PHOSPHORUS LOADING IN AGRICULTURAL AND FORESTED HEADWATER STREAMS IN THE UPPER ETOWAH RIVER BASIN, GEORGIA

by

JAMES JOSHUA ROMEIS

(Under the Direction of C. Rhett Jackson)

ABSTRACT

Few watershed-scale studies have evaluated how phosphorus (P) source and hydrologic transport factors in watersheds managed by poultry operations translate into in-stream P loading. In this study, a combination of continuous (5-minute) streamflow and mixed-frequency water quality data sets were used to estimate total P (TP) loads in three forested (FORS) and nine agricultural (poultry-pasture) (AG) headwater streams (2.4 – 44 ha) in the upper Etowah River basin of Georgia. Specific P source (soil P) and transport (watershed land cover and physical characteristics) factors were also investigated. The data collection duration at study sites ranged between 18 and 22 months. A total of 1,603 water quality samples were collected from the study sites. Significant ($P < 0.1$) inverse relationships were detected between extreme flow response variables (i.e. $Q_{0.1}$) and drainage area and percentage of forest cover. Order-of-magnitude differences in TP and dissolved reactive P (DRP) concentration were observed between AG and FORS sites and among AG sites specifically. At AG sites, stormflow TP concentrations depended on streamflow, but the concentration-flow relationships were strongest on a storm-event basis. At most AG sites, stormflow TP concentrations appeared to reach supply-limited concentrations that were independent of streamflow rate. A documented exception was at an AG site where a storm event was sampled soon after poultry litter application. Three load estimators were examined in the study—planning level, flow-duration rating curves (FDRC), and log-transformed regression models with and without bias-correction techniques. Based on FDRCs, FORS site TP yields ranged between 0.01 and 0.1 kg-P ha^{-1}. At AG sites, the yields ranged 0.031 to 3.17 kg-P ha^{-1}. With confidence intervals factored in, AG site yields ranged 0.025 to 13.1 kg-P ha^{-1}. Total P yields were significantly related ($P < 0.005$) to area-weighted Mehlich-1 soil test P (AWSTP) concentrations. Dissolved reactive P concentrations observed during non-storm flow conditions were significantly related ($P < 0.05$) to AWSTP and P yield. Results suggest that water quality sampling during non-stormflow conditions may be a useful screening tool for watershed scale P risk-based management.

INDEX WORDS: Watershed, Hydrologic response, Load, Phosphorus, Poultry, Forest, Georgia

PHOSPHORUS LOADING IN AGRICULTURAL AND FORESTED HEADWATER STREAMS IN THE UPPER ETOWAH RIVER BASIN, GEORGIA

by

JAMES JOSHUA ROMEIS

B.A., University of Kansas, 1993

M.S., University of Nevada-Reno, 1999

A Dissertation Submitted to the Graduate Faculty of The University of Georgia in Partial Fulfillment of the Requirements for the Degree

DOCTOR OF PHILOSOPHY

ATHENS, GEORGIA

2008

PHOSPHORUS LOADING IN AGRICULTURAL AND FORESTED HEADWATER STREAMS IN THE UPPER ETOWAH RIVER BASIN, GEORGIA

by

JAMES JOSHUA ROMEIS

Major Professor: C. Rhett Jackson

Committee: Todd Rasmussen
David E. Radcliffe
L. Mark Risse
Miguel L. Cabrera

Electronic Version Approved:

Maureen Grasso
Dean of the Graduate School
The University of Georgia
December 2008

DEDICATION

I dedicate my dissertation to my parents, Jim and Dana Romeis, and the rest of my loving family. Thank you all for all your support.

ACKNOWLEDGEMENTS

I wish to express my sincere gratitude to the people whose time and energy directly supported my research and well-being as a student. At the top of the list is my advisor, Dr. Rhett Jackson. Rhett expressed 100% confidence in me, and by doing so, I learned what working independently is all about. I also wish to thank the rest of my Ph.D. committee. Their dedication and unique perspectives benefited me greatly. I wish to thank the hard-working 'behind-the-scenes' field and laboratory personnel who helped with data collection and management. These folks included Philip Brown, Denise Carroll, Tom Maddox, Lisa Dean, Shawn Williams, Brett Porter, John Bryant, Tom Baker, Chris Holliday, Karin Lichtenstein, Josh Erwin, Keith Harris, and Dr. Marco Galang. And, to my friends in Athens and elsewhere, I am grateful to you all for helping me keep the things that truly matter in perspective. Thank you all.

TABLE OF CONTENTS

CHAPTER 1.0

INTRODUCTION

Phosphorus (P) is the limiting nutrient for algal productivity in most of the world's freshwater systems (Wetzel 2001; Carpenter 2005; Withers et al. 2007). Eutrophication, or nutrient enrichment and the associated increase in algal productivity, of freshwater systems can be accelerated by excess P loading from contributing watersheds associated with anthropogenic activities (Correll 1998). Eutrophication can result in various types of water quality degradation including low dissolved oxygen for aquatic life and taste and odor problems for drinking water uses. Eutrophication control emphasizes, in part, reductions of non-point source (NPS) P loads in agricultural and urban watersheds through nutrient planning and use of best management practices.

Non-point source P loading in agricultural watersheds primarily occurs through the interaction, and specifically the co-location, of two modes of P transfer—a P source factor and a hydrologic transport factor (Gburek and Sharpley 1998; Gburek et al. 2000). Source factors are a function of soil, crop, and land management. An important P source factor is soil P content, which has been shown to be positively correlated with P concentration in overland flow (Sharpley et al. 1977, 1978; Pote et al. 1999a, b; Heathwaite and Dils 2000; Sims et al. 2000; Kleinman et al. 2002; Schroeder et al. 2004a). Transport factors include surface (overland) and subsurface flow, soil erosion, and channel transport processes. In most agricultural watersheds with P-enriched mineral soils, 1) P transfer occurs primarily on the land surface via overland flow and soil erosion (Sharpley and Rekolainen 1997; Gburek and Sharpley 1998; Heathwaite and Dils 2000) and 2) most NPS P loading to streams occurs during the most extreme and infrequent storm events (i.e. Pionke et al. 1996, 1997; Dils and Heathwaite 1998; Sharpley et al. 2008a). These findings suggest that the particular factors driving a watershed's hydrologic response to large rain events (i.e. geomorphology, soil characteristics, vegetation, land cover) may be integral to high P loading rates in agricultural watersheds.

Phosphorus management and risk assessment for mitigating P losses in agricultural watersheds has focused on the interaction of P source and transport factors. One recommended approach is targeting P-management measures to critical sources areas (CSAs) where the two factors are co-located and hydrologically-connected to a receiving stream (Pionke et al. 1997; Gburek et al. 2000; Hart et al. 2004). Page et al (2005) found *a priori* identification of CSAs to be difficult, and for risk assessment purposes, proposed that baseflow and streambed P concentrations may be useful as an integrated measure of a watershed's soil P status and hence risk for P loss. With erosion being an important P-transport factor and studies such as McDowell and Wilcock (2007) correlations ($R^2 = 0.44$) between streamflow P and suspended sediment concentrations, suspended sediment may also be a useful P-risk indicator.

The U.S. leads the world in poultry production (U.S. Department of Agriculture (USDA) 2003). Poultry farms generate large volumes of poultry litter, which is a mixture of manure and bedding material such as sawdust, woodstraw, or other materials. Poultry litter can be a valuable organic fertilizer for agricultural land due to its nutrient content (Robinson and Sharpley 1995). This, however, can be problematic because litter application rates typically are based on a crop's nitrogen requirements (Pierson et al. 2001; Schroeder et al. 2004b). Repetitive applications of poultry litter over long time periods can lead to soil P accumulation and subsequent non-point source P loading in receiving streams (Edwards et al. 1996).

The factors for P transfer on the land surface associated with poultry litter application and soil P accumulation are well-studied at plot and hillslope scales (i.e. Giddens and Barnett 1980; Edwards and Daniel 1993; Sauer et al. 2000; Kleinman and Sharpley 2003). Field-scale (0.4 – 8 hectares) studies (Table 1) have been performed in ephemeral, and in some cases, bermed watersheds. Results of those studies show that P concentrations are highly variable and accompanied by order of magnitude differences in P yields (i.e. area-normalized P loading rates). Based on those types of variability, Harmel et al. (2004) recommended more long-term studies of water quality and P loading at both field- and small-watershed scales to investigate the factors driving the variability. Studies of commercial poultry farms may support such research needs. The study by Edwards et al. (1996) (Table 1) was performed on a commercial poultry farm in Arkansas. Recently, small watersheds used for other agricultural practices that are not dedicated for long-term research purposes (termed *non-research catchments* by Page et al. (2005)) have been used (i.e. Hively et al. 2005; Page et al. 2005) for P transfer studies.

In 2002, the State of Georgia ranked #1 in the U.S. in broiler inventory and #6 in layers (USDA 2004). Many of Georgia's poultry farms are small in size and maintain pasture fertilized with the farm's litter (Vervoort et al. 1998). Most poultry sales occur in the northern part of state (USDA 2004). Lander et al. (1998) estimated that in most of north-Georgia's counties, the P in manure generated in those counties could supply over 100% of counties' agronomic P needs for non-leguminous, harvested cropland and hayland. In north-central Georgia, the Lake Allatoona watershed is estimated to have approximately 618 commercial poultry farms. This is based on analysis of aerial photos taken in 1999. Lake Allatoona is a reservoir managed by the U.S. Corps of Engineers for hydropower, drinking water, and recreation for communities northwest of Atlanta. In 2006, due to excessive chlorophyll-*a* concentrations, Lake Allatoona was placed on

Georgia's 303(d) list (http://www.gaepd.org) and scheduled for P Total Maximum Daily Load (TMDL) development. The principal tributary to the reservoir is the upper Etowah River. Because many of the poultry farms identified in the Lake Allatoona basin are located within the upper Etowah River watershed in particular, mitigation of P loads from poultry farms in the upper Etowah River watershed are critical for water quality improvement in Lake Allatoona. Prior to this study, no information was available on P loads or the underlying hydrology and water quality of streams draining poultry farms in the upper Etowah basin.

Study Objectives

The general hypothesis of this research was that the variability of a small agricultural watershed's physical, land cover, and soil P characteristics is reflected in the watershed's hydrologic response, water quality, and thus, P loading rate. The objectives of this research were:

1. To estimate P loading in headwater streams draining both commercial poultry farms and forested watersheds representing reference conditions in the upper Etowah River basin, and

2. To connect variability in hydrologic response by the watersheds to their respective physical and land cover characteristics, and

3. To connect variability in P concentrations and loading in the streams to soil P and other potential risk indicators of P loss.

To fulfill these objectives, continuous (5-minute) streamflow measurement, mixed-frequency water quality sampling, and soil-P sampling were performed in twelve headwater watersheds in the upper Etowah River basin. Nine watersheds were used for different commercial poultry farm operations and three drained National Forest land. Of the streams draining the study watersheds, ten were perennial, one was intermittent, and one was ephemeral.

Streamflow and water quality data from the streams represent approximately 18 watershed years of data total. Methods for load estimation were adapted from methods used primarily in large river studies as methods for load estimation in headwater streams are not well-developed. Methods of data analysis for the hydrologic and water quality studies were mainly empirical. This was due to 1) limitations posed by analyzing data from 12 sites and 2) lack of past information on hydrology and water quality in small streams draining commercial poultry farms.

Organization of Dissertation

While fulfillment of Objective 1 was the primary motivation of this research, the organization of this dissertation is based on the concept that NPS P loading in a watershed is a function of its hydrologic transport and P source factors. Where applicable, discussions pertinent to hydrologic response and P source factors are treated independently. A literature review in Chapter 2 presents concepts and describes previous research on hydrologic response as a function of a watershed's physical and land cover characteristics; source, transport, and risk factors for P transfer in forested and agricultural watersheds; and load estimation methodologies. In Chapter 3, the methods and materials for data collection and analysis used in this study are described. In Chapter 4, results are presented in the order of factors for hydrologic response, water quality variability, and phosphorus load estimation. The discussion in Chapter 5 interprets the main results of this study and relates them to past research. Lastly, Chapter 6 presents the conclusions of this study.

CHAPTER 2

LITERATURE REVIEW

2.1 Hydrologic response

The hydrologic response of a watershed determines how water and solutes are partitioned between atmospheric, surface, and subsurface hydrologic pathways over a range of time scales. Research on hydrologic response has focused on both the process (i.e.Tetzlaff et al. 2008) and end-result (Woodruff and Hewlett 1970) of stormflow generation (i.e. rainfall-runoff). Potentially high spatiotemporal variability of the different hydrologic controls (i.e. climatic, geomorphic, soils, etc.) equates to watersheds having highly variable and yet unique hydrologic response characteristics (i.e. runoff coefficients, peak flow rates) (McDonnell and Woods 2004; Eisenbies et al. 2007). This review highlights past research on 1) stormflow generation processes, 2) categorizing hydrologic controls, and 3) streamflow variability to identify influential controls. Where applicable, this review emphasizes on studies involving headwater catchments in the southeastern U.S.

2.1.1 Stormflow generation in headwater catchments

In the Southeast and other humid regions, the variable source area (VSA) (Betson 1964; Hewlett and Hibbert 1967; Ragan 1967; Dunne and Black 1970a,b) concept is largely accepted as the model for stormflow generation in non-urban, headwater watersheds. The basic VSA concept evolved from observations that during most storm events stormflow does not originate from the entire watershed. Rather, stormflow generation is tied to a dynamic, expanding and contracting near-stream saturated zone that typically represents a small fraction of total drainage area (Hewlett 1982). During a storm event, depending on antecedent soil moisture, rainfall intensity and soil depth, the saturated zone responds to infiltrating rainfall or contributions of unsaturated flow from upslope by rising towards the land surface (Betson and Marius 1969; Nutter 1973). With continued rainfall, the saturated area expands away from the channel. Stormwater discharges to the stream via overland flow and/or groundwater pathways. Overland flow is generated either by rain falling onto areas where the saturated zone intersects the ground surface or via *return flow* (i.e. groundwater seepage) (Dunne and Black 1970a). Overland flow reaching the stream via agricultural fields and roadways constitute part of the VSA model (Hewlett 1982). Mechanisms of groundwater discharge include 1) displacement by lateral throughflow from upslope (Hewlett and Hibbert 1967), 2) displacement caused by increasing pore water pressures in deeper soils (Ragan 1967), and 3) growth of a *saturated wedge* and an accompanying increase in hydraulic gradient between the stream channel and near-stream saturated zone (Sklash and Farvolden 1979). Preferential flow via macropores may play a role by delivering water from the hillslope to the saturated zone (McDonnell 1990) or from the saturated zone to the stream (Pearce et al. 1986).

Variable source areas tend to form within convergent zones (i.e. hillslope hollows) (Anderson and Burt 1978) or where depth to bedrock (Wilson and Dietrich 1987) or other confining layer such as a Bt horizon (Endale et al. 2006) is shallow. Convergent zone locations include slope concavities in plan and in section, zones where soils are thin and have low transmission capacity, and where a temporarily-saturated subsoil layer causes a decrease in hydraulic conductivity (Beven and Kirkby 1979; Ward 1982, 1984).

Weaknesses of the VSA concept are that it fails to specify flow mechanisms and hydrologic pathways operating at different spatial scales such as those associated with threshold responses to storm events (Sidle et al. 2000; McDonnell 2003). A threshold-response may be manifest as an abrupt rise in streamflow or change in water chemistry due to part of the watershed exceeding a threshold level in water storage or two typically disconnected parts of a watershed (i.e. riparian and upland zones) becoming hydrologically-connected (Bracken and Croke 2007). The study of Sidle et al. (2000) demonstrated a threshold response by a zero-order watershed. The authors used different field methods to identify stormflow pathways in a nested set of steep, forested, zero and first-order watersheds in Japan. Over a series of storms within a one-month winter period, substantial overland flow was not observed in an upland zero-order watershed until antecedent moisture and groundwater accumulation exceeded a threshold capacity. Another zero-order watershed did not generate overland flow until a later event. This lag was attributed to the latter watershed having deeper soils and greater water storage capacity. Similar threshold events were reported by Buttle et al. (2004) and Ocampo et al. (2006).

2.1.2 Categories of hydrologic response controls

Different approaches have been used to categorize the controls on hydrologic response. Hewlett and Hibbert (1967) list watershed area, channel length, slope percent, and porous mantle depth as the fundamental dimensions for modeling an undisturbed watershed. For small watersheds, Moldan and Cerny (1994) list the following site characteristics as the prominent influential factors: relief, altitude above sea level, bedrock geology, soil cover, vegetation cover, and human impact. Eisenbies et al. (2007) describe streamflow as the integration of climate, geology, vegetation, and soils. Those factors were split into two groups depending on their susceptibility to human influence. The non-susceptible group, following Benda et al. (2004), included climate, geology, and watershed geometry. Recent proposals for basin classification systems have used similar conventions. For example, Winter (2001) and Wolock et al. (2004)

used land-surface form, geologic texture, and climate characteristics as main variables for grouping basins (~200 km^2) in the U.S. into 'hydrologic landscape regions'.

The concept of hydrologic connectivity has been integrated into discussions in the literature on critical hydrologic response controls. Buttle (2006) note that a limitation of some basin classification systems (i.e. Winter 2001; Wolock et al. 2004) is that they do not specify the relative importance of each control or they do not take into account the potential that the importance may change as a function of location or scale. Buttle (2006) categorizes controls in terms of typology, topology, and topography. Typology describes the relative potential of different controls to partition and store water into surface and subsurface pathways. Topography describes the relative role of hydraulic gradients in transferring water downgradient. Topology is a measure of hydrologic connectivity that describes the relative role spatiotemporally for the drainage network to *modulate* water downgradient. Bracken and Croke (2007) propose a conceptual model of hydrologic connectivity that integrates the VSA concept with landscape characteristics both spatially and temporally. The components included: 1) climatic environment (climate, storm intensity and duration), 2) hillslope runoff potential (infiltration, surface roughness, vegetation, land management, temporal variability), 3) landscape position, 4) delivery pathway, and 5) lateral buffering. Bracken and Croke (2007) propose *volume to breakthrough* as the quantitative, dependent variable that can be measured in the field and predicted by the model. While examples of the model's application were simple, the concept behind the model seems practical because it can account for delivery pathways associated with human activity such as roadways and other features.

In small agricultural watersheds, features associated with different land treatments may constitute controls on hydrologic response. Ludwig et al. (1995) show that dead furrows and field boundaries in addition to topography and structural state of surface soils were correlated with rill occurrence and size in zero-order cultivated catchments. Moussa et al. (2002) modeled the roles of tillage and a ditch network on flooding in a 91-hectare (ha) watershed covered predominantly by vineyards. Tillage decreased runoff coefficients and enabled infiltration. Ditches routed storm runoff to the watershed outlet plus they were sources of groundwater discharge when the water table was below the bed of the ditches. Cattle trails may have similar water routing effects as ditches because repeated travel over the same path by cattle can result in soil compaction, erosion, and initiation of gully formation (Cooke and Reeves 1976; Rostagno 1989; Trimble and Mendel 1995). All of these effects would be critical for faster routing and greater volumes of overland flow to streams.

2.1.3 Analysis of streamflow variability to discern hydrologic response controls

While a streamflow time series provides no direct information on the interactions of factors driving hydrologic response of a watershed, it is still representative of those interactions (Bracken and Croke 2007). One use of streamflow data in this capacity has been through before/after watershed studies. Swank et al. (2001) used a ~20-year streamflow record from a 59-ha forested watershed in the southern Appalachians to discern changes in water yield and hydrograph characteristics due to forest harvesting activities. In the first year after harvesting, annual water yield increased by about 28%. Over the next four years, water yield declined until before/after differences in yield statistically the same. The largest increases in monthly yields after harvesting occurred during summer low-flow months. Results of hydrograph analysis showed significant differences in all hydrograph characteristics (initial flow, peak flow, total quickflow volume and quickflow volumes before and after peak flow, quickflow duration, and recession time) tested except time to peak flow. Another use of streamflow data has been to use its temporal variability as a measure of watershed hydrologic response. Richards (1989) calculated three flow variability measures (ratio measures (i.e. flashiness indices), spread measures, and coefficients of variation of logs of flow) representing *flow responsiveness* for 118 Great Lakes tributaries and related them to basin area. While results did suggest an overall decrease in responsiveness with increasing area, exponential models fit to the data were weak ($R^2<0.30$). The author identified soil type and land use as potential sources of variability that were not considered for in the models.

There were at least two studies of eastern U.S. watersheds that specifically took land use into account as a factor for streamflow variability. Woodruff and Hewlett (1970) tested regression models between a mean hydrologic response factor *R* and 15 different planimetric, hypsometric, and land use (% cleared (i.e. non-urban and non-forest), % forest, % urban) variables using streamflow and precipitation data from 90 watersheds (2 – 100 mi^2) across the eastern U.S. The *R* was computed for each watershed by dividing annual quickflow volumes by annual precipitation depths. Tested individually, none of the variables explained more than 3% of the variability in *R*. Further, no significant correlations were detected. In a later part of the study, a hydrologic response map was developed for the eastern U.S. using data from 201 watersheds. Response patterns tended to be organized by the major physiographic regions (i.e. Piedmont, Appalachian Plateau, etc.) of the eastern U.S.

The second study was by Schoonover et al. (2006) who investigated influence of land cover on the variability of an annual streamflow time series observed in 18 first-, second-, and third-order Piedmont watersheds (500 – 2500 ha) in west Georgia. Land cover categories included urban, developing, pastoral, managed forest, or unmanaged forest. Three or four watersheds were assigned to each land cover category. None of the study watersheds were covered by more than half of their respective assigned cover category. Thirty-two hydrologic variables were computed for each stream. Variables were categorized as frequency, magnitude, duration, flow predictability and flashiness, and baseflow. Data analysis included means testing by least significant difference, non-parametric analysis of variance (Kruskal-Wallace), and Pearson's correlation. There tended to be agreement among the statistically-significant results on the following relationships. First, forested watersheds had lower area-normalized flow minima, maxima, and means. Second, urban and developing watersheds had higher area-normalized flow maxima and flow-frequencies. Last, pastoral watersheds had higher baseflows.

2.1.4 Synopsis and implications

Hydrologic response in watersheds has been studied through both process- and end result-oriented approaches to understanding stormflow generation. In small, humid watersheds, the process of stormflow generation is tied to the VSA as dynamic source of overland flow and groundwater to streams during rainfall events. A limitation of the VSA concept is its ability to accommodate threshold-level hydrologic responses in watersheds. Underlying controls of stormflow generation processes have been categorized differently. The concept of hydrologic connectivity constitutes an important control, especially in small watersheds with networks of roads or other features. End result-oriented studies that were reviewed showed that both geomorphic and land use controls may explain variability in hydrologic response metrics. The implication of the literature reviewed here is that the potential sources and interactions among controls on hydrologic response in watersheds are numerous and can vary both spatially and temporally. This suggests that distinguishing the relative influence of different controls on hydrologic response in one or a group of watersheds may be difficult and may require different analytical approaches.

2.2 Phosphorus source and transport factors

The focus on phosphorus (P) in water quality-based environmental research is largely due to the impairments caused by cultural eutrophication of freshwater systems. Research has demonstrated the important role that P plays as a limiting nutrient for phytoplankton productivity in most lentic freshwater systems (Schindler 1977; Hecky and Kilham 1988; Rabalais 2002). Like terrestrial plants, P is vital for phytoplankton growth. Phytoplankton use P in almost all phases of metabolism (Wetzel 2001). Eutrophication of undisturbed lentic systems is a natural and slow process (Lampert and Sommer 1997). Excess P load loading from external (i.e. point and non-point) sources as well as internal (i.e. sediment release) sources can accelerate eutrophication and result in a biomass increase of phytoplankton and other aquatic plants. Consequences may include blooms of harmful or nuisance algae, oxygen shortages, increased costs for water treatment, and losses of fish, wildlife and recreational resources (Sharpley and Rekolainen 1997; Wilson and Carpenter 1999; Carpenter 2005). Recovery of a eutrophic lake following a reduction of external P loading may take centuries or longer depending on internal loading rates and the size of the P pool in lake sediment (Carpenter 2005). In eutrophic lakes that drain agricultural watersheds with high soil P contents, major changes in soil management may be necessary for lake recovery.

This review highlights how P source and transport factors interact and can regulate hydrologic P transfer processes in forested and agricultural watersheds. Transfer processes in headwater, forested and poultry/pasture-dominated agricultural watersheds in the southern Appalachians and Georgia Piedmont, respectively, are emphasized. In addition, a short discussion is provided that highlights different approaches used to assess agricultural watersheds for risk of P loss to downstream waterbodies. This review begins with a discussion of influential factors for eutrophication in Georgia Piedmont reservoirs.

2.2.1 Factors for phytoplankton growth in Georgia Piedmont reservoirs

There are no natural lakes in the Georgia Piedmont but there are numerous manmade impoundments, or reservoirs, used for water supply, recreation, flood control and other uses (Raschke 1994). Reservoirs in Georgia are different than most north-temperate lakes that are glacial in origin. While the reservoirs can be deep enough to stratify they are monomictic and may stratify longer, such as between April and October (Porter 2004). Such differences are due to a longer growing season in the Southeast plus warmer annual average temperatures and a lack of winter ice cover (Raschke 1993, 1994; Porter et al. 2004; Parker 2004).

Another difference between north-temperate lakes and Georgia reservoirs involves factors for P cycling. Parker (2004) demonstrated how P cycling in reservoirs of the Georgia Piedmont is controlled by the iron (Fe) cycle and inherently linked to influent sediments originating from the Bt horizon of Piedmont soils. The Bt horizons of Piedmont soils are rich in iron (Fe) oxides (Radcliffe and West 2000) and can have large P sorption capacities. Sorption capacity experiments by Parker (2004) showed that Bt soils and reservoir sediments may have maximum P sorption capacities of 500 grams of P per gram (g-P g^{-1}) of soil or greater. Parker (2004) described two mechanisms for P-release from Fe in reservoirs during summer stratification. One mechanism occurs in the epilimnion, where colloidal-sized Fe-P complexes that remain suspended may release P with photosynthesis-induced elevations of pH due to bicarbonate removal. This mechanism is enabled by the characteristically low buffering capacity, alkalinity, and sulfur content of Piedmont surface waters. These characteristics are not typical of north-temperate lakes. The other mechanism for P release occurs in the hypolimnion.

Phosphorus is released through reduction of particulate Fe-P complexes caused by utilization of organic carbon (i.e. respiration) by metal-reducing bacteria. Longer stratification periods may result in a greater amount of P released, even when only more recalcitrant organic carbon is bacterially-available. The phosphate becomes plant-available when the reservoir mixes. The P-availability may be minimized, however, by uptake (i.e. scavenging) of P by iron oxides in the water column. An important watershed management implication of Parker's (2004) research is that efforts to mitigate eutrophication impacts due to P must also take management of both Fe and organic carbon into account.

2.2.2 Phosphorus cycling in forested watersheds

In undisturbed, humid (i.e. forested) watersheds, originating sources of P in soil are weathering of primary minerals through pedogenesis and bulk (wet and dry) atmospheric deposition (Dillon and Kirchner 1975; Walker and Syers 1976; Walbridge et al. 1991). Weathering of P in primary minerals is a geologically-slow process that depends in part on the parent material (Walker and Syers 1976). Annual inputs of P from bulk deposition are typically negligible compared to the size of the P pool in soil and vegetation but the deposition inputs can be significant relative to watershed P losses via streamflow (Ballard 1980; Wood et al. 1984; Swank and Waide 1984; Monk and Day, Jr. 1988). Brady (1990), Walbridge et al (1991), and Sharpley and Rekolainen (1997) review soil P cycling process and present conceptual models of P cycling processes in soils. Those reviews are synthesized below.

Pools of soil P are both organic and inorganic forms. Organic P pools include humus, plant residues, soil microbes, labile organic P (Walbridge et al. 1991; Sharpley and Rekolainen 1997). Organic forms of P include inositol phosphates, phospholipids, nucleic acids, and humic/fulvic acids (Brady 1990; Sharpley 1995). Pools of inorganic P, in addition to primary minerals, include secondary P minerals, occluded P, and labile inorganic P. In non-calcareous soils, secondary minerals include iron (Fe) and aluminum (Al) oxyhydroxides and silicate clays (Brady 1990; Sharpley 1995). Aluminum and Fe oxyhydroxides can be categorized as either amorphous or crystalline. Amorphous Al and Fe oxyhydroxides are the dominant inorganic form in soil P sorption reactions because of greater surface area/mass ratios (Hsu 1977; Shwertmann and Taylor 1977; Walbridge et al. 1991). Phosphorus in most soils is 50 to 75% inorganic with the remainder in organic forms, but the respective ranges of organic and inorganic forms can vary widely (Sharpley 1995).

Of total P content in soil, only 0.01 % of the P may exist in soluble forms (Brady 1990). In unfertilized soils, sources of soluble organic P include direct leaching from plants (i.e. throughfall), leaching from detritus, exudation, and microbial dissolution (Qualls 2000). The major factors for removal of organic P from solution are adsorption to Al and Fe oxyhydroxides, plant root uptake following microbial hydrolysis, and hydrologic transfer to a receiving stream (Anderson 1980; Qualls et al. 2000). Sources of soluble inorganic P include bulk deposition, weathering of primary minerals, desorption from Al and Fe oxyhydroxides, mineralization of organic P, and leaching from plants. The major factors for removal of inorganic P from solution are similar to those for organic P. Exceptions are that root uptake is a direct process and soluble inorganic P may be immobilized through microbial uptake or removed via an anion exchange reaction (Brady 1990; Qualls 2000).

Brady (1990) described the general process of retaining soluble inorganic P through adsorption in terms of pH-dependent precipitation or fixation. In strongly acid soils, P is chemically fixed and precipitated with Al, Fe, or manganese (Mn). In strongly to moderately acid soils, P is fixed by Al and Fe oxyhydroxides. In moderately to weakly acid soils, silicate clays (i.e. kaolinite) fix P. In Ultisols, which are the predominant soil order of the southern Appalachians and Georgia Piedmont, soil P fixation capacity is high due to their acidic and highly weathered nature and associated large quantities of Al and Fe oxyhydroxides (Velbel 1988). This is a critical factor for limiting P availability for plants in Ultisols (Sanchez and Uehara 1980).

In forested watersheds, soluble organic and inorganic P may not be evenly distributed between the forest floor and surface and subsurface soil horizons. Qualls et al. (1991) measured the flux of dissolved organic and inorganic P from the forest canopy to the forest floor and down to mineral soil in an experimental deciduous forested watershed at Coweeta Hydrologic Observatory in the southern Appalachians. The forest floor was a sink for inorganic P from throughfall and not a source of inorganic P to mineral soil. A likely explanation was that microbes immobilized inorganic P. The forest floor and O horizon, in particular, was an important source of organic P to mineral soil. In a different study at Coweeta, Walbridge et al. (1991) showed that the biological and geochemical subcycles that controlled overall P availability in soils were not vertically stratified within the near-surface (0 – 30 cm) mineral horizons. Biological agents appeared to control P dynamics in the forest floor. This latter finding appears to align with the explanation by Qualls et al. (1991) that microbial immobilization controlled inorganic P in the forest floor.

2.2.3 Hydrologic transfer of phosphorus in forested watersheds

Because overland flow is mostly negligible in southern Appalachian forested watersheds, transfer of soluble P to streams occurs via subsurface flow and transfer of insoluble P occurs via soil and channel erosion. Qualls and Haines (1991) and Qualls (2000) hypothesized that *hydrologic short circuiting* of root networks and absence of soil horizons that are high in Al and

Fe oxyhydroxides enable transfer of soluble P loss from soils to streams. A rationale for the hypothesis was the finding by Qualls and Haines (1991) that streamflow concentrations of dissolved organic P were higher than in B and C horizons and headwater seeps. Further, the concentrations increased on rising limb of storm hydrographs. While not explicitly stated by the authors, it is assumed that macropore flow constitutes the type of pathway that short-circuits root networks and biogeochemically-active soil horizons.

As suggested above, forested watersheds tightly conserve P. This is evident from several studies that reported watershed P budgets of forested watersheds in the eastern U.S. From a 13-year study of baseline precipitation in seven untreated, control forested watersheds at Coweeta, Swank and Waide (1988) reported mean annual depositional inputs ranged between 0.08 and 0.12 kilograms of P per hectare (kg-P ha^{-1}). Dry deposition constituted 70.6 % of the bulk precipitation. Mean streamflow outputs ranged between 0.02 and 0.03 kg-P ha^{-1}. Net differences ranged between 0.06 and 0.09 kg-P ha^{-1}. It is important to note that there was substantial variability in the concentration of bulk deposition in precipitation. The mean streamflow phosphate (PO_4-P) concentration was 0.00564 mg-P L^{-1}. The standard error and coefficient of variation were 0.00039 and 0.190, respectively. Hobbie and Likens (1973) developed a watershed P budget for an undisturbed forested watershed at Hubbard Brook. Over a one-year monitoring period, the net difference between rainwater P input (0.108 kg-P ha^{-1}) and streamflow P output (0.021 kg-P ha^{-1}) was 0.087 kg-P ha^{-1}. In both studies, the ratio between depositional P inputs and streamflow P outputs was approximately 5:1. The difference was reflected in forest primary production. Monk and Day, Jr. (1988) estimated primary production rates and the amounts of P in soil and biomass in one of the undisturbed, hardwood watersheds studied by Swank and Waide (1988). During leafout, roughly one-third of P was stored in soil, litter and roots. The remainder was stored in above tree biomass. Bulk deposition inputs and streamflow losses combined accounted for less than 0.01% of the total soil-litter-biomass pool.

Forested watersheds may remain P-conservative following disturbance. Swank (1988) studied changes in stream chemistry in forested watersheds at Coweeta that underwent different cutting and vegetation regrowth treatments. Control streams (Swank and Waide 1988) had PO_4-P concentrations ranging between of 0.001 to 0.002 mg-P L^{-1}. Treated streams had PO_4-P concentrations ranging between of 0.004 to 0.008 mg-P L^{-1}. While the concentrations in treated streams were higher, they still remained low, as noted by the author. Further, there were no pretreatment stream chemistry data, which would be more appropriate for comparison purposes. In terms of P-exports, in one stream draining a clearcut and logged watershed, annual PO_4-P exports were higher (0.03 to 0.12 kg-P ha^{-1}) during the first four years but by the fifth year, the PO_4-P export was back to control stream levels (0.02 kg-P ha^{-1}). The increase in exports was attributed to increases in annual streamflow. Hobbie and Likens (1973) attributed a lack of change in dissolved inorganic P exports following clearcutting in a Hubbard Brook watershed to disruption of biological surface processes causing downward transfer of P from the forest floor to P sinks in the B soil horizon.

2.2.4 Application of fertilizer amendment to agricultural soils

In crop-based, agricultural systems, water, N and P are among the main factors that limit crop yield (Sharpley and Halvorson 1994). Due to different retention and loss mechanisms that limit soil N and P availability, maintenance of crop residues and application of fertilizer amendments to soil are integral to fulfilling crop nutrient requirements and maintaining profitable production (Brady 1990; Sharpley and Halvorson 1994). Organic fertilizers including animal manure and compost can be effective nutrient sources for crops (Brady 1990; Sharpley and Halvorson 1994). Manure may also increase soil organic matter and cover which can then improve soil physical properties, promote infiltration, delay and reduce runoff, and protect against soil erosion (Giddens and Barnett 1980; Sharpley and Halvorson 1994; Gilley and Risse 2000; Kleinman and Sharpley 2003).

In agricultural systems where manure is applied, the optimal application amount depends on the type of manure, its nutrient availability relative to crop requirements and soil nutrient availability, and environmental conditions including temperature, soil moisture and other soil characteristics and microbial activity (Eghball et al. 2002). In terms of P, when manure or other fertilizers are applied, its use by crops and its retention by soil are subject to the similar types of factors controlling P in natural soil-vegetation systems. After application, P may be utilized by the crop with a portion recycled into organic P and fixed by different minerals or clays (Sharpley and Rekolainen 1997). After long-term application at excessive rates, P may accumulate in the near-surface (i.e. upper five cm) soil horizons (Andraski et al. 2003; Schroeder et al. 2004b). Without removal via crop harvest or erosion, the P may continue to accumulate as well as be leached downward via infiltrating rainwater.

Manures are typically applied to crops in order to satisfy N needs (Edwards et al. 1996). Because manures have low N:P ratios (i.e. 2:1 to 6:1) relative to crop N:P requirements (i.e. 7:1 to 11:1), the amount of P applied can exceed the crop's P requirements (Sharpley 1995; Edwards et al. 1996; Heathwaite et al. 2000). After long-term manure application, the end result is accumulation of soil P in excess of crop needs (Edwards and Withers 1998; Haygarth et al. 1998). This can be accentuated in regions of intensive livestock production in two ways. First, the quantity of P in the volume of manure produced may exceed the region's crop P requirements (Sharpley et al. 1993; Kingery et al. 1994; Lander et al. 1998; Ribaudo et al. 2003). Second, manure amendments like poultry litter can be voluminous and costly to transport (Bosch and Napit 1992). Sims et al. (2000) reported that long-term trends in soil-test P values around the world indicated that many regions in the U.S. and around the world have soil-P levels in excess of crop requirements. For counties in the U.S. where manure application is restricted to non-leguminous cropland or hayland, Lander et al. (1998) showed that many of the counties where manure can provide more than 100% of crop P needs overlapped with counties indicating high soil-P availability.

Counties within the north-Georgia poultry production region are among regions in the U.S. shown by Lander et al. (1998) to have both high manure P production and high soil P availability. In 2002, the State of Georgia ranked first in the nation in broiler inventory and sixth in layer inventory (USDA 2004). Most poultry sales occur in the northern part of state (USDA 2004). Many of Georgia's poultry farms are small in size and maintain pasture fertilized with the on-farm poultry litter (Vervoort et al. 1998). Poultry litter differs from manure in that litter also contains feathers, wasted feed, and bedding materials such as sawdust, wheat straw or pine bark shavings (Moore et al. 1995; Robinson and Sharpley 1995). For bone development and other purposes, calcium and phosphorus are added to poultry feed typically as dicalcium phosphate (National Research Council 1994). The pasture vegetation is commonly a mixture of tall-fescue and bermudagrass (Kuykendall et al. 1999). To maintain adequate levels of forage for cattle, relatively high rates of fertilization are needed (Huneycutt et al. 1988). When this is coupled with limited land areas relative to the volumes of litter produced, litter application rates can become excessive (Kuykendall et al. 1999).

2.2.5 Source factors for P transfer in manure-amended soils

Accumulation of soil P beyond agronomic requirements is a critical environmental aspect of manure management because studies (i.e. Sharpley et al. 1977, 1978; Schroeder et al. 2004a) have demonstrated direct relationships between a soil's P content and the P content of storm runoff in contact with the soil. Hydrologic P transfer in agricultural systems primarily occurs via overland flow and soil erosion during storm events (Figure 1) (Pionke et al. 1988; Sharpley et al. 1994; Heathwaite 1997; Gburek and Sharpley 1998; Sharpley et al. 1999). Important determinants of runoff P concentration are the concentration of soil P specifically in the near-surface soil horizon and how much of that horizon interacts with overland flow (Sharpley 2003; Dougherty et al. 2004). Factors such as rainfall intensity, slope, and raindrop energy may influence the depth of interaction (Sharpley 1985; Dougherty et al. 2004). In addition, physical characteristics of the soil surface that influence infiltration may influence the depth including soil texture, structure, aggregate stability, and quality of the soil surface. Another determinant may be a *change point* representing a break in the slopes of two linear relationships that describe soil/runoff-P relationships for a particular soil (McDowell and Sharpley 2001). Soil/runoff-P relationships can be soil-specific (Sharpley 1995) and vary as a function of season (Pote et al. 1999a). Pote et al. (1999b) showed that the relationship varied within a soil series and may be a function of hydrologic response. For a given level of water-extractable P (WEP), soils (3 total sampled) yielding the lowest runoff volumes were those with the lowest runoff dissolved reactive P (DRP) concentrations. After normalizing by the depths of runoff, regression lines between runoff DRP concentration and WEP for each soil were statistically the same ($P<0.05$). The authors suggest that knowledge of site hydrology may improve how soil P can predict runoff P. Most investigations of soil/runoff-P relationships have occurred at the experimental plot scale. At larger spatial scales, Dougherty et al. (2004) noted that the strongest relationships had been shown in *pure soil-pasture systems* where soil, land cover, and management aspects are uniform and minimally-variable. They also noted that at larger watershed scales (i.e. McDowell and Trudgill 2000) mixed land cover types and hydrologic variations would make soil/runoff-P relationships highly variable.

Phosphorus in freshly-applied and residual manure is a potential P source to overland flow independent of soil P content (Figure 1). Studies (i.e. Edwards and Daniel 1993; Sharpley 1995; Vervoort et al. 1998; Kleinman and Sharpley 2003 and others) demonstrate strong positive relationships between manure or litter application rate and P concentration in runoff. Typically, P concentrations of runoff in contact with applied manure are highest during the first rainfall event and then reduce rapidly over subsequent events. As time between poultry manure application and rainfall increases, the potential P concentration in the first or subsequent runoff events may decrease depending on the degree of contact between applied manure and the receiving soil which can enable P adsorption (Edwards and Daniel 1994; Sharpley 1997, Pierson et al. 2001; Kleinman and Sharpley 2003; Schroeder et al. 2004b). Over time, with natural alternations between rain events and dry periods, the amount of P remaining in the residual manure relative to the initial application amount may be substantial. Pierson et al. (2001) showed that DRP concentrations remained above 1.0 mg-P L^{-1} for 19 months following a series of four biannual litter applications to 0.75-ha bermudagrass paddocks. Because poultry manure may have a strong influence on runoff P concentration for a substantial amount of time following application, the influence of soil P on the runoff P concentration may be overwhelmed by that of manure. This was demonstrated by Sauer et al. (2000) and Kleinman et al. (2002).

Rainfall intensity may also influence the P concentration in the first runoff following manure application. Edwards and Daniel (1994) investigated the effects of three application rates (range 54 to 215 kg-TP ha^{-1}) and two rainfall intensities (five and ten cm hr^{-1}) on runoff P concentration collected from grassed plots from the first simulated rain event. As rainfall intensity increased, concentrations decreased on the order of 22 to 36% but the percentage of TP lost from the initial application amount increased by over 250%. This suggests that a dilution effect (Fleming and Cox 1998) may have occurred due to a greater amount runoff relative to soil P source. In all treatments combined, the fraction of TP concentration as DRP relative to TP ranged between 78 and 95 %. As application rate increased, DRP/TP tended to decrease (i.e. from 95% to 82%).

In pasture systems, livestock typically are not significant new P sources when added to a pasture or significant P losses when removed because livestock recycle most of the P they consume (Mays et al. 1980; Barrow 1987). What livestock do represent, however, is a source of spatial and temporal rearrangement of available P due to grazing patterns and camping tendencies which can vary by stocking rate, species, breed, and sex (Mays et al. 1980; Sauer et al. 1999). Like poultry manure, the availability of P from cattle dung is a function of the time since release (McDowell et al. 2006). The potential loss of P from cattle dung can be accentuated through the physical impacts (i.e. soil compaction, decrease of vegetative cover) of livestock and how that can alter hydrologic response. Physical impacts can be a function of grazing intensity, however Kuykendall et al. (1999) showed that grazing method (rotational vs. continuous stocking) did not affect ($P > 0.1$) surface runoff quality or quantity from fields fertilized with broiler litter. McDowell et al. (2007) showed that the impacts of treading alone accounted for about 10% of the overall loss in a plot-scale study aimed at differentiating between relative P contributions from soil, dung, grazed pasture plants, and the added influence of treading. In the latter study, rainfall and treading by cow hooves were both simulated.

2.2.6 Transport factors for P transfer in manure-amended soils

In systems such as pasture where poultry litter is applied, the pools of organic and inorganic P may be large but the actual fractions available for mobilization during a runoff event may be relatively small and on the order of 1-5 % (Dougherty et al. 2004). Mobilization of P (Figure 1) from the P source involves three processes that are based on the amount of the P that is mobilized: 1) physical detachment and entrainment, 2) chemical release or solubilization (Dougherty et al. 2004; Hart et al. 2004; Haygarth et al. 2005a), and 3) incidental losses from manure following contact with rainfall (Withers et al. 2003). Detachment is typically linked to energy processes involving soil erosion including raindrop impact, slaking and overland flow (Dougherty et al. 2004; Haygarth et al. 2005a). Chemical release of P is a function of source P and receiving runoff characteristics. As noted above, different studies have found strong relationships between runoff P and both soil P and manure P. Further, studies have demonstrated numerous sources of variability in these relationships. Sharpley et al. (1981a) developed an empirical model to describe chemical release of P from soil to water in laboratory mixing experiments. Phosphorus release was directly related to desorbable soil P content. The logarithm of P release was linearly related to the logarithms of contact (mixing) time and water:soil ratio. Sharpley et al. (1981b) expanded on the model to describe the release of P from surface soil to runoff using results of soil box experiments with simulated rainfall. The authors showed that average DRP concentration could be predicted using desorbable P, contact time, water:soil ratio plus depth of interaction, soil bulk density, and volume of runoff per unit area (Sharpley 1985).

Once mobilized, the forms of P in stormflow may exist along a broad range of particulate, colloidal, and dissolved ionic forms (Figure 1). Particulate P includes P-containing soil particles and organic matter resulting from erosion of surface soil (Sharpley and Halvorson 1994). Because of preferential transport of clay-sized (< 2 μm) particulates, its content is generally higher than the originating soil source (Sharpley and Halvorson 1994; Heathwaite 1997). Filtration of water through a filter with 0.45-μm pore size has been the standard methodology for differentiating between particulate and dissolved (or soluble) P fractions. Subsequent laboratory analysis of filtrate by the standard Murphy and Riley (1962) colorimetric method is then used to identify the plant-available P fraction. That fraction is widely termed by the literature as DRP (as discussed so far) or soluble reactive P (SRP). Haygarth and Sharpley (2000) criticized this overall approach of how particulate and dissolved P fractions are differentiated and how Murphy-Riley-reactive P represents plant-available P. Their arguments were based on the concepts that that colloidal P may exist in a wide range of sizes (1 nm – 1 μm per Haygarth et al. 2006) and that loosely-bound inorganic P, organic P, and silica may be Murphy-Riley-reactive. For the purposes of this review, the term DRP represents inorganic, plant-available P.

Numerous factors may influence the amount of P mobilized and the resulting runoff P concentration (Dougherty et al. 2004). Concentration-wise, two factors that bridge a P source with hydrology are 1) the contact time between the source and runoff and 2) the runoff to P source ratio (Sharpley et al. 1981a, b; Dougherty et al. 2004). Contact time is a function of different factors including surface roughness (i.e. vegetation, topographical variation), land slope, and slope length (Chow et al. 1988). A slower velocity increases contact time with the source and the potential for a greater P release from the source (Dougherty et al. 2004). An apparent increase in concentration can be countered by a greater runoff:P ratio, such as through a dilution effect (Fleming and Cox 1998; Dougherty et al. 2004) that lowers the P concentration but may still be reflected in an overall increase in P transported (i.e. Edwards and Daniel 1993). Fraction-wise, P in runoff through grass cover has been understood to occur predominantly in the dissolved form (i.e. Sharpley and Halvorson 1994). As noted above, Edwards and Daniel (1993) observed DRP/TP fractions on the order of 80-90% in runoff from grassed plots that varied as a function of manure application rate and rainfall intensity. A greater proportion of particulate P would be expected during larger runoff events and on land surfaces with greater availability of erodible soil and organic matter.

Under certain conditions, subsurface P transfer may be an important component for how P ultimately reaches a stream. Peaty and sandy soils with low fixation capacity typically have high P leaching potentials (Heathwaite 1997). In soils with high fixation capacity, leaching may still be important in cases of P saturation (Heckrath et al. 1995; Heathwaite and Dils 2000; Sims et al. 2000). Preferential flow via macropores and soil cracks can preferentially route runoff to shallow groundwater or to the stream channel in riparian zones (Pearce et al. 1986; McDonnell 1990; Heathwaite 1997; Simard et al. 2000).

Hillslope hydrology is fundamental to P transfer on the landscape (Dougherty et al. 2004). The merging of hillslope hydrology and P source factors is the underlying basis for the P *critical source area* (CSA) concept which focuses on areas of high soil P or frequent manure application with areas having high surface runoff and erosion potentials (Sharpley and Tunney 1998; Dougherty et al. 2004). Gburek and Heald (1974) were among initial authors to propose a P CSA concept. The authors hypothesized that near-stream *partial areas* (i.e. variable source areas) (Betson 1964; Hewlett and Hibbert 1967; Ragan 1967; Dunne and Black 1970a,b) were direct sources of P and among the major P factors for P export by a stream. (A discussion of VSA hydrology is provided in Section 2.1.) Variable source areas may be important for transferring P to streams via both surface runoff and groundwater pathways (Gburek and Sharpley 1998). The CSA concept has been further developed through different studies including Pionke et al. (1988, 1996, 2000), Gburek and Sharpley (1998), Gburek et al. (2000), and others. Further, the need to identify CSAs has become an accepted component of assessing agricultural areas for P export risk (Heathwaite et al. 2000; Heckrath et al. 2008). Studies have explored a variety of innovative methods in attempts to identify CSAs. Methods have included use of runoff collector rings (Pionke et al. 1988), saturation sensors (Zollweg 1996; Gburek and Sharpley 1998; Srinivasan et al. 2000; Leh et al. 2008), analysis of soil P spatial variability (Page et al. 2005), and modeling (Lyon et al. 2006). A recurrent theme of some of these studies has been difficulty in identifying runoff-generating mechanisms.

2.2.7 Influence of streambed, streambank, and pond sediments on in-stream P transfer

The concentrations and forms of P at the edge-of-field may change once delivered to the receiving stream. Stream banks are potential sources of particulate P depending on bank erodibility and the P concentration of bank materials. In a 2-year study of bank erosion in 15 rural 1st and 2nd order streams, Laubel et al. (2003) found that bank erosion rates were significantly related to bank angle, vegetation cover, and overhang and estimated stream power. Smaller erosion rates were observed in streams with riparian woodland and where cattle were fenced off. Bank erosion accounted for 15 to 40% of total P exports. Bank fencing was in place. McDowell and Wilcock (2007) measured loads of suspended sediment (SS) and P loads in a low gradient (2,100 ha) dairying watershed and used ^{137}Cs to identify sources of sediment and P in bank and bed materials. Total P and SS concentrations were linearly related ($R^2 = 0.44$; P <

0.05) but DRP and SS were not related, possibly due to different sources of DRP relative to particulate and organic P sources. Streambed sediment may function as a P source or sink depending on the sediment's equilibrium P concentration (sediment-EPC), which is a concentration that may maintain zero net P sorption or desorption with the ambient water P concentration (Taylor and Kunishi 1971; McDowell and Sharpley 2003). The sediment-EPC can be a function of the biotic processes or fine particle fraction in sediment (Haggard et al. 2004). Haggard et al. (2004) found that sediment-EPCs increased downstream of a wastewater treatment plant. In a study a laboratory mesocosm study on P release from riparian wetland sediments, Surridge et al. (2007) reported that reductive release of P from P-bearing Fe-oxides was identified as potential P source under anaerobic sediment conditions. The sediment represented a transient pool of stored P that could release P back to the stream when WWTP P discharges were reduced. Resuspension of bed materials may also contribute P to a stream (Sharpley and Syers 1979).

Sediment in small ponds draining agricultural or other watersheds may regulate ambient water P concentration in ways similar to large lakes and reservoirs (i.e. Parker 2004). Masuda and Boyd (1994) quantified P fractions in sediments at different depths in a 22-year-old, 400 m^2 experimental fish-feeding pond in Alabama. As a function of sediment depth, TP concentration increased, sorption capacity decreased, and desorption capacity increased. Overall sorption sites were about 50% saturated with P. Dissolved reactive P accounted for 37% of TP in sediments, but only 7% in ambient water. Ruan and Gilkes (2000) investigated P accumulation in water and sediments in 50 dams and farm ponds downstream of agricultural (grazing, cropping, and pasture) watersheds in Australia. Clay materials in sediments and soils were mainly kaolinitic with Al and Fe. Concentrations of TP in pond water and sediments varied by two and by at least three orders of magnitude, respectively. Sediment TP was generally higher than soil TP. Overall, there was a substantial degree of scatter in the results presented. Log-transformations were required to demonstrate significant ($R^2 = 0.32$, $P = 0.001$) linear relationships between different P forms in sediments and dissolved P in pond water.

2.2.8 Previous phosphorus yield estimates for poultry litter-amended pasture sites

Seven field-scale studies (Table 1) were found in the literature that reported edge-of-field P yield estimates for pastures fertilized with poultry manure or litter. No comparable watershed-scale studies were found in the literature. The field-scale studies took place on ephemeral (0.45 - 8.0 ha) experimental (n=5) or commercial (n=2) pastures. All studies required use of earthen berms or other structures to isolate and concentrate runoff to monitoring equipment used for flow measurement and water quality sampling. All runoff was generated by natural rainfall. The studies as a whole represent unique manure application rates, field characteristics including presence of grazing, soil test P concentrations, and climate conditions. With the exception of climate, site characteristics (i.e. soils, vegetation, coverage of manure application) in each study were assumed to be fairly uniform. It is important to note that the results shown in Table 1 represent the *normal* manure application treatments reported by those studies. Any results from experimental manure treatments, such as use of composted (Vervoort et al. 1998) or alum-treated (Moore et al 2000) litter, are not shown in Table 1.

Because of differences among the field-scale studies' objectives and other constraints, there are limitations to any interstudy comparisons that might be made. As shown in Table 1, not all studies reported the same types of results. Methods used for water quality sampling and analysis plus load calculations differed. In addition, methods used to estimate manure P application rates including analysis of P concentration differed or at least were not explained. In some studies it was not clear whether the P yield estimate was based on DRP or TP (or TKP). Across all studies and within several studies, runoff P concentrations and P yields differed by one order of magnitude (0.4 – 17.8 kg-P ha^{-1}).

2.2.10 Methods of assessing risk for phosphorus loss

Assessing a field, farm, or watershed for its potential risk of P loss is an important aspect of mitigating delivery to downstream waterbodies and prioritizing use of best management practices (BMPs) (Page et al. 2005). Areas of P risk-based research have encompassed different methodologies and scales. Methodologies have included soil P testing, indexing methods, simulation modeling and other methods. The primary objective for risk-based soil P testing is to identify critical levels of soil P that correlate with P concentrations in runoff that represent water quality risk (Sharpley and Tunney 2000; Sims et al. 2000). Research on soil P testing has included experimenting with different agronomic and environmental sampling and laboratory extraction (or desorption) methods (Sharpley et al. 2000; Sims et al. 2000; Torbert et al. 2002; Nair et al. 2004; Vadas et al. 2005). Indexing tools combine soil P test data with other factors important for controlling P loss. In the U.S, the Phosphorus Index (P-Index) (Lemunyon and Gilbert 1993; Sharpley 1995) is a federally-recognized risk-based nutrient management planning tool used by agencies and farmers. The P-Index integrates P source (soil, fertilizer, and manure) and transport (erosion, overland flow, subsurface flow) factors into identifying and ranking fields for potential P loss (Sharpley et al. 2008b). Nearly all states use the P-Index either directly or with state-specific modifications (Osmond et al. 2006). The Georgia P-Index method is described by Cabrera et al. (2002). Evolving P-Index research has included incorporation of poultry manure characteristics into the source factors (DeLaune et al. 2004a) and hydrologic return period (Gburek et al. 2000) into the transport factor. Sharpley (2007) categorized simulation models as 1) process-based models (i.e. Soil and Water Assessment Tool (SWAT) (Chaubey et al. 2007) and Hydrologic Simulation Program-Fortran (HSPF) (Radcliffe and Lin 2007); 2) export coefficient models (i.e. Beaulac and Reckhow 1982); and 3) statistical or empirical models (i.e. Kronvang et al. 2003; Andersen et al. 2005). Radcliffe and Cabrera (2007) identify future directions for P modeling research including modeling of runoff-generation areas, soil P pools, and in-stream processes.

Recently, other studies have experimented with P risk assessment tools. Schärer et al. (2005) used simple fuzzy decision trees (i.e. expert system modeling) to predict annual P exports for eleven agricultural watersheds (1.7 – 27.8 km^2) in Switzerland. The decision trees used four input parameters; annual rainfall, agricultural land use, soil P and a baseflow index. Estimates were within the range of estimates from regression models. The results suggested that single events were important for exports of particulate P. In a different study, Page et al. (2005) investigated the potential of using watershed topography (Beven and Kirkby 1979) combined with spatial data on different soil P metrics to identify *a priori* P CSAs in two headwater (22 and 48 ha) agricultural watersheds in the UK. Due to difficulties that were related to how their methodology fit with the spatial scale of the study watersheds, the authors proposed using other *integrated* indicators of soil P status such as baseflow and streambed sediment P concentrations.

2.1.11 Synopsis and implications

Eutrophication of freshwater and estuarine systems is linked to how P is managed on the land surface. Reduction of P loadings to mitigate eutrophication impacts in Georgia Piedmont reservoirs may also need to consider how iron and organic matter loadings are also reduced (Parker 2004). Forested watersheds in the southern Appalachians are highly conservative with respect to P. Forest floors appear to be sinks for inorganic P and sources of organic P to the mineral horizon (Qualls et al. 1991). An important mechanism for P loss from forested watersheds may be short-circuiting of soil horizons and root networks via macropores or other preferential pathways (Qualls and Haines 1991; Qualls 2000).

The poultry production region of north Georgia is among the leading production regions of the U.S. Long-term application of poultry manure to satisfy nitrogen demands of pasture and other crops can result in the accumulation of soil P beyond agronomic needs. The soil P tends to accumulate in the near-surface soil horizons. Surface runoff of P is the primary hydrologic transfer pathway. Accumulation of soil P is highly correlative with P concentration in runoff. During a storm event, the relative loss of soil P in runoff to a stream may be outweighed by incidental P losses from freshly-applied poultry manure or litter. Streambed and bank material can constitute a large source of P to a stream as well.

Numerous P source and hydrologic transport factors ultimately control how P is transferred within agricultural watersheds. Risk-based environmental P management in agricultural watersheds is now focusing on identification of P critical source areas where P source areas are co-located with runoff-generation areas such as VSAs. Page et al. (2005) reported difficulty in identifying P CSAs within two small commercial agricultural watersheds. From a risk-based perspective, the authors recommended baseflow and streambed P as potential P risk indicators for agricultural watersheds.

No studies were identified in the literature that reported P loading or yield estimates for small, commercial agricultural watersheds where poultry operations are predominant. However, seven field-scale studies were identified (Table 1). Two studies were performed on commercial poultry farms and the remaining five were performed at non-commercial, experimental research sites. The soil, hydrologic, and land and manure management parameters of the studies are assumed to represent the variability of the conditions and manure management practices held on many commercial farms. Findings from the field-scale studies shown in Table 1 plus the many plot-scale studies in the literature suggest that runoff P concentrations and yields exhibit order-of-magnitude variability and that variability is highly time-dependent. This implies that P in streamflow exhibits similar levels of variability. That variability may be accentuated or dampened by the influence of watershed-scale P source (i.e. watershed soil P variability, proximity to stream, streambed P) and transport (variations in topography and land cover) factors.

2.3 Load Estimation

Estimation of a pollutant or constituent load is a routine activity of many hydrologists and surface water quality managers today. Loading integrates the hydrologic and biogeochemical transfer processes of a constituent within a watershed and in a stream specifically (Semkin et al. 1994; Aulenbach and Hooper 2006). Load estimation is fundamental to watershed mass balance studies (Semkin et al. 1994), total maximum daily load (TMDL) development (Whiting 2006), and detection of loading rate trends (Kronvang and Bruhn 1996). It is also a means for developing land use-based export coefficients (Beaulac and Reckhow 1982) and calibrating or verifying streamwater loads predicted by different types of watershed models (Smith et al. 1997).

In the water quality field of hydrology, the term *load* refers to the mass flux of a constituent transported past the cross-sectional area of a stream location. Mass flux comprises both advective and diffusive fluxes that are mathematically represented in two terms, respectively, in Equation 1:

$$J_x = u_x C - D_m \frac{\partial C}{\partial x} \qquad (1)$$

where:

J_x = one-dimensional mass flux in x-direction (M L^{-2} T^{-1})

u_x = velocity (L T^{-1})

C = concentration (M L^{-3})

D_m = molecular diffusion coefficient (from Fick's First Law) (M L^{-2} T^{-1})

x = length (L)

Accounting for conservation of mass, hydrodynamic dispersion and negating sources or sinks, Equation 1 above can be derived to form the one-dimensional advection-dispersion or mass transport equation for a conservative constituent (Fischer et al. 1979; Martin and McCutcheon 1999):

$$\frac{\partial \overline{C}}{\partial t} + \overline{u}\frac{\partial \overline{C}}{\partial x} = D_x \frac{\partial^2 \overline{C}}{\partial x^2} \qquad (2)$$

where:

D_x dispersion coefficient (M L^{-2} T^{-1})

$\overline{C}$ mean concentration (M L^{-3})

$\overline{u}$ mean velocity (L T^{-1})

The dispersion coefficient D_x, defined below, represents both advective and molecular diffusion.

$$D_x = D_m + \alpha_x \overline{u_x} \qquad (3)$$

where:

α_x dispersivity (L)

Conventional representation of a loading rate integrates continuous traces of both flow and a constituent's concentration:

$$L(t) = \int Q(t)C(t)dt \qquad (4)$$

where:

L = loading rate ($M\ T^{-1}$)

Q = streamflow ($L^3\ T^{-1}$)

C = constituent concentration ($M\ L^{-3}$)

The term *yield* represents a loading rate that is normalized by the contributing watershed drainage area of the stream location where the estimate is applied. Note that consistent units are required for use of the equation above as well as other equations shown in this section.

Equation 4 implies that continuous flow and concentration measurements are required to obtain the most accurate load estimates. Typically, concentration measurement limits accurate load estimation as the costs of continuous sample collection can be high relative to the costs of continuous streamflow measurement. When continuous concentration measurement is not performed, an error is likely to be introduced into the resulting load estimate (Walling and Webb 1985). The magnitude of the error depends, in part, on how the data generated from a sampling program represents the true hydrochemical behavior of the analyte in the basin of interest (Johnes 2007). Stream chemistry naturally changes with time in response to seasonal fluctuations or long-term trends such as climate or land use change (Cooper 2004).

Load estimation has been a research focus for decades (see references identified by Walling 1977; Cohn et al. 1992; Cooper and Watts 2002; Horowitz 2003). A common objective of much load-estimation research is to identify methods that bridge sampling and streamflow measurement frequencies with the appropriate mathematics, or load estimators, in order to estimate a load with an acceptable level of uncertainty. This has been the basis for numerous studies (i.e. Richards and Holloway 1987; Rekolainen et al. 1991; Kronvang and Bruhn 1996; Schleppi et al. 2006) that have compared the use of different estimators with data collected at different frequencies. Preston et al. (1989) tested sampling strategies with different estimators and found that no class of estimators performed best for all strategies. Richards and Holloway (1987) used Monte Carlo methods to evaluate errors of different sampling strategies on phosphorus load estimates in Great Lakes tributaries. Sampling frequency and pattern, load estimation method, watershed size, and flow-concentration relationships were influential on the resulting estimation error. Further, interactions among those factors were also possible. In small watersheds where concentration exhibits large or rapid changes during stormflow conditions, subdaily sampling frequencies may be necessary to maintain errors at acceptable levels. Automated sampling equipment (autosamplers) can provide critical support to programs requiring sample collection at small time intervals (e.g. Walling 1977; Rekolainen et al. 1991; Horowitz 1995, Harmel et al. 2003, 2006a; King et al. 2005).

2.3.1 Estimator types

Past authors have assigned different classes and naming conventions to distinguish among load estimator types. Thomas (1985) distinguished between statistical and non-statistical techniques which depend on whether or not the sampling probabilities are known. Preston et al. (1989) describes three classes—averaging, regression models, and ratio estimators. Cohn (1995) reviewed three methods and different modifications for each. The methods included estimating a continuous concentration trace (i.e. rating curves), direct estimation, and other methods. Phillips et al. (1999) distinguished between extrapolation- and interpolation-based procedures—both of which largely overlapped with the classes of Preston et al. (1989) and Cohn (1995). Schwartz and Naimann (1999) distinguished between planning-level and riverine estimators. Aulenbach and Hooper (2006) described four estimator classes—averaging, period-weighted approaches, regression-model (or rating curve methods), and ratio estimators. This review describes three (regression, direct estimation, and planning level) of the above estimators without partiality to any particular set of estimator. Regression estimators are emphasized because they are among the more commonly-used estimators when a continuous streamflow time-series is available.

2.3.1.1 Regression models

Regression models and rating curves for load estimation purposes are fairly synonymous and are among the most common load estimators studied (i.e. Walling 1977; Johnson 1979; Dolan et al. 1981; Crawford 1991; Kronvang and Bruhn 1996; Haggard et al. 2003). These estimators typically use ordinary least squares (OLS) to predict concentration or load as a function of streamflow (Ferguson 1986a, 1987; Koch and Smillie 1986a). Other independent variables such as time of year may also be used (Cohn 1989). Reasons for the popularity of regression models are their convenience (Cohn et al. 1992) and that they are appropriate for use with *opportunistic* (Cooper and Watts 2002), mixed-frequency, or non-probability-based data. A potential problem with regression models, however, involves the logarithmic transformation of the model data (i.e. dependent and independent variables) that is typically required to linearize the model data and stabilize residual error variance (Crawford 1991). A simple linear form of this model (adapted from Cohn 1995) is shown in Equation 5.

$$\ln L(t) = \beta_0 + \beta_1 \cdot \ln Q(t) + \varepsilon \qquad (5)$$

where:

β_0, β_1 are model coefficients representing intercept and slope, respectively,

L(t) is observed instantaneous load (M T^{-1}). Note that concentration (C) can be used in place of load (L).

Q(t) is observed instantaneous flow (L^3 T^{-1}).

ε is model residual error. Error is assumed to be random and independent and identically distributed (IID) normal with a mean of zero and constant variance.

Past authors have included additional terms on the right side of Equation 5. Cohn et al. (1992) developed a seven-parameter log-linear model that included a flow-squared term, two time terms, and sine and cosine terms to represent seasonal fluctuations. Hysteresis terms can be included in the model. Separate models can also be developed for rising vs. falling hydrograph limbs. In addition, separate models may be used to represent different magnitudes of flow (Glysson 1987).

When model fitting is complete, load estimation using the fitted model requires back-transformation, or exponentiation, of model predictions to arithmetic space:

$$L_{\exp}(t) = \exp\left[\beta_0 + \beta_1 \cdot \ln Q(t)\right] \qquad (6)$$

where:

L_{exp} represents L in arithmetic space after back-transformation from log space.

Application of the back-transformed model (Equation 6) to predict the loading rate as a function of flow (Q) at a specific time (t) results in the prediction of the geometric mean or median loading rate and not the mean loading rate and hence, the loading rate is biased low assuming the distribution of observed data in arithmetic space exhibits positive skew (Miller 1984; Thomas 1985; Ferguson 1986a,b; Koch and Smillie 1986a,b; Hirsch et al. 1993; Cohn et al. 1989; Cohn 1995). The magnitude of the underestimation is related to the variance of the residuals and can be at least 50% (Miller 1984; Ferguson 1986a, 1987; Koch and Smillie 1986a; Cohn et al. 1992). Crawford (1991) provides an in-depth discussion of the bias and reviews other model approaches involving maximum likelihood estimation and non-linear models as alternatives to OLS. It is important to note that the bias discussed here is specific to the modeling component of load estimation using log-transformed regression models. That bias does not represent biases incurred from other sources such as through water quality sampling.

Three different methods, or bias-correction factors (BCFs), have been used to eliminate the back-transformation bias described above. Thomas (1985), Ferguson (1986a,b), and Koch and Smillie (1986a,b), described what Cohn et al. (1989) termed the Quasi Maximum Likelihood Estimator (QMLE). Using the concepts that 1) the back-transformed residuals are lognormally distributed and 2) the bias is dependent on the residual standard deviation (s_ε), the bias and associated correction factor are represented by $\exp(s_\varepsilon^2\ 2^{-1})$. The QMLE model form is:

$$L_{qmle}(t) \equiv \exp\left[\beta_0 + \beta_1 \cdot \ln Q(t) + \frac{s_\varepsilon^{\ 2}}{2}\right] \tag{7}$$

where:

L_{qmle} represents L in arithmetic-space with the QMLE correction factor applied

$\frac{s_\varepsilon^2}{2}$ QMLE correction factor

Use of L_{qmle} assumes that 1) the log-log regression model is linear, 2) residuals in LN-space are normally-distributed, 3) residuals have equal variance for all LN-transformed streamflows, and 4) the model data represent a random sample of all possible data points (Ferguson 1986b).

The second BCF is the non-parametric *smearing* method that Thomas (1985) and Koch and Smillie (1986a) adapted from Duan (1983):

$$L_{sm}(t) = \exp[\beta_0 + \beta_1 \cdot \ln Q(t)] \cdot (\frac{1}{N} \cdot \sum_{i=1}^{N} \exp e_i) \tag{8}$$

where:

L_{sm} represents L in arithmetic-space with the smearing correction factor applied

N number of pairs of measured instantaneous flow and load used in model calibration

ε_i model residual associated with i^{th} observed flow and load pair.

While use of L_{sm} does not assume normally-distributed residuals, it still assumes that assumptions 1, 3, and 4 listed above are satisfied (Ferguson 1986b).

The third BCF, the Minimum Variance Unbiased Estimator (MVUE) (Cohn et al. 1989), represents the minimum variance unbiased estimator when the assumed log-linear model is appropriate (Cohn 1995). A motivation for the MVUE was that, while the L_{qmle} and L_{sm} may yield acceptable results for many applications, the two estimators do not entirely remove bias and can even overestimate loads by a large margin (Cohn et al. 1989). As an unbiased alternative, the authors presented the Minimum Variance Unbiased Estimator (MVUE):

$$L_{mvue} = L_{\exp} \cdot g_m \left[\frac{m+1}{2m} (1 - V) s_\varepsilon^{\ 2} \right] \tag{9}$$

where:

g_m is a Bessel function (2nd order ordinary differential equation) the authors derived

m is the number of data pairs used in model calibration minus the number of model parameters

V is a function of explanatory variables (Runkel et al. 2004)

The MVUE follows previous work by Bradu and Mundlak (1970). Crawford (1991) provided a short review of the MVUE and noted that, instead of generating a single value as the BCF, it generates individual corrections for each observation. The MVUE can be run with a FORTRAN computer program. It is also the BCF used in the LOADEST program developed by Runkel et al. (2004) and supported by the USGS (http://water.usgs.gov/software/loadest).

Cohn et al (1989) compared the performance of the L_{mvue} with L_{exp} and L_{qmle} using sets of generated model data. Cohn et al. (1989) concluded that both L_{exp} and L_{qmle} can provide adequate results for a number of conditions. Exceptions were in the case of small sample sizes or estimating loads for high-flow periods. Cohn (1995) stated that the L_{qmle}, L_{sm}, and L_{mvue}

provide similar estimates if 1) the log-linear model is approximately correct, 2) at least 30 pairs of data are used for model calibration, and 3) and the model is not used to estimate loads for flow ranges in which there are no observed data.

A problem for log-linear regression estimators is estimating the precision of the load estimate. Cohn (1995) noted that this procedure is not simple and refers to the mathematical models of Gilroy et al. (1990) for computing both bias and precision to arrive at the mean square error (MSE) for all four regression estimators described above. The derivation of those methods is not straightforward. The probabilistic sampling methods of Thomas (1985; 1988a, b) and Thomas and Lewis (1993, 1995) facilitate confidence interval estimation but their methods require external dataloggers to control autosamplers. The results of Ferguson (1987) suggest approximate confidence intervals can be estimated using sample size, residual scatter and regression model slope but, from review of that study, the method is not readily apparent (Ferguson 1986b). Preston et al. (1989) defined precision of the estimators they tested as the inverse of the standard error of the load estimate. They summed the normalized square of the precision value with the normalized bias squared to arrive at a normalized MSE used to compare results of different estimators. Robertson and Roerish (1999) used the normalized MSE described by Preston et al. (1989) plus standard errors, median absolute errors, and average absolute errors to compare loads estimated via different sampling strategies.

Another problem of using log-linear regression methods is autocorrelation of model residuals. Regression models based on time series of data are commonly positively correlated as residuals as consecutive observations typically have the same sign (Mendenhall and Sincich 2003). When sampling frequency is relatively high and observations are closely spaced in time, autocorrelation is almost guaranteed (Helsel and Hirsch 2002). When autocorrelation is present, regression coefficients remain unbiased, but their variance is underestimated plus confidence and prediction intervals are incorrectly spaced too close together (Helsel and Hirsch 2002). Cohn et al. (1992) stated that load estimators based on log-linear models appear to be *relatively insensitive* to such conditions.

Numerous studies have evaluated the performance of two, three, or all four regression estimators by comparing the respective load estimates with a *true* observed load. Walling (1977) and Ferguson (1986b) noted that factors such as sampling error may outweigh the bias and that use of LN-transformed models may still ultimately result in overprediction or further underprediction of loads. Thomas (1985) criticized the L_{qmle} and L_{sm} methods as being inadequate remedies to underestimation bias and noted that they do not account for other biases, such as outliers, or poor model specification. Walling and Webb (1985) reviewed a small number of studies in which use of L_{qmle} and L_{sm} failed to improve load estimates relative to the uncorrected model. In their own study, they found that the QMLE and smearing BCFs did not improve the reliability (accuracy and precision) of sediment load estimates over the uncorrected (i.e. L_{exp}) model compared to actual loads. Further, the uncorrected model did not produce reliable estimates. Notable explanations included scatter resulting from lack of coincidence in high sediment concentrations with high stormflows, exhaustion and hysteresis effects, and overall difficulty in representing how the majority of sediment loading (~75%) was delivered by the most infrequent (<5%) streamflows. Preston et al. (1989) found that the bias and precision of the L_{qmle}, L_{mvue}, and a robust regression estimator they tested were inconsistent. Performance depended on the analyte and the strength of the flow-concentration relationship. None of the regression estimators were superior to the other (averaging, ratio) estimators that were evaluated. Results of Phillips et al. (1999) suggested that the accuracy and precision of the L_{exp}, L_{qmle}, and

L_{sm} estimators they tested were inversely related to basin size. Guo et al. (2002) found that estimates from L_{exp} plus a simple ratio estimator and flow-weighted averaging estimator exhibited lower bias and root mean square error compared to L_{sm} and L_{mvue} for the sampling frequencies and monitoring period durations they tested.

2.3.1.2 Direct estimation

Direct estimation involves summing a set of weighted instantaneous loads (Cohn 1995) or load estimates that correspond to different time periods or different flow intervals. Of the direct estimation methods identified in the literature, all require use of a continuous record of streamflow. Time- or *period-weighting* might be used when sampling data are collected uniformly or randomly in time (Cohn 1995). One approach to period-weighting (i.e. Likens et al. 1977; Dann et al. 1986) is to establish a series of regular or irregular time intervals (i.e. days, weeks, etc.) within a study period of interest, multiply the mean concentration of all samples collected within each interval by the total flow volume for that interval, and then sum all individual products (loads) to arrive at a total load. Another period-weighting approach (i.e. Tonderski et al. 1995; Larson et al. 1995) has been to estimate concentrations for non-sampling periods by linearly interpolating between a time series of observed concentrations. Total load is calculated by summing the individual loads representing the combination of interpolated and observed concentrations and their respective flows.

Flow-weighting is another type of direct estimation method. It is similar to the first period-weighting approach described above except that the proportion of time that streamflow occurred within each interval must be incorporated into the calculations. As an alternative to least-squares regression, Verhoff et al. (1980) described a flow-duration rating curve (FDRC) that was used to estimate total phosphorus (TP) loads in tributaries to Lake Erie. Flow intervals were established by dividing the range between the minimum and maximum flow rates into a set of equally-spaced flow intervals. An average loading rate was calculated by summing the products of the mean load for each interval by the percent of time that flow occurred within that interval. A total load was then calculated by multiplying the average loading rate by the number of days for the period of interest. Verhoff et al. (1980) described a method for calculating a confidence interval to accompany the average and total loads. Cohn (1995) derived the FDRC calculations of Verhoff et al. (1980) and described it as a *stratified sampling* method. Flow-weighting methods may be advantageous when flows vary significantly over time or when concentrations within a flow interval are highly correlated (Dann et al. 1986; Semkin et al. 1994). Of five estimators compared by Walling and Webb (1985), the Verhoff FDRC method closely approximated a true load, but it also had a low degree of precision.

2.3.1.3 Planning-level estimators

Planning-level estimators are different than the other estimators reviewed here in that they represent a generalized approach to load estimation that does not require consideration of sampling characteristics (i.e. frequency) or relationships between streamflow and concentration (Schwartz and Naimann 1999). The calculation involved in planning-level estimation is multiplying a cumulative flow volume by a single, characteristic concentration (Schwartz and Naimann 1999). Characteristic concentrations may include the mean, median, or geometric mean of a concentration data set. Schwartz and Naimann (1999) showed how the mean, median, and geometric mean can all result in biased mean annual loads. In contrast, Rasmussen (2001) (unpublished manuscript) showed how using geometric averages of concentrations and flows can result in unbiased load estimates.

2.3.2 Small watershed studies

Few studies have investigated load estimators, sampling strategies, and associated estimation errors with data from very small (<1000 ha) to headwater (<50 ha) streams. Rekolainen et al. (1991) evaluated the accuracy and precision offour averaging estimators and one ratio estimator with phosphorus data collected from two (564 and 1540 ha) agricultural watersheds. The lowest overall errors resulted from the combination of averaging estimators with mixed-frequency data comprising flow-proportional data from peak flows in conjunction with regular (systematic) intervals. Dann et al. (1986) compared seven methods representing variations of regression, period-weighting (direct estimation), and averaging to estimate sulfate loads in a 123-ha forested watershed. A period-weighted approach resulted in the best load estimates. Aulenbach and Hooper (2006) presented the *composite method* which combined a hyperbolic regression model that used non-transformed data with a period-weighted approach. The authors applied their method to a stream draining a forested, 41-ha watershed and tested different subsampling scenarios from a multi-frequency data set for estimating alkalinity and chloride loads. Overall, estimation errors depended on sampling design, and in particular the degree to which large storms were sampled, patterns in regression model residuals, and the estimation time interval. Toor et al. (2008) tested four low-frequency sampling strategies with a regression model to estimate nutrient and sediment loads in an ephemeral stream. The authors expressed caution in using regression methods with low-frequency data to estimate short term (≤ 1-year) loads in small watersheds. Reasonably accurate load estimates were possible, however, with multiple (~three) years of low-frequency data. Intensive autosampling was recommended for short-duration studies requiring intensive sampling.

2.3.3 Synthesis and implications

From the studies reviewed here that compared estimator performance across a full range of basin sizes, it is apparent that there are no perfect sampling/estimator combinations. Performance depends on the analyte, sampling interval, monitoring period, and the basin specifically. For phosphorus load estimation in particular, Johnes (2007) concluded that further research is necessary in watersheds with significant quickflow hydrologic response, such as in certain headwater watersheds that can exhibit times of concentration on the order of minutes. Sampling and load estimation is further complicated by flow-concentration (Q-C) hysteresis during storm events or temporal modifications in Q-C relationships during different seasons or due to land management changes. If large percentages of loading occur during stormflow conditions, intensive sampling using automated samplers (autosamplers) may be required. Automated sampling equipment (autosamplers) can provide critical support to programs requiring sample collection at small time intervals (e.g. Walling 1977; Rekolainen et al. 1991; Horowitz 1995, Harmel et al. 2003; King et al. 2005).

CHAPTER 3.0

METHODS AND MATERIALS

3.1 Upper Etowah River basin description

3.1.1 Ecoregion

The upper Etowah River basin (Figure 2) is located in north Georgia at the southern end of the Southern Appalachian Mountains. It is positioned within the Blue Ridge and Piedmont Level III ecoregions (Omernik 1987). The corresponding Level IV ecoregions are the Southern Metasedimentary Mountains and Southern Inner Piedmont.

3.1.2 Hydrography, climate, and geology

The Etowah River (hydrologic unit 03150104) originates in the foothills of the Southern Appalachian Mountains (Figure 2). As it flows out of the Appalachians, it flows in a south-to-westerly direction through the Georgia Piedmont. At the Etowah River's confluence with the Oostanaula River in northwest Georgia, it forms the Coosa River before flowing into Alabama. The Coosa River is part of the larger Alabama River system which joins the Tombigbee River to form the Mobile River before emptying into the Gulf of Mexico. Within Georgia, the Etowah River is impounded by Lake Allatoona, a reservoir northwest of Atlanta and managed by the U.S. Army Corps of Engineers (USACE) for flood control, hydropower, water supply, water quality, recreation, and fish and wildlife management (information available from the USACE at http://allatoona.sam.usace.army.mil; last accessed September 27, 2008). The designated uses for water quality of the Etowah River and Lake Allatoona are drinking water and recreation (Georgia Environmental Protection Division 1998). For this study, the upper Etowah River basin constitutes the drainage area (1,588 square kilometers) above Lake Allatoona at Canton near the inflow to Lake Allatoona (Figure 2).

From water years 1897 to 2007, mean annual flow of the Etowah River at Canton (U.S. Geological Survey (USGS) Site Number 2392000) ranged between 14.4 and 56.0 cubic meters per second ($m^3 s^{-1}$) (information available from USGS at http://waterdata.usgs.gov; last accessed June 5, 2008). The long-term mean discharge is 34.2 $m^3 s^{-1}$. Between 1941 and 1970, mean annual unit-area runoff of the upper Etowah basin ranged approximately between 0.0142 and 0.0283 $m^3 s^{-1}$ per square kilometer (km^2) (or 0.142 and 0.283 liters per second per hectare ($L s^{-1} ha^{-1}$) with higher runoff at the top of the basin decreasing to lower runoff downriver (USGS 1982).

The climate of the Georgia Mountain and Piedmont regions is humid and temperate. Overall, temperatures vary between cool winters and warm-to-hot summers (Georgia State Climate Office 1998a, b). The average annual temperatures of the Georgia Mountain region range between 10 and 16 degrees Celsius (ºC) (Georgia State Climate Office 1998a). The average annual temperature of the Piedmont region is 32 ºC (Georgia State Climate Office 1998b). Monthly precipitation within each region is fairly consistent with the exception of drier months tending to occur late summer through early fall (Georgia State Climate Office 1998a, b). Mean annual precipitation of five weather stations operated through the Georgia Automated Environmental Monitoring Network (GAEMN) (http://www.griffin.uga.edu/aemn; see Alpharetta, Dahlonega, Ellijay, Gainesville, and Rome) that surround the upper Etowah basin ranges between 1400-1650 mm yr^{-1}. Precipitation is typically higher within the Etowah's headwater region due to orographic effects associated with differences in elevation between its headwaters (~ 640 m above mean sea level (msl)) and the lower basin (258 m msl at Canton).

The geologic parent material of the upper Etowah basin is metamorphic (Georgia Geologic Survey 1976, U.S. Environmental Protection Agency 2007). Rocks are Blue Ridge and Piedmont crystalline types that are predominantly mica schist and intermediate gneiss with biotite, quartzite, and amphibolite. The surficial geology is Quarternary to Tertiary.

Soil surveys of the counties encompassing the Etowah basin were performed by McIntyre (1972) and Jordan et al. (1973). Soils are described as acidic, highly weathered, well-drained, and having textures ranging from sandy loam to clay. Ultisols (Udults) are the predominant soil order present.

3.1.2 Land management

The upper Etowah River basin is shared by Cherokee, Dawson, Lumpkin, and Pickens counties. Principal towns include Ball Ground, Dahlonega, and Dawsonville. The majority of the land cover in the basin is forested, however some portions of the basin are rapidly urbanizing. Lin et al. (2007) estimated that in 2001 the basin was 77% forest, 13% pasture, 9% urban, and less than 1% row crop. The urban land cover percentage reflected a 302% increase since 1992.

Poultry-based agriculture has been practiced in Dawson and Lumpkin (and presumably Cherokee and Pickens) Counties since the 1940s (McIntyre 1972). In 1997 and 2002, there were 275 and 239 poultry farms, respectively, in the four counties that encompass the upper Etowah basin (USDA 2004). In 2002, 239 poultry farms within the four counties around the Etowah basin sold 14,057,005 broilers and layers combined. Of the total sold, 97.3 percent were broilers (USDA 2004). Of all 159 Georgia counties, the four counties within the Etowah Basin ranked between 14th and 24th in number of broilers sold in 2004.

3.1.6 Aquatic life

Aquatic life in the Etowah River basin is highly diverse (Burkhead et al. 1997; Etowah Aquatic Habitat Conservation Plan Steering Committee (HCPSC) 2007). It includes ten imperiled species that include three federally listed fishes. The amber darter (*Percina antesella*) and Etowah darter (*Etheostoma etowahae*) are listed as endangered. The Cherokee darter (*Etheostoma scotti*) is listed as threatened. The Etowah and Cherokee darters are endemic to the Etowah River. The Etowah Aquatic Habitat Conservation Plan (HCP) (HCPSC 2007) was developed to meet requirements of the federal Endangered Species Act for the protection of the listed fishes and other imperiled aquatic life in the Etowah River basin (HCPSC 2007). The HCP focuses on stressors associated with urbanization as other sources such as agriculture and forestry are declining in the Etowah River basin.

3.2 Study sites

Data were collected from twelve sites (Figure 2) for this study. All sites were located on headwater streams in the upper Etowah River basin. Three of the streams' watersheds were forested (FORS) and nine were agricultural (AG). Water quality conditions of the three forested (FORS) streams were assumed to represent reference hydrologic and water quality conditions for the upper Etowah basin.

Selection of study sites occurred in Fall 2004 and Winter 2005. Sites FORS-1, -2, and -3 were located in the Blue Ridge Wildlife Management Area of the Chattahoochee National Forest. Forest site selection was based on identification of first-order blue-line streams on USGS 7.5' quadrangle maps located within both the Chattahoochee National Forest and Etowah River basin area. Forest site selection emphasized two criteria: 1) road accessibility within 50 m of the site and 2) ability to install a primary (i.e. weir or flume) or secondary (culvert) flow control structure for flow measurement. All AG project sites (AG-4 through AG-12) were located on private land that was entirely managed for different commercial poultry (broiler) farm operations. Examples of the operations included poultry houses, pasture, roads, barns, stackhouses, farmer dwellings, and undeveloped land including small patches of forest. Sites AG-5 and AG-6 were located on adjacent streams draining areas of the same poultry farm. Selection of AG sites occurred through visits to commercial poultry farms in the upper Etowah basin and meetings with farm operators. The sites were selected in a similar manner as done by Edwards et al. (1996) in their study of commercially-operated agricultural watersheds. In addition, selection emphasized access and use of a primary flow control structure.

Physical characteristics of the site watersheds and streams are presented in Table 2. The data was obtained through manual measurements using ArcMap 9 Version 9.2 (ArcMap) (ESRI 2006) with digital raster graphics of USGS 7.5' topographic maps. Watershed and stream slopes were estimated by dividing their estimated flow path lengths by their respective ranges in elevation (McCuen 2005).

Ten of the twelve streams flowed perennially during the study. The stream at AG-4 flowed intermittently between July and September 2006. The drainage at AG-12 was ephemeral. Appendix A provides information on soil mapping units within the site watersheds. Ponds were located in the FORS-1, AG-9, and AG-11 watersheds (Tables 2 and 3). The three ponds had different percentages of surface area (4.1%, 6.5%, and 3.5%, respectively) and contributing drainage area (85.4%, 63.5, and 91.4%, respectively) relative to total watershed area. The watershed for site AG-4 also contained a pond, but the pond was not addressed in this study because its percentages of surface area and contributing drainage area relative to total watershed area were about 1% and 40%, respectively.

Estimates of land cover distribution for the study sites are provided in Table 3. Estimates of forested cover in FORS watersheds do not take into account stream channel corridor areas or small clearings for wildlife or from timber activities. The land cover percentages for AG watersheds were estimated through manual delineation using ArcMap with digital ortho quarter quad (DOQQ) satellite images collected in 1999. Aerial photographs available in Google Earth Version 4.3 (Google 2008) were used to supplement the DOQQs. In Table 3, for the AG watersheds, the "Forest" category refers to concentrated areas of arboral vegetation within either upland or riparian zones. "Pasture" includes grassed areas dedicated for livestock grazing or hay. Initially, the pasture at AG-7 was not grazed, however midway through the project, the farm owners at AG-7 cleared additional vegetation for a small number of horses to graze. Examples of "other vegetated" land cover include sparsely forested uplands and grassed areas surrounding various structures (i.e. barns and farmers' homes) located in some watersheds. "Impervious" areas include paved roads and rooftops on poultry houses and other structures. "Unpaved" areas include gravel and "dirt" roads plus fenced-in, unvegetated areas for livestock (i.e. horse or sheep pens).

The AG watersheds differed in terms of number of poultry houses and bird capacity (Table 4); poultry-litter management; presence, type and intensity of livestock grazing; and on-farm BMPs. A survey of approximately 30 questions was administered to all farm owners. The survey questions covered topics such as application rates and other management practices involving poultry litter, how bird mortality was handled, presence of cattle or other livestock, and if soil nutrient testing was performed. Information from the survey applied to the entire farm and not the site specifically. Farmers at sites AG-4 and AG-8 did not respond to the survey. Highlights from the survey are presented in Table 4. Information on livestock access to stream channels at all sites plus the number and type of livestock at AG-4, -7, -8, -9, and -11 was based on field observation.

3.3 Data collection

Sites were instrumented with hydrologic monitoring and automated sampling equipment between January and July 2005. Dismantling of sites occurred between October and December 2006. Data collection at project sites ranged between 18 and 22 months. The 15 months between July 1, 2005, and September 30, 2006, represents the data collection period common to all twelve sites.

3.3.1 Hydrologic monitoring

Eleven of the twelve project streams were instrumented with 0.610-m (or 2-foot) aluminum H-flumes (Brakensiek et al. 1979). The maximum flow capacity of a 0.610-m H-flume is 314 L s^{-1} (or 11.1 cubic feet per second (Grant and Dawson 2001). Figures 3 shows an upstream view of the H-flume installed at FORS-3. Figure 4 shows a top view of the H-flume at AG-7. The Manning equation was the basis for flow measurement in a piped road culvert at FORS-1. Plywood wingwalls were constructed at ephemeral AG-12 to direct runoff through the H-flume. In the cumulative uncertainty analysis by Harmel et al. (2006b), the authors cited Slade (2004) in using a ± 5-10 percent uncertainty for streamflow measurements using pre-calibrated flow control structures that use stage-discharge relationships and that are properly designed and installed.

Each site was equipped with one Teledyne Isco (ISCO) (http:\\www.isco.com) 24-bottle, 6700- or 6712-series autosampler (Figure 5) (ISCO 2007); one ISCO 720 submerged probe module for water level measurement; and one ISCO 674 rain gage (Figure 6). Autosamplers were stored in locked, wooden shelters located within 2-4 m of the H-flumes or culvert. The

ISCO 720 submerged probe functions as a vented pressure transducer. The probes have a level measurement accuracy ± of 0.008 and 0.012 m for vertical distances 0.01-1.52 and >1.52 m, respectively (ISCO 2005). The probes were placed in stilling wells attached to the H-flumes (Figures 3 and 6). At FORS-1, the probe was placed at the upstream end of the culvert. The ISCO 6700 and 6712 autosamplers, which have datalogging capacities, convert water level measurements to streamflow via pre-programmed stage-discharge relationships for H-flumes and other flow control structures. For flow measurement in a culvert pipe using the Manning equation, the sampler requires information on culvert pipe radius, slope, and the roughness coefficient. The ISCO 674 rain gage (Figure 6) has a 0.1-mm sensitivity and capacity of 38 centimeters per hour (cm hr^{-1}). Its accuracy is ± 1.5% at 5 cm hr^{-1} and 3.5-9% up to 13 cm hr^{-1}) (ISCO 2002). Rain gages were located between two and ten m of the autosamplers. Tree canopy partially covered rain gages at the three forested sites plus sites AG-6, AG-9, and AG-11.

Streamflow and rainfall data were recorded at five-minute intervals. All data stored by the ISCO 6712 autosamplers were retrieved at field sites using ISCO Rapid Transfer Devices. The data were uploaded to a personal computer and managed using ISCO Flowlink (versions 4.16 and 5) software.

Streamflow data editing was required for all sites. Most edits were to correct erroneously high streamflow due to sediment accumulation in H-flumes. Remaining edits were to estimate flow at sites where the data was missing due to battery failure or equipment damage. This was accomplished through use of double mass curve and linear regression methods in which streamflow relationships were generated using data collected from nearby project sites. Streamflow data were not estimated for sites with missing data on streams draining reservoirs.

Rainfall data were estimated for sites where rain gages were damaged, removed for repair, clogged by debris, or covered by leaves. Rainfall data estimation was required for all sites except AG-8 and AG-10. Estimation for individual sites was based on adaptation of rainfall data from nearby sites as well rain gages (Figure 2) operated by the Georgia Automated Environmental Monitoring Network (GAEMN) (http://www.griffin.uga.edu/aemn) and the USGS (http://ga.www.usgs.gov).

3.3.2 Water quality monitoring

3.3.2.1 Sampling program

The water quality sampling program adapted recommendations of Robertson and Roerish (1999) and Robertson (2003) for one-year and two or more year duration load estimation studies based on their own studies of small (14-110 km^2) streams. Conceptually, the program was similar to sampling strategy #4 investigated by Rekolainen et al. (1991). Water sampling occurred at a mixed-frequency consisting of biweekly grab (BWG) sampling coupled with stormflow sampling. The majority of BWG samples were collected during non-storm streamflow conditions. No BWG samples were collected at AG-12. The sample collection capabilities of the ISCO autosamplers were used solely for collection of stormflow samples.

During most of 2005, storm sampling varied between time- and flow-based approaches. By December 2005, a storm-sampling objective was established that was aimed at characterizing both the event-mean concentration (EMC) and intrastorm variation between concentration and flow over a storm hydrograph resulting from a one-year 24-hour rain event. The rain depth for an event of this magnitude in north-central Georgia ranges between 7.6 and 8.9 cm (Hershfield 1961).

To fulfill the above objective, two-part programs were created for each site in which the autosamplers, once enabled by a site-specific stream level rise, would simultaneously collect one flow-weighted composite sample (Part A) and multiple discrete samples (Part B). The first six to eight bottles (Figure 5) were reserved for Part A samples. Multiplexing rates of 10 to 20 samples per bottle were used. Flow-pacing varied by site and by season. After a storm event occurred, the Part A bottles that received samples were capped and returned to UGA where they were later combined in a churn splitter. Once analyzed by the laboratory, the water sample poured from the churn splitter represented a flow-weighted EMC. The bottles that remained for Part B were filled on a non-uniform time basis. Typically, the first four bottles were filled at short intervals ranging between every 5 to 15 minutes. If the autosampler remained enabled, the time intervals gradually slowed to frequencies of every four to six hours. Only one sample per bottle was collected under Part B. Each bottle represented one discrete sample for laboratory analysis.

The success of the two-part storm sampling programs varied by site and by storm. Some storms that were sampled by Part B were not sampled adequately by Part A. For example, it was common for small rain events to result in two or three Part B samples but no Part A samples. The reverse occurred as well.

Following storm sample retrieval, a subset of the samples was selected and processed for laboratory analysis. Selection emphasized 1) greater numbers of samples from larger storm events and 2) having similar numbers of samples evenly distributed from the rising and falling limbs of storm hydrographs. With all sites and storms combined, the number of discrete storm samples selected for analysis ranged between one and 17 samples. The approximate number of storm hydrographs sampled at each of the eleven perennial and intermittent sites ranged between 16 and 40. At ephemeral site AG-12, approximately eleven storm hydrographs were sampled.

Over the entire data collection period, a total of 1,603 discrete water quality samples were collected from the study streams as a whole. That number excludes quality control samples described in Section 3.3.3. Between 110 and 183 samples were collected from each of the eleven perennial and intermittent streams. Between 40 and 50 BWG samples were collected at each of the eleven sites with the remainder representing storm samples. At AG-12, 53 samples were collected solely from storm runoff.

3.3.2.2 Sample handling, processing, and storage

Biweekly grab samples were collected manually in triple-rinsed, 500-mL polyethylene bottles. The bottles were filled by placing the bottle immediately below the flume outfall and collecting the stream water before it mixed with water circulating in the scour hole below the flume. Storm samples were collected via flexible polyethylene sample intake tubing and placed in one-liter polyethylene bottles contained within the autosamplers (Figures 3, 5, and 6). Before each storm sample was collected, the autosampler purged and rinsed the sample line with water to be sampled. At most of the sites, the sample intakes were located in the scour holes below the flume outfalls. At AG-12, the intake was placed approximately two centimeters above the flume floor.

Biweekly grab samples were transported back to the laboratory in plastic tubs under ambient outdoor conditions on the same day of sample collection. Storm samples were retrieved between one and four days after sample collection and then transported back to UGA in plastic tubs under ambient outdoor air conditions. Upon return to UGA, BWG and storm samples were placed in a refrigerator at approximately 2.0 ºC and stored overnight before being processed for analysis. On a few occasions, such as over weekends, samples were refrigerated for 2-3 days after their return.

3.3.2.3 Laboratory analysis

Laboratory analyses for water samples included total P (TP), dissolved reactive P (DRP), turbidity, and total suspended solids (TSS). The Soil Physics Laboratory within the UGA Crop and Soil Sciences Department was utilized for all turbidity and TSS analyses plus all processing of samples for subsequent P analyses. The Analytical Chemistry Laboratory (http://www.uga.edu/sisbl) within the University of Georgia's Odum School of Ecology performed all TP and DRP analyses.

Turbidity was measured using a Hach Company (Loveland, Colorado) 2100 turbidimeter. Total suspended solids were measured by filtering water sample through a 47-mm 0.45-micron (µm) cellulose nitrate filter using in-line vacuum suction with a 250-mL Buchner filter flask and a porous, glass filter holder. For water samples with turbidity below 100 Nepholometric Turbidity Units (NTU), 250 mL were filtered. When turbidity was above 100 NTU, only 100 mL were filtered. Following filtration, the residue on the filter was dried at 103-105 ºC and then weighed. The filtrate water was retained for DRP analysis.

Approximately 15 mL of both raw, unfiltered sample water plus the filtrate resulting from filtration for TSS were poured into 20-mL scintillation vials and frozen until analysis for TP and DRP, respectively. Total P analysis utilized an alkaline persulfate digestion that followed Koroleff (1983) with modifications by Qualls (1989). The digests plus all DRP samples were analyzed by automated colorimetry using an AlpKem autoanalyzer in accordance with Standard Method 4500-P F. Laboratory detection levels ranged between 0.001 and 0.005 milligrams of P of per liter (mg-P L^{-1}). For data analysis purposes, laboratory results reported as below detection were assumed to be one-half of the detection level.

3.3.3 Quality control

A quality control (QC) program was developed to mitigate sampling errors associated with routine field and laboratory data collection procedures. The QC program described here is exclusive of the QC procedures maintained by the Analytical Chemistry Laboratory. As part of routine site maintenance, water levels were measured manually to ensure that correct water levels were recorded by autosamplers at all sites. Most bottles used for water sample collection including both 500-mL Nalgene and one-liter ISCO bottles were site-dedicated and never used across land use types. For example, bottles used at AG sites were never subsequently used at FORS sites, and vice versa. The 500-mL and one-liter sample bottles plus all glassware and funnels used for sample filtration were cleaned and decontaminated using triple-rinses of tap and deionized (DI) water, a minimum of a 24-hour soak in a 1% v/v hydrochloric acid bath, a second DI triple-rinse, and then air drying. Scintillation vials were not reused.

Water QC samples were collected as part of the QC program that included both field- and laboratory-based samples. Field QC samples included field duplicates (FD) and "comparison" samples. Field duplicates were mostly collected during non-storm conditions along with BWG samples. The FD method entailed pre-rinsing and filling one 500-mL Nalgene bottle immediately after a first bottle was pre-rinsed and filled. Comparison samples were collected by programming an ISCO autosampler to instantaneously fill a one-liter ISCO bottle (known as a *manual grab* in ISCO programming terminology) at approximately the same time that a pre-rinsed 500-mL Nalgene bottle was collected (or grabbed) directly from the stream. The majority of those latter grab samples described were BWG samples. Laboratory QC samples included DI water blanks and different DI rinsates to check for contamination of reused sample bottles (termed bottle rinsate or BR) and laboratory equipment (filtration apparatus) (termed equipment check or CK) used to process samples including glassware and 0.45-µm filters. A DI rinsate was collected by directly filling a scintillation vial directly with DI water. A BR was filled by triple-rinsing and then filling a clean, acid-rinsed sample bottle with DI water. A CK was collected by *running* (i.e. manually, via gravity, etc.) DI water through the different types of laboratory equipment.

3.3.4 Soil sampling

Soil samples were collected between February and April 2006 from all study watersheds in order to characterize the soil test P (STP) levels of different land cover types and then relate the variability of STP to variability of P in streamflow (described in Section 3.4.2). Examples of land cover types included pasture, areas around poultry houses, and forest. Radcliffe et al. (Accepted) used the STP data in their SWAT watershed model of the Etowah River basin to estimate soluble P concentrations in runoff from different land cover types.

ArcView GIS 3.2 (ESRI 1999) was used to delineate and estimate the aerial coverage of the land cover areas. The procedure was similar to the process described previously in Section 3.2 using DOQQs. Between three and nine areas were delineated within the AG watersheds. From each area, between seven and ten randomly-located cores (2-cm diameter; 0-10 cm depth) were collected using a push probe and then composited. At the FORS watersheds, cores were collected from two transects from both sides of the stream (one in or near the riparian zone and one at mid-slope) and composited for a total of four samples per FORS watershed. At FORS-1, a fifth composite sample was collected from a wetland at the inflow to the pond in the watershed. All composited samples were analyzed for Mehlich-1 STP following Mehlich (1953) and Isaac and Johnson (1983).

An area-weighted average STP concentration was calculated for each AG watershed by summing the products of each individual land cover area's STP concentration multiplied by its respective percentage of total watershed area. For each FORS site, the median STP concentration of the four or five samples that were collected was used without area-weighting.

3.3.5 Management of monitoring data

As noted in Section 3.3.1, hydrologic data recorded by ISCO autosamplers were managed using ISCO Flowlink software. All water quality data were managed in a Microsoft Access software database. The size of the database was 11.1 megabytes. All STP data were managed using Microsoft Excel software. Hydrologic and water quality data were exported into Microsoft Excel prior to performance of any data analysis.

3.4 Data analysis

3.4.1 Hydrologic variation

Analyses of hydrologic variation were aimed at supporting comparisons of intersite and land use-based hydrologic conditions and assessing relationships between hydrologic variability and the physical characteristics and predominant land cover conditions of the project watersheds. All analyses were based on data collected during the 15 months between July 1, 2005, and September 30, 2006, during which all monitoring sites were in operation. Unless otherwise noted, all streamflow data were normalized by watershed area.

3.4.1.1 Water balance calculations

Water balance calculations were based on subtraction of total streamflow from rainfall for the 15-month period. The residuals were assumed to represent evapotranspiration (ET), unmeasured groundwater and hyporheic flow below the flow-measurement location (i.e. flume or culvert), and data collection errors. Watershed storage for the 15-month period was assumed negligible.

3.4.1.2 Flow duration curves, flashiness indices, and low-flow statistics

Flow-duration curves were generated for all sites using methods described by Searcy (1959). Five-minute streamflow was related to the percent of time the streamflow was exceeded.

Flashiness index (FI) calculations followed Richards (1989) and were in the form of Q_a/Q_b where a = flow-exceedance percentile and b = 100 – a. Flashiness indices included: Q_{20}/Q_{80}, Q_{10}/Q_{90}, Q_5/Q_{95}, $Q_1/_{99}$, and $Q_{0.1}/_{Q99.9}$. Richards (1989) did not investigate a $Q_{0.1}/_{Q99.9}$. Flashiness indices were not calculated for AG-12.

Seven-, 14- and 30-day low flows (7LQ, 14LQ, 30LQ, respectively) were calculated for all perennial and intermittent sites. The calculations were based on the daily means of the five-minute streamflow data.

3.4.1.3 Storm event hydrologic analyses

This analysis focused on computing different storm response variables using data from the ten storm events having the highest peak flow (Q_p) rates during the 15-month common data period. Selection of storm response variables for analysis was adapted from Swank et al. (2001). From streamflow and rainfall data directly, Q_p, the flow (Q_o) immediately prior to hydrograph rise, the time (T_p) to peak flow (represented by the duration between Q_o and Q_p), and storm event rainfall depth were identified Hydrograph separation was used to identify the volume of quickflow (Q_{qk}). Hydrograph separation followed the constant slope method of Hewlett and Hibbert (1967) to separate Q_{qk} from delayed, or base-, flow. Following conversion to metric units and adaptation to five-minute time intervals, the slope 4.59 x 10^{-4} L s^{-1} ha^{-1} 5-min^{-1} was applied immediately following Q_o and continued until intersection with the recession limb. This is exemplified in Figure 7 which shows the intersection of storm hydrograph observed at site AG-8 with computed delayed flow. In Figure 7, the area between the hydrograph and delayed flow line represents Q_{qk}. The sum of Q_{qk} and the area under the delayed flow line represents total stormflow (Q_{tot}). Remaining metrics included the percentages of Q_{qk} in relation to 1) Q_{tot} and 2) the total rainfall distributed over the watershed.

3.4.1.4 Diurnal flow fluctuations

Analysis of diurnal flow fluctuations focused on the 26 days of streamflow data recorded between August 31, 2005, and September 25, 2005, at the eleven perennial and intermittent sites. The period was the most consistently dry period across all study sites as a whole. September 2005 was the driest month over the entire project (Table 5). Due to "noise" in the five-minute streamflow data recorded at some project sites, one-hour mean streamflow data were used in the analyses for all sites. In addition, hydrograph separation was used to remove quickflow from the streamflow time series associated with a small number of rain events at sites AG-10 and AG-11.

Specific analyses included calculation of the daily AMP and ET loss reflected in the diurnal streamflow fluctuations. To calculate the AMP, the maximum and minimum streamflow rates were identified within the 00:00-12:00 and 12:00-24:00 time periods, respectively, of each day. The AMP was calculated as one-half the difference between the maximum and minimum flow rates. Estimation of daily ET loss was adapted from the 'missing streamflow' method described by Bond et al. (2002). The method for this study used the maximum one-hour mean flow used in the AMP calculations, the time (in decimal days) that the maximum flow occurred, and the total flow between every two adjacent daily flow maxima. At the time of each flow maximum, baseflow was assumed to be at its maximum and ET was assumed to be zero. Across all sites, the average duration between adjacent maxima ranged between 23.1 and 24.3 hours.

Standard errors ranged between 0.33 and 1.14 hrs. Following Bond et al. (2002), straight lines representing the maximum baseflow were interpolated between every two adjacent flow maxima. An example using streamflow data at FORS-2 is shown in Figure 8. The interpolated, straight-line and actual flow for each intermaxima time period were then summed. The difference between the two was assumed to represent a fraction of the daily ET loss from each watershed.

3.4.1.5 Relation of hydrologic response variables to watershed characteristics

Non-parametric correlation analysis (Spearman's rho (r_s)) coupled with simple linear regression modeling by least squares was used to test relationships between hydrologic response variables and watershed physical and land cover characteristics. Response variables were grouped into three categories: 1) high flow variables from the storm event analyses plus the $Q_{0.1}$, Q_1, Q_5, Q_{10}, and Q_{20} from the FDCs; 2) low flow variables including 7LQ, 14LQ, 30LQ and results of diurnal flow analyses; and 3) flow range variables represented by FIs. The specific high flow variables from storm event analyses were the medians of each sites' ten storm Q_p, T_p, Q_{tot}, the percent of Q_{qk} to Q_{tot} (Q_{qk}/Q_{tot}), and the percent of Q_{qk} to total rainfall (Q_{qk}/rain). The low flow variables from diurnal flow analyses were the medians of each site's daily streamflow AMP and daily ET representing 'missing streamflow.' Site AG-12 and the three sites with ponds were excluded from this analysis. Watershed characteristics included both physical and land cover characteristics. Physical characteristics included 1) drainage area, 2) monitoring site elevation, 3) watershed slope, 4) watershed length, 5) stream length, and 6) stream slope. Land cover percentages (in decimal fraction) included: 1) forest, 2) pasture, 3) other vegetated, 4) unpaved, and 5) impervious (Table 3), plus 6) the sum of all non-forested land cover types (impervious, other vegetated, pasture, and undeveloped (IOVPU)) combined. All correlation analyses were conducted using SAS v9.1 (SAS) (SAS Institute, Inc. 2003) with an, *a priori*, alpha (α) = 0.05 probability level. Any significantly correlated data pair was retained for use with linear regression to identify significant linear relationships between response variables and watershed characteristics. SAS was used for all linear regression model estimation.

3.4.2 Water quality variation

The purpose of analyzing water quality variation was to 1) compare intersite and inter-land use water quality conditions and 2) investigate relationships among water quality parameters and between streamflow TP and STP. Laboratory results resulting from BWG and stormwater sampling were treated as separate data sets.

Summary statistics and box-whisker graphs were generated for TP, DRP, and TSS observed in BWG and storm samples collected at every project site. Analysis of variance using the non-parametric Kruskal-Wallis (K-W) test was initially pursued to compare sites in terms of the above parameters. Prior to initiating K-W tests, the Bartlett's test for equal variance was applied to all sites' data sets using SAS. Use of both non- and natural log (LN)-transformed data representing all parameters and sample types consistently failed Bartlett's test. For that reason, analysis of variance was not further pursued.

The fraction of TP concentration as DRP (DRP/TP) in BWG and storm samples was estimated for all sites by dividing a sample's DRP concentration by its respective TP concentration. Samples having DRP concentrations greater than the corresponding TP concentration were excluded from this analysis. Across all sites and sample types combined, between 0 and 17 of those instances occurred. Frequency was greatest at the four sites (FORS-1, -2, -3 and AG-7) where overall P concentrations were the lowest and near laboratory detection levels.

As with hydrologic response data, correlation analysis (Spearman's rho) coupled with simple linear regression modeling were used to test intersite relationships within the following data group pairings:

1) median BWG TP vs. median storm TP,

2) median BWG TSS vs. median storm TSS,

3) median BWG TSS vs. median BWG TP,

4) median storm TSS vs. median storm TP,

5) area-weighted STP vs. median BWG TP,

6) area-weighted STP vs. median storm TP,

7) area-weighted STP vs. median BWG DRP,

8) area-weighted STP vs. median storm DRP,

9) area-weighted STP vs. mean BWG DRP/TP,

10) area-weighted STP vs. mean storm DRP/TP,

11) high STP vs. median BWG TP,.

12) high STP vs. median storm TP,

13) high STP vs. median BWG DRP, and

14) high STP vs. median storm DRP

Within each pairing, the first variable listed was the independent variable used in regression model estimation. All analyses were performed using SAS with an, *a priori*, $\alpha = 0.05$ probability level. LN-transformation of model variables was used in cases where initial model results were insignificant.

Hysteresis dynamics between TP concentration and streamflow were investigated using data from storm events sampled by five or more samples. Line plots of TP vs. streamflow were used to identify positive (clockwise), negative (counterclockwise), or neither types of patterns over the course of the sampled storm events. This investigation emphasized storms with uniformly-shaped hydrographs that were sampled with an approximately-even distribution of samples (five-sample minimum) collected from the rising and falling hydrograph limbs. Further, only data from AG sites were included because of low TP concentrations observed in FORS site samples.

3.4.3 Load estimation

Three classes of load estimators were utilized for this study: planning-level, direct estimation, and log-linear regression modeling. For each site and estimator, a total load (i.e. kilograms of P (kg-P)) was estimated for the entire data collection period respective to a site. Then, each load was normalized by watershed area and converted to an annual yield estimate in units kg-P per hectare (kg-P ha^{-1}). The conversion to annual yield was based on multiplication of the total load times the number of days of streamflow measurement divided by 365 days per year. For all but two planning-level estimators, an estimate of the precision, or error,was computed and then normalized to accompany the yield estimate.

3.4.3.1 Planning-level

Three planning-level TP load estimates were computed for each site. In each case, the cumulative flow volume observed at each site was multiplied by a characteristic P concentration for the site following Schwartz and Naimann (1999). The three characteristic concentrations were 1) the median TP concentration of all BWG samples, 2) the median TP concentration of all storm samples, and 3) the geometric mean of all BWG and storm samples combined. Each product represented a total load for the entire monitoring period. To arrive at an average daily loading rate, the product was divided by the number of days of streamflow measurement. The three estimates were termed L_{bwg}, L_{stm}, and L_{geo}, respectively.

The L_{bwg} and L_{stm} estimates were assumed to represent lower and upper bounds, respectively, of the actual loads at each site. That approach was less conservative than using the observed maximum storm and minimum BWG sample concentrations as the two characteristic concentrations. Precision values for the L_{bwg} and L_{stm} were not estimated.

The steps to compute L_{geo} and its confidence interval (CI) are presented below.

$$L_{geo} = k \cdot \frac{V_{tot} \cdot \exp(u_{geo})}{n_{mp}} \tag{10}$$

where:

u_{geo}	is the mean of the natural logarithms of all observed TP concentrations for a site
$\exp(u_{geo})$	is the geometric mean of the TP concentrations
V_{tot}	is the cumulative flow volume for the monitoring period
n_{mp}	is the number of days in the monitoring period that streamflow data were collected
k	is a units conversion factor

A 95% confidence interval (CI) assuming a log-normal distribution was computed for each L_{geo} estimate. The lower and upper limits of the L_{geo} CI are shown in Equations 11 and 12, respectively:

$$CI_{\log eo} = \frac{\exp(u_{geo})}{\exp(\sigma_{geo})} \tag{11}$$

where:

σ_{geo}	is the standard deviation of the natural logarithms of all observed instantaneous TP concentrations

$\exp(\sigma_{geo})$ is the geometric standard deviation of the TP concentrations

$$CI_{upgeo} = \exp(u_{geo}) \cdot \exp(\sigma_{geo}) \tag{12}$$

The upper and lower CI limits were multiplied by cumulative flow volume and normalized to annual yield. Similar to the L_{bwg} and L_{stm} estimates, the L_{geo} CIs were assumed to bracket the actual TP loads and yields of each site.

3.4.3.2 Direct estimation

Flow-duration rating curves (FDRCs) following the methods of Verhoff et al. (1980) were developed for all sites. The main steps of the method as used in this study are described below. Note that the method requires derivation of flow duration curves (FDCs) as an initial step. Those were derived for all sites following the approach described in the hydrologic data analysis (Section 3.4.1.2) with two exceptions. First, all months of streamflow data were used instead of the 15 months used previously and second, the streamflow data were in liters per second ($L\ s^{-1}$) units.

The first step was to divide the range between the minimum and maximum flow rates at a site by a user-specified number that resulted in a set of equally-spaced flow intervals, or bins. Second, all observed instantaneous loads were allocated to the intervals. Third, for each interval, the mean and standard error of the instantaneous loads were computed. For this study, a minimum of three instantaneous loads were allocated to each interval. Fourth, the mean loads were summed to represent the average daily load for the monitoring period. Fifth, a variance was computed from of the sum of the products of the squares of the standard errors and percentages of time each flow interval occurred. A 95% CI was computed from the square root of the variance. Finally, the total load and associated CI for the full monitoring period were estimated by multiplying the two terms times the number of days of the monitoring period.

Between 18 and 30 flow intervals were established in developing FDRCs for the eleven perennial and intermittent sites. The average was 23 intervals. Eleven intervals were used for ephemeral site AG-12. For all sites, some flow intervals had to be combined to satisfy the requirement that at least three instantaneous loads were allocated to each flow interval. The average flow-exceedance percentile for which that occurred was 7.63% for the eleven perennial and intermittent sites. It was 0.56% for AG-12.

3.4.3.3 Regression

Log-linear regression models were used to estimate TP loads for the nine agricultural (AG) sites. Regression modeling was not performed for FORS sites due to complications posed by sample TP concentrations reported below laboratory detection limits. The natural logarithm of instantaneous load represented the dependent variable and the natural logarithm of instantaneous Q represented the independent variable. Natural logarithm-transformed concentration-flow models were also developed but only for load-flow regression model evaluation. This is discussed later in this section. For each site, all combined BWG and storm sample TP data were used in model calibration. All model estimation was based on ordinary least methods using SAS at an, *a priori* , $\alpha = 0.05$ probability level.

Two model forms were fitted to the calibration data sets. One was Equation 5 (see Section 2.3.1.1) and Equation 13:

$$\ln L(t) = \beta_0 + \beta_1 \cdot \ln Q(t) + \beta_2 (\ln Q(t))^2 + \varepsilon \qquad (13)$$

where:

β_2 is a model coefficient.

Addition of the flow-squared term in Equation 13 was recommended through personal communication by Brent Aulenbach (USGS), Robert Hirsch (USGS), and Peter Richards

(Heidelberg University) to remove quadratic or curvilinear patterns evident in particular regression model scatter plots. Stepwise regression in SAS (α= 0.05) was used for all AG sites to determine if the additional term was significant and improved calibration.

The regression models were evaluated in three ways following recommendations for regression model evaluation by Hirsch et al. (1993), Helsel and Hirsch (2002), Mendenhall and Sincich (2003), and Kutner et al. (2004). First, the statistical significance and standard errors of the calibrated model coefficients were examined. Model R^2 values for load-flow (L-Q) as well as concentration-flow (C-Q) model forms were also examined. Concentration-flow model R^2 values of 0.2 (personal communication, Brent Aulenbach) or higher generally indicate a C-Q correlation that warrants either C-Q or L-Q regression model development for load estimation. Second, results of different residual (normal and studentized) and influence diagnostic tests were examined. Those are listed here:

1) Kolmogorov-Smirnov (K-S) test for normality of model residuals,

2) standard deviation (s_ε) of model residuals,

3) Kendall's tau correlation (τ_ε) between neighboring, lag one residuals (i.e. ε_i and ε_{i-1}),

4) Durbin-Watson (D-W) test for autocorrelation,

5) 1st-order autocorrelation coefficient (φ_ε) of model residuals,

6) number of residual Cook's *D* values greater than 0.7, and

7) number of the absolute values of studentized residuals (ε_{si}) greater than or equal to 2.0.

Third, graphs involving observed and predicted instantaneous loads and model residuals were examined. Note that all discussion here refers to loads and residuals in LN space.

Back-transformation of model predictions was completed in three ways: straightforward exponentiation (Equation 6) and with the QMLE (Equation 7) and smearing (Equation 8) BCFs.

For final load estimation, the back-transformed models were used to predict a five-minute trace of instantaneous TP load from the five-minute streamflow observed at each site. To arrive at a total load, each instantaneous load was multiplied by five minutes and then summed.

The precision of each regression-based load and yield estimates were evaluated using a weighted mean absolute error (WMAE):

$$WMAE = \frac{1}{N}\sum\left(QE\% \cdot \left|L_{obs\,i} - L_{pred\,i}\right|\right) \tag{14}$$

where:

L_{obsi} is the observed instantaneous of the ith observed data pair

L_{predi} is the predicted instantaneous load based on the ith observed Q

QE% is the flow-exceedance percentile of the ith observed Q from flow-duration curves

A ± one WMAE was applied to each regression model estimate to facilitate comparison with results from other estimators.

CHAPTER 4.0

RESULTS

4.1 Climatic and regional hydrologic conditions during study period

Based on data from the GAEMN-Dahlonega weather station (Figure 2), precipitation in the upper Etowah River basin was below average during most of the study period. Figure 9 shows that at Dahlonega, monthly rainfall between January 2005 and September 2006 was above average for only five of the 21 months that bracketed the full monitoring period of all sites combined. Factoring in the USGS' precipitation data, there appeared however to be some spatial variability in rainfall over the upper Etowah basin as a whole. The general trend over the 21-month period was average to above-average precipitation near the beginning of the study and well-below average rainfall towards the end. Mean annual flow in the Etowah River at Canton in water years 2005 and 2006 were 39.4 and 20.1 $m^3 s^{-1}$, respectively (information available from USGS at http://waterdata.usgs.gov; last accessed June 5, 2008). The two flows were about 15% above and 39% below the mean annual flow of 34.2 $m^3 s^{-1}$, respectively, for years 1897 to 2007. Between January 2005 and September 2006, the Palmer Hydrological Drought Index (PHDI) for north-central Georgia evolved from predominantly *moderately-moist* conditions in 2005 to *mid-range* conditions in 2006 (information available from the National Climatic Data Center at http:\\www.ncdc.noaa.gov\oga\ncdc.html; last accessed September 27, 2008).

Above-average rainfall in July and August 2005 was largely due to an active tropical storm season. From a rainfall-runoff perspective, the most influential tropical storm for the upper Etowah River basin was Hurricane Dennis, which made landfall in Florida on July 10, 2005, and then moved north-northwestward over Alabama and then Mississippi on July 11 as a tropical depression (Beven 2005). The Etowah River at Canton began to receive rainfall from the storm on July 10. On July 11, 2005, the 84.6 mm of rainfall reported at Canton was the second highest daily rainfall over that time period. On July 12, 2005, the mean daily streamflow in the Etowah River at Canton was 240 $m^3 s^{-1}$. That was the highest streamflow reported by the USGS for that site between January 1, 2005, and September 30, 2006.

4.2 Hydrologic variation at study sites

For the 15-month (July 1, 2005, to September 30, 2006) period common to all sites, total rainfall on the 12 sites ranged from a low of 1,275 mm at site AG-9 to a high of 1,699 mm at site FORS-3 (Figure 10). Rainfall depths were linearly related ($P = 0.0004$; $R^2 = 0.7316$) to site elevation (Figure 11). When converted to a monthly basis, these results suggest that monthly rainfall increased at approximately 0.11 mm per one-meter rise in elevation. At the perennial and intermittent sites, water balance residuals accounted for 43% (AG-6) to 87% (AG-8) of the total rainfall at the study sites (Figure 10).

Streamflow was continuous throughout the study period at the three forested (FORS) sites and seven of the nine agricultural (AG) sites (Appendix B). At site AG-4, streamflow was intermittent between July and September 2006. The stream was dry for approximately 36 days. Site AG-12 was an ephemeral stream that flowed only during and after rainfall. To varying extents, the streamflow time series shown in Appendix A demonstrate seasonal variations or study-long declines in streamflow concurrent with the trend in the climatic conditions understood for the north-Georgia region. The time series for FORS-3 appears to demonstrate both trends. In Fall 2005, streamflow increased presumably due to the onset of cooler temperatures and low transpiration rates. However, with persistent below-average rainfall from winter through August

2006, streamflow exhibited a continuous decline. At AG-5, which was minimally forested, no seasonal fluctuations were apparent and a downward trend in streamflow was not suggested until Spring 2006.

Flow duration curves for the eleven perennial and intermittent sites were similar between the 80% and 1% exceedance levels (Figure 12). (Note that curves for individual sites are shown in Appendix E as part of results (see Section 3.4.3.2) on the use of flow-duration rating curves to estimate TP loads.) Within that exceedance level range, there were no apparent differences between the AG and FORS sites; however there were order-or-magnitude intersite differences. Below the 1% exceedance level, AG site FDCs were notably higher than FORS site FDCs. This was particularly the case for AG-5, AG-6, and AG-9, which had the three highest streamflows at the 0.1% ($Q_{0.1}$) exceedance level. Above the 80% exceedance level, the variations among the FDCs did not appear to be based on land use.

The overall variation among the perennial and intermittent sites' FDCs is partially reflected in their flashiness indices (FIs) (Figure 13). The Q_5/Q_{95}, Q_1/Q_{99}, and $Q_{0.1}/Q_{99.1}$ FIs for AG-4 were not computed because the Q_{95}, Q_{99}, and $Q_{99.1}$ were 0.0 L s^{-1} ha^{-1} (Figure 12). The high FIs computed for sites FORS-2 and AG-8, -9, and -11 may be explained by their low flow-exceedance percentiles between Q_{90} and $Q_{99.9}$ Conversely, high FIs at AG-6 may be explained by flows at the high (i.e. $Q_{0.1}$) end of the FDC spectrum. There was no suggestion of a difference between the AG and FORS site FIs.

For most study sites, the dates of the ten storm events that were analyzed were spread over the full 15-month common monitoring period (Figure 14). Note that sites FORS-1 and ephemeral AG-12 were not included in storm event analyses. There were differences however among the sites in the numbers of events that occurred in July and August 2005, which represented the peak months of the 2005 tropical storm season. The rainfall depth ranges of the storms at all sites were fairly similar (Figure 15). Median rainfall depths of the ten storms analyzed at each site ranged between 19.4 and 34.9 mm. Of the six storm event response variables that were analyzed (Figures 16 - 21), only peak flow (Q_p) (Figure 17) and the relative percentage of quickflow to total stormflow (Q_{qk}/Q_{tot}) (Figure 21) appeared to differ by land use type (i.e. AG vs. FORS). Intersite differences in initial streamflow rates (Q_o) (Figure 16) may have been influenced by variability in both antecedent conditions prior to storm events and the storm event dates (Figure 14) relative to hydrologic conditions over the study period.

Some of the patterns and intersite variability exhibited in the different boxplots suggest important similarities or differences about the study sites in terms of hydrologic response. The intersite variability in quickflow volume (Q_{qk}) (Figure 19) across all sites mirrored that of Q_p (Figure 17) with the exception of AG-11. At most sites, quickflow volumes accounted for less than 20% of storm rainfall depths (Figure 20). The outstanding exceptions were sites AG-5, AG-6, and AG-9 which exhibited the some of highest Q_p's, Q_{qk}'s, and Q_{qk}/Q_{tot}'s. For AG-5 and AG-6, in particular, those results concur with water balance results previously presented. The two highest streamflow volumes and two lowest water balance residuals occurred at those two sites.

Most mean 7-, 14-, and 30-d low flows (Figure 22) computed for the eleven perennial and intermittent occurred between June and September 2006 (Appendix A) as *mid-range* drought (based on PHDI) conditions became established in north-central Georgia. No land use-based differences in mean low flows among the sites were suggested from the data reflected in Figure 22. The same case applied to amplitudes (Figure 23) and daily evapotranspiration (ET) (Figure 24) estimates based on diurnal streamflow fluctuations observed in September 2005. As could be expected, the pattern of intersite differences in amplitudes and ET mirrored one another. The order-of-magnitude differences in the two variables at FORS-1 compared to all other sites may have been due to evaporation from the pond there or streamflow measurement errors. It may have been the latter as the amplitude and ET at pond sites AG-9 and AG-11 were the lowest of all AG sites. One general difference among all sites was the trend in daily flows. Daily flows at some sites such as FORS-3 (Figure 25) demonstrated steeper recessions than other sites such as AG-7 (Figure 26). Possible explanations for this would be larger groundwater reserves following the July and August 2005 tropical storm seasons and/or steeper near-stream hydraulic gradients.

4.3 Hydrologic response relationships

Correlations (Spearman's rho) among watershed characteristics were evaluated prior to assessment of relationships involving response variables. Most physical characteristics were either positively or negatively correlated (Table 6). For example, stream and watershed length plus watershed slope were positively correlated with drainage area. This would be expected due to basic morphometric relationships involving watershed area and relief (Ritter 1978). Watershed slope and study site elevation were positively correlated which would also be expected. Among land cover characteristics, forest cover tended to exhibit correlative relationships with other land cover types based on pasture coverage. Impervious, unpaved, and other vegetated (OV) land covers were all positively correlated with each other. Forest cover was either positively or negatively correlated with all physical characteristics except site elevation. The *impervious, OV, pasture, and undeveloped (*IOVPU) cover category, which is a direct inverse of forest cover, exhibited the same correlations as forest cover except with different signs. The correlations among land cover and physical relationships were likely influenced by the coincidence that the three forest sites, with 100% forest cover, had the largest drainage areas and highest site elevations and watershed slopes (Table 6). Regardless, because forest cover and drainage area tended to exhibit the most frequent significant ($P < 0.1$) correlations with other characteristics they were retained for further analysis involving relationships with hydrologic response factors.

Of all response factors tested (Table 6), only three factors exhibited a significant correlation with either drainage area or percent forest cover. The 0.01 flow-exceedance percentile ($Q_{0.1}$) was inversely correlated with drainage area and the fraction of forest cover. No significant linear relationships were detected, however, between $Q_{0.1}$ and either watershed characteristic. The remaining factors showing significant correlation were based on top 10 storm event analyses. Median Q_ps were inversely related to drainage area (Figure 27) ($P = 0.0872$; $R^2 = 0.4100$) and forest cover (Figure 28) ($P = 0.0971$; $R^2 = 0.3914$). As shown, linear models were fit to both sets of data, but inverse or exponential decay models may have described the relationships better. This would partly be a function of AG-6 (identified), which appears to be an outlier in both figures. While the two pond sites (AG-9 and AG-11) shown in the figures were not included in the regression analyses, they do not appear to be outliers. This suggests that the ponds at AG-9 and AG-11 did not dampen stormflow response to large storm events. This is supported by the relatively high Q_ps observed at AG-9 (Figure 17). Median percentages of Q_{qk}/Q_{tot} (Figure 21) were inversely related to drainage area (Figure 29) ($P = 0.0163$; $R^2 = 0.6456$) and forest cover (Figure 30) ($P = 0.0006$; $R^2 = 0.8756$). In contrast to relationships above involving Q_p, AG-6 is not an apparent outlier in either figure. Plus, linear models appear to describe both relationships appropriately, even if the models were to include the pond sites.

4.4 Phosphorus concentrations

4.4.1 Quality control samples

Laboratory results of deionized (DI) water-based quality control (QC) samples suggested that any P contamination of study site samples was negligible. The mean ± standard error of TP and DRP concentrations of all DI-based QC samples were within the range (0.001-0.005 mg-P L^{-1}) of minimum detection levels (MDLs) of P reported by the Analytical Chemistry Laboratory for P (Table 8). The absolute values of the mean differences between original and field duplicate (FD) samples collected from FORS and AG sites for TP (Figure 31) were 0.009 mg-P L^{-1} and 0.031 mg-P L^{-1}, respectively. In original and FD samples collected for DRP (Figure 32), the values for FORS and AG sites were 0.004 mg-P L^{-1} and 0.013 mg-P L^{-1}, respectively. It is important to note that most FD samples were collected during non-storm conditions while collecting biweekly grab (BWG) samples. The results reported here may not represent the differences between the two sample types during stormflow conditions.

Laboratory results of QC samples aimed at estimating potential errors via ISCO autosampling suggested that any differences in P concentrations between autosamples and ambient water quality conditions were relatively small (Table 9). At FORS sites, for both TP and DRP, mean errors ± the associated standard errors between autosamples and grab samples collected directly from flume outlets were within the range of laboratory P method detection limits (MDLs). At AG sites, differences in both DRP and TP concentrations between the two samples types were greater than at the FORS sites. At most sites, especially with DRP, the magnitudes and ranges of errors tended to approximate and overlap with the P MDL range. These results are further depicted in Figures 33 and 34 which combine results for DRP and TP, respectively, from all sites. The scatter in both graphs appears to be evenly distributed about the

1:1 lines shown. This was tested by fitting linear regression models to the data and using two-tailed t-test methods with regression model output (slope and standard error) to test whether the slopes were significantly different than 1.0. For TP, the respective t-statistic, critical t-value, and P-value (probability to fail to reject H_o: slope = 1) were 1.65, 1.99, and 0.1032. For DRP, the respective t-statistic, critical t-value, and P-value were 0.109, 1.99, and 0.9137. For both analytes, and especially for DRP, these results suggest that ISCO-collected samples were representative of ambient water quality conditions. It is important to note that the majority of ISCO-based comparison samples were collected during non-storm conditions.

4.4.2 Total phosphorus

Time series graphs of TP concentrations observed in BWG and storm samples observed at the study sites are shown along with streamflow (L s^{-1}) time series in Appendix C. Scatter plots of TP concentrations vs. streamflow are shown in Appendix D. At FORS sites, minimal differences were apparent between the ranges of TP concentration observed in both BWG (Figure 35) and storm (Figure 36) samples. The interquartile TP concentrations of both sample types ranged between 0.001 and 0.01 mg-P L^{-1}. At most, Appendix C suggests that there were weak relationships overall between TP concentration and flow at the forest sites. Stronger relationships appear to have occurred when evaluated on a storm-by-storm basis (Appendix C). It is important to note that because the ranges of P concentration observed in the forested streams of this study were typically at or near the limits (0.001 – 0.005 mg-P L^{-1}) of laboratory detection, the results should not be used for strict comparison purposes.

Observed TP concentrations in streamflow at AG sites (Appendix C; Figures 35 and 36), demonstrated substantial differences between BWG and storm samples. At some sites, such as AG-6, -8, and -11, the BWG TP time series (Appendix C) suggest sinusoidal-like trends that appear to have coincided with clusters of storm hydrographs. At site AG-7, BWG sample TP concentrations were comparable to FORS sites (Figure 35). The site's storm sample TP concentrations, however, were mostly one order-of-magnitude higher than FORS sites (Figure 36). At all other AG sites, TP concentrations of BWG samples were typically one order-of-magnitude higher than FORS sites while in storm samples, TP concentrations were typically two orders-of-magnitude higher. In storm samples in particular, interquartile ranges varied between zero (i.e. AG-4, -7, and -11) and three (i.e AG-8) orders of magnitude higher.

With the exceptions of AG-4, AG-10, and AG-11, positive concentration-flow (C-Q) relationships at AG sites were apparent but with a moderate-to-high degree of scatter (Appendix D). Because the x- and y-axis scales are different for each site shown in Appendix D, relative intersite differences in slope cannot be inferred. With some exceptions, for storm events when at least five or more samples were collected at a site, the range of TP concentrations observed within each sample set tended to overlap with other sets collected from the same site. The important points to emphasize are that 1) the range of TP concentrations observed within each sample set could vary by one or two orders-of-magnitude over the course of the hydrograph and 2) any two sets of overlapping storm event concentrations may have been associated with entirely different stormflow conditions (i.e. peak flow, hydrograph duration, etc.). One exception to the former point is demonstrated by the December 14-15, 2005, storm event sampled at AG-6 (Appendix C). The storm samples shown were collected within one or two weeks after the farmer there had spread poultry litter. The application represented the annual fertilization of pasture there. The stormflow associated with that event was substantially lower than most other sampled storm events. By the time the next group of storm samples was collected in March 2006, the range of TP concentrations was back within the range of most other storm event samples. Other exceptions were observed in storm samples collected at AG-10 and AG-11. At both sites, the storm sample TP concentration time-series suggest a positive trend with time.

At some AG sites, TP concentration hysteresis was observed in sets of storm samples. To exemplify this, plots of TP concentration as a function of flow are presented from 3-4 storm events sampled at sites AG-4, -6, -8, -9, and -12 (Figures 37 - 41, respectively). The numbers in the scatter-plots show the numeric sequence of samples selected from the larger group of sample bottles filled by the ISCO over the hydrograph. All of the storms shown from AG-4 and AG-6 exhibited counterclockwise hysteresis between TP concentration and flow. At AG-8, AG-9, and AG-12, a mixture of hysteretic patterns were exhibited including lack of patterns altogether. Asymptotic relationships between TP concentration and flow were suggested by some storm events shown for the five sites. The strongest cases of this were apparent in Figure 37 for AG-4 where all storms shown suggest an asymptotic relationship. The relationship is also suggested in Figures 38 (AG-6) and 39 (AG-8) but to a lesser extent than compared to AG-4.

From a risk-based perspective, TP concentrations in water samples varied with soil test P (STP). Median storm sample TP concentrations across all study sites were linearly related to both area-weighted STP concentrations (AWSTP) (Table 10) (Figure 42) and the highest STP concentration (HISTP) (Figure 43) observed within each watershed. These results suggest that median TP concentrations in storm samples across all sites increased at an approximate rate of 0.002–0.005 mg-P L^{-1} per unit mg-P kg^{-1} soil, depending on how soil P in the watersheds was represented. BWG sample TP concentrations were also related to STP. LN-transformation was required to obtain a significant model fit between median BWG TP concentrations and AWSTP

(Figure 44). Transformation was not required to obtain a significant model fit between median BWG TP and HISTP (Figure 45).

From a different risk perspective, TP concentrations in storm samples exhibited relationships with TP concentrations in BWG samples. Storm and BWG sample median TP concentrations were correlated (r_s =0.7727; P= 0.0053) (Figure 46), but natural log-transformation of both variables was required to obtain a significant linear model fit to the data (Figure 47).

4.4.3 Dissolved reactive phosphorus

Intersite differences in the fraction of TP concentration as DRP (DRP/TP) in both BWG and storm samples did not appear to be land use-based (Figure 48). In FORS site samples overall, DRP/TP fractions were about 20 to 40 percent. Any differences between FORS site BWG and storm sample DRP/TP fractions may be negligible as the majority of DRP concentrations in FORS site BWG and storm samples (see Figures 35, 36, 49, and 50) were within the range of laboratory P MDLs. At most AG sites, DRP/TP fractions in both BWG and storm samples were greater than what were observed at FORS sites. Further, AG site storm sample DRP/TP fractions tended to be higher than BWG samples. Exceptions to both of these trends were observed at AG-7 and pond site AG-11.

Patterns in the intersite and land-use based differences in BWG and storm sample DRP concentrations (Figures 49 and 50) were comparable to the differences observed for TP (Figures 35 and 36). Notable exceptions again involved sites AG-7 and -11. The difference in storm sample DRP concentrations at AG-7 vs. the FORS sites was not as distinct as it was with TP (Figure 36). At AG-11, BWG and storm sample DRP concentrations compared to other AG sites were lower than what was observed with TP. These results involving AG-7 and -11 concur with results presented above regarding the sites' BWG/TP percentages.

As with the risk-based analyses for TP, DRP concentrations in water samples varied as a function of STP and water sample type. Median storm sample DRP concentrations across all study sites were linearly related to AWSTP (Table 10) (Figure 51). These results suggest that median storm sample DRP increased about 0.003 mg-P L^{-1} per unit of mg-P kg^{-1} of AWSTP. LN-transformation was required to obtain a significant model fit between median storm sample DRP and high HISTP (Figure 52). Median BWG sample DRP concentrations were linearly related to AWSTP (Figure 53). LN-transformation was required to obtain a significant model fit between median BWG sample DRP and high HISTP (Figure 54). Median storm sample DRP concentrations were related to respective sites' median BWG sample DRP concentrations (Figures 55 and 56).

The degree to which the fraction of TP as DRP (DRP/TP) was related to AWSTP at study sites depended on sample type (BWG vs. storm) and whether pond sites (FORS-1, AG-9, and AG-11) were included in the analysis. When data from all twelve sites were included, a significant ($P = 0.0597$; $R^2 = 0.3106$) linear relationship was obtained between mean storm DRP/TP and AWSTP (Figure 57). No significant correlation or linear relationship was obtained between BWG DRP/TP and AWSTP when data from all sites were included. When data was restricted to the non-pond sites only, the relationships between DRP/TP and AWSTP improved. Mean non-pond BWG DRP/TP was weakly correlated (Spearman rho $r_s = 0.6429$; $P = 0.0856$) with AWSTP. A significant linear relationship was not obtained between the two variables. Mean non-pond storm DRP/TP was linearly related ($P = 0.0158$; $R^2 = 0.5886$) to AWSTP (Figure 58).

4.5 Suspended sediment concentrations

No DI-based QC samples were prepared for TSS analysis. The absolute values of the mean differences between original and field duplicate (FD) samples collected from FORS and AG sites for TSS were 3.70 mg L^{-1} and 32.5 mg L^{-1}, respectively (Figure 59). Results of ISCO-based QC samples (Table 9; Figure 60) compared with direct grab samples suggest that autosampler TSS concentrations at most sites, while highly variable, almost consistently exceeded ambient TSS concentrations. As with TP and DRP (Section 4.4.1), two-tailed t-test methods with regression model output (slope and standard error) were used to test if the slope (Figure 60) was significantly different than 1.0. The respective t-statistic, critical t-value, and P-value (probability to reject H_o: slope = 1) were 10.3 (absolute value of -10.3), 1.99, and <0.0001. These results suggest that ISCO-collected samples for TSS were not representative of ambient water quality conditions. One reason for the difference may involve how the intake tubing for autosamplers was positioned in the scour holes immediately below flume outlets. Typically, there was sediment continuously circulating in the scour holes that was visibly not representative of sediment being discharged by the flumes. Another reason may be that autosamplers did not sample isokinetically—the intake velocity exceeded stream water velocity. As stated above with TP, most samples collected for these comparisons were done so during non-storm conditions. It is possible that under high flow conditions, the stream water in the scour hole was well-mixed and representative of flow through the flume.

Land use-based differences in TSS concentrations of BWG and storm samples (Figures 61 and 62, respectively) were less than that what were observed with P in the two sample types. Within the two land use types, there was greater variability among FORS sites and less variability among AG sites. Sites such as FORS-2, AG-7, and AG-10, which typically exhibited low water sample P concentrations compared to other sites, exhibited high TSS concentrations. In contrast, ephemeral AG-12, which exhibited high P concentrations in stormflow, exhibited low TSS concentrations. This was likely associated with the dense-grass cover maintained throughout the watershed. No statistically significant relationships were detected between the median TSS concentrations from the two sample types (i.e. storm TSS vs. BWG TSS) (Figure 63). This was the case for both regression and correlation (r_s =0.4954; P= 0.1212) analyses of LN-transformed variables.

Total suspended solids concentration was tested as a risk-based indicator of TP concentrations. Median TP concentrations in both BWG and storm samples were linearly related to BWG and storm sample TSS concentrations (Figures 64, 65, and 66). Linear regression results shown in Figure 66 suggest that median TP concentrations increased about 0.003 and 0.001 mg-P L^{-1} per mg L^{-1} increase in median TSS in BWG and storm samples, respectively.

4.6 Phosphorus load estimates

At FORS sites, all planning-level TP yield estimates were within 0.001 to 0.01 kg-P ha^{-1} (Figure 67; Appendix F). Forested site geometric mean-based yields (L_{geo}) overlapped with flow-duration rating curve-based (L_{fdrc}) yields. Across all AG sites, TP yields via L_{geo} ranged 0.031 (AG-7) to 2.88 (AG-6) kg-P ha^{-1} (Appendix F). With CIs factored in, the yields ranged 0.007 to 13.1 kg-P ha^{-1}. The CIs were comparable to the ranges between the BWG (L_{bwg}) and storm (L_{stm}) sample-based yields. Further, the ranges of the planning-level estimates encompassed those of the L_{fdrc} and regression estimators (Figure 67).

Instantaneous TP load data used for L_{fdrc} estimation were collected over wide ranges of streamflows observed at study sites (Appendix E). At FORS sites, L_{fdrc} yields were within 0.01 to 0.1 kg-P ha^{-1} (Figure 67). At AG sites, the yields ranged 0.031 (AG-7) to 3.17 kg-P ha^{-1} (AG-

6). With CIs factored in, the yields ranged 0.025 to 13.1 kg-P ha^{-1}. The intersite variability in TP L_{fdrc}-based yields mirrors intersite variability in storm TP concentrations (Figure 36). Compared to the regression-based yield estimates, AG site L_{fdrc} yields captured the ranges of the L_{exp} yields. Yields via the other two regression estimators (L_{qmle} and L_{sm}) were typically higher than L_{fdrc} yields.

Stepwise regression methods in SAS selected Equation 13 for six sites (AG-4 through AG-9). Equation 5 was selected for three sites (AG-10 through AG-12) (Table 11). All regression models and coefficients were significant ($P < 0.05$). Standard errors of model coefficients were typically low relative to their respective coefficients. The C-Q model R^2 for site AG-4 (0.180) suggests an overall weak relationship between TP concentration and flow that may limit interpretation of regression model load estimates for that site. Kolmogorov-Smirnov tests for normality of model residuals passed (indicated by $P > 0.05$) for six AG sites and failed for three AG sites. Results of Kendall's tau (b) and Durbin-Watson tests indicated autocorrelation was present in the residuals of all regression models. Results of Cook's *D* tests indicated there were no highly influential observations used in calibration of the different AG site models. The average rate that absolute values of ε_{si} exceeded 2.0 was 5.2 percent. A rate of 5 percent is indicative of a normal distribution (Helsel and Hirsch 2002).

Further presentation of regression model calibration results focuses on sites AG-5, -6, -7 and -11 as they reflect the variability of AG site data used in model calibration, the two equation forms (Equations 5 and 13) used for model calibration, and the diagnostics shown in Table 11 and summarized above. For all four sites, the relationship between observed (L_{obs}) and predicted (L_{pred}) TP loads appear linear and distributed evenly about a 1:1 line (Figures 68-71). Note that the data discussed here is in LN-space and has not undergone transformation back to arithmetic space. The time series of residuals for AG-5, -6, -7, and -11 demonstrated periodic bias, or autocorrelation (Figures 72-75). Random mixtures of positive (>0) and negative (<0) residuals appeared to be short-lived. For AG-11 (Figure 75) in particular, the residuals exhibited a cyclic or sinusoidal pattern. These latter results may be a function of representativeness and temporal resolution monitoring data, both short- and long-term variations in C-Q relationships, and simplicity of the model equations.

Three regression-based TP yields were estimated for each AG site—one developed without bias correction (L_{exp}) applied and two with bias correction (L_{qmle} and L_{sm}) applied. While the QMLE is appropriate for back-transforming model estimates with normally-distributed residuals, for this study it was applied to all sites, independent of whether residuals passed the Kolmogorov-Smirnov test.

Yield estimates via L_{qmle} and L_{sm} always exceeded L_{exp} estimates (Figure 67; Appendix F). This was expected due to how L_{qmle} and L_{sm} are mathematically defined to correct back-transformation bias (Equations 7 and 8). The magnitude of the exceedance depends on the variance of the original calibrated model's residuals. While the weighted mean absolute errors (WMAEs) of the L_{qmle} and L_{sm} yield typically overlapped, the nonparametric L_{sm} may be a better representative of the two due to failure of Kolmogorov-Smirnov tests for three AG sites. The range that L_{sm} yields exceeded L_{exp} yields was between 22 % (AG-11) and 128 % (AG-10). The differences in P yield between the two estimators were correlated with the standard deviation of model residuals (s_{ε}) ($r_s = 0.950$, $P < 0.05$) (Figure 76) (Table 11). (As s_{ε} went up, the difference between L_{sm} and L_{exp}, in terms of P yield, went up.) The magnitude of the correction factors used by both the L_{sm} and L_{qmle} methods were directly a function of s_{ε}. (As s_{ε} went up, the numerical value of the correction factor went up.)

The range in s_ε was further explored based on the concepts that 1) L_{sm} was a more accurate predictor of actual loads and 2) the magnitude of s_ε was related to the degree that L_{exp} underpredicted actual loads. These concepts do not appear to be supported, however, by Figures 77, 78, and 79 which compare observed instantaneous loads with predicted loads as a function of streamflow observed at sites AG-5, -10, and -11, respectively. Those three sites were chosen because they represent the range in the percent differences between the L_{exp} and L_{sm} yields (Figure 76). For each site, all predicted loads were within the range of observed loads. Persistent underpredictions of observed loads via L_{exp} were not apparent. This may be due, in part, to the high degree of variability of TP concentrations, and hence instantaneous loading, as a function of flow at most AG sites. While underprediction bias may be inherent to using the L_{exp} regression estimator, without having "true" loading data, there is not strong evidence to support the use of either L_{sm} or L_{qmle} over L_{exp} in this study.

As a measure of regression-model performance, time series of five-minute predicted TP loads were compared with observed TP loads using data from sites AG-5, -7, and -10. These sites were chosen because they reflect almost the full range in TP yields estimated for AG sites (Figure 67; Appendix F). Plus, like above, they reflect the two equations (Equations 5 and 13) used for model calibration and variations in model diagnostics (Table 11). This evaluation was restricted to modeling results based on the L_{exp} estimator only. Predicted TP loading (Figures 76, 78, and 80) for sampled storm events appeared to match the majority of observed instantaneous storm sample TP loads for each site. To variable extents, the regression models overpredicted the observed loads based on BWG sampling, which primarily represented non-storm flow conditions. Detailed comparisons of predicted and observed loads are further necessary to help determine how well the regression models predicted the observed loads. The initial results presented here suggest that additional model specification or use of separate models may be necessary to represent loading during non-storm flow conditions. Model specification could be based on the concept that the predominant P source areas and transport mechanisms can be different during storm and non-storm flow conditions.

The relative contributions of stormflow and non-storm flow conditions to total TP loading was explored by relating cumulative TP loads at AG-5, AG-7, and AG-10 based on regression modeling (L_{exp}) to observed streamflow. A 10% flow-exceedance for each site (Figure 12; Appendix E) was assumed to represent the approximate break between storm and non-storm flow conditions. Flows less than the 10% exceedance (i.e. 5% or Q_5) represent storm flow conditions and flows above the 10% exceedance (i.e. 90% or Q_{99}) represent non-storm flow conditions. The 10% flow-exceedance percentiles for sites AG-5, -7, and AG-10 were approximately 2.0, 1.0, and 1.3 mm d^{-1}, respectively. For AG-5, 2.0 mm d^{-1} represents approximately 16% (Figure 81) of the cumulative load. This suggests that 84% of TP loading at AG-5 occurred via the highest 10% of streamflow. The 84%-value may be a conservative estimate given that the AG-5 regression model appeared to overpredict loading during non-storm flow conditions. For AG-7, 1.0 mm d^{-1} represents approximately 35% (Figure 83) of the cumulative load. For AG-10, 1.3 mm d^{-1} represents approximately 51% (Figure 85) of the cumulative load. These latter results suggest that, compared to AG-5, smaller proportions of the cumulative TP loads at AG-7 and AG-10 occurred via stormflow.

Regression-model load estimation was not performed for the three forested sites and hence, continuous time-series and cumulative estimated TP loading could not be evaluated for those sites. As previously noted, results (Figures 35 and 36; Appendices C and D) show that the differences in TP concentration as a function of sample type (and assumedly streamflow) at forested sites were apparently minimal. When concentrations were converted to loads, such as for site FORS-3 (Figure 86), the differences between the two flow regimes became more apparent.

Section 3.3.2.1 described a two-part autosampling method used to collect a flow-weighted composite sample over a storm hydrograph while at the same time collecting multiple discrete samples. Those two types of data are used here to evaluate regression-based load estimates for four storm events at both AG-4 and AG-10. Table 12 shows the storm event dates, the duration and flow volume of the hydrographs that were sampled by the Part A ISCO programs, the number of flow-weighted samples composited for laboratory analysis, the resulting TP concentration, and the observed TP load based on the product of the flow volume and composite sample TP concentration. At both sites, L_{exp}, L_{sm}, and L_{qmle} both under- and overpredicted observed loads. If all three estimates overpredicted the observed load, then L_{exp} was least biased. Conversely, if all estimates underpredicted the observed load, then L_{exp} was the most biased. These results concur with results shown in Figures 77, 78, and 79. Across most flow ranges, all three estimators both under- and overpredicted observed instantaneous loads, but overall, their predictions appear to fit within the greater variability of observed loads.

The intersite differences in P yield rates were assumedly due to how different P source and transport factors in each study watershed were integrated over the study period. Spearman correlation and stepwise regression analyses were performed in SAS in order to identify which source and transport factors investigated in this study were most closely related to annual P yields. The L_{fdrc} P yields were selected as the dependent variable because 1) the method for calculating L_{fdrc} and its confidence interval is established in the literature and 2) the L_{fdrc} yield estimates were consistently in the mid-part of the overall range of estimates at each site.

Independent variables included area-weighted Mehlich-1 (M1) soil test P (AWSTP), high M1 STP (HISTP), fraction of forest cover, watershed drainage area and 15-month total rainfall. Hydrologic response variables were not included in the analysis because response is dependent on the interactions among forest cover, drainage area, and rainfall. Total P yield was positively correlated ($P < 0.005$) to AWSTP ($r_s = 0.8182$) and HISTP ($r_s = 0.8182$). Yield was negatively correlated ($P < 0.05$) to forest cover ($r_s = -0.7248$), drainage area ($r_s = -0.6105$), and rainfall ($r_s = -0.6150$). Two iterations of stepwise regression analysis were performed to identify the strongest relationship between TP yield and the independent variables. When AWSTP, forest cover, drainage area, and rainfall were available as dependent variables, SAS selected AWSTP ($P = 0.003$; $R^2 = 0.6426$) (Figure 87). When the analysis was run with HISTP substituted for AWSTP, SAS selected drainage area ($P = 0.0568$; $R^2 = 0.3464$). These results suggest that AWSTP was most closely related to the L_{fdrc} yield estimates, with AWSTP explaining about 64% of the overall P yield variability.

The relationship between P loading and soil P was further evaluated by plotting annual TP load (not area-normalized) versus estimated total mass of M1 STP (based on AWSTP) in the upper 10 cm of soil in each watershed. Use of the 10-cm depth corresponds to the depth of soil core samples collected from each watershed in 2006. A uniform bulk density of 1.65 megagrams (Mg) per cubic meter of soil was assumed for each watershed. As used in the analyses above, TP loading was based on use of the L_{fdrc} estimator. Results suggest a positive relationship existed between the two variables (Figure 88). With the TP load estimates converted to annual yield (kg-P ha^{-1}) and the mass of soil P in the upper 10 cm of soil area-normalized (kg-P ha^{-1}), the results suggest that the mass of M1STP in each AG watershed was 140 to 160 times greater than the annual yield. It is important to note that Mehlich-1 STP represents an agronomic measurement of plant-available soil P. It does not represent the total amount of P in the soil or that which is water-soluble.

Correlation and linear regression analyses were performed to identify relationships between TP yields and different P water quality variables representing potential risk-based screening tools. First, Spearman correlation analyses were performed in SAS to test correlations between yield and median DRP and TP concentrations in both BWG and storm samples collected at study sites. Significant ($P < 0.05$) positive correlations were detected between yield and all four variables: 1) median BWG DRP ($r_s = 0.8995$); 2) median storm DRP ($r_s = 0.8581$); 3) median BWG TP ($r_s = 0.8273$); and 4) median storm TP ($r_s = 0.8811$). Significant linear relationships were detected between yield and three of the four variables: 1) median BWG DRP ($P = 0.0003$; $R^2 = 0.7818$) (Figure 89), 2) median storm DRP ($P = 0.0011$; $R^2 = 0.6742$); and 3) median storm TP ($P = 0.003$; $R^2 = 0.6020$). A significant linear relationship was not detected between yield and median BWG TP ($P = 0.2372$; $R^2 = 0.1512$).

CHAPTER 5.0

DISCUSSION

5.1 Hydrologic response

Few differences in hydrologic response characteristics were observed between the AG and FORS sites as a whole. The main differences between the two land use types appeared to be associated only with high stormflow conditions. The non-pond forest sites typically had lower $Q_{0.1}$s, Q_ps, and Q_{qk}/Q_{tot}s. Schoonover et al. (2006) showed that watersheds in the west Georgia Piedmont with unmanaged and managed forest cover had significantly ($P < 0.05$) lower mean, maximum, and minimum area-normalized streamflows compared to pasture-dominated watersheds. Smith (1992) found that the hydrologic effects from afforestation of a riparian zone in a grazed, pastured watershed reduced peak flows during small storm events but not during large events. The small storm effect was attributed to stream channel and riparian zone interception combined with a reduction in the aerial extent of variable source areas. During large events, variable source area runoff generation occurred from >40 % of the watershed, which was consistent with pre-afforestation runoff generation. These differences suggest an agreement with the threshold concept (i.e. Sidle et al. 2000; Buttle et al. 2004; Ocampo et al. 2006; Eisenbies 2007) that differences in hydrologic response between low- and high-flow events are linked to different hydrologic controls. In this study, response variables associated with low-flow events were not specifically investigated. From evaluation of flow duration curves, there were some order-of-magnitude differences among the study sites' Q_{20}s and Q_{30}s, but the differences did not appear to be land use-based.

For the same three variables above ($Q_{0.1}$, Q_p, and Q_{qk}/Q_{tot}) shown to be related to forest cover, similar relationships were also observed with drainage area. The only notable difference between the relationships involving forest cover and drainage area was suggested by their relationships with Q_{qk}/Q_{tot}, which were more closely related to forest cover. The lack of clarity in differentiating between the relationships involving forest cover and drainage area may be due, in part. to the coincidences that the forested watersheds also had the largest drainage areas and steepest watershed slopes. The low number (n = 8) of data sets used in the regression analyses and the use of medians may have been important limitations on the analyses. The correlation between drainage area and forest cover and lack of correlation between response variables and other land cover types (i.e. % pasture, % impervious, etc.) aligns with studies (i.e. Woodruff and Hewlett 1970; Hewlett and Bosch 1984) that found undetectable effects of land use on stormflow characteristics.

Of most hydrologic variables investigated, results for the two neighboring watersheds of AG-5 and AG-6 tended to stand out compared to the other AG sites. The two sites had the lowest relative water balance residuals and consistently exhibited high levels of stormflow response (i.e. Q_1, Q_p, etc.). The sites also, however, exhibited high relative values for the low metrics (i.e. Q_{99}, 7-day low flow, etc) that were investigated. The two sites had the smallest drainage areas and shortest stream lengths of all perennial and intermittent AG sites. Both watersheds at AG-5 and AG-6 were covered mostly by cattle-grazed pasture. Cattle had access to both stream channels. Riparian vegetation was minimal along the stream channel at AG-5. A swale connected the head of the stream channel at AG-6 with a gully that received runoff from poultry houses house and an unpaved road. A cattle trail encircled the stream channel of both sites. Additional trails crossed the channels through the streambeds. While no geomorphic data were collected from the two stream channels, both were incised. At AG-6, banks were nearly vertical in some locations with heights exceeding the heights of cattle. All of these factors combined with heir small drainage areas could explain the anomalous hydrologic response characteristics of the two watersheds. Small drainage areas and short stream lengths could equate to short lag times, less floodplain storage capacities, and higher unit-area peak flows (Ritter 1978). Below-average rainfall during most of the study period may have accentuated grazing pressure on pasture vegetation which would promote runoff potential due to reductions of interception, roughness, and transpiration (Hofmann and Ries 1991). Lack of riparian vegetation minimized canopy interception of rainfall and enabled greater stream channel interception (Smith 1992). Cattle trails, with exposed and compacted soil cover, plus the linkage among the poultry houses, roads, and gully at AG-6 diminished watershed infiltration potential and directly connected the stream channels with upslope runoff (Ludwig et al. 1995; Trimble 1995; Moussa et al. 2002; Bracken and Croke 2007). High runoff potentials, erodible soils typical of the Piedmont, plus continued channel access by cattle could have combined to result in stream bank and bed erosion (Trimble 1995). A lowered stream elevation intersected with the shallow water table could have resulted in higher area-normalized rate of baseflow. Another explanation for higher baseflow is a discrepancy between the contributing areas of groundwater (larger) and surface water (smaller).

While AG watersheds appeared to exhibit their own unique response signals, none of the other response variables were related to the land cover or physical characteristics tested. A variety of factors may have been involved in this finding. First, the 15-month common monitoring period is an important limitation. Studies such as Swank et al. (2001) were based on roughly 20 years of precipitation and streamflow data for one watershed. Secondly, assuming rainfall at the GAEMN climate station at Dahlonega was representative of the study area as a whole, precipitation was below average for about 11 of those 15 months. Below-average rainfall would result in depleted soil moisture and groundwater reserves that would then act to dampen hydrologic response to the storm events that did occur. This concept is supported to varying extents by the streamflow time series shown for study sites in Appendix B. In each watershed, the spatial organization of the different land cover types, small scale hydrologic features (i.e. roads, ditches, erosional zones), spatial and temporal variations in soil characteristics, and unique physical characteristics likely added dimensions of variability in hydrologic response that simple correlation and regression analyses could not identify (Cassel et al. 1983; Ludwig et al. 1995; Moussa et al. 2002; Page et al. 2005; Buttle 2006; Endale et al. 2006). Multivariate methods such as principal components analysis would be one approach to identifying what combinations of watershed characteristics were statistically most influential on hydrologic response.

The AG pond sites (AG-9 and AG-11) were expected to have unique response signals such as lower peak flows (McCuen 2005), longer times to peak flow, and overall stable, non-flashy streamflow characteristics. Results were mixed at AG-11 and none of these expectations were supported by AG-9. The AG-9 watershed had the highest estimated percentage (15.7 %) of impervious and unpaved (i.e. gravel roads) land cover combined of all AG watersheds. That percentage implies a high degree of hydrologic connectivity within the watershed. Assuming the pond was shallow (Declerck et al. 2006) and had low detention capacity, it is possible that surface runoff during storm events was routed quickly through the pond. Another possibility is that runoff from some areas of the watershed entered the stream below the pond but upstream of the monitoring location.

5.2 Factors for variability in phosphorus concentration

Past investigations of P in forested and otherwise undeveloped streams showed P concentrations to be fairly low. In undisturbed, hardwood forested watersheds at Coweeta, Swank and Waide (1988) reported mean annual stream phosphate (PO_4-P) concentrations of 0.001 to 0.002 mg-P L^{-1}. Phosphate concentrations in streams draining disturbed watersheds at Coweeta were slightly higher with a range of 0.003 to 0.005 mg-P L^{-1} (Swank 1988). Clark et al. (2000) reported summary statistics for TP and dissolved orthophosphate concentrations observed in streams (18 to about 2,500 km^2) monitored throughout the U.S. between 1990 and 1995 by the USGS for its Hydrologic Benchmark Network (HBN) program. Median dissolved orthophosphate concentrations in streams draining 43 Hydrologic Benchmark Network basins were <0.01 mg-P L^{-1}. Median TP concentrations in streams draining 41 HBN basins were 0.02 mg-P L^{-1}. In this study, P concentrations in most samples collected from the forested streams (FORS-1, -2, and -3) were comparable or less than those reported for the Coweeta and HBN streams discussed above. Mean DRP concentrations in BWG and storm samples combined from each forested stream ranged 0.002 to 0.003 mg-P L^{-1}. Median DRP concentrations in all forested streams were 0.001 mg-P L^{-1}. Median TP concentrations ranged 0.003 to 0.004 mg-P L^{-1}.

Low P input rates to the forested watersheds combined with high rates of P retention by soils, terrestrial vegetation, streambed sediments, and aquatic plants (i.e. bryophytes) were all possible factors for the low P concentrations in the forested streams. The low percentages of DRP relative to TP in both BWG and storm samples suggest that the majority of P was either in an organic or particulate form. During storm events, high discharge would flush P from sediments, stream banks, and other sources (Meyer and Likens 1979). This would explain the short, storm-specific increases in TP concentration visible in the streamflow and TP concentration time series shown in Appendix C.

Overlap between AG and FORS stream P concentrations was minimal. The main exception was at AG-7 during non-storm conditions, which is suggested by the magnitude of DRP and TP concentrations observed in AG-7 BWG samples (Figure 35). At the other AG sites, the higher ranges of TP and DRP in BWG samples may have resulted from several different source/transport factors. Anaerobic conditions in riparian soils or buried channel sediments could favor release of P from reduced iron and aluminum oxyhydroxides to shallow groundwater before it entered the stream (Jordan et al. 1993; Carlyle and Hill 2001; Surridge et al. 2007). If groundwater entering the stream was low in P concentration relative to the sediment equilibrium phosphate concentration (EPC), the sediment could release P to the stream (Taylor and Kunishi 1971; Meyer 1979; McDowell and Sharpley 2003; Haggard et al. 2004). Another explanation is transfer of P to shallow groundwater as leachate via throughflow, percolation, or preferential flow in contact with high P soils (Heckrath et al. 1995; Heathwaite 1997; Sims et al. 2000). Following the studies cited here, redox- and EPC-based mechanisms would explain detection of the DRP detected in the BWG samples. The remaining non-DRP fraction detected in BWG samples could reflect slow, continual entrainment of fine particulate and Murphy-Riley unreactive colloidal P (Turner et al. 2004) from sediment and bank materials. The variations of P in BWG samples over time, which at some sites appeared to fluctuate with streamflow rates during non-storm conditions, may have been linked to variations in groundwater discharge or timing of BWG sample collection relative to a preceding storm event.

While it is apparent that P concentrations (C) in AG streams were related to streamflow (Q), Appendix D and the LN-transformed C-Q R^2-values shown in Table 11 suggest that C-Q relationships varied by site and across sites as a whole. Further, results suggest that P C-Q relationships at some AG sites were asymptotic and indicative of P dilution (Edwards and Daniel 1994; Fleming and Cox 1998) or supply-limitation. Using TP as a basis, the strongest P C-Q relationships for AG sites as well as FORS sites were apparent during individual storm events. In Appendix C, TP concentration time series for all AG sites show that TP concentrations typically rose (or spiked) concurrently with storm hydrographs. Study-wide, however, storm event TP concentrations at most AG sites appeared to reach limits that were independent of respective hydrograph peaks. At sites AG-5, AG-7, and AG-8 in particular, the ranges of TP concentrations observed during the July 2005 tropical storm events were similar to those collected from smaller events much later in the study. This concentration-limiting effect could be due to P supply-limitation from the hillslope and channel source areas. This is equivalent to a dilution effect (Edwards and Daniel 1994; Fleming and Cox 1998) caused by higher rainfall intensities or stormwater runoff rates.

The asymptotic behavior of storm event TP C-Q relationships (Section 4.4.2) shown in Figures 37, 38, and 39 for sites AG-4, AG-6, and AG-8, respectively, supports the P supply-limiting concept discussed above. The asymptote represents the P concentration-limit. The most mostly counterclockwise hysteretic patterns shown in the figures suggest that the primary sources of P in those streams were located on hillslopes or in their upstream channels (Lefrancois et al. 2007). Assuming hillslopes were the primary P source areas at AG sites, the P concentration-limit at each site would be a function of the P supply in the soil, vegetation and residual manure on the hillslope relative to the mobilization potential of storm runoff.

An exception to the supply-limiting effect would be in the case of a storm event occurring soon after poultry litter was applied. A documented example of this is in the

December 2005 storm event sampled at AG-6 that occurred shortly after poultry litter was applied. That particular storm event can be considered a supply-sustaining P transfer event that was likely due to high incidental losses P from the freshly-applied poultry litter on the land surface. During the remainder of the year, hillslope soils and channel sources predominated. This differentiation in the relative weighting of soil and manure P sources agrees with studies such as Sauer et al. (2000) and Kleinman et al. (2002).

More data is necessary to determine if and when the supply-limiting effect above is applicable. Interpretations from the results of this study are limited because the majority of storm events that occurred at AG sites were not sampled and of those that were sampled, sometimes only one or two samples were collected and analyzed. Further, sample collection did not always coincide with the storm hydrograph peak. Another factor is that precipitation during most months of the study was below average. Overall drier antecedent moisture conditions would dampen hydrologic response and thus the potential for P mobilization on the hillslope. During the ~18 months that each AG site was monitored, the number of poultry litter applications at farms where litter is applied was small since farmers typically fertilize pasture one or two times per year. Poultry litter cake may have been applied more frequently but the volumes of cake are relatively small compared to litter applications. At AG-10, both BWG and storm event TP concentrations appeared to exhibit a positive time trend over the study. Another uncertainty is how suspended sediment at individual sites varied with streamflow during individual storm events and over time.

As in the hydrologic response analysis, pond site AG-11 demonstrated a unique P signal compared to other AG sites but pond site AG-9 did not. The ranges of TP concentrations in BWG and storm samples were both the highest of all sites. The ranges of DRP concentrations in both samples, and specifically the percentages of DRP relative to TP in both sample types (Figure 48) were the lowest of all AG sites. Throughout most of the study period, during field visits to AG-11, the pond was green in color, which is suggestive of an active phytoplankton community. Low DRP in streamflow at AG-11 may have resulted from a combination of retention and uptake of inorganic P by pond sediments (Masuda and Boyd 1994) and phytoplankton, respectively. The higher concentrations of TP at AG-11 relative to AG-9 may have been partially due to differences in poultry litter management at the two farms (Table 4).

5.3 Estimators and indicators of phosphorus loading

The primary motivation for this study was to estimate P loads in headwater streams draining both agricultural and forested watersheds in the upper Etowah River basin of north Georgia. Three load estimator types were employed. Planning-level estimators represented a generalized approach that required basic mathematics combined with the use of two pieces of data--a characteristic P concentration and a cumulative streamflow volume for the period of interest. Two types of characteristic concentration were used. In one type, the median BWG (L_{bwg}) and storm (L_{stm}) TP concentrations were used in tandem to represent upper and lower bounds on actual P loading rates. The geometric mean (L_{geo}), the second type of characteristic concentration, has been both criticized (Schwartz and Naimann 1999) and supported (Rasmussen 2001). In this study, use of the geometric mean appeared appropriate for use with the mixed-frequency water quality data sets. It was advantageous because a confidence interval (CI) could be estimated and that a strong C-Q relationship was not necessary. Use of the L_{fdrc} estimator developed by Verhoff et al. (1980) has been used in different published studies, but it also has been criticized (Walling and Webb 1985) in the literature. Regression estimators are among the most-studied estimators. Much of the research interest focuses on correction of the bias incurred from back-transformation of model estimates initially derived in log space. A well-recognized weakness of using regression estimators via least squares is characterizing the precision of a regression-based load estimate. For this study, a weighted mean absolute error (WMAE) was estimated and used.

At most sites, with the CIs included, L_{geo} planning-level yield estimates bracketed the ranges of the L_{bwg} and L_{stm} planning-level estimators plus they typically encompassed the ranges of yields estimated via the L_{fdrc} and the three regression estimators (L_{exp}, L_{qmle}, and L_{sm}). Similarly, the L_{fdrc} yield estimates and their respective CIs typically overlapped with the L_{exp} yield estimates and their respective WMAEs. For AG sites, the use of bias-correction techniques (i.e. L_{qmle} and L_{sm}) for regression-based load estimation did not appear warranted. This may be due to the high degree of variability in concentration and hence, instantaneous load. The L_{exp} estimator showed better agreement with the non-regression estimators.

With all AG sites and estimators taken into account, the relative site-to-site TP yield rankings typically remained the same regardless of what estimator was used for comparison. For example, with L_{geo}, L_{fdrc}, and L_{exp} estimates combined, sites AG-6 and AG-5 always had the highest and second-highest yields, respectively, of all sites. Similarly, sites AG-4, -10, -9, and -7 had the sixth, seventh, eighth, and ninth lowest yield estimates, respectively. The third, fourth, and fifth yield rankings were shared among sites AG-8, AG-9, and AG-12, but not always in the same order.

The TP yields (Figure 67; Appendix F) estimated for the nine AG sites were comparable to those reported by seven previous field-scale studies (Table 1) of pastures fertilized with poultry litter. Using the L_{fdrc} yield estimates as a basis, annual TP yields for the nine AG sites ranged 0.031 to 3.17 kg-P ha^{-1}. With confidence intervals factored in, the annual yields ranged

0.025 to 13.1 kg-P ha^{-1}. The range in annual P yield estimates reported in the previous studies (Table 1) was 0.10 to 17.8 kg-P ha^{-1}. The nine AG-site TP yields estimated in this study were also comparable to the TP yields estimated by Schroeder et al. (2004b) from 2-m^2 hay-covered plots fertilized by one of three different poultry litter application rates. At the end of ten simulated rainfall events, TP yields were 2.12, 4.22, and 9.66 kg-P ha^{-1} for application rates of two, seven, and 13 megagrams (Mg) of litter (Mg-litter) per hectare, respectively.

The overlap among the TP yields estimated at the plot-scale (Schroeder et al. 2004b), field-scale (Table 1), and headwater watershed-scale (this study) studies discussed above suggests that P loading studies of small (two m^2 to 27 ha) agricultural drainages can be scalable. In this study, however, a weak inverse relationship ($P = 0.0797$; $R^2 = 0.3747$) was detected between natural log (LN)-transformed TP yield (L_{fdrc} estimator) and LN-transformed drainage area of the nine AG watersheds (Figure 90). Studies that focused directly on the relationship between P yield and drainage area found that P yield and area were not directly scalable. Those studies, however, focused on watersheds with wider ranges in area. T.-Prairie and Kalff (1986) compiled TP yields reported by studies of 14 agricultural watersheds with 70% or more pasture cover. The median and interquartile range of drainage area of the 14 watersheds were 0.42 and 0.11 to 57.3 km^2, respectively. Log-transformed annual TP yield (kg-P km^{-2}) decreased ($P < 0.05$) at a rate of 0.411 times the log-transformed drainage area (km^2) (i.e. log TP yield = 1.562 – 0.411*log area). Haygarth et al. (2005b) estimated TP yields in stormflow at six locations in a nested headwater-to-river channel study within the River Taw basin in the United Kingdom. Drainage areas of the six locations ranged between 30-m^2 and 86,200 ha. Results of that study suggested an inverse relationship between TP yield and area however no statistical analyses were performed. Yields ranged between 0.116 kg-P ha^{-1} (30 m^2 plot) and 0.05 kg-P ha^{-1} (4,000 and

86,200 ha mainstem river sites). Both T.-Prairie and Kalff (1986) and Haygarth et al. (2005b) attributed the lack of scalability in P yield to factors such as attenuation through floodplain deposition.

Part of the overlap among P yields reported by this study, Schroeder et al (2004b), and those in Table 1 may be similarities in soil test P (STP). Soil test P concentrations for the nine AG watersheds (AWSTP range 25.7 to 186 mg-P kg^{-1}) in this study and the five previous field-scale studies (Table 1) (range 10.7 to 187 mg-P kg^{-1}) were closely comparable and both encompassed the STP concentrations of the plots studies by Schroeder et al. (2004b). Average Mehlich-3 STP concentrations of the plots were 32.3, 37.5, and 62.5 for the two, seven, and 13 Mg-litter ha^{-1} treatments, respectively, at the end of the ten simulated rainfall events. Another factor for the overlap in reported P yields may be due to limited potential for downgradient attenuation, especially in the plot- and field-scale studies.

The P-risk indicators investigated for this study included two soil P data types (AWSTP and high STP (HISTP), P concentrations in BWG and storm samples, SS concentrations in both BWG and storm samples, drainage area, percent of watershed in forest cover, and rainfall. Of the different source and transport indicators tested, the strongest indicator for TP yield at AG sites was AWSTP. The transport factors (rainfall, area, forest cover) were outweighed by AWSTP. To varying extents, both DRP and TP concentrations in BWG samples were related to AWSTP. These results support the proposal by Page et al. (2005) that baseflow P concentration may be an effective surrogate measure of a watershed's soil P status. In this study, because DRP concentrations of BWG samples were also related to TP yield, baseflow DRP concentration may also be an effective measure of a watershed's P loading rate. Hess et al. (2007) described the use of pre-screening tools as an initial step for planners prior to development of a phosphorus index

(P-Index) for a field. At a watershed scale, baseflow sampling would constitute the prescreening.

CHAPTER 5.0

CONCLUSIONS

A combination of continuous streamflow and mixed-frequency water quality data sets were used in this study to estimate TP loads and yields in three forested (FORS) and nine agricultural (AG) (poultry-pasture) headwater watersheds. Because P loading integrates variability in hydrologic response with variability in P concentration, factors for hydrologic response and streamflow P variability were also investigated. Specific attention was also given to identifying indicators of potential P loss from the watersheds that were studied.

Precipitation was below-average during most of the ~18 month study period. An important exception was June-to-August 2005 when precipitation was about 70% above average. The overall below-average precipitation may have dampened the study watersheds' hydrologic response signals and potential for P loss to streams.

Between AG and FORS sites as whole, there were few differences in their hydrologic response characteristics. The main differences between the two land use types appeared to be associated only with response variables ($Q_{0.1}$, Q_p, and Q_{qk}/Q_{tot}) representing high and infrequent stormflow conditions. $Q_{0.1}$, Q_p, and Q_{qk}/Q_{tot} exhibited significant inverse relationships with both drainage area and percentage of forest cover. Interpretation of these findings was complicated by the coincidence that the forested watersheds had the largest watershed drainage areas and slopes.

Mean dissolved reactive P (DRP) concentrations (0.002 to 0.003 mg-P L^{-1}) in FORS streams were comparable to mean annual phosphate concentrations reported by Swank and

Waide (1988) and Swank (1988) for hardwood (0.001 to 0.002 mg-P L^{-1}) and disturbed (0.003 to 0.005 mg-P L^{-1}) forested streams, respectively, in the southern Appalachian Mountains. Median DRP (0.001 mg-P L^{-1}) and total P (TP) (0.003 to 0.004 mg-P L^{-1}) concentrations in FORS streams were comparable to median dissolved orthophosphate (<0.01 mg-P L^{-1}) but less than TP (0.02 mg-P L^{-1}) concentrations, respectively, reported by Clark et al. (2000) for streams draining Hydrologic Benchmark Network basins monitored by the USGS. The FORS streams appeared to exhibit concentration-flow (C-Q) dependence on an individual storm event basis, but over the entire study period, the relative differences between non-storm and storm condition P concentrations were minimal.

At most AG sites, the ranges in P concentration of biweekly grab (BWG) and storm samples exceeded those of the FORS sites by at least one order-of-magnitude. In some cases, the differences were as high as three orders-of-magnitude. Among the AG sites specifically, intersite difference in P concentration as a function of site and sample type were also at order-of-magnitude levels. Stormflow P concentrations did depend on streamflow, but like the FORS sites, the C-Q relationships appeared to be strongest on a storm-event basis. Phosphorus C-Q relationships at some AG sites were asymptotic and indicative of P dilution (Fleming and Cox 1998; Edwards and Daniel 1994) or supply-limitation. A documented exception occurred at an AG site where a storm event was sampled soon after poultry litter application. When dilution or supply-limitation effects were apparent during high stormflow rates, actual P loading rates were still relatively high.

Three types of load estimator were investigated—planning-level (L_{bwg}, L_{geo}, and L_{stm}), flow duration rating curve (L_{fdrc}), and log-transformed linear regression with (L_{qmle} and L_{sm}) and without (L_{exp}) bias-correction techniques. Planning-level estimators were used to identify approximate bounds of actual loading rates. They also served as a basis for comparison with the other estimators. A weighted mean absolute error (WMAE) technique was developed to estimate the precision for regression-model load estimates. Results of regression modeling suggested that the use of bias-correction techniques were unnecessary. At most sites, L_{geo} planning-level TP yield estimates bracketed the ranges of the L_{bwg} and L_{stm} planning- level estimators plus they typically encompassed the ranges of yields estimated via all three regression estimators. Yield estimates and respective confidence intervals (CI) and WMAEs of the L_{fdrc} and L_{exp} estimators typically overlapped. Comparisons of observed and predicted TP loads for three sites based on the L_{exp} estimator suggested that model predictions matched the range of observed loading during storm events but overpredicted loading during non-storm flow conditions. With all AG sites and estimators taken into account, the relative site-to-site TP yield rankings typically remained the same regardless of what estimator was used for comparison. Based on flow-duration rating curve methods, FORS site TP yields ranged between 0.01 to 0.1 kg-P ha^{-1}. The yields at AG sites ranged 0.031 to 3.17 kg-P ha^{-1}. The AG sites yields ranged 0.025 to 13.1 kg-P ha^{-1} with CIs factored in. The TP yields estimated for the nine AG sites were comparable to those reported by seven previous field-scale studies of pastures fertilized with poultry litter.

Of the different source (soil P) and hydrologic transport (forest cover, drainage area, rainfall) variables examined, TP yields exhibited the strongest relationships with area-weighted Mehlich-1 soil test P (AWSTP) concentrations. To varying extents, both DRP and TP concentrations in BWG samples were related to AWSTP. Further, DRP concentrations in BWG samples were related to P yield. In addition to supporting Page et al. (2005) on the use of base flow P concentrations as a surrogate measure for watershed soil P, results of this study suggest baseflow DRP concentration may be an effective measure of a watershed's P loading rate. These findings have potential for use in a P-based management and risk assessment framework such as the Phosphorus Index applied at the watershed scale. Baseflow sampling is first performed as a screening measure. Soil sampling then follows either on a watershed-wide basis or potentially through emphasis on land areas with high soil or where fertilizer application is planned.

REFERENCES

Ammerman, J.W., Raleigh, R.H., Case, D.A. and Cotner, J.B., 2003. Phosphorus defiency in the Atlantic: an emerging paradigm in oceanography. Eos, Transactions of the American Geophysical Union, 84(18).

Andersen, H.E., Kronvang, B. and Larsen, S.E., 2005. Development, validation and application of Danish empirical phosphorus models. Journal of Hydrology, 304(1-4): 355-365.

Anderson, G., 1980. Assessing organic phosphorus in soils. In: F.E. Khasawneh, E.C. Sample and E.J. Kamprath (Editors), The Role of Phosphorus in Agriculture. ASA-CSSA-SSSA, Madison, Wisconsin, pp. 411-432.

Anderson, M.G. and Burt, T.P., 1978. Role of topography in controlling throughflow generation. Earth Surface Processes and Landforms, 3(4): 331-344.

Andraski, T.W., Bundy, L.G. and Kilian, K.C., 2003. Manure history and long-term tillage effects on soil properties and phosphorus losses in runoff. Journal of Environmental Quality, 32(5): 1782-1789.

Aulenbach, B.T. and Hooper, R.P., 2006. The composite method: an improved method for stream-water solute load estimation. Hydrological Processes, 20(14): 3029-3047.

Ballard, R., 1980. Phosphorus nutrition and fertilization of forest trees. In: F.E. Khasawneh, E.C. Sample and E.J. Kamprath (Editors), The Role of Phosphorus in Agriculture. ASA-CSSA-SSSA, Madison, Wisconsin, pp. 763-804.

Barrow, N.J., 1987. Return of nutrients by animals. In: R.W. Snaydon (Editor), Managed Grasslands. Elsevier, Oxford, England, pp. 181-186.

Beaulac, M.N. and Reckhow, K., 1982. An examination of land use-nutrient export relationships. Water Resource Bulletin, 18: 1013-1024.

Benda, L., Andras, K., Miller, D. and Bigelow, P., 2004. Confluence effects in rivers: Interactions of basin scale, network geometry, and disturbance regimes. Water Resources Research, 40(5).

Betson, R.P., 1964. What is watershed runoff? Journal of Geophysical Research, 69(8): 1541-1552.

Betson, R.P. and Marius, J.B., 1969. Source areas of storm runoff. Water Resources Research, 5(3): 574-&.

Beven, J., 2005. Tropical Cyclone Report: Hurricane Dennis, 4-13 July 2005. National Hurricane Center. National Oceanic and Atmospheric Administration. Available at http://www.nhc.noaa.gov/pdf/TCR-AL042005_Dennis.pdf.

Beven, K. and Kirkby, M.J., 1979. A physically based, variable contributing area model of basin hydrology. Hydrobiologia, Hydrological Sciences Bulletin(24): 43-69.

Beven, K. and Wood, E.F., 1983. Catchment geomorphology and the dynamics of runoff contributing areas. Journal of Hydrology, 65(1-3): 139-158.

Bond, B.J., Jones , J.A., Moore, G., Phillips, N., Post, D., and McDonnell, J.J., 2002. The zone of vegetation influence on baseflow revealed by diel patterns of streamflow and vegetation water use in a headwater basin. Hydrological Processes, 16(8): 1671-1677.

Bosch, D.J. and Napit, K.B., 1992. Economics of transporting poultry litter to achieve more effective use as fertilizer. Journal of Soil and Water Conservation, 47(4): 342-346.

Bracken, L.J. and Croke, J., 2007. The concept of hydrological connectivity and its contribution to understanding runoff-dominated geomorphic systems. Hydrological Processes, 21(13): 1749-1763.

Bradu, D. and Mundlak, Y., 1970. Estimation on lognormal linear models. Journal of the American Statistical Association, 65(329): 198-211.

Brady, N.C., 1990. The Nature and Properties of Soils, 10th ed. Macmillan Publishing Company, New York, 621 pp.

Brakensiek, D.L., Osborn, H.B. and Rawls, W.J., 1979. Field Manual for Research in Agricultural Hydrology. Agriculture Handbook 224. U.S. Department of Agriculture, 550 pp.

Burkhead, N.M., Walsch, S.J., Freeman, B.W. and Williams, J.D., 1997. Status and restoration of the Etowah River, an imperiled southern Appalachian river ecosystem. In: G.A. Benz and D.E. Collins (Editors), Aquatic fauna in peril: the southeastern perspective. Special Publication No. 1, Southeast Aquatic Research Institute, Lenz Design & Communications, Decatur, Georgia.

Buttle, J., 2006. Mapping first-order controls on streamflow from drainage basins: the T^3 template. Hydrological Processes, 20: 3415-3422.

Buttle, J.M., Dillon, P.J. and Eerkes, G.R., 2004. Hydrologic coupling of slopes, riparian zones and streams: an example from the Canadian Shield. Journal of Hydrology, 287(1-4): 161-177.

Cabrera, M.L., Franklin, D.H., Harris, G.H., Jones, V.H., Kuykendall, H.A., Radcliffe, D.E., Risse, L.M., and Truman, C.C., 2002. The Georgia Phosphorus Index. The University of Georgia and U.S. Department of Agriculture, pp. 10.

Carlyle, G.C. and Hill, A.R., 2001. Groundwater phosphate dynamics in a river riparian zone: effects of hydrologic flowpaths, lithology, and redox chemistry. Journal of Hydrology, 247(3-4): 151-168.

Carpenter, S.R., 2005. Eutrophication of aquatic ecosystems: Bistability and soil phosphorus. Proceedings of the National Academy of Sciences of the United States of America, 102(29): 10002-10005.

Cassel, D.K., 1983. Spatial and temporal variability of soil physical properties following tillage of Norfolk loamy sand. Soil Science Society of America Journal, 47(2): 196-201.

Chaubey, I., Migliaccio, K.W., Green, C.H., Arnold, J.G. and Srinivasan, R., 2007. Phosphorus modeling in Soil and Water Assessment Tool (SWAT) model. In: M.L. Cabrera and D.E. Radcliffe (Editors), Modeling Phosphorus in the Environment. CRC Press, Inc., Boca Raton, Florida, pp. 163-188.

Chow, V.T., Maidment, D.R. and Mays, L.W., 1988. Applied Hydrology. McGraw-Hill, Inc. , New York, 572 pp.

Clark, G.M., Mueller, D.K. and Mast, M.A., 2000. Nutrient concentrations and yields in undeveloped stream basins of the United States. Journal of the American Water Resources Association, 36(4): 849-860.

Cohn, T.A., 1995. Recent advances in statistical methods for the estimation of sediment and transport in rivers. Reviews of Geophysics, 33: 1117-1123.

Cohn, T.A., Caulder, D.L., Gilroy, E.J., Zynjuk, L.D. and Summers, R.M., 1992. The validity of a simple statistical-model for estimating fluvial constituent loads - an empirical study involving nutrient loads entering Chesapeake Bay. Water Resources Research, 28(9): 2353-2363.

Cohn, T.A., Delong, L.L., Gilroy, E.J., Hirsch, R.M. and Wells, D.K., 1989. Estimating constituent loads. Water Resources Research, 25(5): 937-942.

Cooke, R.U. and Reeves, R.W., 1976. Arroyos and Environmental Change in the American South-West. Clarendon Press, Oxford, 213 pp.

Cooper, D.M., 2004. Some effects of sampling design on water quality estimation in streams. Hydrological Sciences Journal, 49(6): 1055-1080.

Cooper, D.M. and Watts, C.D., 2002. A comparison of river load estimation techniques: application to dissolved organic carbon. Environmetrics, 13(7): 733-750.

Correll, D.L., 1998. The role of phosphorus in the eutrophication of receiving waters: A review. Journal of Environmental Quality, 27(2): 261-266.

Crawford, C.G., 1991. Estimation of suspended-sediment rating curves and mean suspended-sediment loads. Journal of Hydrology, 129: 331-348.

Dann, M.S., Lynch, J.A. and Corbett, E.S., 1986. Comparison of methods for estimating sulfate export from a forested watershed. Journal of Environmental Quality, 15(2): 140-145.

Declerck, S., De Bie, T., Ercken, D., Hampel, H.,Schrijvers, S.,Van Wichelen, J.,Gillard, V., Mandiki, R., Losson, B., Bauwens, D., Keijers, S., Vyverman, W., Goddeeris, B., De Meester, L., Brendonck, L., and Martens, K., 2006. Ecological characteristic's of small farmland ponds: Associations with land use practices at multiple spatial scales. Biological Conservation, 131(4): 523-532.

DeLaune, P.B., Moore, P.A., Carman, D.K., Sharpley, A.N., Haggard, B.E., and Daniel, T.C., 2004a. Development of a phosphorus index for pastures fertilized with poultry litter - Factors affecting phosphorus runoff. Journal of Environmental Quality, 33(6): 2183-2191.

DeLaune, P.B.. Moore, P.A., Carman, D.K., Sharpley, A.N., Haggard, B.E., and Daniel, T.C., 2004b. Evaluation of the phosphorus source component in the phosphorus index for pastures. Journal of Environmental Quality, 33(6): 2192-2200.

Dillon, P.J. and Kirchner, W.B., 1975. Effects of geology and land-use on export of phosphorus from watersheds. Water Research, 9(2): 135-148.

Dils, R.M. and Heathwaite, A.L., 1998. Development of an iron oxide-impregnated paper strip technique for the determination of bioavailable phosphorus in runoff. Water Research, 32(5): 1429-1436.

Dolan, D.M., Yui, A.K. and Geist, R.D., 1981. Evaluation of river load estimation methods for total phosphorus. Journal of Great Lakes Research, 7(3): 207-214.

Dougherty, W.J., Fleming, N.K., Cox, J.W. and Chittleborough, D.J., 2004. Phosphorus transfer in surface runoff from intensive pasture systems at various scales: A review. Journal of Environmental Quality, 33(6): 1973-1988.

Duan, N., 1983. Smearing estimate: A nonparametric retransformation method. Journal of the American Statistical Association, 78(383): 605-610.

Dunne, T. and Black, R.D., 1970a. An experimental investigation of runoff production in permeable soils. Water Resources Research, 6(2): 478-490.

Dunne, T. and Black, R.D., 1970b. Partial area contributions to storm runoff in a small New England watershed. Water Resources Research, 6(5): 1296-1311.

Edwards, A.C. and Withers, P.J.A., 1998. Soil phosphorus management and water quality: a UK perspective. Soil Use and Management, 14: 124-130.

Edwards, D.R. and Daniel, T.C., 1993. Effects of poultry litter application rate and rainfall intensity on quality of runoff from fescuegrass plots. Journal of Environmental Quality, 22(2): 361-365.

Edwards, D.R. and Daniel, T.C., 1994. Quality of runoff from fescuegrass plots treated with poultry litter and inorganic fertilizer. Journal of Environmental Quality, 23(3): 579-584.

Edwards, D.R., Daniel, T.C., Murdoch, J.E. and Moore, P.A., 1996. Quality of runoff from four northwest Arkansas pasture fields treated with organic and inorganic fertilizer. Transactions of the ASAE, 39(5): 1689-1696.

Eghball, B., Wienhold, B.J., Gilley, J.E. and Eigenberg, R.A., 2002. Mineralization of manure nutrients. Journal of Soil and Water Conservation, 57(6): 470-473.

Eisenbies, M.H., Aust, W.M., Burger, J.A. and Adams, M.B., 2007. Forest operations, extreme flooding events, and considerations for hydrologic modeling in the Appalachians - A review. Forest Ecology and Management, 242(2-3): 77-98.

Elser, J.J., Marzolf, E.R. and Goldman, C.R., 1990. Phosphorus and nitrogen limitation of phytoplankton growth in the freshwaters of North America: a review and critique of experimental enrichments. Canadian Journal of Fisheries and Aquatic Sciences, 47(7): 1468-1477.

Endale, D.M., Fisher, D.S. and Schomberg, H.H., 2006. Soil water regime in space and time in a small Georgia piedmont catchment under pasture. Soil Science Society of America Journal, 70(1): 1-13.

ESRI, 1999. ArcView GIS 3.2. Available at http://www.esri.com.

ESRI, 2006. ArcMap Version 9.2. Available at http://www.esri.com.

Etowah Aquatic Habitat Conservation Plan Steering Committee, 2007. Draft Etowah Aquatic Habitat Conservation Plan. August 15, 2007. Available at http:///www.etowahhcp.org.

Ferguson, R.I., 1986a. River loads underestimated by rating curves. Water Resources Research, 22(1): 74-76.

Ferguson, R.I., 1986b. River loads underestimated by rating curves - reply. Water Resources Research, 22(13): 2123-2124.

Ferguson, R.I., 1987. Accuracy and precision of methods for estimating river loads. Earth Surface Processes and Landforms, 12(1): 95-104.

Fischer, H.B., List, E.J., Koh, R.C.Y., Imberger, I. and Brooks, N.H., 1979. Mixing in Inland and Coastal Waters. Academic Press, New York, 483 pp.

Fleming, N.K. and Cox, J.W., 1998. Chemical losses off dairy catchments located on a texture-contrast soil: Carbon, phosphorus, sulfur, and other chemicals. Australian Journal of Soil Resources, 36: 979-995.

Gburek, W.J. and Sharpley, A.N., 1998. Hydrologic controls on phosphorus loss from upland agricultural watersheds. Journal of Environmental Quality, 27(2): 267-277.

Gburek, W.J., Sharpley, A.N., Heathwaite, L. and Folmar, G.J., 2000. Phosphorus management at the watershed scale: a modification of the phosphorus index. Journal of Environmental Quality, 29(1): 130-144.

Georgia Geologic Survey, 1976. Geologic Map of Georgia. State Map 3 (1:500,000).

Georgia State Climate Office, 1998a. Climatology of Georgia Mountains. Driftmeir Engineering Center, University of Georgia, Athens. Available at http://www.bae.uga.edu/climate.

Georgia State Climate Office, 1998b. Climatology of Georgia Piedmont. Driftmeier Engineering Center, University of Georgia, Athens. Available at http://www.bae.uga.edu/climate.

Giddens, J. and Barnett, A.P., 1980. Soil loss and microbiological quality of runoff from land treated with poultry litter. Journal of Environmental Quality, 9(3): 518-520.

Gilley, J.E. and Risse, L.M., 2000. Runoff and soil loss as affected by the application of manure. Transactions of the ASAE, 43(6): 1583-1588.

Gilroy, E.J., Hirsch, R.M. and Cohn, T.A., 1990. Mean square error of regression-based constituent transport estimates. Water Resources Research, 26(9): 2069-2077.

Glysson, G.D., 1987. Sediment transport curves. U.S. Geological Survey Open File Report 87-218. U.S. Geological Survey, 47 pp.

Google, 2008. Google Earth Version 4.3. Available at http://earth.google.com.

Grant, D.M. and Dawson, B.D., 2001. Isco Open Channel Flow Measurement Handbook. Isco, Inc., Lincoln, Nebraska, 501 pp.

Guo, Y.P., Markus, M. and Demissie, M., 2002. Uncertainty of nitrate-N load computations for agricultural watersheds. Water Resources Research, 38(10).

Haggard, B.E., Ekka, S.A., Matlock, M.D. and Chaubey, I., 2004. Phosphate equilibrium between stream sediments and water: Potential effect of chemical amendments. Transactions of the ASAE, 47(4): 1113-1118.

Haggard, B.E., Moore, P.A., Chaubey, I. and Stanley, E.H., 2003. Nitrogen and phosphorus concentrations and export from an Ozark Plateau catchment in the United States. Biosystems Engineering, 86(1): 75-85.

Harmel, R.D., King, K.W., Haggard, B.E., Wren, D.G. and Sheridan, J.M., 2006a. Practical guidance for discharge and water quality data collection on small watersheds. Transactions of the ASABE, 49(4): 937-948.

Harmel, R.D., Cooper, R.J., Slade, R.M., Haney, R.L. and Arnold, J.G., 2006b. Cumulative uncertainty in measured streamflow and water quality data for small watersheds. Transactions of the ASABE, 49(3): 689-701.

Harmel, R.D., King, K.W. and Slade, R.M., 2003. Automated storm water sampling on small watersheds. Applied Engineering in Agriculture, 19(6): 667-674.

Harmel, R.D., Torbert, H.A., Haggard, B.E., Haney, R. and Dozier, M., 2004. Water quality impacts of converting to a poultry litter fertilization strategy. Journal of Environmental Quality, 33(6): 2229-2242.

Hart, M.R., Quin, B.F. and Nguyen, M.L., 2004. Phosphorus runoff from agricultural land and direct fertilizer effects: A review. Journal of Environmental Quality, 33(6): 1954-1972.

Haygarth, P.M., Bilotta, G.S., Bol, R., Brazier, R.E., Butler, P.J., Freer, J., Gimbert, L.J., Granger, S.J., Krueger, T., Macleod, C.J.A., Naden, P., Old, G., Quinton, J.N., Smith, B., and Worsfold, P., 2006. Processes affecting transfer of sediment and colloids, with associated phosphorus, from intensively farmed grasslands: an overview of key issues. Hydrological Processes, 20(20): 4407-4413.

Haygarth, P.M., Chapman, P.J., Jarvis, S.C. and Smith, R.V., 1998. Phosphorus budgets for two contrasting grassland farming systems in the UK. Soil Use and Management, 14: 160-167.

Haygarth, P.M., Condron, L.M., Heathwaite, A.L., Turner, B.L. and Harris, G.P., 2005b. The phosphorus transfer continuum: Linking source to impact with an interdisciplinary and multi-scaled approach. Science of the Total Environment, 344(1-3): 5-14.

Haygarth, P.M. and Jarvis, S.C., 1997. Soil derived phosphorus in surface runoff from grazed grassland lysimeters. Water Research, 31(1): 140-148.

Haygarth, P.M. and Sharpley, A.N., 2000. Terminology for phosphorus transfer. Journal of Environmental Quality, 29(1): 10-15.

Haygarth, P.M., Wood, F.L., Heathwaite, A.L. and Butler, P.J., 2005a. Phosphorus dynamics observed through increasing scales in a nested headwater-to-river channel study. Science of the Total Environment, 344(1-3): 83-106.

Heathwaite, A.L., 1997. Sources and pathways of phosphorus loss from agriculture. In: H. Tunney, O.T. Carton, E.S. Brookes and A.E. Johnston (Editors), Phosphorus Loss from Soil to Water. CAB International, New York, pp. 205-223.

Heathwaite, A.L. and Dils, R.M., 2000. Characterising phosphorus loss in surface and subsurface hydrological pathways. Science of the Total Environment, 251: 523-538.

Heathwaite, L., Sharpley, A. and Gburek, W., 2000. A conceptual approach for integrating phosphorus and nitrogen management at watershed scales. Journal of Environmental Quality, 29(1): 158-166.

Heckrath, G., Bechmann, M., Ekholm, P., Ulen, B., Djodjic, F., and Andersen, H. E., 2008. Review of indexing tools for identifying high risk areas of phosphorus loss in Nordic catchments. Journal of Hydrology, 349(1-2): 68-87.

Heckrath, G., Brookes, P.C., Poulton, P.R. and Goulding, K.W.T., 1995. Phosphorus leaching from soils containing different phosphorus concentrations in the Broadbalk Experiment. Journal of Environmental Quality, 24(5): 904-910.

Hecky, R.E. and Kilham, P., 1988. Nutrient limitation of phytoplankton in freshwater and marine environments: a review of recent evidence on the effects of enrichment. Limnology and Oceanography, 33(4): 796-822.

Helsel, D.R. and Hirsch, R.M., 2002. Statistical Methods in Water Resources. Techniques of Water-Resources Investigations of the United States Geological Survey, Book 4, Hydrologic Analysis and Interpretation, Chapter A3. U.S. Department of the Interior, U.S. Geological Survey. Available at: http://pubs.usgs.gov/twri/twri4a3-new.pdf.

Hess, P., Eisenhauer, B. and Joern, B., 2007. Challenges to using and implementing phosphorus indices in nutrient management planning: an MMP perspective. In: M.L. Cabrera and D.E. Radcliffe (Editors), Modeling Phosphorus in the Environment. CRC Press, Inc., Boca Raton, Florida, pp. 333-349.

Hewlett, J.D., 1982. Principles of Forest Hydrology. University of Georgia Press, Athens, Georgia, 183 pp.

Hewlett, J.D. and Bosch, J.M., 1984. The dependence of storm flows on rainfall intensity and vegetal cover in South Africa. Journal of Hydrology, 75(1-4): 365-381.

Hewlett, J.D. and Hibbert, A.R., 1967. Factors affecting the response of small watersheds to precipitation in humid areas. In: W.L. Sopper and H.W. Lull (Editors), International Symposium on Forest Hydrology, Pergamon, Oxford, pp. 275-290.

Hirsch, R.M., Helsel, D.R., Cohn, T.A. and Gilroy, E.J., 1993. Statistical analysis of hydrologic data. In: D.R. Maidment (Editor), Handbook of Hydrology. McGraw-Hill, Inc., New York.

Hively, W.D., Bryant, R.B. and Fahey, T.J., 2005. Phosphorus concentrations in overland flow from diverse locations on a New York dairy farm. Journal of Environmental Quality, 34(4): 1224-1233.

Hobbie, J.E. and Likens, G.E., 1973. Output of phosphorus, dissolved organic carbon, and fine particulate carbon from Hubbard Brook watersheds. Limnology and Oceanography, 18(5): 734-742.

Hofmann, L. and Ries, R.E., 1991. Relationship of soil and plant characteristics to erosion and runoff on pasture and range. Journal of Soil and Water Conservation, 46: 143-147.

Horowitz, A.J., 1995. The Use of Suspended Sediment and Associated Trace Elements in Water Quality Studies. International Association of Hydrological Sciences Special Publication No. 4. IAHS Press, Wallingford, Oxfordshire, United Kingdom, 58 pp.

Horowitz, A.J., 2003. An evaluation of sediment rating curves for estimating suspended sediment concentrations for subsequent flux calculations. Hydrological Processes, 17(17): 3387-3409.

Howarth, R.W., 1988. Nutrient limitation of net primary production in marine ecosystems. Annual Review of Ecology and Systematics, 19: 89-110.

Hsu, P.A., 1977. Aluminum hydroxides and oxyhydroxides. In: J.B. Dixon and S.B. Weed (Editors), Minerals in Soil Environments. Soil Science Society of America, Madison, Wisconsin, pp. 99-143.

Huneycutt, H.G., West, C.P. and Phillips, J.M., 1988. Responses of bermudagrass, tall fescue, and tall fescue-clover to broiler litter and commercial fertilizer. Arkansas Experimental Station Bulletin 913. University of Arkansas, Fayetteville.

Isaac, R. A. and W. C. Johnson. 1983. High speed analysis of agricultural samples using inductively coupled plasma-atomic emission spectroscopy. Spectrochemica Acta. 38B: 277-282.

Johnes, P.J., 2007. Uncertainties in annual riverine phosphorus load estimation: Impact of load estimation methodology, sampling frequency, baseflow index and catchment population density. Journal of Hydrology, 332(1-2): 241-258.

Johnson, A.H., 1979. Estimating solute transport in streams from grab samples. Water Resources Research, 15(5): 1224-1228.

Jordan, D.H., Bramlett, G.L., Gaither, G.A., R.J. Tate, B., M.M. and Murphy, J.O., 1973. Soil Survey of Cherokee, Gilmer, and Pickens Counties, Georgia. U.S. Department of Agriculture Soil Conservation Service. U.S. Government Printing Office, Washington, D.C. 73 p.

Jordan, T.E., Correll, D.L. and Weller, D.E., 1993. Nutrient interception by a riparian forest receiving inputs from adjacent cropland. Journal of Environmental Quality, 22: 467-473.

King, K.W., Harmel, R.D. and Fausey, N.R., 2005. Development and sensitivity of a method to select time- and flow-paced storm event sampling intervals for headwater streams. Journal of Soil and Water Conservation, 60(6): 323-331.

Kingery, W.L., Wood, C.W., Delaney, D.P., Williams, J.C. and Mullins, G.L., 1994. Impact of long-term land application of broiler litter on environmentally related soil properties. Journal of Environmental Quality, 23(1): 139-147.

Kleinman, P.J.A. and Sharpley, A.N., 2003. Effect of broadcast manure on runoff phosphorus concentrations over successive rainfall events. Journal of Environmental Quality, 32(3): 1072-1081.

Kleinman, P.J.A., Sharpley, A.N., Moyer, B.G. and Elwinger, G.F., 2002. Effect of mineral and manure phosphorus sources on runoff phosphorus. Journal of Environmental Quality, 31(6): 2026-2033.

Koch, R.W. and Smillie, G.M., 1986a. Bias in hydrologic prediction using log-transformed regression-models. Water Resources Bulletin, 22(5): 717-723.

Koch, R.W. and Smillie, G.M., 1986b. River loads underestimated by rating curves - comment. Water Resources Research, 22(13): 2121-2122.

Koroleff, F., 1983. Simultaneous oxidation of nitrogen and compounds by persulfate. In: K. Grasshoff, M. Eberhardt and K. Kremling (Editors), Methods of Seawater Analysis. Verlag Chemie, Weinheimer, FRG, pp. 168-169.

Kronvang, B., Bechmann, M., Pedersen, M.L. and Flynn, N., 2003. Phosphorus dynamics and export in streams draining micro-catchments: Development of empirical models. Journal of Plant Nutrition and Soil Science-Zeitschrift Fur Pflanzenernahrung Und Bodenkunde, 166(4): 469-474.

Kronvang, B. and Bruhn, A.J., 1996. Choice of sampling strategy and estimation method for calculating nitrogen and phosphorus transport in small lowland streams. Hydrological Processes, 10(11): 1483-1501.

Kutner, M.H., Nachtsheim, C.J. and Neter, J., 2004. Applied Linear Regression Models. McGraw-Hill Irwin, New York, 698 pp.

Kuykendall, H.A., Cabrera, M.L., Hoveland, C.S., McCann, M.A. and West, L.T., 1999. Stocking method effects on nutrient runoff from pastures fertilized with broiler litter. Journal of Environmental Quality, 28(6): 1886-1890.

Lampert, W. and Sommer, U., 1997. Limnoecology: The ecology of lakes and streams. Oxford University Press, New York, 382 pp.

Lander, C.H., Moffitt, D. and Alt, K., 1998. Nutrients available from livestock manure relative to crop growth requirements. Resource Assessment and Strategic Planning Working Paper 98-1, U.S. Department of Agriculture Natural Resources Conservation Service, 38 pp.

Larson, S.J., Capel, P.D. and Goolsby, D.A., 1995. Relations between pesticide use and riverine flux in the Mississippi River basin. Chemosphere, 31(5): 3305-3321.

Laubel, A., Kronvang, B., Hald, A.B. and Jensen, C., 2003. Hydromorphological and biological factors influencing sediment and phosphorus loss via bank erosion in small lowland rural streams in Denmark. Hydrological Processes, 17(17): 3443-3463.

Lefrancois, J., Grimaldi, C., Gascuel-Odoux, C. and Gilliet, N., 2007. Suspended sediment and discharge relationships to identify bank degradation as a main sediment source on small agricultural catchments. Hydrological Processes, 21(21): 2923-2933.

Leh, M.D., Chaubey, I., Murdoch, J., Brahana, J.V. and Haggard, B.E., 2008. Delineating runoff processes and critical source areas in a pasture hillslope of the Ozark Highlands. Hydrological Processes, 22. DOI: 10.1002/hyp.7021.

Lemunyon, J.L. and Gilbert, R.G., 1993. The concept and need for a phosphorus assessment-tool. Journal of Production Agriculture, 6(4): 483-486.

Likens, G.E., Bormann, F.H., Pierce, R.S., Eaton, J.S. and Johnson, N.M., 1977. Biogeochemistry of a forested ecosystem. Springer-Verlag, New York.

Ludwig, B., Boiffin, J., Chadoeuf, J. and Auzet, A.V., 1995. Hydrological structure and erosion damage caused by concentrated flow in cultivated catchments. Catena, 25(1-4): 227-252.

Lyon, S.W., McHale, M.R., Walter, M.T. and Steenhuis, T.S., 2006. The impact of runoff generation mechanisms on the location of critical source areas. Journal of the American Water Resources Association, 42(3): 793-804.

Martin, J.L. and McCutcheon, S.C., 1999. Hydrodynamics and Transport for Water Quality Modeling. Lewis Publishers, Boca Raton, Florida, 794 pp.

Masuda, K. and Boyd, C.E., 1994. Phosphorus fractions in soil and water of aquaculture ponds built on clayey Ultisols at Auburn, Alabama. Journal of the World Aquaculture Society, 25(3): 379-395.

Mays, D.A., Wilkinson, S.R. and Cole, C.V., 1980. Phosphorus nutrition of forages. In: F.E. Khasawneh, E.C. Sample and E.J. Kamprath (Editors), The Role of Phosphorus in Agriculture. ASA-CSSA-SSSA, Madison, Wisconsin, pp. 805-846.

McCuen, R.H., 2005. Hydrologic analysis and design. Pearson Prentice Hall, Upper Saddle River, N.J., xix, 859 pp.

McDonnell, J.J., 1990. A rationale for old water discharge through macropores in as steep, humid catchment. Water Resources Research, 26(11): 2821-2832.

McDonnell, J.J., 2003. Where does water go when it rains? Moving beyond the variable source area concept of rainfall-runoff response. Hydrological Processes, 17(9): 1869-1875.

McDonnell, J.J. and Woods, R., 2004. On the need for catchment classification. Journal of Hydrology, 299(1-2): 2-3.

McDowell, R. and Trudgill, S., 2000. Variation of phosphorus loss from a small Catchment in south Devon, UK. Agriculture, Ecosystems & Environment, 79(2-3): 143-157.

McDowell, R.W., Muirhead, R.W. and Monaghan, R.M., 2006. Nutrient, sediment, and bacterial losses in overland flow from pasture and cropping soils following cattle dung deposition. Communications in Soil Science and Plant Analysis, 37(1-2): 93-108.

McDowell, R.W., Nash, D.M. and Robertson, F., 2007. Sources of phosphorus lost from a grazed pasture receiving simulated rainfall. Journal of Environmental Quality, 36(5): 1281-1288.

McDowell, R.W. and Sharpley, A.N., 2001. Approximating phosphorus release from soils to surface runoff and subsurface drainage. Journal of Environmental Quality, 30(2): 508-520.

McDowell, R.W. and Sharpley, A.N., 2003. Uptake and release of phosphorus from overland flow in a stream environment. Journal of Environmental Quality, 32(3): 937-948.

McDowell, R.W. and Wilcock, R.J., 2007. Sources of sediment and phosphorus in stream flow of a highly productive dairy farmed catchment. Journal of Environmental Quality, 36(2): 540-548.

McIntyre, C.L., 1972. Soil Survey for Dawson, Lumpkin, and White Counties, Georgia. U.S. Department of Department of Agriculture Soil Conservation Service. U.S. Government Printing Office, Washington, D.C. 106 p.

McLaughlin, K., Kendall, C., Silva, S.R., Young, M. and Paytan, A., 2006. Phosphate oxygen isotope ratios as a tracer for sources and cycling of phosphate in North San Francisco Bay, California. Journal of Geophysical Research-Biogeosciences, 111(G3).

Mehlich, A., 1953. Determination of P, K, Ca, Mg, and NH4. Soil Testing Division, North Carolina Department of Agriculture, Raleigh. Available at http://www.ncagr.com/agronomi/pdffiles/mehlich53.pdf.

Mendenhall, W. and Sincich, T., 2003. Regression Analysis. Pearson Education, Inc., Upper Saddle River, New Jersey, 880 pp.

Meyer, J.L., 1979. Role of sediments and bryophytes in phosphorus dynamics in a headwater stream ecosystem. Limnology and Oceanography, 24(2): 365-375.

Meyer, J.L. and Likens, G.E., 1979. Transport and transformation of phosphorus in a forest stream ecosystem. Ecology, 60(6): 1255-1269.

Miller, D.M., 1984. Reducing transformation bias in curve fitting. The American Statistician, 38(2): 124-126.

Moldan, B. and Cerny, J., 1994. Small catchment research. In: B. Moldan and J. Cerny (Editors), Biogeochemistry of Small Catchments. Chichester, West Sussex, England, John Wiley & Sons, Inc., pp. 1-29.

Monk, C.D. and Day, J., F.P., 1988. Biomass, primary production, and selected nutrient budgets for an undisturbed hardwood watershed. In: W.T. Swank and J. Crossley, D.A. (Editors), Forest Hydrology and Ecology at Coweeta. Springer-Verlag, New York, pp. 151-160.

Moore, P.A., Daniel, T.C., Sharpley, A.N. and Wood, C.W., 1995. Poultry manure management - environmentally sound options. Journal of Soil and Water Conservation, 50(3): 321-327.

Moore, P.A.J., Daniel, T.C. and Edwards, D.R., 2000. Reducing phosphorus runoff an inhibiting ammonia loss from poultry manure with aluminum sulfate. Journal of Environmental Quality, 29: 37-49.

Moussa, R., Voltz, M. and Andrieux, P., 2002. Effects of the spatial organization of agricultural management on the hydrological behaviour of a farmed catchment during flood events. Hydrological Processes, 16(2): 393-412.

Murphy, J. and Riley, J.P., 1962. A modified single solution method for determination of phosphate in natural waters. Analytica Chimica Acta, 26(1): 31-36.

Nair, V.D. and Harris, W.G., 2004. A capacity factor as an alternative to soil test phosphorus in phosphorus risk assessment. New Zealand Journal of Agricultural Research, 47(4): 491-497.

National Research Council, 1994. Nutrient Requirements of Poultry: Ninth Revised Edition. National Academy Press, Washington, D.C.

Newbold, J.D., Elwood, J.W., Oneill, R.V. and Vanwinkle, W., 1981. Measuring nutrient spiralling in streams. Canadian Journal of Fisheries and Aquatic Sciences, 38(7): 860-863.

Nutter, W.L., 1973. The role of soil water in the hydrologic behavior of upland basins, Field Soil Moisture Regime. Soil Science Society of America, pp. 181-193.

Ocampo, C.J., Sivapalan, M. and Oldham, C., 2006. Hydrological connectivity of upland-riparian zones in agricultural catchments: Implications for runoff generation and nitrate transport. Journal of Hydrology, 331(3-4): 643-658.

Omernik, J.M., 1987. Ecoregions of the coterminous United Stated. Annals of the Associatoin of American Geographers, 77(1): 118-125.

Osmond, D.L., Cabrera, M.L., Feagley, S.E., Hardee, G.E., Mitchell, C.C., Moore, P.A., Mylavarapu, R.S., Oldham, J.L., Stevens, J.C., Thom, W.C., Walker, F., and Zhang, H., 2006. Comparing ratings of the southern phosphorus indices. Journal of Soil and Water Conservation, 61(6): 325-337.

Page, T., Haygarth, P.M., Beven, K.J., Joynes, A., Butler, T., Keeler, C., Freer, J., Owens, P.N., and Wood, G.A., 2005. Spatial variability of soil phosphorus in relation to the topographic index and critical source areas: Sampling for assessing risk to water quality. Journal of Environmental Quality, 34(6): 2263-2277.

Parker, A.K., 2004. The Role of Iron-Rich Sediment in the Biogeochemical Cycling of Phosphorus in Georgia Piedmont Impoundments. Ph.D. Dissertation, University of Georgia, Athens, 119 pp.

Pearce, A.J., Stewart, M.K. and Sklash, M.G., 1986. Storm runoff generation in humid headwater catchments 1. Where does the water come from? Water Resources Research, 22(8): 1263-1272.

Phillips, J.M., Webb, B.W., Walling, D.E. and Leeks, G.J.L., 1999. Estimating the suspended sediment loads of rivers in the LOIS study area using infrequent samples. Hydrological Processes, 13(7): 1035-1050.

Pierson, S.T., Cabrera, M.L., Evanylo, G.K., Kuykendall, H.A., Hoveland, C.S., McCann, M.A., and West, L.T., 2001. Phosphorus and ammonium concentrations in surface runoff from grasslands fertilized with broiler litter. Journal of Environmental Quality, 30(5): 1784-1789.

Pionke, H.B., Gburek, W.J. and Sharpley, A.N., 2000. Critical source area controls on water quality in an agricultural watershed located in the Chesapeake Basin. Ecological Engineering, 14(4): 325-335.

Pionke, H.B., Gburek, W.J., Sharpley, A.N. and Schnabel, R.R., 1996. Flow and nutrient export patterns for an agricultural hill-land watershed. Water Resources Research, 32(6): 1795-1804.

Pionke, H.B., Gburek, W.J., Sharpley, A.N. and Zollweg, J.A., 1997. Hydrological and chemical controls on phosphorus loss from catchments, Phosphorus Loss from Soil to Wate. CAB International, Wallingford, U.K., pp. 225-242.

Pionke, H.B., Hoover, J.R., Schnabel, R.R., Gburek, W.J., Urban, J.B.. and Rogowski, A.S., 1988. Chemical-hydrologic interactions in the near-stream zone. Water Resources Research, 24(7): 1101-1110.

Porter, K., Saunders, P., Haberyan. K., Macubbin, A., Jacobsen, T., and Hodson, R., 2004. Annual cycle of autotrophic and heterotrophic production in a small, monomictic Piedmont lake (Lake Oglethorpe): analog for the effects of climatic warming on dimictic lakes. Limnology and Oceanography, 41(5): 1041-1051.

Pote, D.H., Daniel, T.C., Nichols, D.J., Moore, P.A., Miller, D.M., and Edwards, D.R., 1999a. Seasonal and soil-drying effects on runoff phosphorus relationships to soil phosphorus. Soil Science Society of America Journal, 63(4): 1006-1012.

Pote, D.H., Daniel, T.C., Nichols, D.J., Sharpley, A.N., Moore, P.A., Miller, D.M., and Edwards, D.R., 1999b. Relationship between phosphorus levels in three Ultisols and phosphorus concentrations in runoff. Journal of Environmental Quality, 28(1): 170-175.

Preston, S.D., Bierman, V.J. and Silliman, S.E., 1989. An evaluation of methods for estimation of tributary mass loads. Water Resources Research, 25(6): 1379-1389.

Qualls, R.G., 1989. Determination of total nitrogen and phosphorus using persulfate oxidation: a modification for small sample volumes using the method of Koroleff (1983). Ph.D. dissertation Thesis, University of Georgia, Athens, GA.

Qualls, R.G., 2000. Comparison of the behavior of soluble organic and inorganic nutrients in forest soils. Forest Ecology and Management, 138(1-3): 29-50.

Qualls, R.G. and Haines, B.L., 1991. Geochemistry of dissolved organic nutrients in water percoloating through a forest ecosystem. Soil Science Society of America Journal, 55(4): 1112-1123.

Qualls, R.G., Haines, B.L. and Swank, W.T., 1991. Fluxes of dissolved organic nutrients and humic substances in a deciduous forest. Ecology, 72(1): 254-266.

Rabalais, N.N., 2002. Nitrogen in aquatic ecosystems. Ambio, 31(2): 102-112.

Radcliffe, D.E. and Cabrera, M.L., 2007. Suggestions to improve modeling of phosphorus. In: D.E. Radcliffe and M.L. Cabrera (Editors), Modeling Phosphorus in the Environment. CRC Press, Boca Raton, Florida, pp. 405-415.

Radcliffe, D.E. and Lin, Z., 2007. Modeling phosphorus with Hydrologic Simulation Program-Fortran. In: M.L. Cabrera and D.E. Radcliffe (Editors), Modeling Phosphorus in the Environment. CRC Press, Inc., Boca Raton, Florida, pp. 189-214.

Radcliffe, D.E. and West, C.P., 2000. MLRA 136: Southern Piedmont. In: Water and Chemical Transport in Soils of the Southeastern U.S. Southern Cooperative Series Bulletin #395. Available at http://soilphysics.okstate.edu/S257/cover.html

Ragan, R.M., 1967. An experimental investigation of partial area contributions. International Association of Scientific Hydrology, 76: 241-251.

Raschke, R.L., 1993. Guidelines for assessing and predicting eutrophication status of small southeastern piedmont impoundments. Environmental Services Division, U.S. Environmental Protection Agency, Athens, Georgia.

Raschke, R.L., 1994. Phytoplankton bloom frequencies in a population of small southeastern impoundments. Lake and Reservoir Management, 8(2): 205-210.

Rasmussen, T.C., 2001. Determination of average concentrations and loads. Unpublished manuscript.

Rekolainen, S., Posch, M., Kamari, J. and Ekholm, P., 1991. Evaluation of the accuracy and precision of annual phosphorus load estimates from 2 agricultural basins in Finland. Journal of Hydrology, 128(1-4): 237-255.

Ribaudo, M.O., Gollehon, N.R. and Agapoff, J., 2003. Land application of manure by animal feeding operations: Is more land needed? Journal of Soil and Water Conservation, 58(1): 30-38.

Richards, R.P., 1989. Measures of flow variability for Great Lakes tributaries. Environmental Monitoring and Assessment, 13(2-3): 361-377.

Richards, R.P. and Holloway, J., 1987. Monte-Carlo studies of sampling strategies for estimating tributary loads. Water Resources Research, 23(10): 1939-1948.

Ritter, D.F., 1978. Process Geomorphology. Wm. C. Brown, Dubuqe, Iowa, 603 pp.

Robertson, D.M., 2003. Influence of different temporal sampling strategies on estimating total phosphorus and suspended sediment concentration and transport in small streams. Journal of the American Water Resources Association, 39(5): 1281-1308.

Robertson, D.M. and Roerish, E.D., 1999. Influence of various water quality sampling strategies on load estimates for small streams. Water Resources Research, 35(12): 3747-3759.

Robinson, J.S. and Sharpley, A.N., 1995. Release of nitrogen and phosphorus from poultry litter. Journal of Environmental Quality, 24(1): 62-67.

Rostagno, C.M., 1989. Infiltration and sediment production as affected by soil surface conditions in a shrubland of Patagonia, Argentina. Journal of Range Management, 42(5): 382-385.

Ruan, H.D. and Gilkes, R.J., 2000. Phosphorus accumulation in farm ponds and dams in southwestern Australia. Journal of Environmental Quality, 29(6): 1875-1881.

Runkel, R.L., Crawford, C.G. and Cohn, T.A., 2004. Load Estimator (LOADEST): a FORTRAN program for estimating constituent loads in streams and rivers. U.S. Geological Survey Techniques and Methods Book 4, Chapter A5. U.S. Department of the Interior, pp. 75.

Sanchez, P.A. and Uehara, G., 1980. Management considerations for acid soils with phosphorus fixation capacity. In: F.E. Khasawneh, E.C. Sample and E.J. Kamprath (Editors), The Role of Phosphorus in Agriculture. ASA-CSSA-SSSA, Madison, Wisconsin, pp. 655-680.

SAS Institute, Inc., 2003. SAS for Windows, v. 9.1, Cary, N.C.

Sauer, T.J., Daniel, T.C., Moore, P.A., Coffey, K.P., Nichols, D.J., and West, C.P., 1999. Poultry litter and grazing animal waste effects on runoff water quality. Journal of Environmental Quality, 28(3): 860-865.

Sauer, T.J., Daniel, T.C., Nichols, D.J., West, C.P., Moore, P.A., and Wheeler, G.L., 2000. Runoff water quality from poultry litter-treated pasture and forest sites. Journal of Environmental Quality, 29(2): 515-521.

Schärer, M., Page, T. and Beven, K., 2006. A fuzzy decision tree to predict phosphorus export at the catchment scale. Journal of Hydrology, 331(3-4): 484-494.

Schindler, D.W., 1977. Evolution of phosphorus limitation in lakes. Science, 195(4275): 260-262.

Schleppi, P., Waldner, P.A. and Fritschi, B., 2006. Accuracy and precision of different sampling strategies and flux integration methods for runoff water: comparisons based on measurements of the electrical conductivity. Hydrological Processes, 20(2): 395-410.

Schoonover, J.E., Lockaby, B.G. and Helms, B.S., 2006. Impacts of land cover on stream hydrology in the west Georgia piedmont, USA. Journal of Environmental Quality, 35(6): 2123-2131.

Schroeder, P.D., Radcliffe, D.E., Cabrera, M.L. and Belew, C.D., 2004a. Relationship between soil test phosphorus and phosphorus in runoff: Effects of soil series variability. Journal of Environmental Quality, 33(4): 1452-1463.

Schroeder, P.D., Radcliffe, D.E. and Cabrera, M.L., 2004b. Rainfall timing and poultry litter application rate effects on phosphorus loss in surface runoff. Journal of Environmental Quality, 33(6): 2201-2209.

Schwartz, S.S. and Naiman, D.Q., 1999. Bias and variance of planning level estimates of pollutant loads. Water Resources Research, 35(11): 3475-3487.

Schwertmann, U. and Taylor, R.M., 1977. Iron oxides. In: J.B. Dixon and S.B. Weed (Editors), Minerals in Soil Environments. Soil Science Society of America, Madison, Wisconsin, pp. 145-180.

Searcy, J.K., 1959. Flow-duration curves. Water-Supply Paper 1542-A. Manual of Hydrology: Part 2. Low-Flow Techniques. U.S. Geological Survey. Washington, D.C.

Semkin, R.G., Jeffries, D.S. and Clair, T.A., 1994. Hydrochemical methods and relationships for study of stream output from small catchments. In: B. Moldan and J. Cerny (Editors), Biogeochemistry of Small Catchments. John Wiley and Sons, Inc., Chichester, West Sussex, England, pp. 163-187.

Sharpley, A.N., 1985. Depth of surface soil-runoff interaction as affected by rainfall, soil slope, and management. Soil Science Society of America Journal, 49: 1010-1015.

Sharpley, A.N., 1995. Soil phosphorus dynamics: agronomic and environmental impacts. Ecological Engineering, 5(2-3): 261-279.

Sharpley, A.N., 1997. Rainfall frequency and nitrogen and phosphorus runoff from soil amended with poultry litter. Journal of Environmental Quality, 26(4): 1127-1132.

Sharpley, A.N., 2003. Soil mixing to decrease surface stratification of phosphorus in manured soils. Journal of Environmental Quality, 32(4): 1375-1384.

Sharpley, A.N., 2007. Modeling phosphorus movement from agriculture to surface waters. In: D.E. Radcliffe and M.L. Cabrera (Editors), Modeling Phosphorus in the Environment. CRC Press, Boca Raton, Florida, pp. 3-19.

Sharpley, A.N., Ahuja, L.R., Yamamoto, M. and Menzel, R.G., 1981a. The kinetics of phosphorus desorption from soil. Soil Science Society of America Journal, 45(3): 493-496.

Sharpley, A.N., Ahuja, L.R. and Menzel, R.G., 1981b. The release of soil phosphorus to runoff in relation to the kinetics of desorption. Journal of Environmental Quality, 10(3): 386-391.

Sharpley, A.N., Chapra, S.C., Wedepohl, R., Sims, J.T.,Daniel, T.C., and Reddy, K.R., 1994. Managing agricultural phosphorus for protection of surface waters - issues and options. Journal of Environmental Quality, 23(3): 437-451.

Sharpley, A.N, Foy, B. and Withers, P., 2000. Practical and innovative measures for the control of agricultural phosphorus losses to water: An overview. Journal of Environmental Quality, 29(1): 1-9.

Sharpley, A.N., Gburek, W.J., Folmar, G. and Pionke, H.B., 1999. Sources of phosphorus exported from an agricultural watershed in Pennsylvania. Agricultural Water Management, 41(2): 77-89.

Sharpley, A.N. and Halvorson, A.D., 1994. The management of soil phosphorus availability and its impact on surface water quality. In: R. Lal and B.A. Stewart (Editors), Soil Processes and Water Quality. Lewis Publishers, Boca Raton, Florida, pp. 7-91.

Sharpley, A.N., Kleinman, P.J.A., Heathwaite, A.L., Gburek, W.J., Folmar, G.J., and Schmidt, J.R., 2008a. Phosphorus loss from an agricultural watershed as a function of storm size. Journal of Environmental Quality, 37(2): 362-368.

Sharpley, A.N., Kleinman, P.J.A., Heathwaite, A.L., Gburek, W.J., Weld, J.L., and Folmar, G.J., 2008b. Integrating contributing areas and indexing phosphorus loss from agricultural watersheds. Journal of Environmental Quality, 37(4): 1488-1496.

Sharpley, A.N. and Rekolainen, S., 1997. Phosphorus in agriculture and its environmental applications. In: H. Tunney, O.T. Carton, E.S. Brookes and A.E. Johnston (Editors), Phosphorus Loss from Soil to Water. CAB International, New York, pp. 1-53.

Sharpley, A.N. and Smith, S.J., 1989. Prediction of soluble phosphorus transport in agricultural runoff. Journal of Environmental Quality, 18(3): 313-316.

Sharpley, A.N., Smith, S.J. and Bain, W.R., 1993. Nitrogen and phosphorus fate from long-term poultry litter applications to Oklahoma soils. Soil Science Society of America Journal, 57(4): 1131-1137.

Sharpley, A.N. and Syers, J.K., 1979. Phosphorus inputs into a stream draining an agricultural watershed. 2. Amounts contributed and relative significance of runoff types. Water Air and Soil Pollution, 11(4): 417-428.

Sharpley, A.N., Syers, J.K. and Tillman, R.W., 1978. Improved soil-sampling procedure for prediction of dissolved inorganic phosphate concentrations in surface runoff from pasture. Journal of Environmental Quality, 7(3): 455-456.

Sharpley, A.N., Tillman, R.W. and Syers, J.K., 1977. Use of laboratory extraction data to predict losses of dissolved inorganic phosphate in surface runoff and tile-drainage. Journal of Environmental Quality, 6(1): 33-36.

Sharpley, A.N. and Tunney, H., 2000. Phosphorus research strategies to meet agricultural and environmental challenges of the 21st century. Journal of Environmental Quality, 29(1): 176-181.

Sidle, R.C., Tsuboyama, Y. Noguchi, S., Hosoda, I., Fujieda, M., and Shimizu, T., 2000. Stormflow generation in steep forested headwaters: a linked hydrogeomorphic paradigm. Hydrological Processes, 14(3): 369-385.

Simard, R.R., Beauchemin, S. and Haygarth, P.M., 2000. Potential for preferential pathways of phosphorus transport. Journal of Environmental Quality, 29(1): 97-105.

Sims, J.T., Edwards, A.C., Schoumans, O.F. and Simard, R.R., 2000. Integrating soil phosphorus testing into environmentally based agricultural management practices. Journal of Environmental Quality, 29(1): 60-71.

Sklash, M.G. and Farvolden, R.N., 1979. Role of groundwater runoff. Journal of Hydrology, 43(1-4): 45-65.

Slade, R.M., 2004. General Methods, Information, and Sources for Collecting and Analyzing Water-Resources Data. CD-ROM. Copyright 2004 Raymond M. Slade, Jr.

Smith, C.M., 1992. Riparian afforestation effects on water yields and water quality in pasture catchments. Journal of Environmental Quality, 21: 237-245.

Smith, R.A., Schwarz, G.E. and Alexander, R.B., 1997. Regional interpretation of water-quality monitoring data. Water Resources Research, 33(12): 2781-2798.

Srinivasan, M.S., Wittman, M.A., Hamlett, J.M. and Gburek, W.J., 2000. Surface and subsurface sensors to record variable runoff generation areas. Transactions of the ASAE, 43(3): 651-660.

Surridge, B.W.J., Heathwaite, A.L. and Baird, A.J., 2007. The release of phosphorus to porewater and surface water from river riparian sediments. Journal of Environmental Quality, 36(5): 1534-1544.

Swank, W.T., 1988. Stream chemistry responses to disturbance. In: W.T. Swank and J. Crossley, D.A. (Editors), Forest Hydrology and Ecology at Coweeta. Springer-Verlag, New York, pp. 339-357.

Swank, W.T., Vose, J.M. and Elliott, K.J., 2001. Long-term hydrologic and water quality responses following commercial clearcutting of mixed hardwoods on a southern Appalachian catchment. Forest Ecology and Management, 143(1-3): 163-178.

Swank, W.T. and Waide, J.B., 1988. Characterization of baseline precipitation and stream chemistry and nutrient budgets for control watersheds. In: W.T. Swank and J. Crossley, D.A. (Editors), Forest Hydrology and Ecology at Coweeta. Springer-Verlag, New York, pp. 57-79.

T.-Prairie, Y. and Kalff, J., 1986. Effect of catchment size on phosphorus export. Water Resources Bulletin, 22(3): 465-470.

Taylor, A.W. and Kunishi, H.M., 1971. Phosphate equilibria on stream sediment and soil in a watershed draining an agricultural region. Journal of Agricultural and Food Chemistry, 19(5): 827-831.

Teledyne Isco, 2002. Isco 674 Rain Gage. Lincoln, NE: Teledyne Isco, Inc. Available at http://www.isco.com.

Teledyne Isco, 2005. Isco Submerged Probe Flow Module. Lincoln, NE: Teledyne Isco, Inc. Available at: http://www.isco.com.

Teledyne Isco, 2007. Isco 6712 Full-size Portable Sampler. Lincoln, NE: Teledyne Isco, Inc. Available at http://www.isco.com.

Tetzlaff, D., McDonnell, J.J., Uhlenbrook, S., McGuire, K.J., Bogaart P.W., Naef, F., Baird, A.J., Dunn, S.M., and Soulsby, C., 2008. Conceptualizing catchment processes: simply too complex? Hydrological Processes, 22(11): 1727-1730.

Thomas, R.B., 1985. Estimating total suspended sediment yield with probability sampling. Water Resources Research, 21(9): 1381-1388.

Thomas, R.B., 1988a. Measuring sediment yields of storms using PSALT. . Sediment Budgets. Proceedings of Porte Alegre Symposium. IAHS Publication No. 174: 315-322.

Thomas, R.B., 1988b. Monitoring baseline suspended sediment in forested basins: the effects of sampling. Hydrological Sciences Journal, 33(5): 499-514.

Thomas, R.B. and Lewis, J., 1993. A comparison of selection at list time and time-stratified sampling for estimating suspended sediment loads. Water Resources Research, 29(4): 1247-1256.

Thomas, R.B. and Lewis, J., 1995. An evaluation of flow-stratified sampling for estimating suspended sediment loads. Journal of Hydrology, 170(1-4): 27-45.

Tonderski, A., Grimvall, A., Dojlido, J.R. and Vandijk, G.M., 1995. Monitoring nutrient transport in large rivers. Environmental Monitoring and Assessment, 34(3): 245-269.

Toor, G.S., Harmel, R.D., Haggard, B.E. and Schmidt, G., 2008. Evaluation of regression methodology with low-frequency water quality sampling to estimate constituent loads for ephemeral watersheds in Texas. Journal of Environmental Quality, 37: 1847-1854.

Torbert, H.A., Daniel, T.C., Lemunyon, J.L. and Jones, R.M., 2002. Relationship of soil test phosphorus and sampling depth to runoff phosphorus in calcareous and noncalcareous soils. Journal of Environmental Quality, 31(4): 1380-1387.

Trimble, S.W. and Mendel, A.C., 1995. The cow as a geomorphic agent - a critical review. Geomorphology, 13(1-4): 233-253.

Turner, B.L., Kay, M.A. and Westermann, D.T., 2004. Colloidal phosphorus in surface runoff and water extracts from semiarid soils of the western United States. Journal of Environmental Quality, 33(4): 1464-1472.

U.S. Department of Agriculture, 2003. Patterns of World Poultry Consumption and Production. Economic Research Service, Available at http://www.ers.usda.gov/publications/WRS03/dec03/wrs0302/wrs0302b.pdf.

U.S. Department of Agriculture, 2004. 2002 Census of Agriculture. Available at http://www.nass.usda.gov/census/census02.

U.S. Environmental Protection Agency, 2007. Ecoregions of Alabama and Georgia. Map. ftp://ftp.epa.gov/wed/ecoregions/al_ga/alga_front.pdf. Last accessed August 23, 2007.

U.S. Geological Survey, 1982. Average Annual Runoff, Draft-Storage Regions, and Location of Gaging Stations. Water Resources Investigations Open-File Report 82-557, Plate 1. Prepared in conjunction with Georgia Department of Natural Resources Environmental Protection Division.

Vadas, P.A., Kleinman, P.J.A., Sharpley, A.N. and Turner, B.L., 2005. Relating soil phosphorus to dissolved phosphorus in runoff: A single extraction coefficient for water quality modeling. Journal of Environmental Quality, 34(2): 572-580.

Velbel, M.A., 1988. Weathering and soil-forming processes. In: W.T. Swank and J. Crossley, D.A. (Editors), Forest Hydrology and Ecology at Coweeta. Springer-Verlag, New York, pp. 93-103.

Verhoff, F.H., Yaksich, S.M. and Melfi, D.A., 1980. River nutrient and chemical-transport estimation. Journal of the Environmental Engineering Division-ASCE, 106(3): 591-608.

Vervoort, R.W., Radcliffe, D.E., Cabrera, M.L. and Latimore, M., 1998. Field-scale nitrogen and phosphorus losses from hayfields receiving fresh and composted broiler litter. Journal of Environmental Quality, 27(5): 1246-1254.

Walbridge, M.R., Richardson, C.J. and Swank, W.T., 1991. Vertical-distribution of biological and geochemical phosphorus subcycles in 2 southern Appalachian forest soils. Biogeochemistry, 13(1): 61-85.

Walker, T.W. and Syers, J.K., 1976. The fate of phosphorus during pedogenesis. Geoderma, 15(1): 1-19.

Walling, D.E., 1977. Assessing accuracy of suspended sediment rating curves for a small basin. Water Resources Research, 13(3): 530-538.

Walling, D.E. and Webb, B.W., 1985. Estimating the discharge of contaminants to coastal waters by rivers - some cautionary comments. Marine Pollution Bulletin, 16(12): 488-492.

Ward, R.C., 1982. The fountains of the deep and the windows of heaven: Perplexity and progress in explaining the response of rivers to precipitation. University of Hull, Hull, United Kingdom, 30 pp.

Ward, R.C., 1984. On the response to precipitation of headwater streams in humid areas. Journal of Hydrology, 74(1-2): 171-189.

Wetzel, R.G., 2001. Limnology. Academic Press, San Diego, 1006 pp.

Whiting, P.J., 2006. Estimating TMDL background suspended sediment loading to great lakes tributaries from existing data. Journal of the American Water Resources Association, 42(3): 769-776.

Wilson, C.J. and Dietrich, W.E., 1987. The contribution of bedrock groundwater flow to storm runoff and high pore pressure development in hollows, Erosion and Sedimentation in the Pacific Rim. International Association of Scientific Hydrology, pp. 49-59.

Wilson, M.A. and Carpenter, S.R., 1999. Economic valuation of freshwater ecosystem services in the United States: 1971-1997. Ecological Applications, 9(3): 772-783.

Winter, T.C., 2001. The concept of hydrologic landscapes. Journal of the American Water Resources Association, 37(2): 335-349.

Withers, P.J.A. and Haygarth, P.M., 2007. Agriculture, phosphorus and eutrophication: a European perspective. Soil Use and Management, 23(s1): 1-4.

Withers, P.J.A., Ulen, B., Stamm, C. and Bechmann, M., 2003. Incidental phosphorus losses - are they significant and can they be predicted? Journal of Plant Nutrition and Soil Science-Zeitschrift Fur Pflanzenernahrung Und Bodenkunde, 166(4): 459-468.

Wolock, D.M., Winter, T.C. and McMahon, G., 2004. Delineation and evaluation of hydrologic-landscape regions in the United States using geographic information system tools and multivariate statistical analyses. Environmental Management, 34: S71-S88.

Wood, T., Bormann, F.H. and Voigt, G.K., 1984. Phosphorus cycling in a northern hardwood forest - biological and chemical control. Science, 223(4634): 391-393.

Woodruff, J.F. and Hewlett, J.D., 1970. Predicting and mapping the average hydrologic response for the eastern United States. Water Resources Research, 6(5): 1312-1326.

Zollweg, J.A., Gburek, W.J. and Steenhuis, T.S., 1996. SMoRMod - A GIS-integrated rainfall-runoff model. Transactions of the ASAE, 39(4): 1299-1307.

TABLES

Table 1. Previous estimates of field-scale phosphorus yields from poultry manure-amended pastures.

Study	Location	Field drainage area (ha)	Field characteristics Soil texture / Cover Vegetation Grazed?	Soil Test P Mean *Range in means*	Amendment Type (Frequency) Mean rate (Min - Max)	Runoff DRP Conc. Mean *or range in means* (Min - Max)	Runoff TP Conc. Mean *or range in means* (Min - Max)	Annual P yield Mean *or range in means*
Edwards et al. (1996)[a]	Northwest Arkansas	1.23	Silt loam Fescue / Yes	177	Manure (2x) 164 (119 – 209) as ‘P’	2.93 (0.55 – 15.7)	NP	4.3
		1.06	Sandy/grav. loam Fescue / Yes	187	Litter (5x) 61.2 (43 – 71) as ‘P’	2.93 (1.02 – 24.4)	NP	1.6
Vervoort et al. (1998)	Georgia Coastal Plain	0.45	Sandy loam Bermuda/fescue / No	NP	Litter (5x) 109 (73.4 – 148) as TKP	3.3 (NP - 7.9)	NP	0.40
		0.45	Sandy loam Bermuda/fescue / No	NP	Litter (5x) 58.4 (45.3 – 73.9) as TKP	1.2 (NP – 1.8)	NP	0.10
Kuykendall et al. (1999)	Georgia Piedmont	0.75	Sandy loam Bermuda/fescue / Yes	47 *28 – 62*	Litter (4x) 123 (102 – 174) as TP	*5.08 – 8.22* NP	*6.75 – 12.8* NP	*11.6 – 17.8*
Moore et al. (2000)[a]	Northwest Arkansas	0.405	Silt loam Fescue / No	NP	Litter (3x) NP[c]	*3.23 – 7.94* NP	*4.23 - 8.69* NP	3.9
Pierson et al. (2001)[b]	Georgia Piedmont	0.75	Sandy loam Bermuda/fescue / Yes	NP *13 – 81*	Litter (4x) 118 (103 – 159) as TP	*1.29 – 7.35* (0.4 – 19)	NP	6.8
Harmel et al. (2004)	Texas Blackland Prairie	2.3	Black clay Kleingrass / No	49.7 *10.8 – 66.5*	Litter (2x) 6.7 as TP	*0.66 – 1.09* (NP – 1.56)	NP	*0.6 – 1.2*
		8.0	Black clay Bermudagrass / No	30.0 *15.9 – 37.6*	Litter (2x) 13.4 as TP	*1.29 – 2.29* (NP – 3.96)	NP	*0.4 – 0.6*
Toor et al. (2008)	Texas Blackland Prairie	8.0	Black clay Bermudagrass / No	35.8 *20.3 – 44.1*	Litter (NP) 6.7 as ‘P’	*0.61 – 1.11* NP	*0.68 – 1.13* NP	*0.56 – 1.15*

[a] = Commercial farm study;
[b] = Six sites total included in study. Data for individual sites were not specified by author.
[c] = Mean application rate of 6,244 (4,460 – 7136) kg ha^{-1} on “as-is” basis. P-based application rate not specified.
NP = not provided in study.
Phosphorus yields reported as kg-P ha^{-1} yr^{-1}. Soil test P reported as mg-P kg^{-1}. Any mean values reported in studies are shown without parentheses. Values shown in italics represent a range of mean values reported. Any values shown in parentheses represent specific minima or maxima that were reported.

Table 2. Physical characteristics of study watersheds

Site	Monitoring site elevation (msl)	Watershed area (ha)	Watershed slope (%)	Pond area (ha)	Stream length[2] (m)	Stream slope[2] (%)
FORS-1	439	44.1	5.33	1.8	1160	3.2
FORS-2	503	27.9	10.1	NA	541	4.0
FORS-3	533	30.8	12.6	NA	600	2.6
AG-4	320	27.0	5.7	0.23[3]	821	3.4
AG-5	351	2.83	5.9	NA	90	5.0
AG-6	351	2.43	5.1	NA	82	5.5
AG-7	323	9.71	7.9	NA	386	6.4
AG-8	433	7.28	7.2	NA	226	6.8
AG-9	343	10.5	5.4	0.68	360	2.2
AG-10	460	19.0	10.0	NA	310	5.0
AG-11	433	15.8	6.6	0.56	247	3.8
AG-12[1]	381	3.24	7.0	NA	195	6.3

[1]Ephemeral watershed; stream slope based on slope of watershed valley
[2]Length and slope of streams in watersheds FORS-1, AG-4, AG-9, and AG-11 are based on full extent of stream with no pond as shown in USGS topographic maps
[3]Pond at AG-4 not addressed in study
NA = not applicable

Table 3. Estimates of land cover percentage for study watersheds

Site	% Forest	% Pasture	% Other vegetated	% Impervious	% Unpaved	% Pond[2]	% Stream corridor
FORS-1	100.0	0.0	0.0	0.0	0.0	4.1	NE
FORS-2	100.0	0.0	0.0	0.0	0.0	NA	NE
FORS-3	100.0	0.0	0.0	0.0	0.0	NA	NE
AG-4	54.1	15.3	25.2	4.0	1.0	NA[3]	0.9
AG-5	2.7	83.1	13.3	0.0	1.0	NA	1.2
AG-6	13.5	42.7	23.2	6.4	1.3	NA	1.4
AG-7	35.0	40.1	7.3	6.3	1.0	NA	2.6
AG-8	32.4	0.0	49.8	6.2	1.1	NA	1.3
AG-9	23.8	42.8	11.4	9.6	6.1	6.5	0.3
AG-10	36.5	63.1	0.0	0.0	0.0	NA	0.7
AG-11	27.0	47.4	4.7	4.7	1.4	3.5	0.2
AG-12[1]	9.8	83.7	0.0	6.9	0.0	NA	NA

Notes
[1]Ephemeral watershed
[2]Percentages of contributing drainage area relative to total watershed area at FORS-1, AG-9, and AG-11 were approximately 85.4%, 63.5%, and 91.4%, respectively
[3]Watershed for site AG-4 contained pond but not addressed in study due to its relative percentage (~1.0%) of total watershed area and percentage (40%) of contributing drainage area
NA = not applicable
NE = not estimated

Table 4: Information on poultry farm management of agricultural watersheds in study.

Site	No. poultry houses	Average. no. birds raised per year	Annual tons litter/cake produced	Percent of litter/cake applied	Litter/cake application rate	No./type livestock	Livestock access to stream channel
AG-4	3	NP	NP	NP	NP	NP / cattle	Yes
AG-5,-6	3	300,000	75/250	100/100	2 tons/acre	200 cattle	Yes
AG-7	3	302,500	60/150	50 / 25	5 tons/acre	NP/ horses	Yes
AG-8	2	NP	NP	NP	NP	NA	NA
AG-9	2	156,000	20/75	80/0	1 load/2.5 acres	NP / goats	No
AG-10	12	1,104,000	750/1800	95/0	5 tons/acre	30-100 cattle	Yes
AG-11	5	332,500	2/20	100/100	2 tons/acre	NP / cattle	No
AG-12	3	300,000	22.5/114	100/0	1.12 tons/acre	48 sheep + 1 cow	Yes

NA = not applicable
No. = number of
NP = information not provided

Table 5. Monthly precipitation totals reported for sites in Upper Etowah River operated by Georgia Automated Environmental Monitoring Network and U.S. Geological Survey.

Month-Year	GAEMN Station at Dahlonega[1] (mm)		USGS Sites in Upper Etowah River Basin			
	Observed (mm)	% of 1930-1996 mean	Etowah River at Canton[2] (mm)	Etowah River at GA 9, near Dawsonville[2] (mm)	Etowah River near Dahlonega[2] (mm)	Settingdown Creek near Ball Ground[2] (mm)
Mar-05	171	0.97	184	160	NA	NA
Apr-05	121	0.92	126	114	NA	NA
May-05	36	0.30	50	44	NA	NA
Jun-05	186	1.72	49	166	NA	NA
Jul-05	243	1.68	383	224	NA	NA
Aug-05	232	1.77	135	173	NA	NA
Sep-05	8	0.07	13	11	NA	NA
Oct-05	65	0.68	50	65	70	71
Nov-05	101	0.84	97	89	102	38
Dec-05	104	0.54	106	128	152	150
Jan-06	140	0.87	126	106	132	104
Feb-06	61	0.40	97	85	92	125
Mar-06	52	0.29	94	85	84	84
Apr-06	82	0.62	103	89	101	91
May-06	54	0.46	26	42	56	55
Jun-06	82	0.76	64	60	78	27
Jul-06	57	0.39	44	61	57	76
Aug-06	56	0.43	160	99	115	94
Sep-06	195	1.83	44	128	155	76
Sum	*2044*	*0.97*	*1953*	*1443*	*NA*	*NA*

[1] Site located at Blackstock Vineyards and Winery in White County, GA. Data and additional site information available from Georgia Automated Environmental Monitoring Network at http://www.griffin.uga.edu/aemn/cgi-bin/AEMN.pl?site=GADH.
[2] Additional data and site information available from U.S. Geological Survey at http://waterdata.usgs.gov/ga
NA = Data not available. First full month of available precipitation data was October 2005.

Table 6. Results of Spearman correlation analyses among physical and land cover watershed characteristics. Correlations significant at the α=0.05 level are indicated by bold with asterisk sign in grey-shaded cell. Correlations significant at the α=0.10 level are indicated by bold with asterisk sign only. (A = drainage area; E = site elevation; L_s = stream length; S_s = stream slope; L_w = watershed length; S_w = watershed slope; IOVPU = impervious, other vegetation (OV), pasture, and undeveloped; land cover characteristics represent percentage of watershed area.)

Variable	A	E	L_s	S_s	L_w	S_w	Forest	Pasture	Impervious	OtherVeg (OV)	Pasture+OV	Unpaved	IOVPU
A	1.0	0.4217	**0.9342***	**-0.7711***	**0.9342***	**0.7066***	**0.9578***	-0.5891	-0.5551	-0.5277	**-0.8855***	-0.5806	**-0.9578***
E		1.0	0.0838	-0.3193	0.1796	**0.7904***	0.4819	-0.4173	-0.6061	-0.6504	-0.3615	-0.5295	-0.4819
L_s			1.0	**-0.6946***	**0.9524***	0.4762	**0.8743***	-0.5611	-0.3425	-0.2928	**-0.8743***	-0.3932	**-0.8743***
S_s				1.0	**-0.7186***	-0.3713	**-0.6988***	0.2086	**0.6508***	0.4786	0.5542	**0.6763***	**0.6988***
L_w					1.0	0.4524	**0.9222***	-0.5611	-0.3171	-0.3172	**-0.8503***	-0.3425	**-0.9222***
S_w						1.0	**0.7066***	-0.4636	**-0.6342***	**-0.8051***	**-0.6347***	**-0.6596***	**-0.7066***
Forest							1.0	**-0.6627***	-0.4466	-0.5645	**-0.9277***	-0.4721	**-1.0000***
Pasture								1.0	0.0130	0.0000	**0.8345***	-0.0650	**0.6627***
Impervious									1.0	**0.6369***	0.2424	**0.9730***	0.4466
OtherVeg (OV)										1.0	0.3682	**0.7408***	0.5645
Pasture+OV											1.0	0.2680	**0.9277***
Unpaved												1.0	0.4721
IOVPU													1.0

Table 7. Results of Spearman's rho correlation analyses between hydrologic response variables and drainage area and percentage of forest cover in study watersheds. Correlations significant at the α = 0.05 level are indicated by bold with asterisk sign in grey-shaded cell.

Response variable	Drainage area	Percent forest cover
Q_o	-0.0240	-0.0719
Q_p	**-0.7785***	**-0.7785***
T_p	-0.2169	-0.0843
Q_{qk}	-0.6108	-0.5509
Q_{tot}	-0.3234	-0.2634
Q_{qk}/Q_{tot}	**-0.9222***	**-0.8982***
Q_{qk}/Q_{rain}	-0.2395	-0.2515
$Q_{0.1}$	**-0.7425***	**-0.7545***
Q_1	-0.2156	-0.1796
Q_5	-0.2515	-0.2515
Q_{10}	-0.2515	0.2515
Q_{20}	-0.2874	-0.3114
Q_{50}	-0.2874	-0.3114
Q_{80}	-0.2036	-0.2874
Q_{90}	-0.2874	-0.3593
Q_{95}	-0.2771	-0.3494
Q_{99}	-0.2108	-0.3193
$Q_{99.9}$	-0.1677	-0.2635
$Q_{0.1}/Q_{99.9}$	-0.4643	-0.3424
Q_1/Q_{99}	-0.3214	-0.1802
Q_5/Q_{95}	0.1429	0.3063
Q_{10}/Q_{90}	0.1677	0.2515
Q_{20}/Q_{80}	-0.0599	0.0240
AMP	-0.2755	-0.2994
ET	-0.4578	-0.4458
7LQ	0.3253	-0.3916
14LQ	-0.2395	-0.3234
30LQ	-0.2048	-0.3012

Table 8. Results of deionized water-based quality control samples collected for phosphorus analyses (Min=minimum; Max=maximum; SE=standard error)

Analyte	Sample Type	n	Mean	SE	Min	Max
Total P	BR	29	0.0038	0.0003	0.0000	0.0458
	CK	25	0.0048	0.0001	0.0000	0.0838
	DI	21	0.0033	0.0002	0.0000	0.0235
Dissolved Reactive P	BR	29	0.0011	0.0001	0.0000	0.0051
	CK	25	0.0012	0.0001	0.0000	0.0075
	DI	21	0.0006	0.0001	0.0000	0.0050

Table 9. Mean errors and standard errors between laboratory results of ISCO autosamples versus grab samples collected directly from flume outlets. Calculations were based on subtraction of grab sample concentration from autosample concentration. For each analyte, the number of sample pairs across sites used to calculate errors ranged between 7 and 11. TP and DRP errors reported as mg-P L^{-1}. TSS errors reported as mg L^{-1}.

Site	TP		DRP		TSS	
	Mean error	SE	Mean error	SE	Mean error	SE
FORS-1	0.001	0.002	0.001	0.000	-36.1	13.9
FORS-2	-0.003	0.002	0.000	0.000	-75.3	62.6
FORS-3	0.002	0.002	0.000	0.000	-12.7	7.98
AG-4	0.009	0.028	0.007	0.008	-19.1	9.33
AG-5	0.002	0.018	0.000	0.012	41.3	40.7
AG-6	0.012	0.017	0.008	0.015	-80.4	28.6
AG-7	0.009	0.006	0.001	0.006	-284	118.9
AG-8	0.001	0.014	0.005	0.008	-12.0	10.0
AG-9	-0.007	0.005	0.000	0.001	-80.6	48.8
AG-10	-0.010	0.009	-0.004	0.003	-7.28	5.44
AG-11	-0.014	0.020	0.000	0.001	-5.75	2.46

Table 10. Mehlich-1 soil test phosphorus concentrations observed at study watersheds.

Study site	Land cover no.	Land cover description	Land cover area (ha)	[1]Percent of total sampled watershed	Soil P (mg-P/kg)	Area-weighted soil P (mg-P/kg)
FORS-1	1	Riparian/river left	NE	NA	2.25	
	2	Riparian/river right	NE	NA	4.05	
	3	Upland/river left	NE	NA	2.57	
	4	Upland/river right	NE	NA	3.11	
	5	Wetland above pond	NE	NA	4.51	
		Total / Median	***44.13***			***3.11***
FORS-2	1	Riparian/river right	NE	NA	3.00	
	2	Upland/river right	NE	NA	3.02	
	3	Riparian/river left	NE	NA	3.87	
	4	Upland/river left	NE	NA	2.22	
		Total / Median	***28.03***			**3.01**
FORS-3	1	Riparian/river right	NE	NA	3.84	
	2	Upland/river right	NE	NA	3.60	
	3	Riparian/river left	NE	NA	2.84	
	4	Upland/river left	NE	NA	3.19	
		Total / Median	***30.83***			***3.39***
FORS-4	1	Forested area	15.29	0.54	4.68	2.55
	2	Residential	1.17	0.04	22.62	0.94
	3	Pasture	3.04	0.11	103.60	11.23
	4	Pasture	0.69	0.02	115.50	2.85
	5	Pasture	0.73	0.03	66.85	1.73
	6	Chicken house	3.05	0.11	26.21	2.84
	7	Storage area	4.13	0.15	24.35	3.58
		Total	***28.10***	***1.00***		***25.72***
AG-5	1	Horse pen	0.29	0.11	59.40	6.66
	2	Riparian	0.31	0.12	24.80	2.93
	3	Pasture	2.02	0.77	228.83	176.12
		Total	***2.63***	***1.00***		***185.71***
AG-6	1	Forested area	0.28	0.14	10.61	1.47
	2	Pasture	0.92	0.45	220.45	99.02
	3	Chicken house perimeter	0.85	0.41	78.98	32.57
		Total	***2.06***	***1.00***		***133.06***
AG-7	1	Lawn and pine trees	0.63	0.07	4.94	0.32
	2	Horse pasture	2.66	0.27	9.48	2.60
	3	Pasture	3.75	0.39	54.70	21.16
	4	Unnamed	0.48	0.05	127.70	6.27
	5	Unnamed	0.81	0.08	0.00	0.00
	6	Pasture	1.37	0.14	24.45	3.45
		Total	***9.71***	***1.00***		***33.80***
AG-8	1	Grass field	0.73	0.10	62.85	6.38
	2	Forested	2.86	0.40	10.26	4.06
	3	Grass and briars	1.68	0.23	27.71	6.47
	4	Grass field and lawn	1.94	0.27	176.95	47.56
		Total	***7.21***	***1.00***		***64.48***
AG-9	1	Pasture	1.38	0.16	147.40	23.24
	2	Residential	0.74	0.08	6.48	0.55
	3	Residential and pasture combined	1.32	0.15	66.90	10.06
	4	Farm	1.63	0.19	12.87	2.39
	5	Woodland	0.63	0.07	4.74	0.34
	6	Chicken house perimeter	1.76	0.20	33.97	6.81
	7	Trailer and contained area	0.42	0.05	50.40	2.42
	8	Resident	0.70	0.08	64.90	5.18
	9	Pasture/resident	0.19	0.02	35.24	0.76
		Total	***8.78***	***1.00***		***51.74***
AG-10	1	Forest	5.55	0.29	5.08	1.48
	2	Pasture	0.81	0.04	25.32	1.08
	3	Pasture hillslope	1.37	0.07	143.50	10.34
	4	Pasture/trees	1.02	0.05	5.90	0.32
	5	Forest/pasture	1.32	0.07	9.02	0.62
	6	Hilly pasture	5.06	0.27	30.09	7.98
	7	Hilly pasture	3.92	0.21	138.80	28.57
		Total	***19.06***	***1.00***		***50.39***
AG-11	1	Forested area	3.33	0.22	6.45	1.43
	2	East end of chicken house	0.21	0.01	31.47	0.44
	3	West end of chicken house	0.66	0.04	6.78	0.30
	4	North end of chicken house	0.44	0.03	44.91	1.31
	5	South end of chicken house	1.13	0.08	275.40	20.75
	6	Pasture	3.85	0.26	196.90	50.55
	7	Residential	2.99	0.20	17.28	3.44
	8	North end of pond	1.34	0.09	136.40	12.18
	9	East end of pond	1.06	0.07	97.95	6.93
		Total	***15.01***	***1.00***		***97.32***
AG-12	1	Valley flat, along channel	0.41	0.13	101.80	13.64
	2	Sheep pen	0.10	0.03	70.00	2.21
	3	Chicken/sheep/stackhouse	0.30	0.10	12.91	1.27
	4	Pasture/river-right	1.41	0.46	151.00	69.25
	5	Pasture/river-left	0.85	0.28	234.75	65.09
		Total	***3.08***	***1.00***		***151.46***

Notes
[1]The total land cover areas for study watershed do not equate to the areas reported in Table 2 because a) the areas above were estimated using aerial photographs (vs. 7.5' topographic maps for Table 2) and b) some study watersheds were not fully sampled such as those with ponds.
NA = not applicable; NE = not estimated

Table 11. Results of residual diagnostics and influence statistics for regression modeling used for load estimation.

	AG-4		AG-5		AG-6		AG-7		AG-8		AG-9		AG-10		AG-11		AG-12	
Model	Value	SE	Value	SE	Value	SE	Value	SE	Value	SE	Value	SE	Value	SE	Value	SE	Value	SE
β_0	-5.034	0.143	-4.248	0.106	-3.744	0.090	-7.316	0.109	-4.955	0.137	-5.610	0.144	-5.747	0.173	-4.631	0.086	-3.370	0.107
β_1	1.067	0.111	2.009	0.099	1.822	0.056	2.181	0.139	1.883	0.067	1.707	0.077	1.351	0.067	1.193	0.038	1.422	0.048
β_2	0.072	0.027	-0.096	0.036	-0.098	0.019	-0.185	0.046	0.100	0.035	-0.130	0.031	--	--	--	--	--	--
N	183		143		175		125		123		109		142		112		57	
R^2 for C	0.180		0.587		0.636		0.456		0.608		0.458		0.162		0.190		0.590	
R^2 for L	0.749		0.876		0.920		0.805		0.871		0.863		0.742		0.890		0.942	
Residuals																		
K-S (P-value)	0.079* (0.023)		0.057 (>0.150)		0.081* (<0.010)		0.081* (0.044)		0.049 (>0.150)		0.056 (>0.150)		0.056 (>0.150)		0.065 (>0.150)		0.078 (>0.150)	
s_ε	1.037		1.035		0.921		1.061		1.157		1.122		1.282		0.632		0.644	
τ_ε	<0.0001		<0.0001		<0.0001		0.0012		<0.0001		<0.0001		<0.0001		<0.0001		<0.0001	
D-W	1.126		0.858		1.168		1.479		1.143		0.803		0.891		1.013		0.876	
φ_ε	0.424		0.567		0.415		0.258		0.425		0.555		0.550		0.484		0.546	
Cook's D >0.7	0		0		0		0		0		0		0		0		0	
abs(ε_{si}) > 2	9		6		11		6		8		4		8		6		3	

Notes

β_0, β_1, β_3 regression model coefficients
SE standard error of model coefficient
N number of data pairs used in model calibration
R^2 for C coefficient of determination between natural logarithms of TP concentration and streamflow in model
R^2 for L coefficient of determination between natural logarithms of TP load and streamflow in model
K-S Kolmogorov-Smirnov statistic for normal distribution.
* indicates K-S statistics is insignificant at $\alpha = 0.05$ and indicative of normal distribution of model residuals
s_ε standard deviation of model residuals
τ_ε Kendall's tau statistic for autocorrelation between model residuals neighboring in time
D-W Durbin-Watson test statistic for autocorrelation in model residuals
φ_ε first-order autocorrelation coefficient for model residuals
D Cook's distance statistic
abs(ε_{si}) absolute value of studentized residual

Table 12. Comparison of observed storm event total phosphorus loads based on composite samples with predicted loads via regression estimators. Observed load (L_{obs}) represents the product of sampled stormflow and composite sample total phosphorus concentration. Numbers in parentheses represent the percent difference of estimated load with observed load. Negative values indicate underestimation. Positive values indicate overprediction.

Site	Date of storm event	Duration of hydrograph sampled (hours)	Number of samples collected	Volume of sampled stormflow (L)	Composite sample TP conc. (mg-P L^{-1})	L_{obs} load (kg)	L_{exp} load (kg) (%)	L_{qmle} load (kg) (%)	L_{sm} load (kg) (%)
AG-4	12/4/2006	1.8	55	158,020	0.37	0.0585	0.0311 (-46.9)	0.0532 (-9.1)	0.0494 (-15.6)
	1/2/2006	19.3	56	441,969	0.11	0.0487	0.0611 (23.5)	0.103 (111.3)	0.0956 (96.4)
	2/11/2006	19.8	14	221,171	0.05	0.0111	0.0199 (79.7)	0.0342 (208)	0.0317 (186)
	3/20/06	26.4	79	1,593,633	0.13	0.199	0.362 (81.8)	0.620 (211)	0.576 (189)
AG-10	12/15/2005	20.6	40	463,381	0.18	0.0835	0.0356 (-57.7)	0.0721 (-17.7)	0.0811 (-2.9)
	1/17/2006	21.0	53	1,174,157	0.11	0.129	0.127 (-1.8)	0.258 (99.6)	0.290 (124)
	3/20/06	18.3	30	565,187	0.06	0.0340	0.0563 (65.6)	0.114 (236)	0.129 (278)
	10/17/2006	11.2	46	684,756	0.42	0.288	0.0838 (-70.9)	0.170 (-40.9)	0.191 (-33.5)

FIGURES

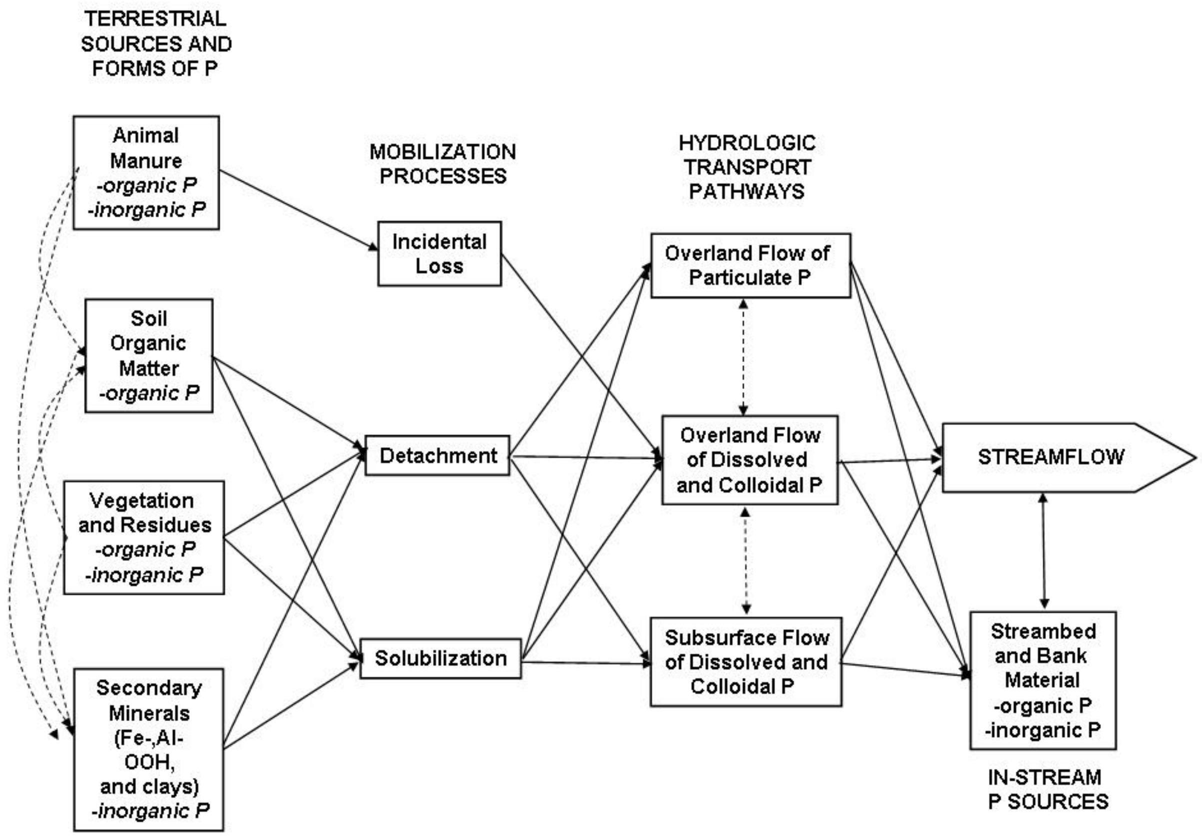

Figure 1. Conceptualization of hydrologic transfer of phosphorus from terrestrial and in-stream sources to a stream during a storm. The figure is not intended to represent all possible phosphorus source-mobilization-pathway combinations.

.

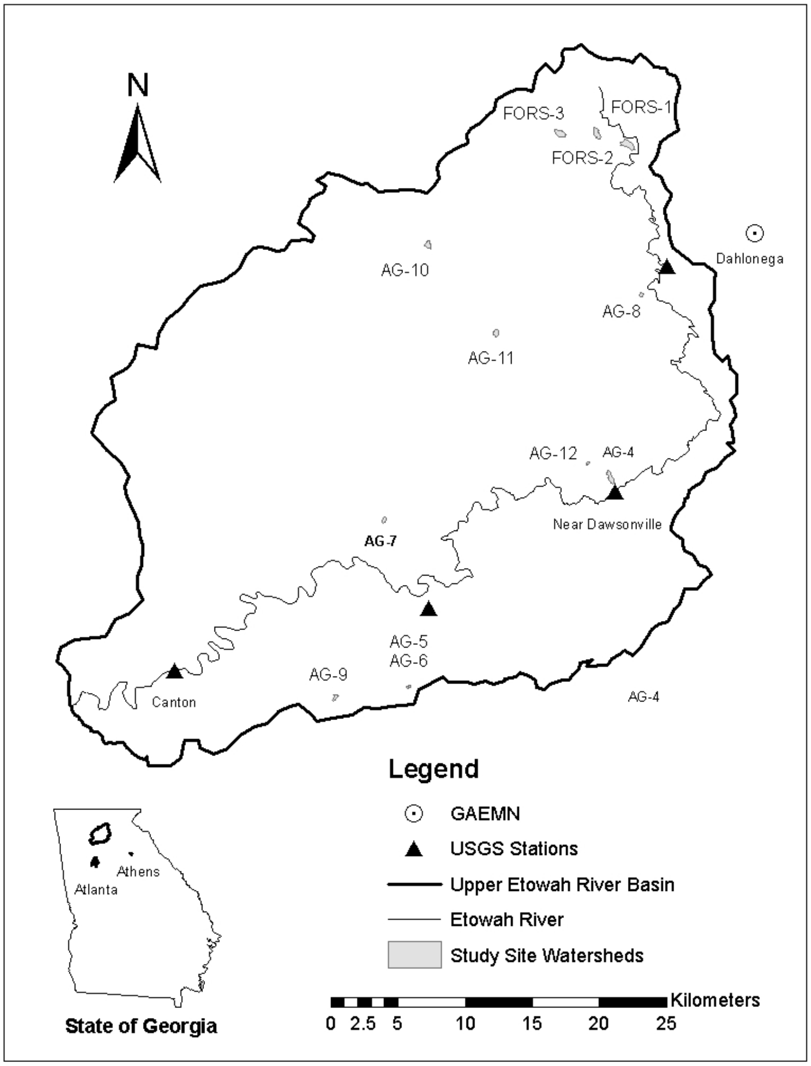

Figure 2. Map of upper Etowah River basin and study sites. Map shows locations of the twelve study sites plus climate and streamflow monitoring locations maintained by Georgia Automated Environmental Monitoring Network (GAEMN) and U.S. Geological Survey (USGS).

Figure 3. Upstream view of two-foot H-flume installed at study site FORS-3. Wingwalls at the upstream entrance to the flume were built into both streambanks. Photo also shows a) stilling well where ISCO 720 submerged probe was installed for level measurement and b) intake tubing positioned in scour hole below flume nose.

Figure 4. Topview of two-foot H-flume installed at study site AG-7. Stilling well is positioned on left-hand side of flume nose. ISCO 720 probe and sample intake tubing were not installed at time of photo.

Figure 5. ISCO 6700 autosampler and wooden shelter installed at AG-10. Photo shows lower half of autosampler on ground surface with 24 one-liter bottles. Upper half of autosampler is resting inside shelter. ISCO 720 module attached to 6700 is in foreground. Autosampler lid rests on top of shelter.

Figure 6. Two-foot H-flume, ISCO 674 rain gage, sample intake tubing, and wooden shelter containing ISCO autosampler installed at AG-4.

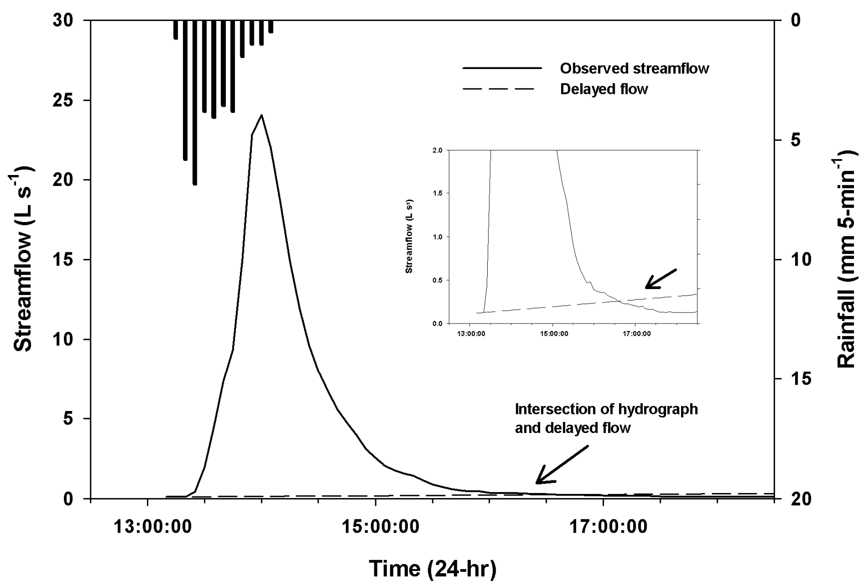

Figure 7. Example of hydrograph separation method following Hewlett and Hibbert (1967).

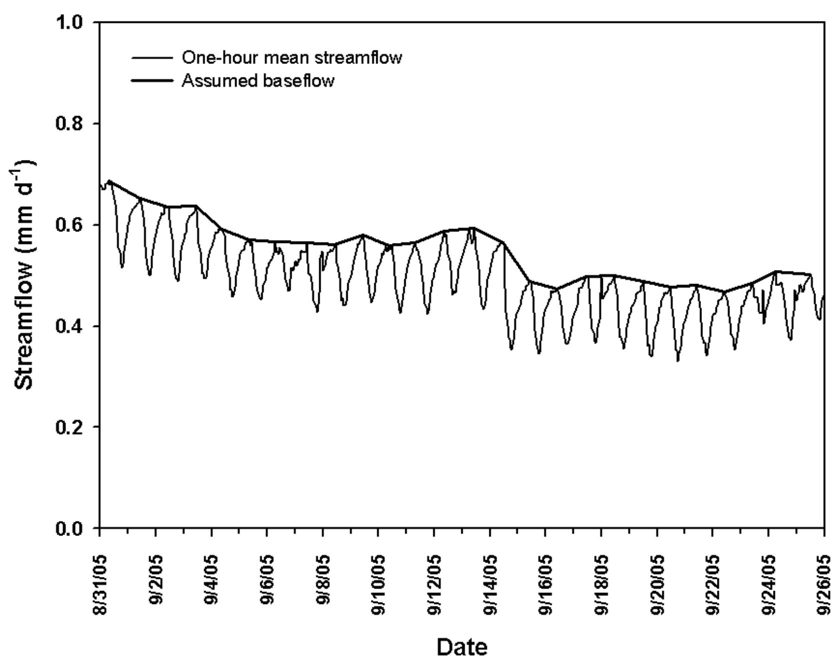

Figure 8. Example of how daily evapotranspiration (ET) was estimated following Bond et al. (2002). The inverted, triangular-shaped areas between the assumed baseflow and one-hour streamflow represent ET.

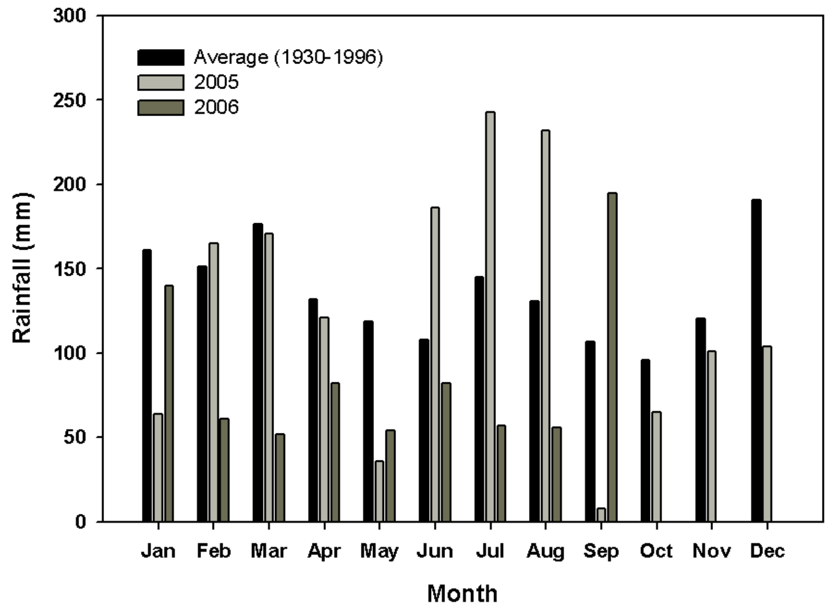

Figure 9. Observed and long-term average monthly precipitation totals reported by Georgia Automated Environmental Monitoring Network for climate station at Dahlonega, Georgia.

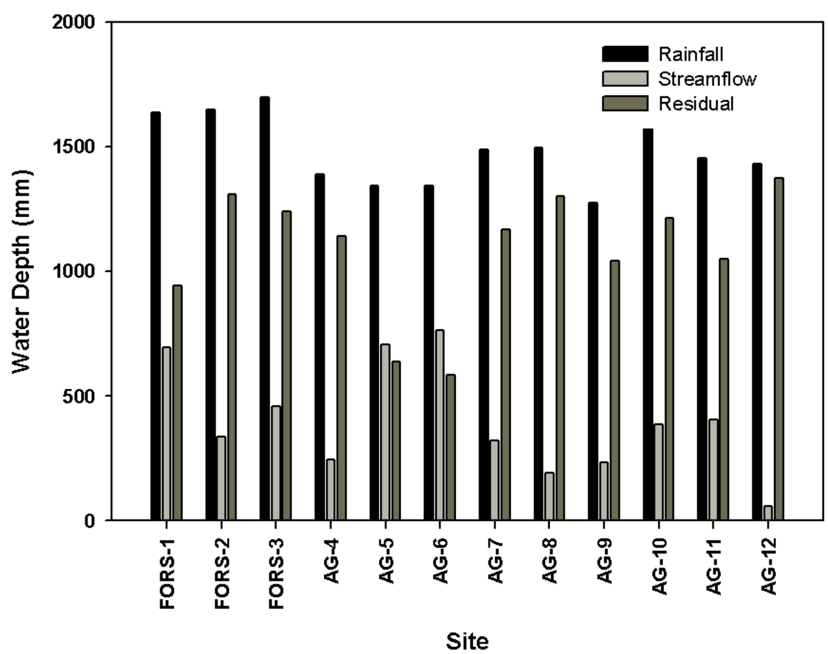

Figure 10. Observed rainfall and streamflow with computed ET residuals for study sites during 15-month common monitoring period.

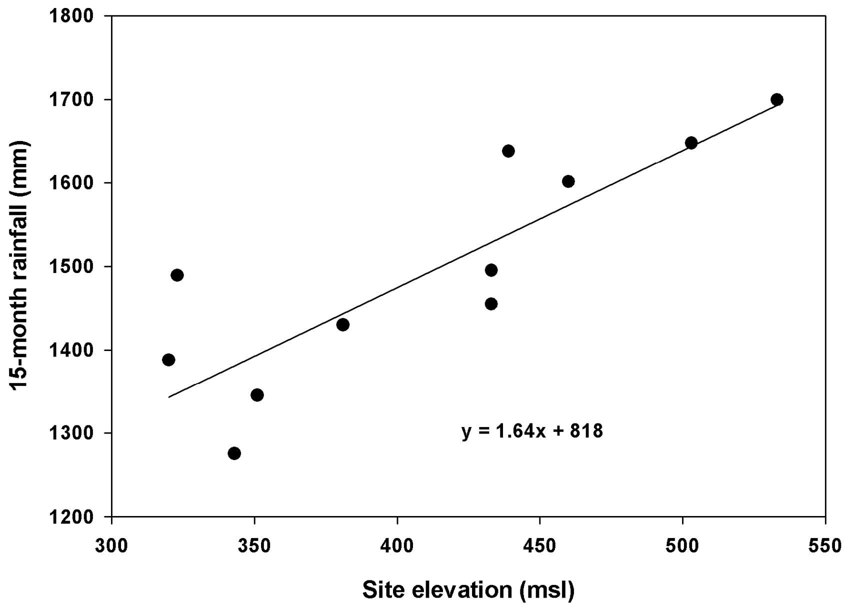

Figure 11. Relationship between observed 15-month rainfall and site elevation of study sites (P = 0.0004; R^2 = 0.7316).

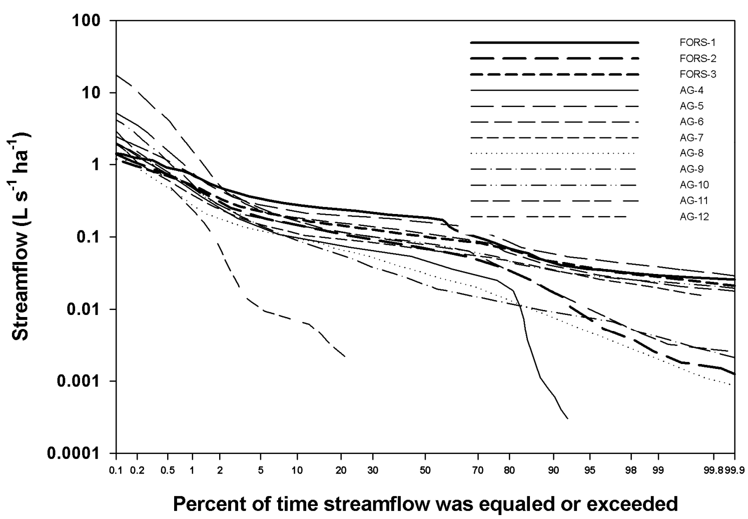

Figure 12. Flow-duration curves for study sites during 15-month common monitoring period.

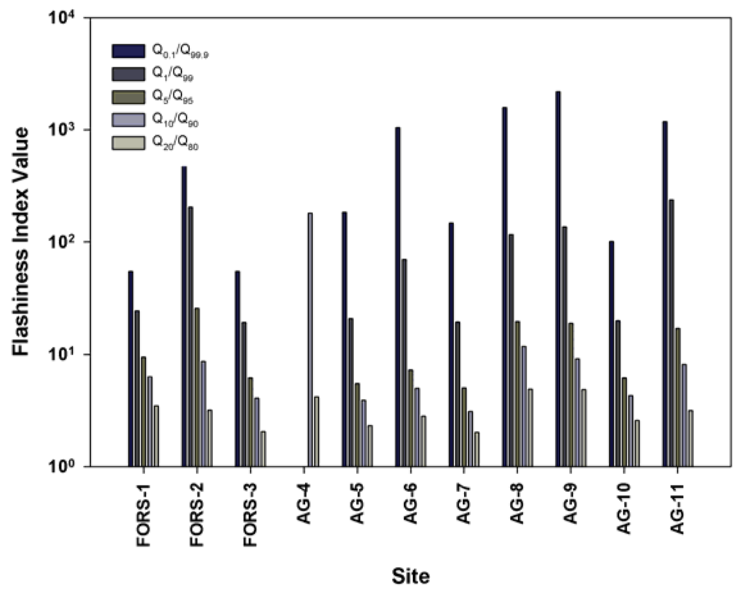

Figure 13. Flashiness indices computed for perennial and intermittent sites for 15-month common monitoring period. The $Q_{0.1}/Q_{99.9}$, Q_1/Q_{99}, and Q_5/Q_{95} are not shown for AG-4 because of intermittent flow conditions observed between July and August 2006. Site AG-12 excluded from analysis.

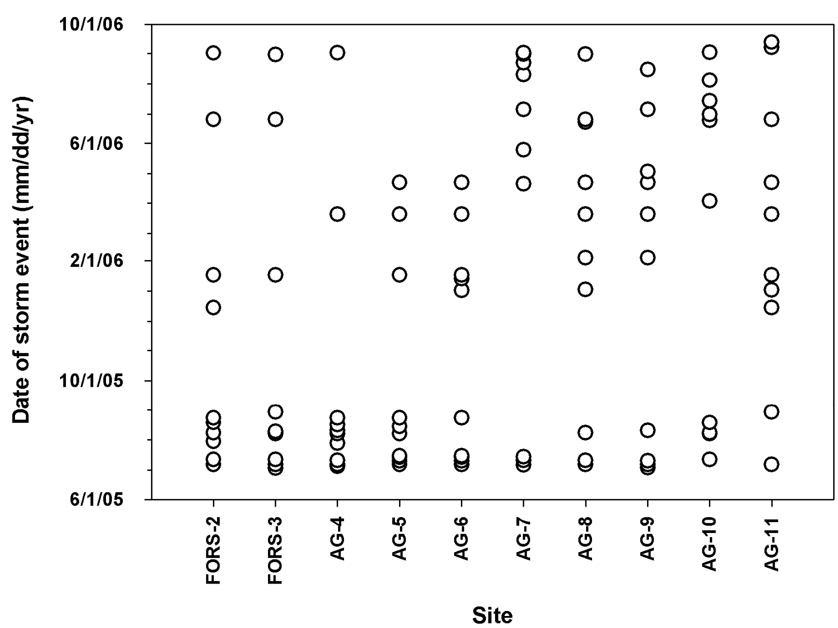

Figure 14. Dates of top 10 storm events analyzed at study sites. Sites FORS-1 and AG-12 excluded from analysis.

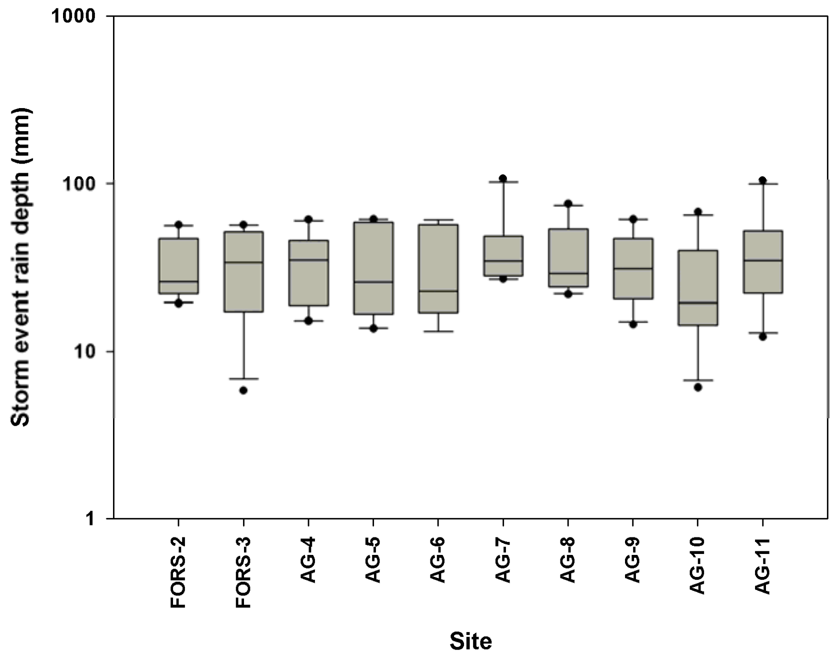

Figure 15. Rainfall depths of top 10 storm events analyzed at study sites. Sites FORS-1 and AG-12 excluded from analysis.

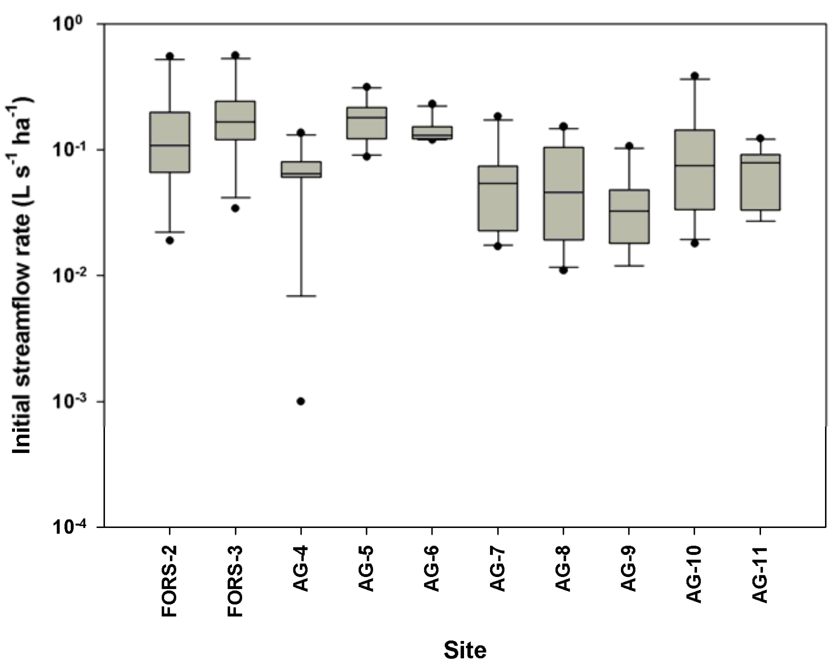

Figure 16. Initial streamflow rate of top 10 storm events analyzed at study sites. Site FORS-1 excluded from analysis. Sites FORS-1 and AG-12 excluded from analysis.

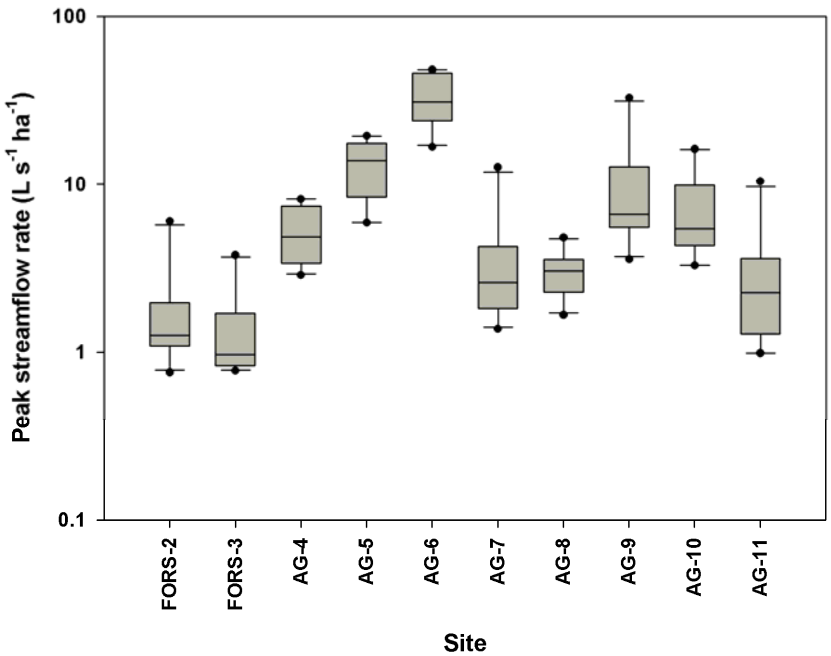

Figure 17. Peak streamflow rate of top 10 storm events analyzed at study sites. Sites FORS-1 and AG-12 excluded from analysis.

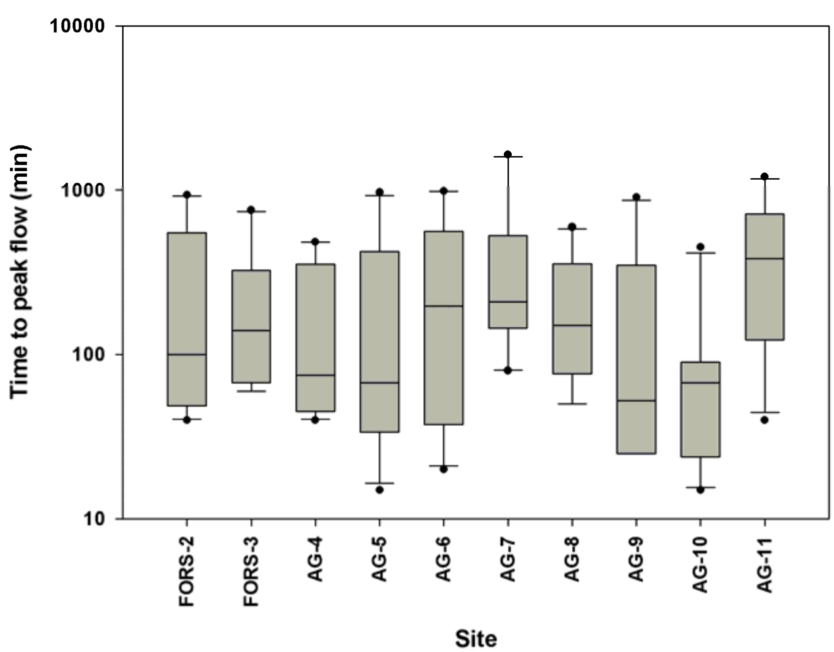

Figure 18. Time to peak streamflow of top 10 storm events analyzed at study sites. Sites FORS-1 and AG-12 excluded from analysis.

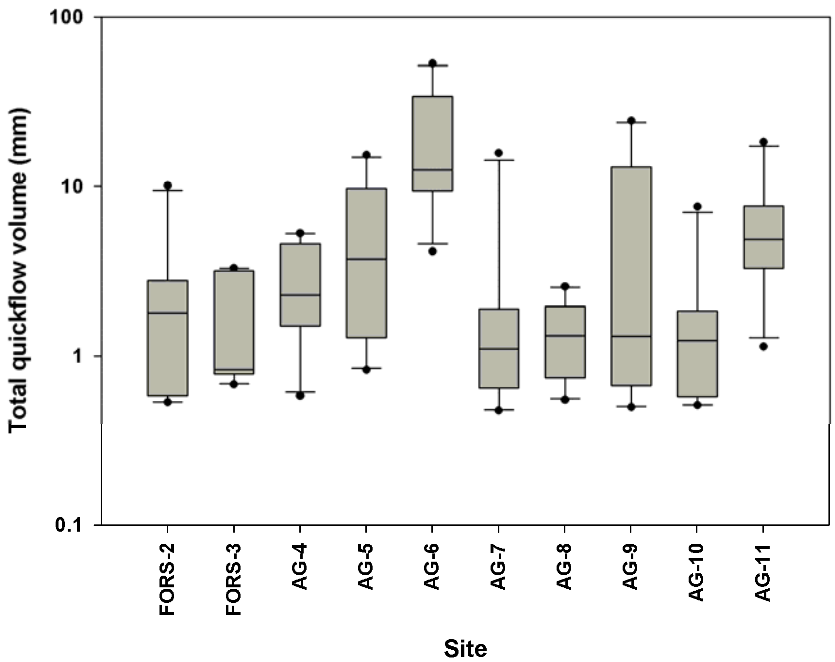

Figure 19. Total quickflow volume of top 10 storm events analyzed at study sites. Sites FORS-1 and AG-12 excluded from analysis.

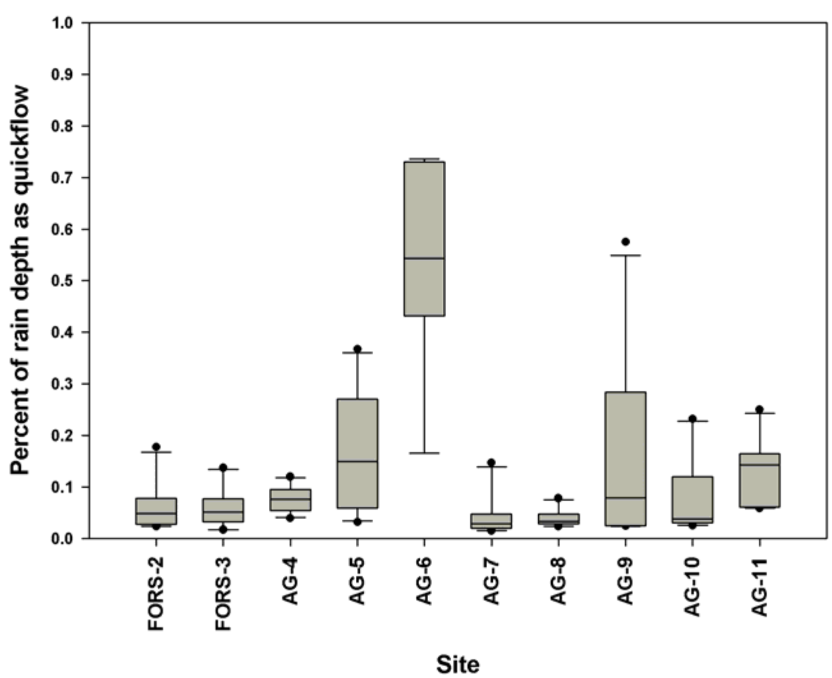

Figure 20. Fraction of rain depth as quickflow of top 10 storm events analyzed at study sites. Sites FORS-1 and AG-12 excluded from analysis.

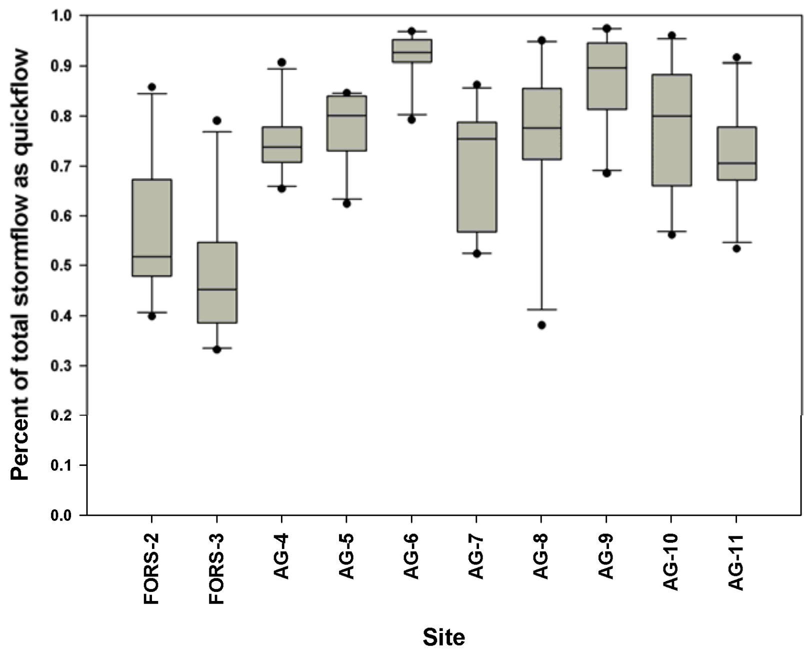

Figure 21. Fraction of total stormflow as quickflow of top 10 storm events analyzed at study sites. Sites FORS-1 and AG-12 excluded from analysis.

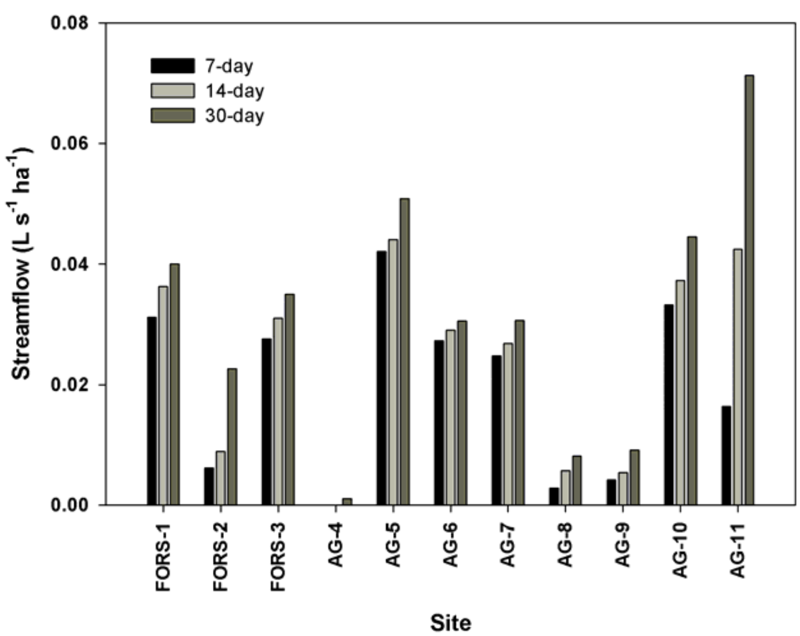

Figure 22. Average 7-, 14-, and 30-day low flows computed from 15-month common monitoring period. Site AG-12 excluded from analysis.

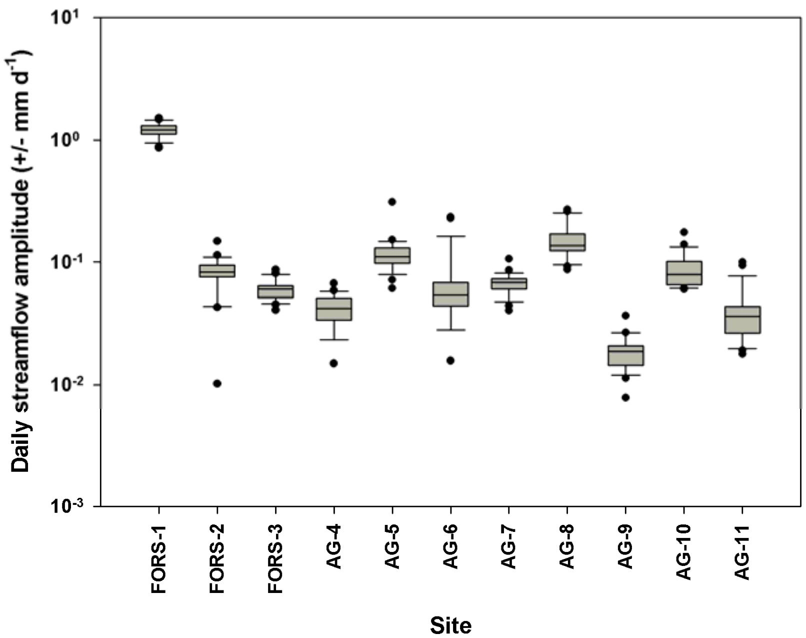

Figure 23. Amplitudes of diurnal streamflow fluctuations at perennial and intermittent sites in September 2005. Site AG-12 excluded from analysis.

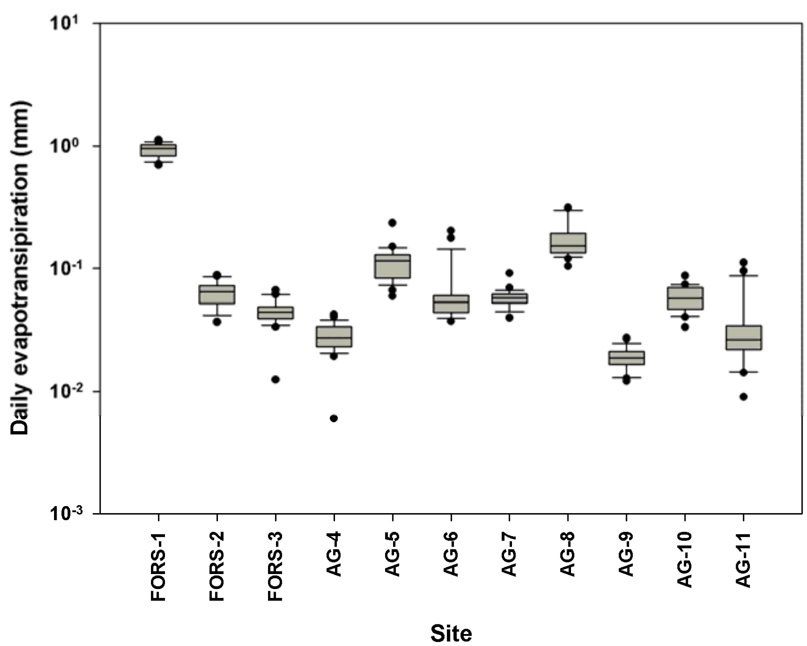

Figure 24. Daily ET estimates for perennial and intermittent sites in September 2005 based on 'missing streamflow' method. Site AG-12 excluded from analysis.

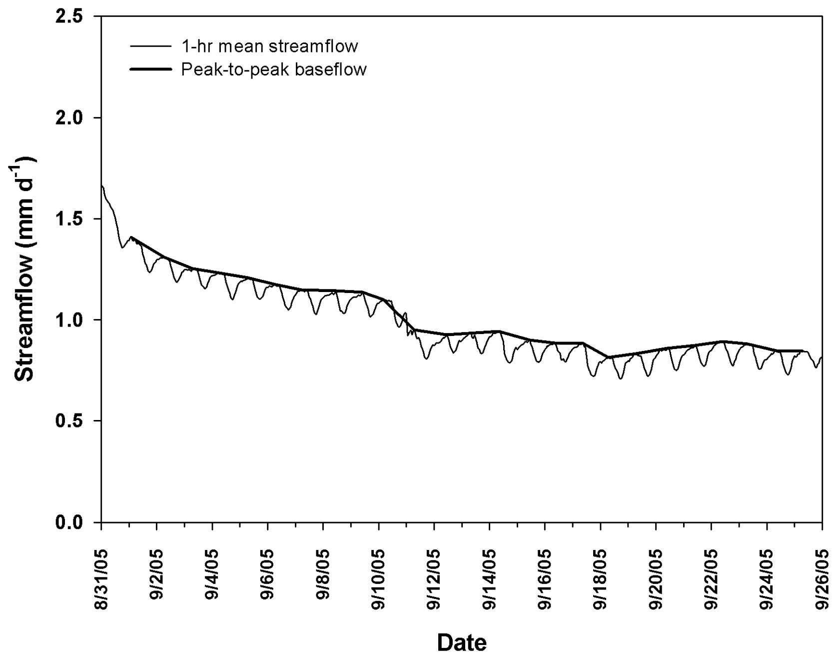

Figure 25. Mean hourly streamflow time series observed at FORS-3 over September 2005.

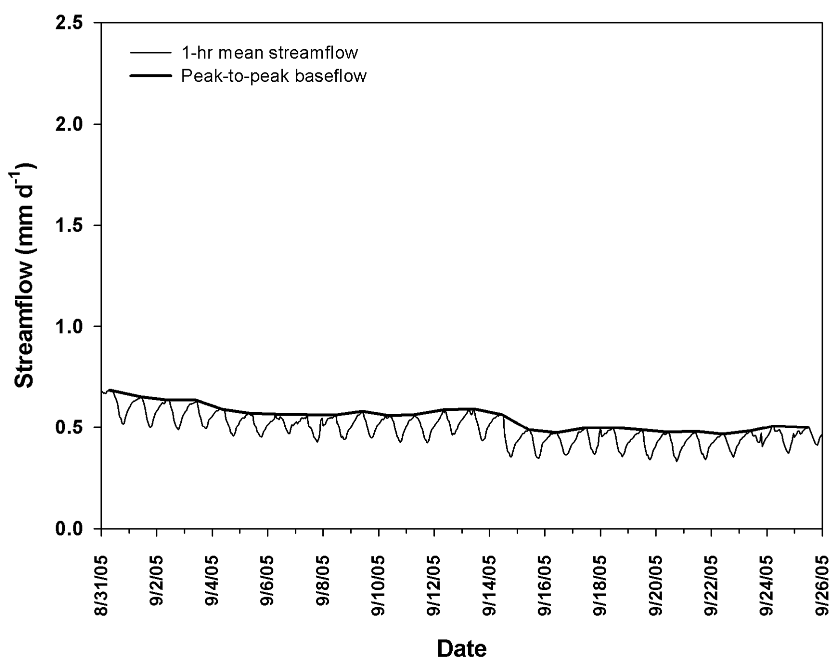

Figure 26. Mean hourly streamflow time series observed at AG-7 over September 2005.

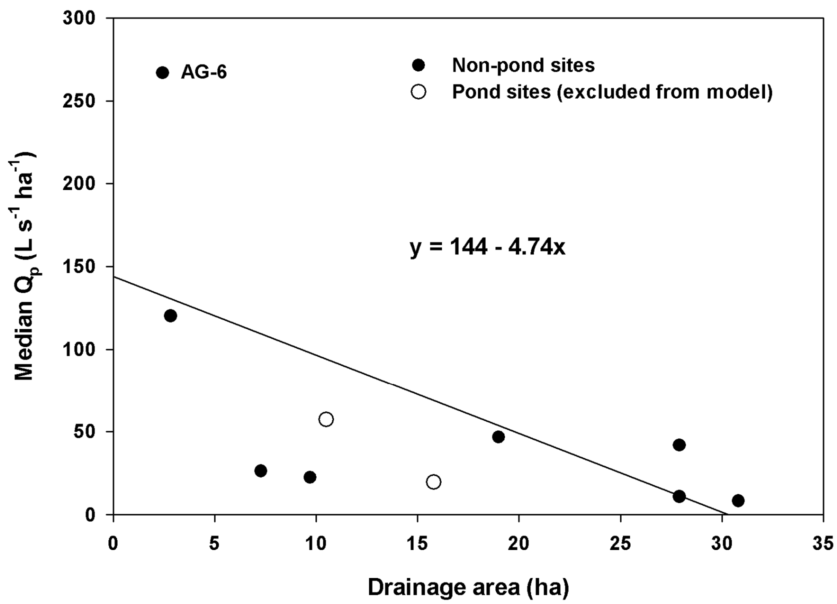

Figure 27. Relationship between median peak flow rates in top 10 storm events and watershed drainage area ($P = 0.0872$; $R^2 = 0.4100$). Sites FORS-1 and AG-12 excluded from analysis.

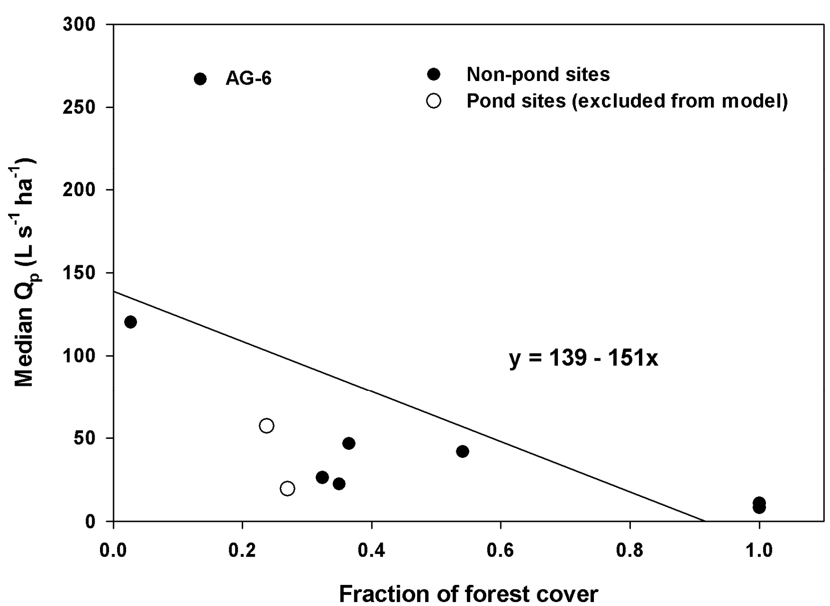

Figure 28. Relationship between median peak flow rates in top 10 storm events and fraction of forest cover in watersheds ($P = 0.0971$; $R^2 = 0.3914$). Sites FORS-1 and AG-12 excluded from analysis.

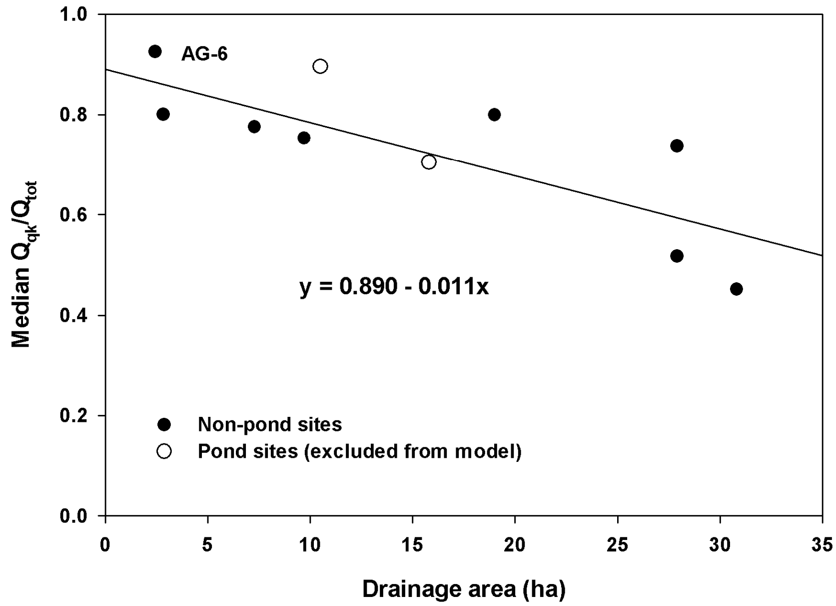

Figure 29. Relationship between median fraction of total stormflow as quickflow and watershed drainage area ($P = 0.0163$; $R^2 = 0.6456$). Sites FORS-1 and AG-12 excluded from analysis.

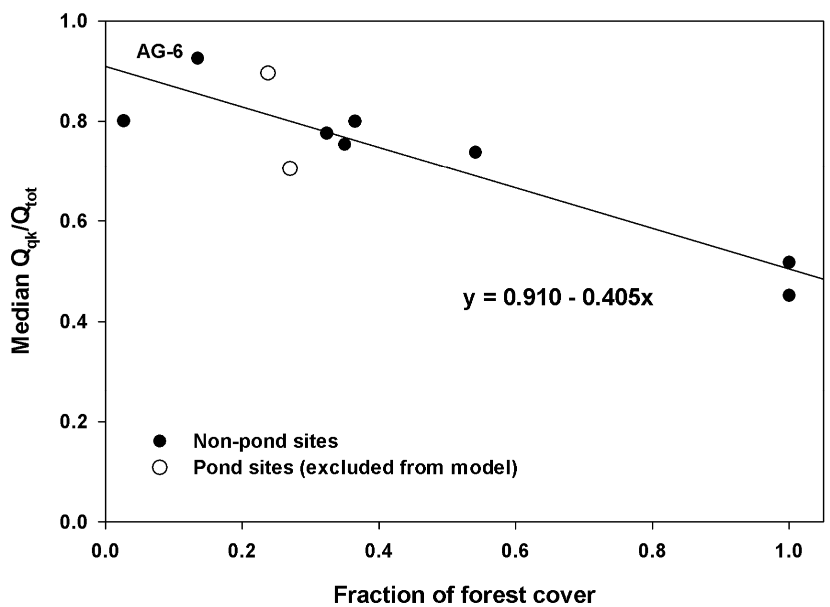

Figure 30. Relationship between median fraction of total stormflow as quickflow and fraction of forest cover in watershed ($P = 0.0006$; $R^2 = 0.8756$). Sites FORS-1 and AG-12 excluded from analysis.

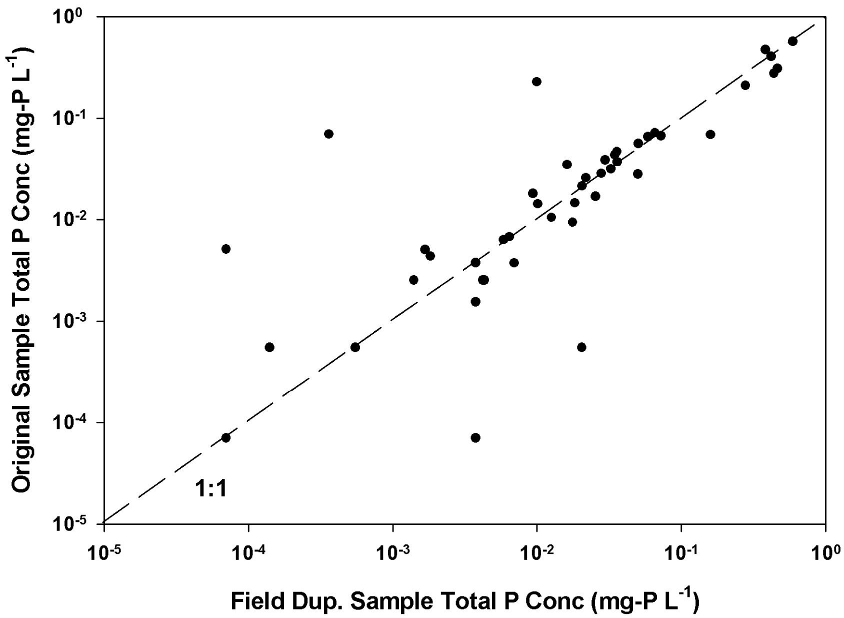

Figure 31. Scatter plot comparing total P concentrations in field duplicate quality control samples with original field samples. The dashed line represents a 1:1 relationship.

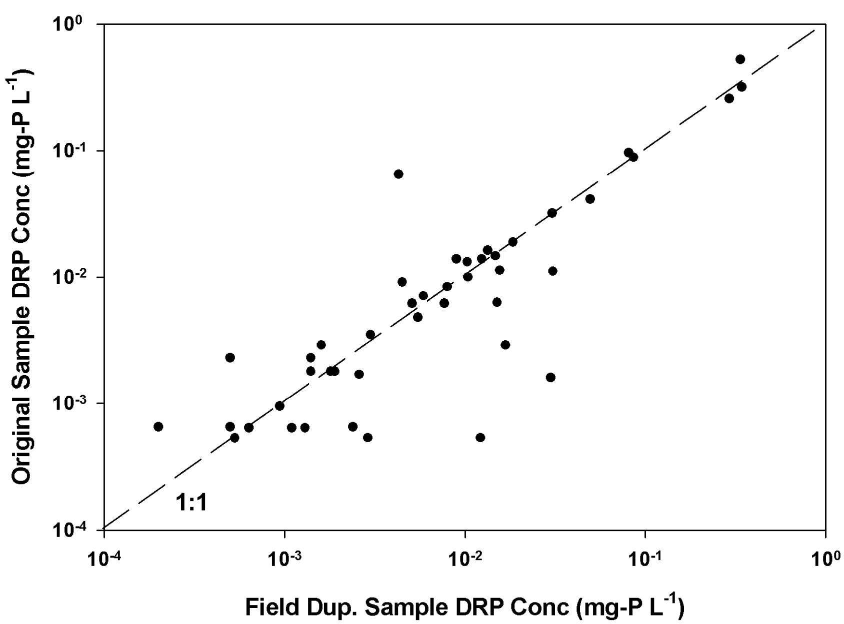

Figure 32. Scatter plot comparing dissolved reactive P concentrations in field duplicate quality control samples with original field samples. The dashed line represents a 1:1 relationship.

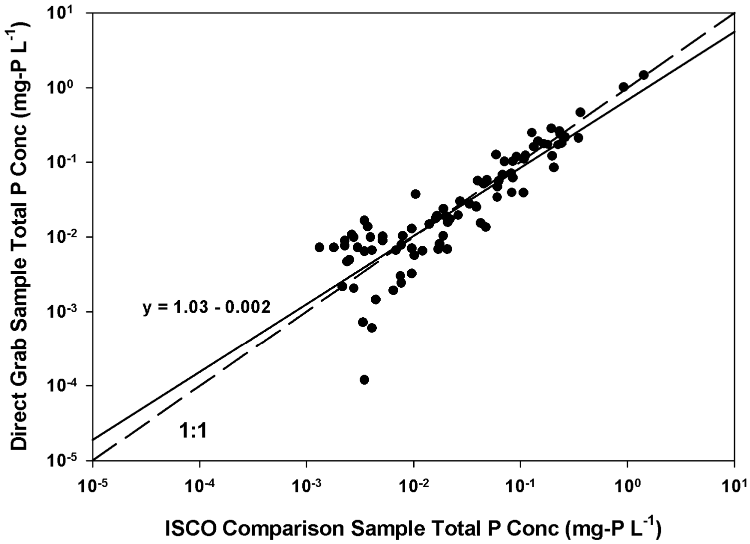

Figure 33. Scatter plot and linear regression model of total P concentrations in ISCO-based comparison QC samples versus grab samples collected directly from flume outlets. (P-value probability to fail to reject (H_o: slope = 1) = 0.1032; R^2-value = 0.9675).

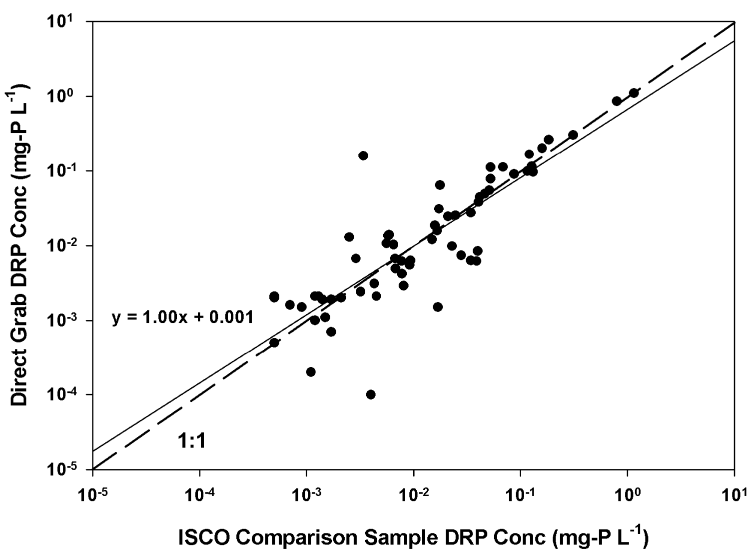

Figure 34. Scatter plot and linear regression model of dissolved reactive P concentrations in ISCO-based comparison QC samples versus grab samples collected directly from flume outlets. (P-value (probability to fail to reject H_o: slope = 1) = 0.9137; R^2-value = 0.9849).

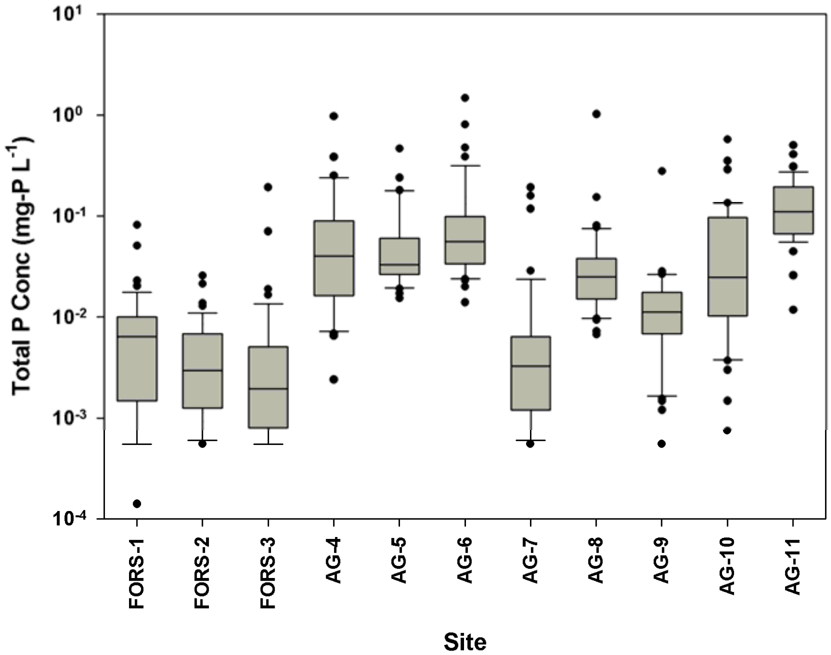

Figure 35. Total P concentrations in BWG samples collected at perennial and intermittent sites.

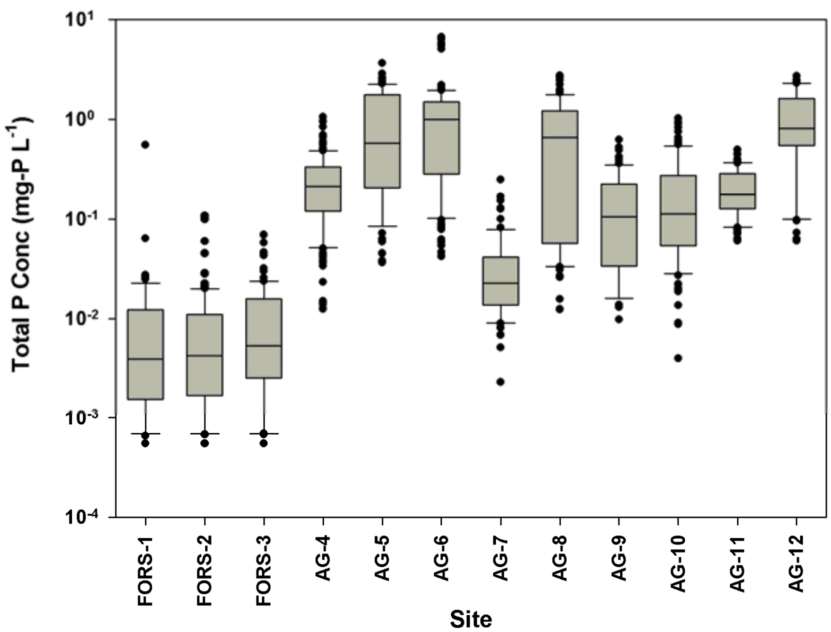

Figure 36. Total P concentrations in storm samples collected at all sites.

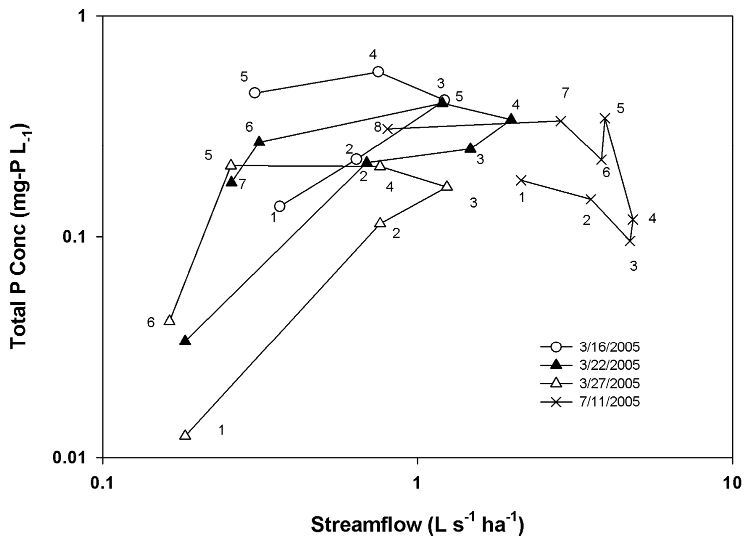

Figure 37. Relationships between TP concentration and streamflow observed during storm events at AG-4.

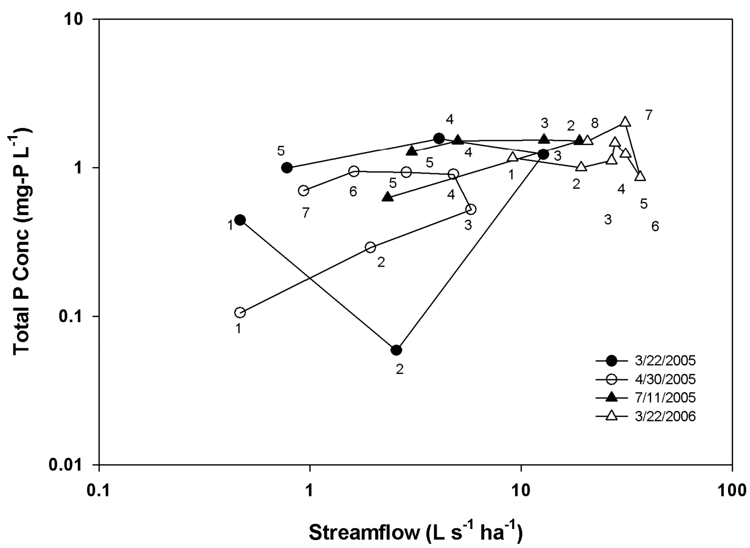

Figure 38. Relationships between TP concentration and streamflow observed during storm events at AG-6.

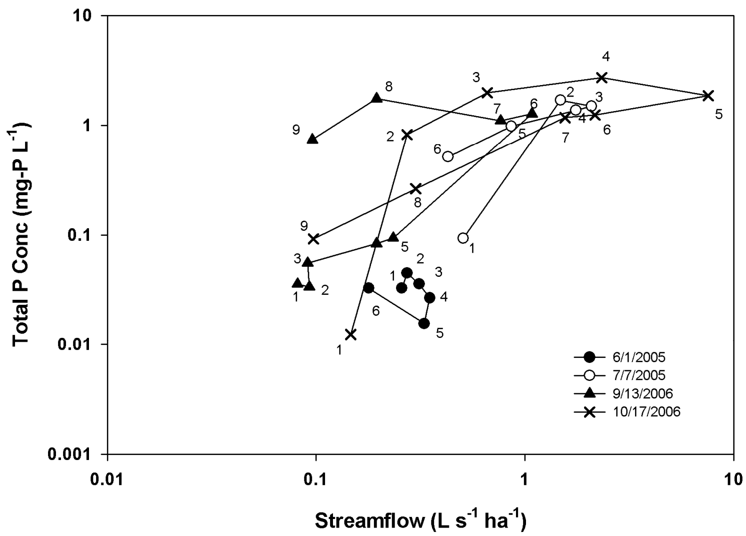

Figure 39. Relationships between TP concentration and streamflow observed during storm events at AG-8.

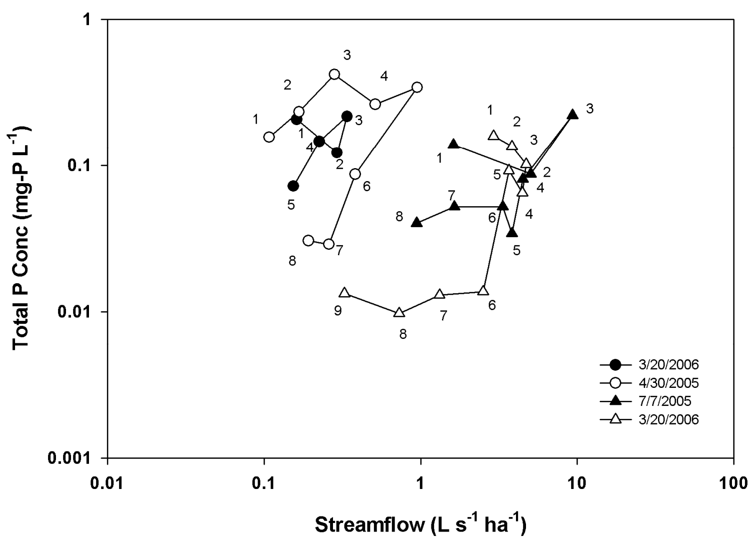

Figure 40. Relationships between TP concentration and streamflow observed during storm events at AG-9.

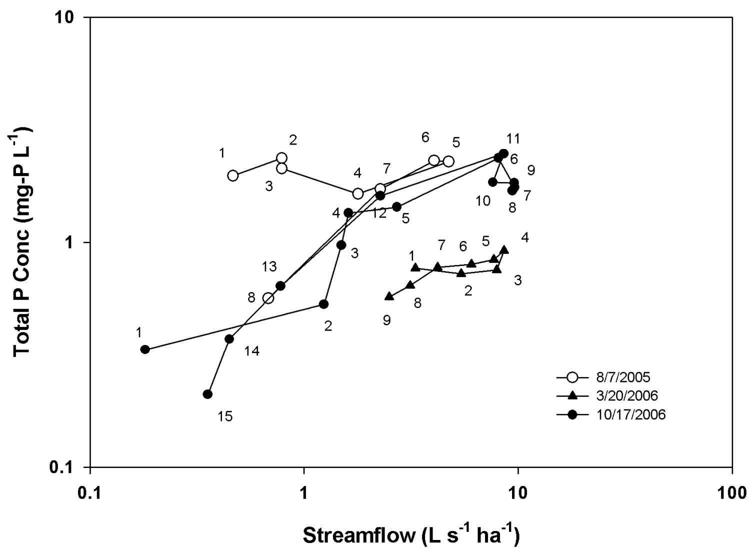

Figure 41. Relationships between TP concentration and streamflow observed during storm events at AG-12.

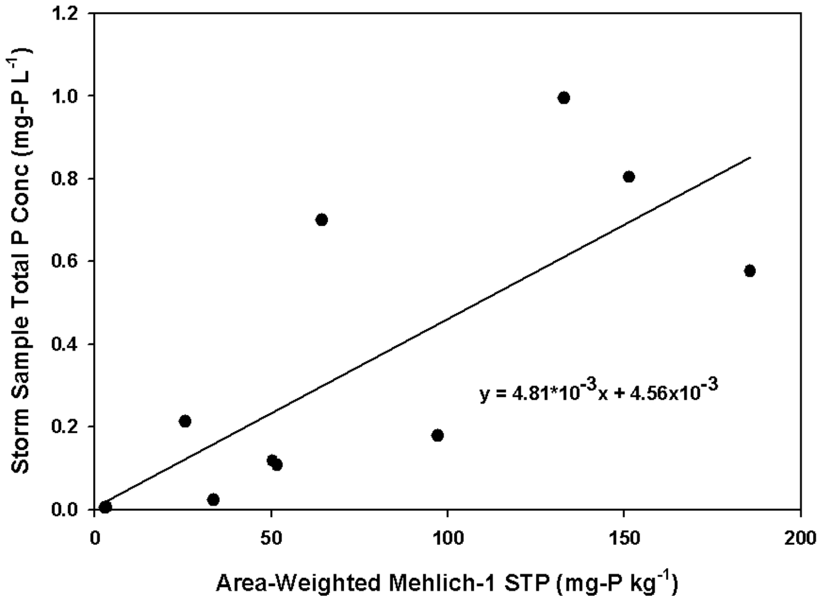

Figure 42. Relationship between median TP concentrations in storm samples and area-weighted Mehlich-1 STP (P=0.0022; R^2=0.6244).

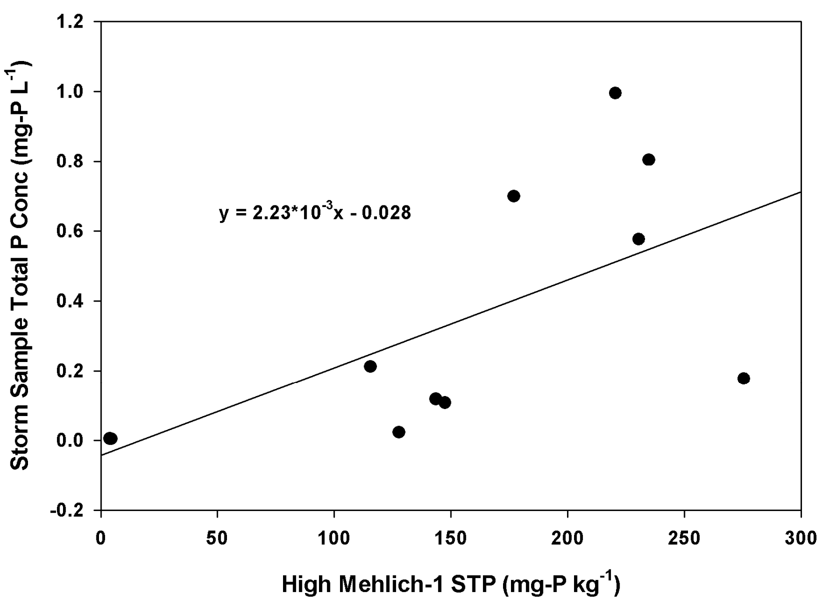

Figure 43. Relationship between median TP concentrations in storm samples and high Mehlich-1 STP (P=0.0395; R^2=0.3914).

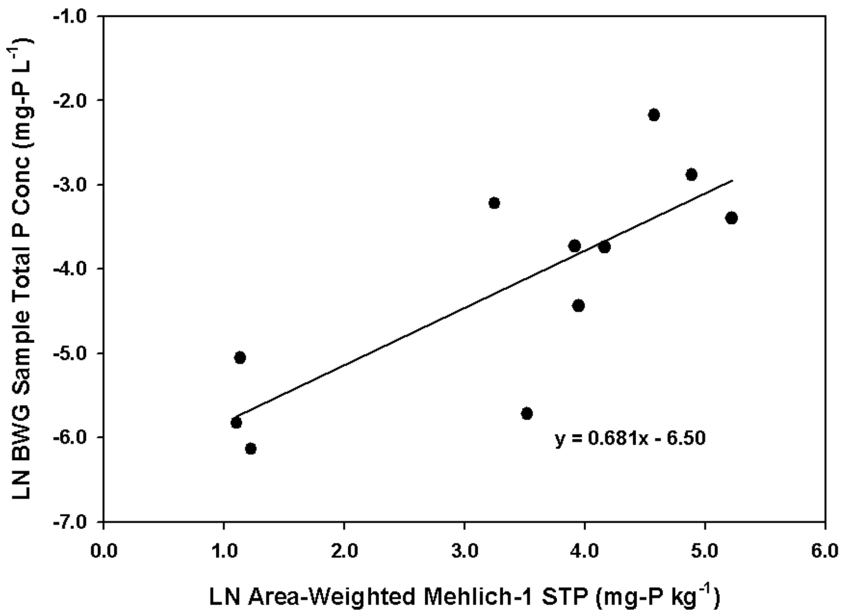

Figure 44. Relationship between LN-transformed median TP concentrations in BWG samples and LN-transformed area-weighted Mehlich-1 STP (P=0.0040; R^2=0.6202).

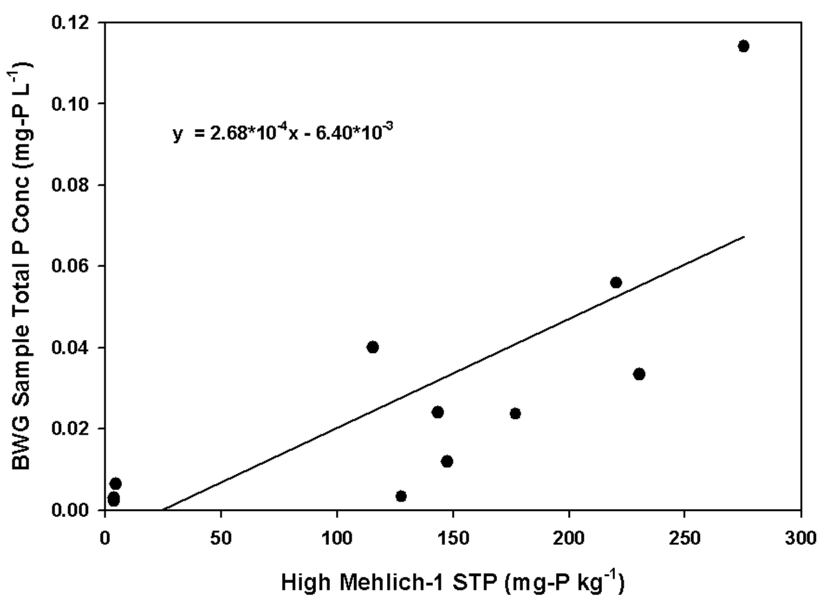

Figure 45. Relationship between median TP concentrations in BWG samples and high Mehlich-1 STP (P=0.0062; R^2 = 0.5837).

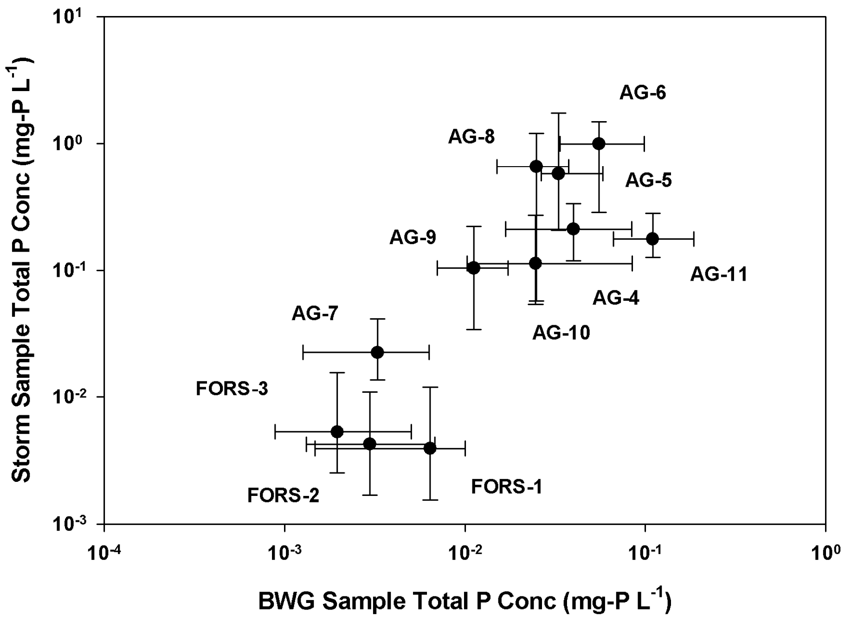

Figure 46. Scatter plot of median TP concentrations of storm and BWG samples. Error bars show interquartile ranges.

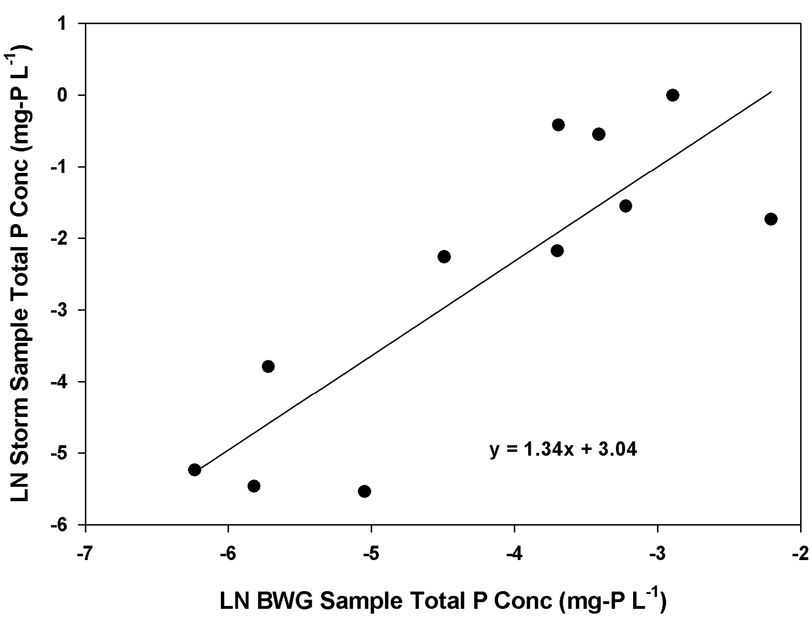

Figure 47. Relationship between LN-transformed median TP concentrations in storm samples and BWG samples ($P=0.0012$; $R^2=0.7085$).

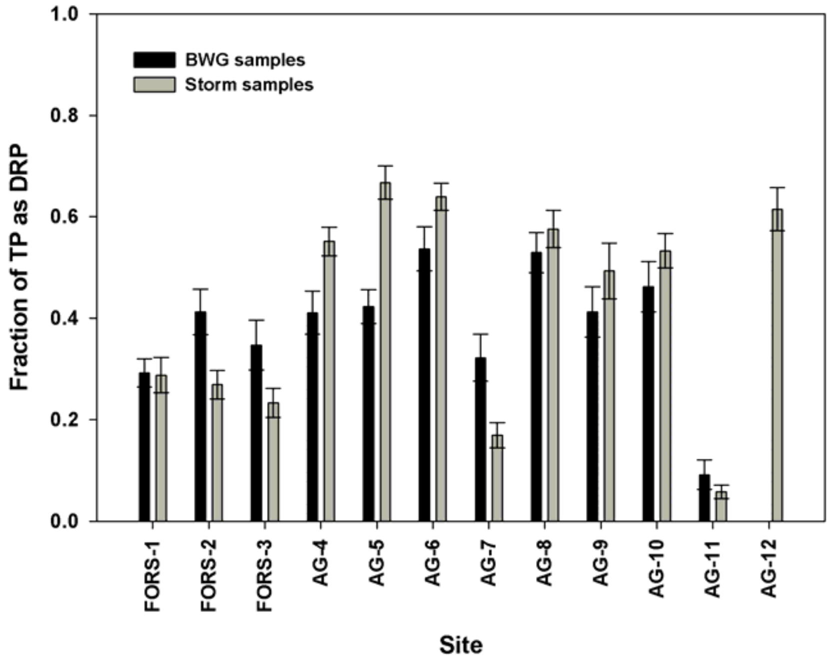

Figure 48. Fraction of TP as DRP in BWG and storm samples. Error bars indicate +/- one standard error.

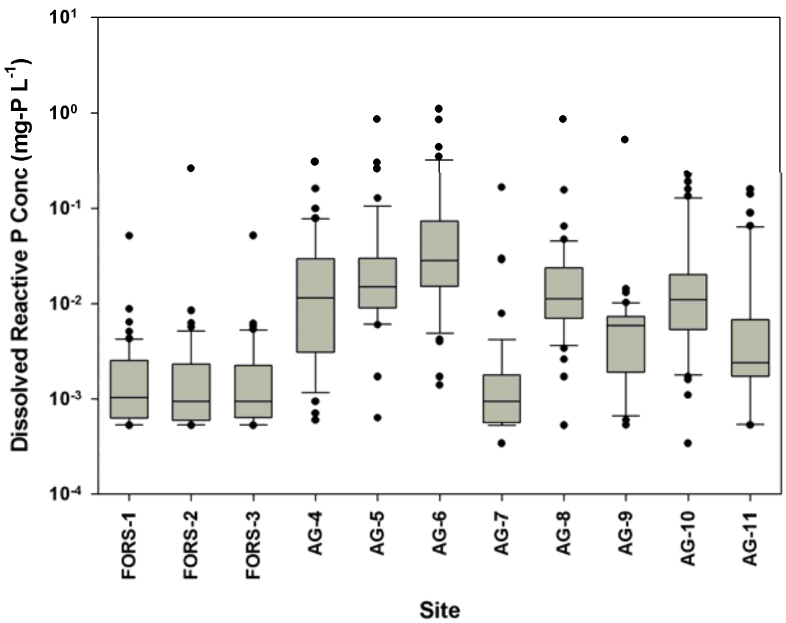

Figure 49. Dissolved reactive P concentrations in BWG samples collected at perennial and intermittent sites.

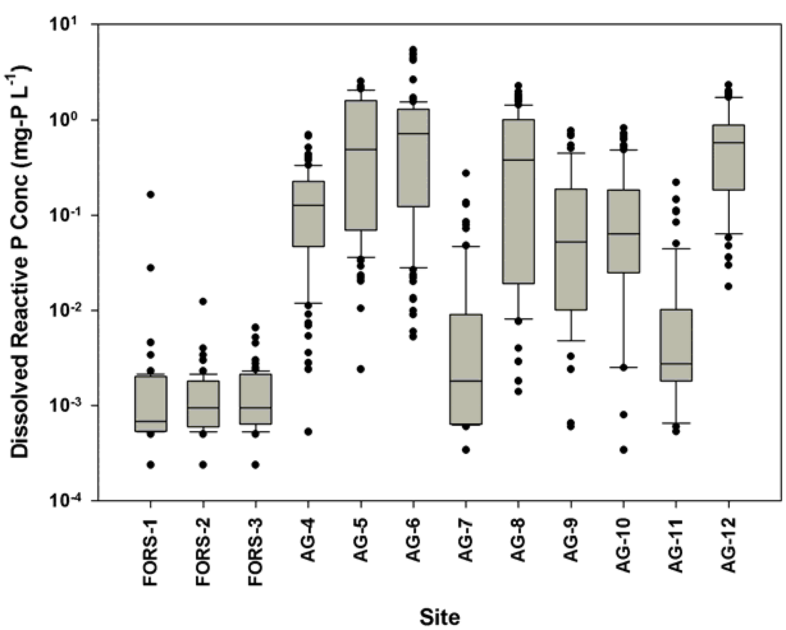

Figure 50. Dissolved reactive P concentrations in storm samples collected at all study sites.

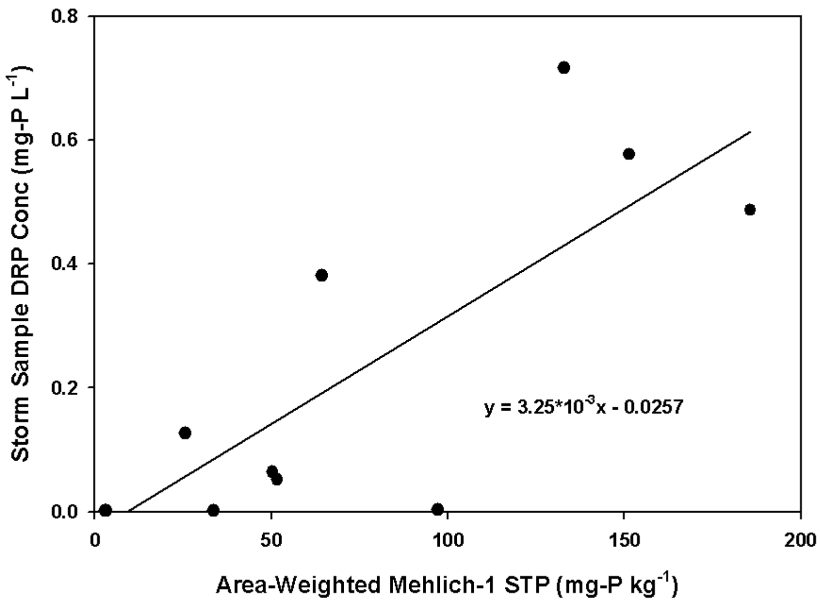

Figure 51. Relationship between median DRP concentrations in storm samples and area-weighted Mehlich-1 STP ($P=0.0058$; $R^2=0.5888$).

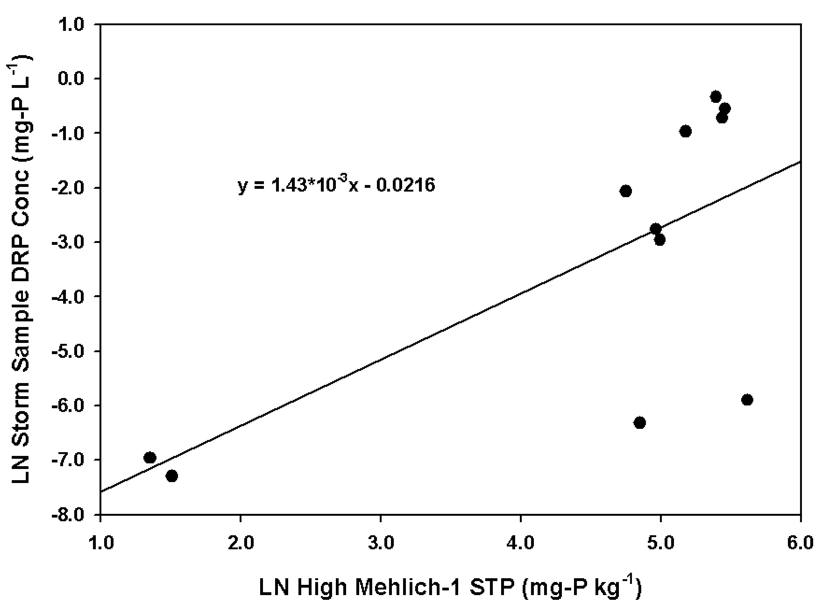

Figure 52. Relationship between LN-transformed median DRP concentrations in storm samples and LN-transformed high Mehlich-1 STP ($P=0.0107$; $R^2=0.5332$).

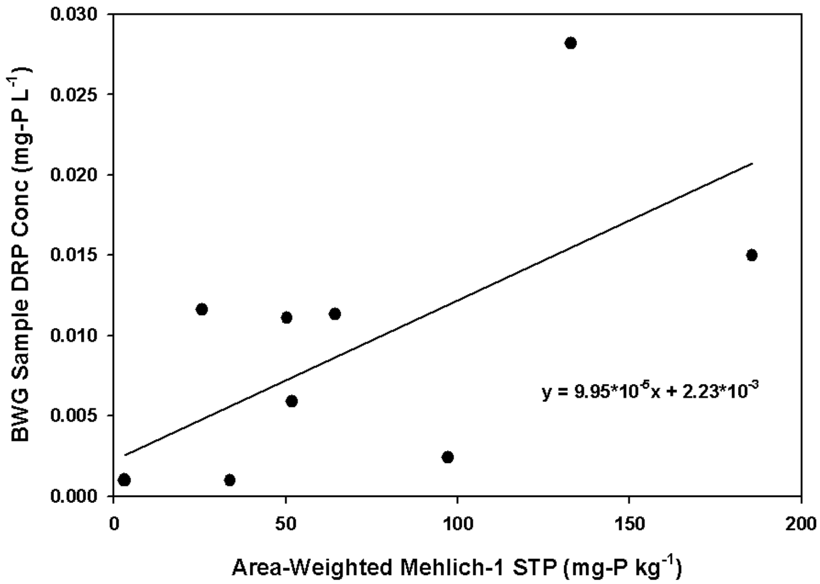

Figure 53. Relationship between median DRP concentrations in BWG samples and area-weighted Mehlich-1 STP (P=0.0201; R^2=0.4687).

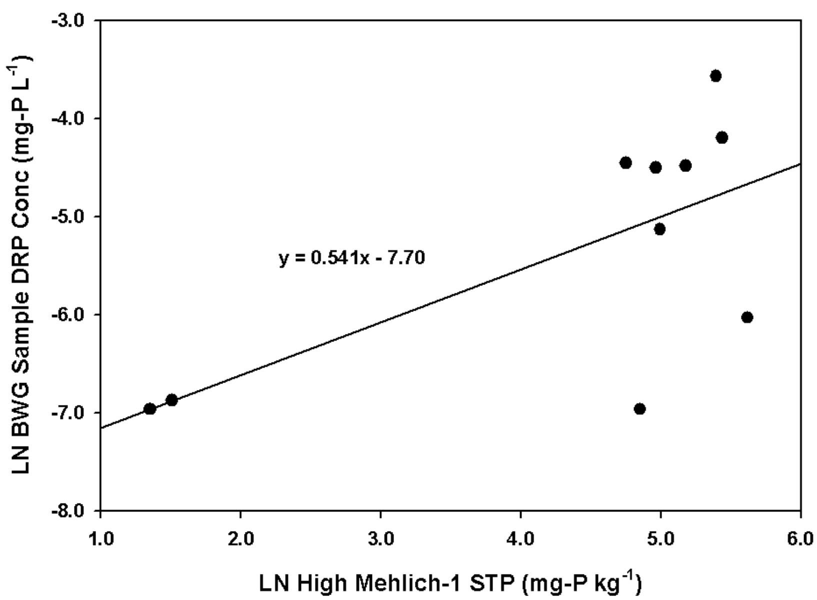

Figure 54. Relationship between LN-transformed median DRP concentrations in BWG samples and LN-transformed high Mehlich-1 STP (P<0.0001; R^2=0.5293).

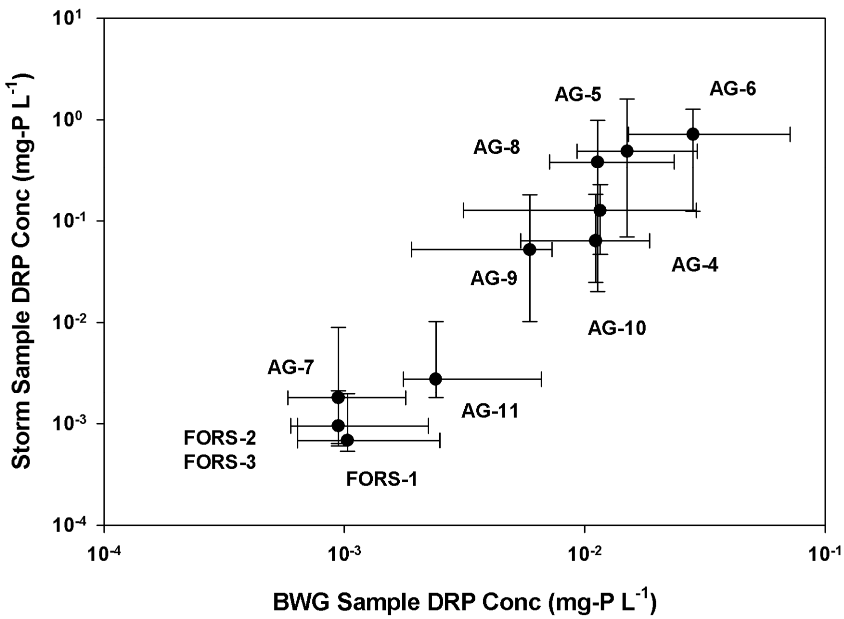

Figure 55. Scatter plot of median TP concentrations of storm and BWG samples. Error bars show interquartile ranges.

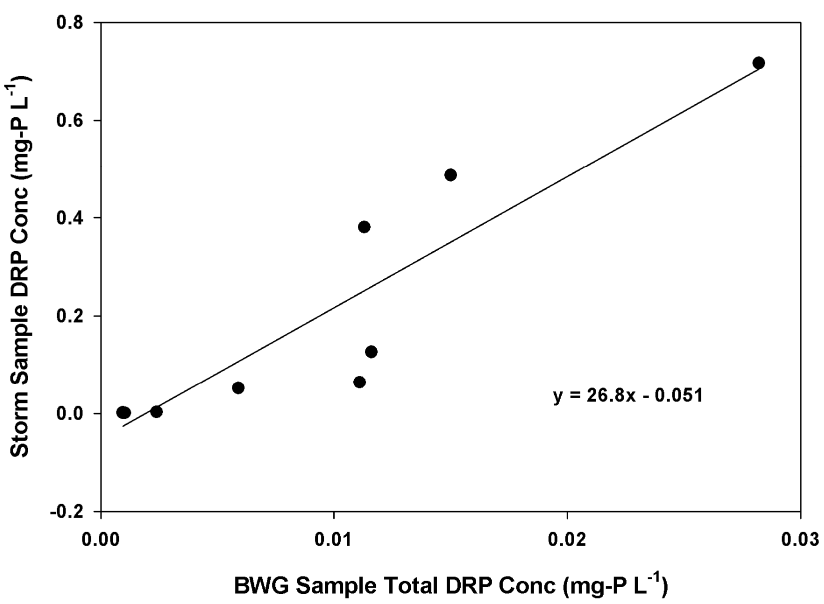

Figure 56. Relationship between median DRP concentrations in storm samples and BWG samples ($P<0.0001$; $R^2=0.8489$).

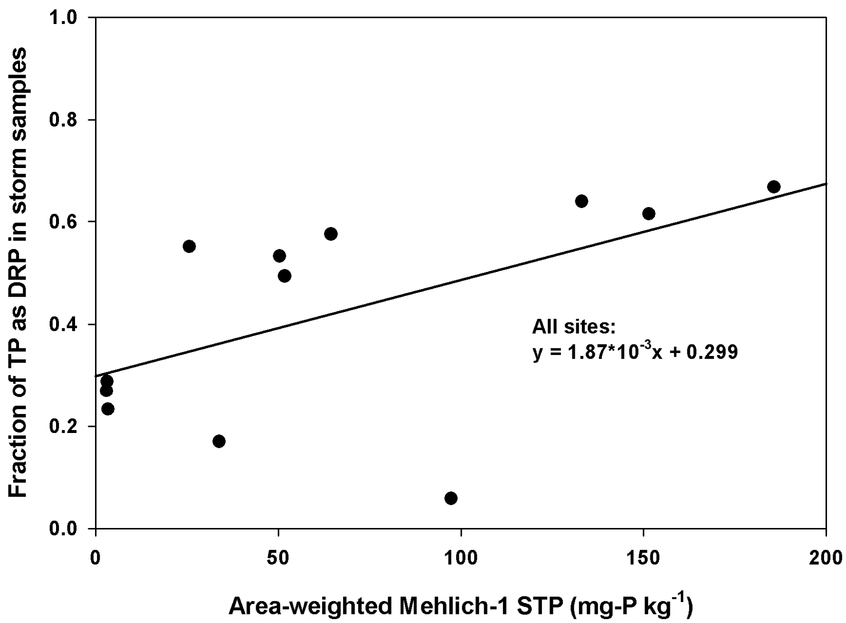

Figure 57. Relationship between fraction of TP concentration as DRP in storm samples from all sites and area-weighted Mehlich-1 STP (P = 0.0597; R^2 = 0.3106).

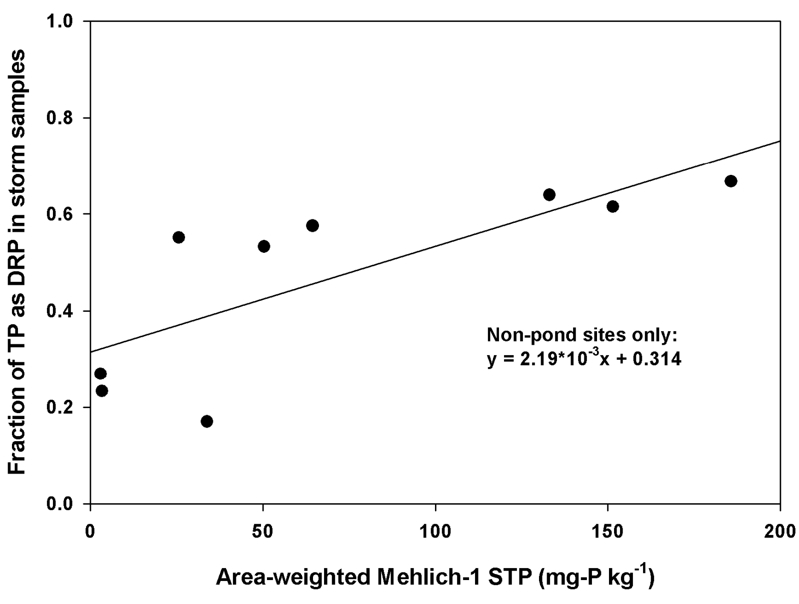

Figure 58. Relationship between fraction of TP concentration as DRP in storm samples from non-pond sites and area-weighted Mehlich-1 STP (P = 0.0158; R^2 = 0.5886).

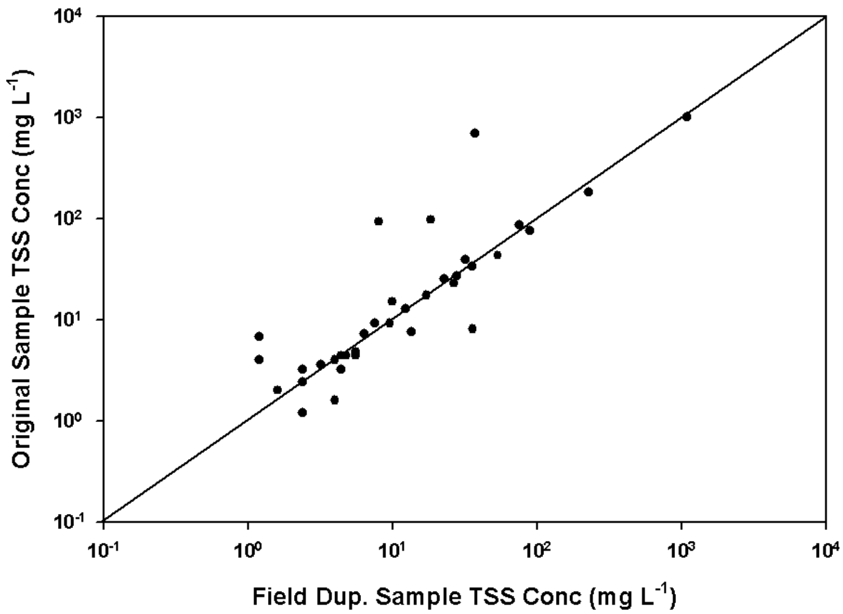

Figure 59. Scatter plot comparing total suspended solids concentrations in field duplicate quality control samples with original field samples. The dashed line represents a 1:1 relationship.

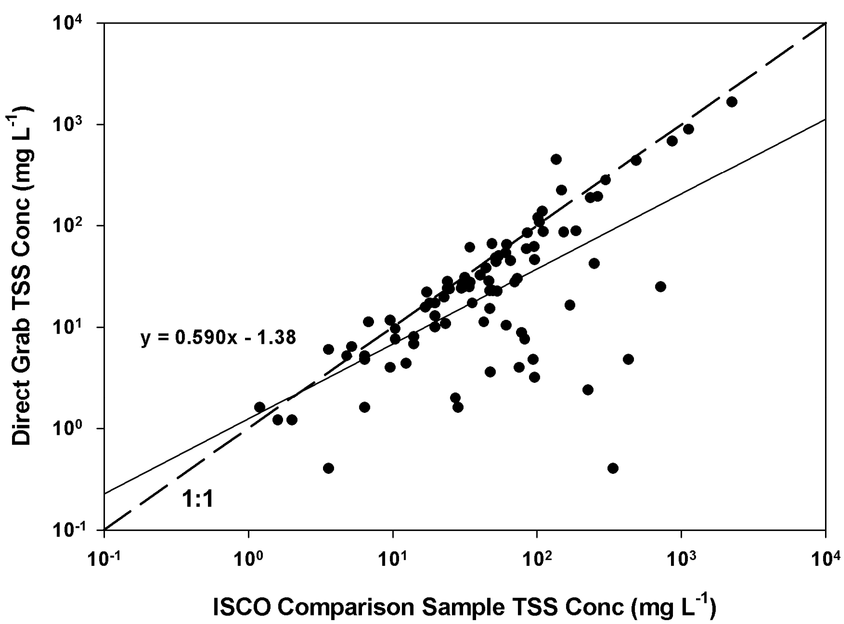

Figure 60. Scatter plot and linear regression model of total suspended solids concentrations in ISCO-based comparison QC samples versus grab samples collected directly from flume outlets. (P-value (probability to fail to reject H_o: slope = 1) <0.0001; R^2 = 0.7082). The dashed line represents a 1:1 relationship.

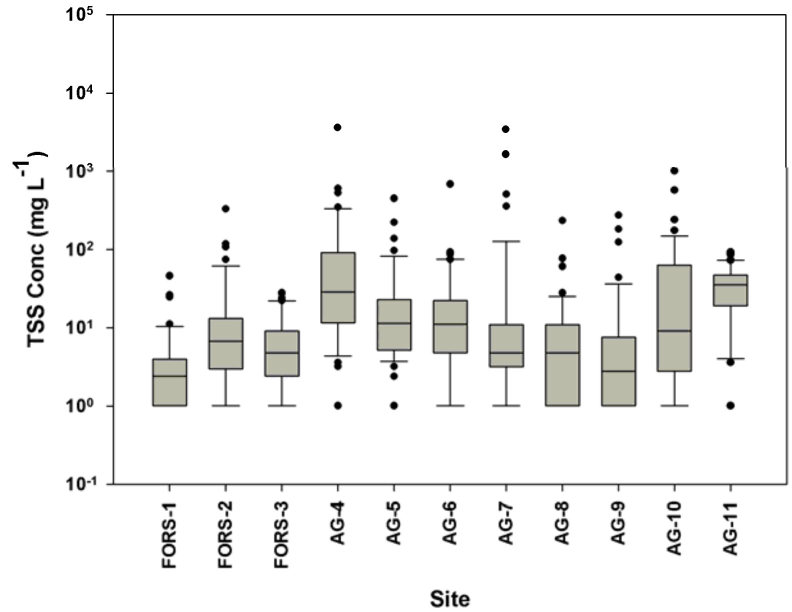

Figure 61. Total suspended solids concentrations in BWG samples collected at perennial and intermittent sites.

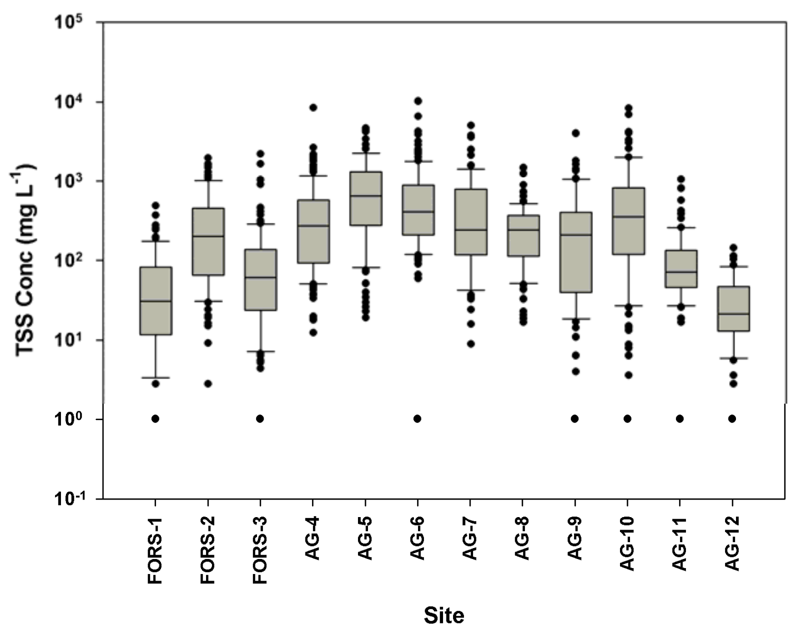

Figure 62. Total suspended solids concentrations in BWG samples collected at all sites.

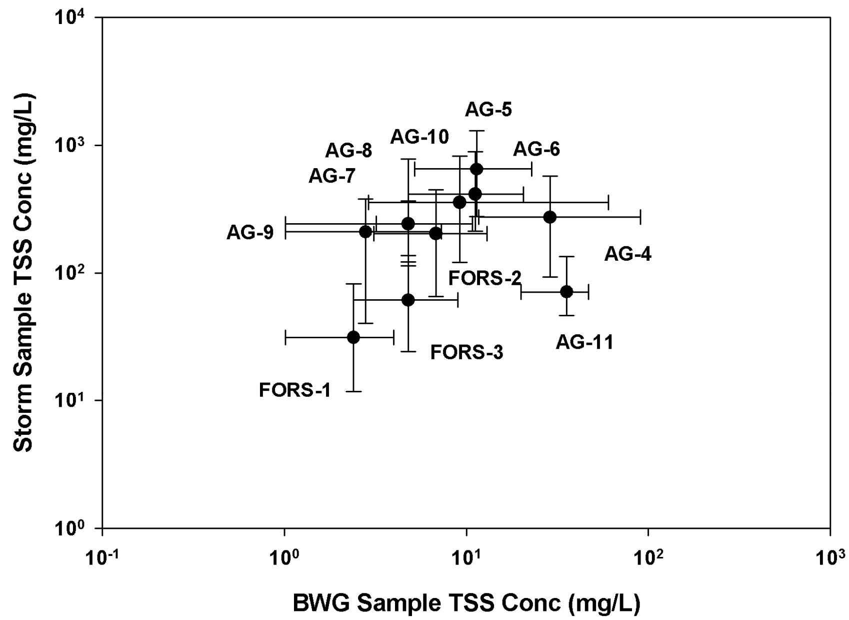

Figure 63. Scatter plot of median TSS concentrations of storm and BWG samples. Error bars show interquartile ranges.

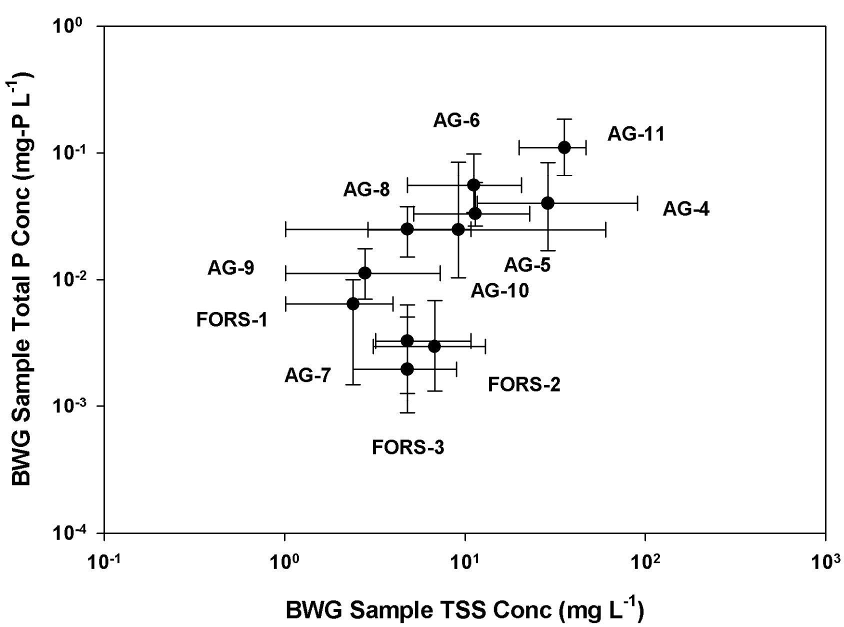

Figure 64. Scatter plot of median TP and TSS concentrations in BWG samples. Error bars show interquartile ranges.

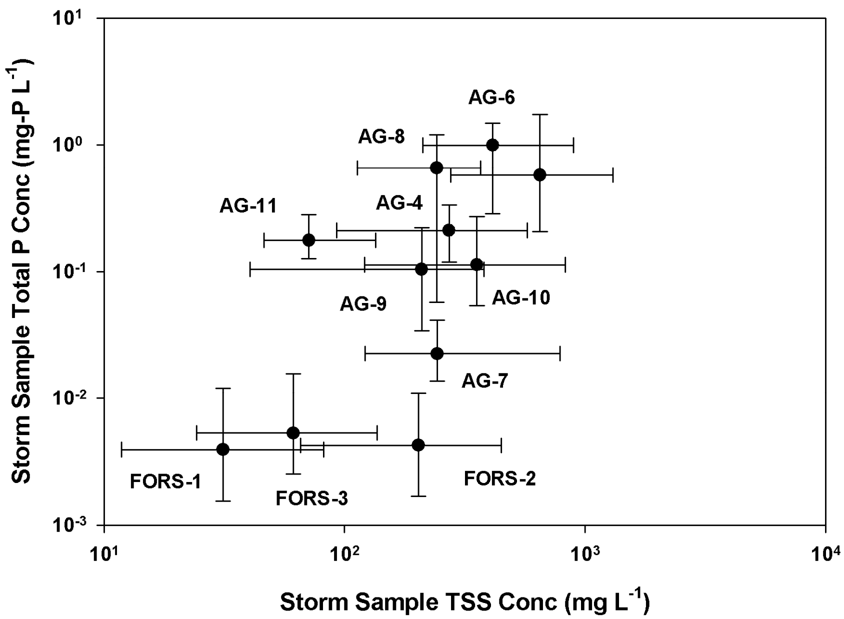

Figure 65. Scatter plot of median TP and TSS concentrations in storm samples. Error bars show interquartile ranges. Ephemeral site AG-12 was not included in the analysis.

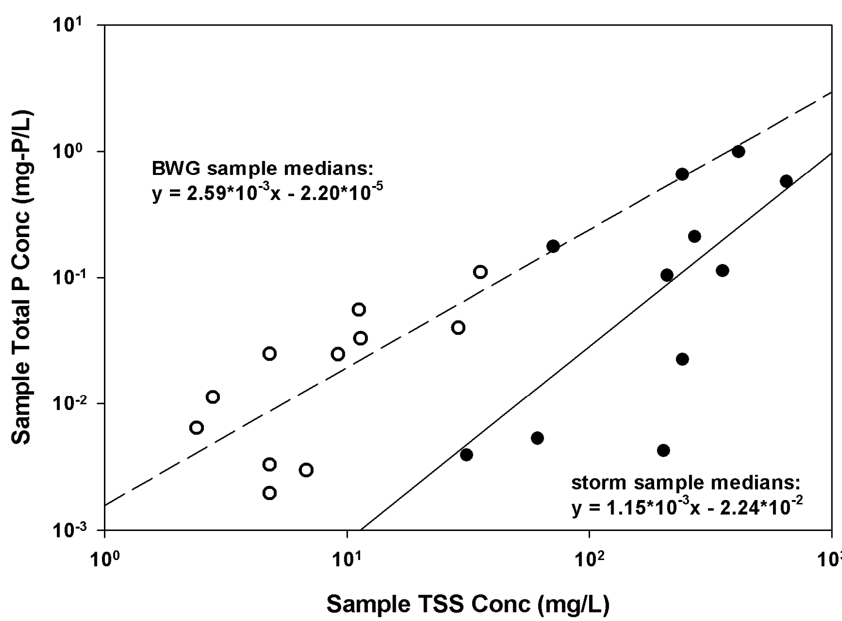

Figure 66. Relationships between median TP and TSS concentrations in BWG ($P=0.0008$; $R^2=0.7308$) and storm samples ($P<0.0471$; $R^2=0.3700$). Ephemeral site AG-12 was not included in the analysis.

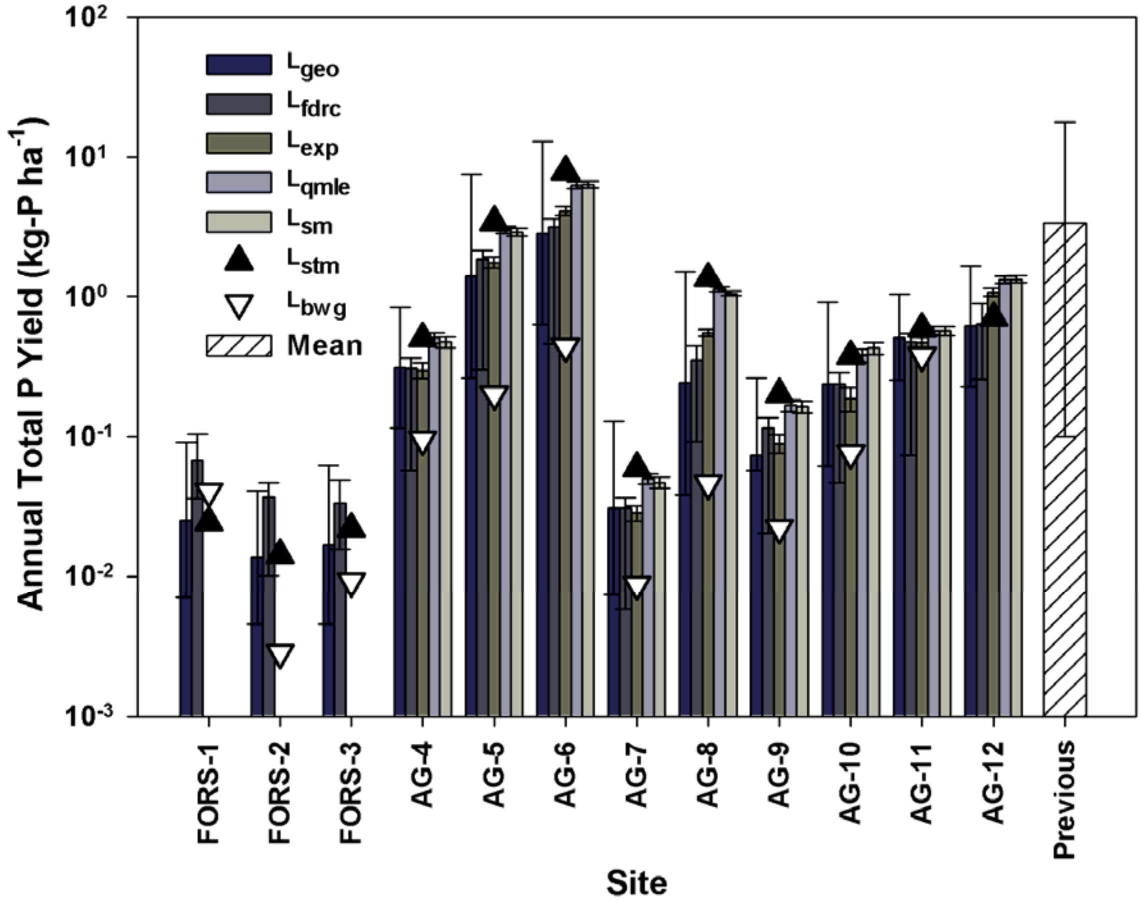

Figure 67. Annual TP yield estimates based on all load estimators investigated in study. Also shown are the mean and range of TP yields reported in previous field-scale studies (Table 1) of poultry manure-amended pastures.

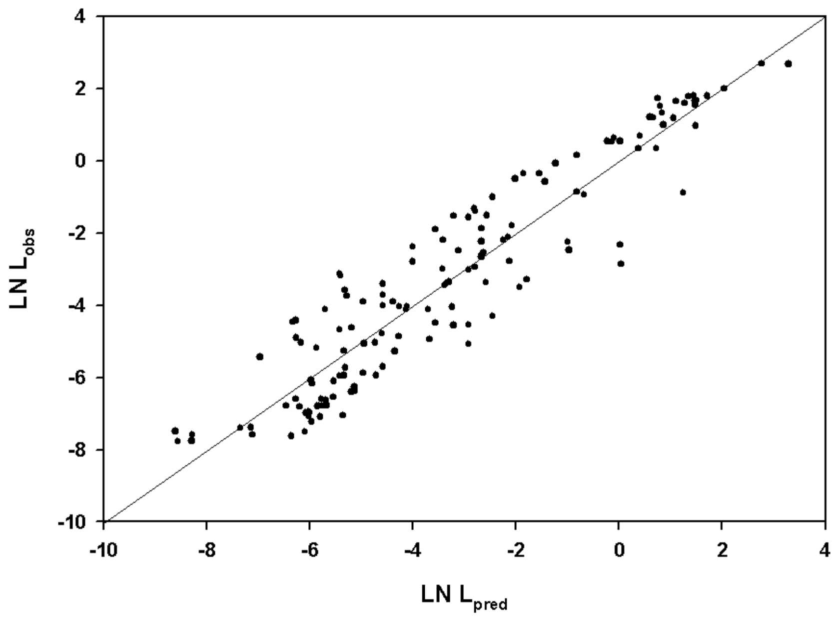

Figure 68. Comparison of observed instantaneous TP loads with predicted loads based on regression model calibration for AG-5. Line shown represents 1:1 line.

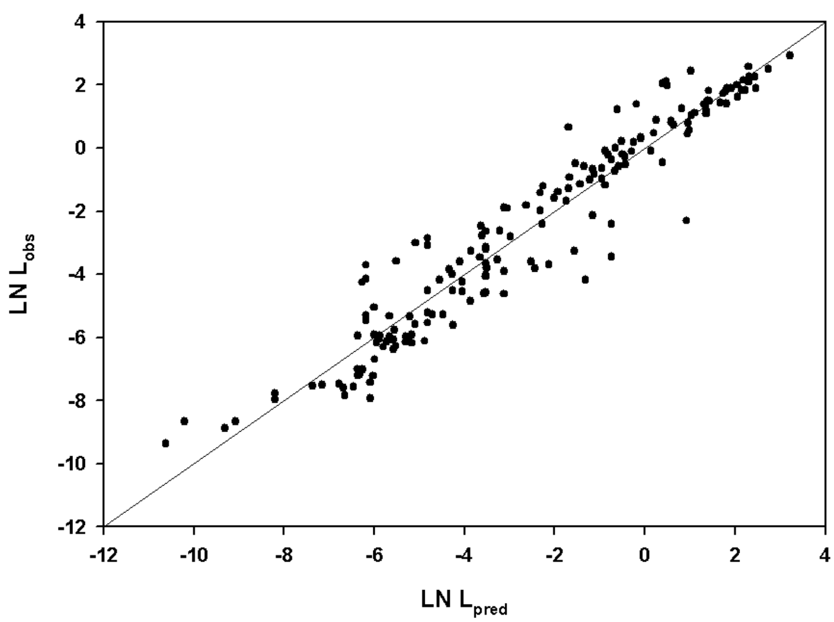

Figure 69. Comparison of observed instantaneous TP loads with predicted loads based on regression model calibration for AG-6. Line shown represents 1:1 line.

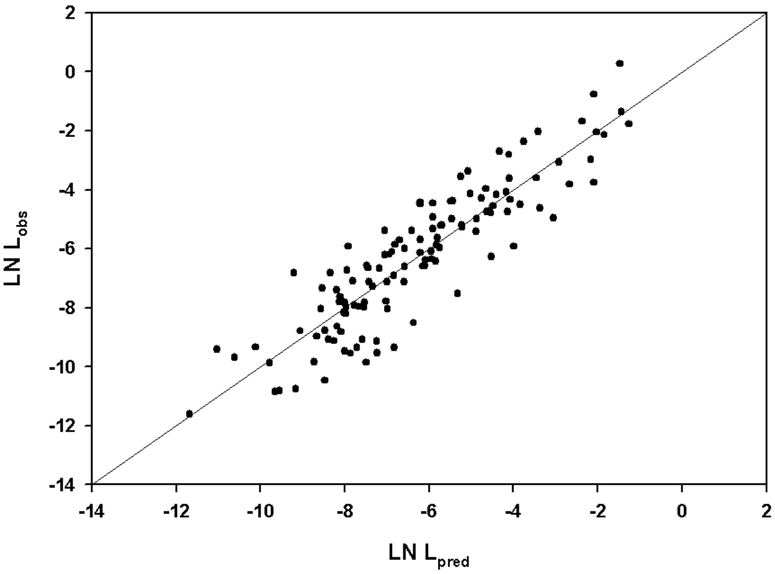

Figure 70. Comparison of observed instantaneous TP loads with predicted loads based on regression model calibration for AG-7. Line shown represents 1:1 line.

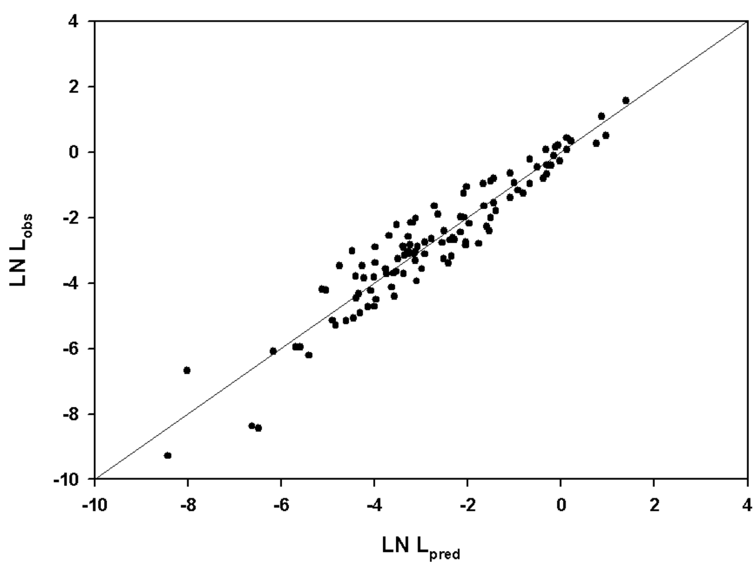

Figure 71. Comparison of observed instantaneous TP loads with predicted loads based on regression model calibration for AG-11. Line shown represents 1:1 line.

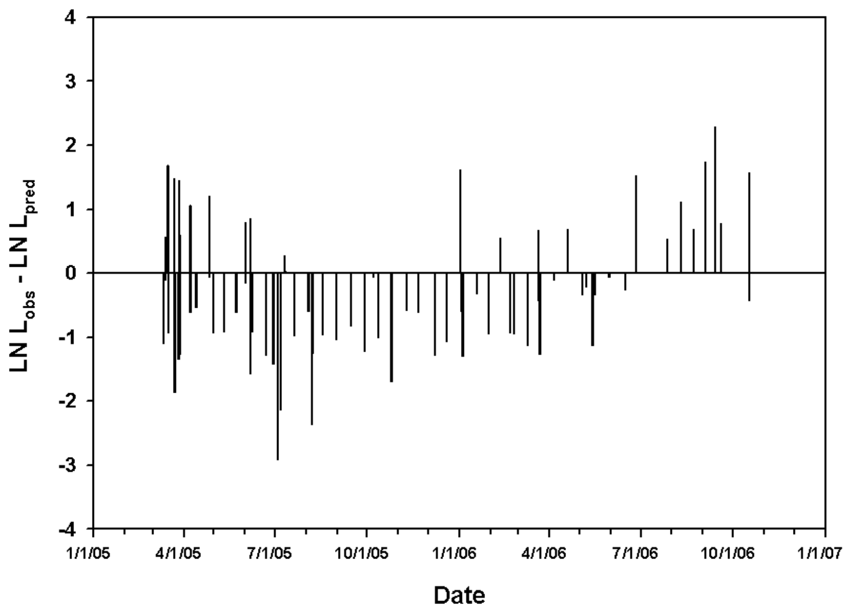

Figure 72. Time series of regression model residuals for AG-5.

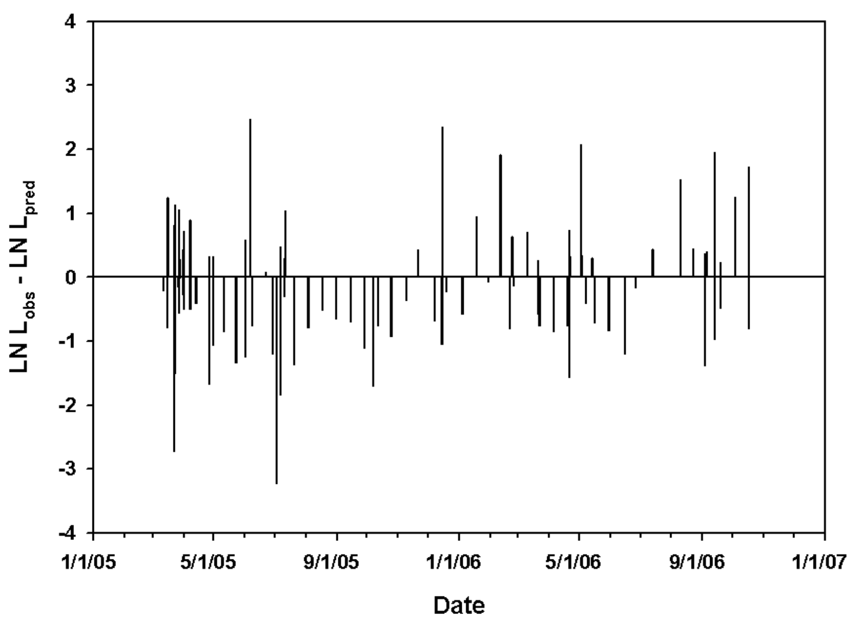

Figure 73. Time series of regression model residuals for AG-6.

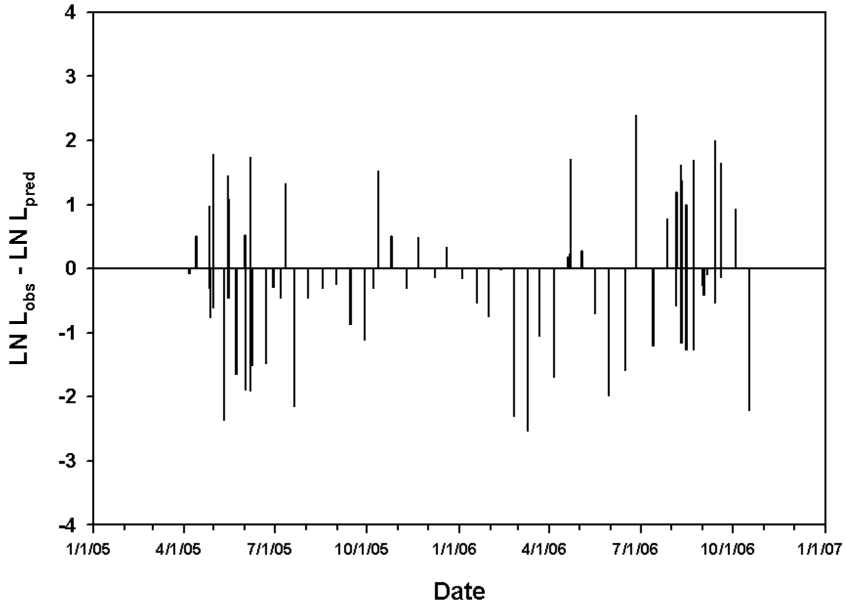

Figure 74. Time series of regression model residuals for AG-7.

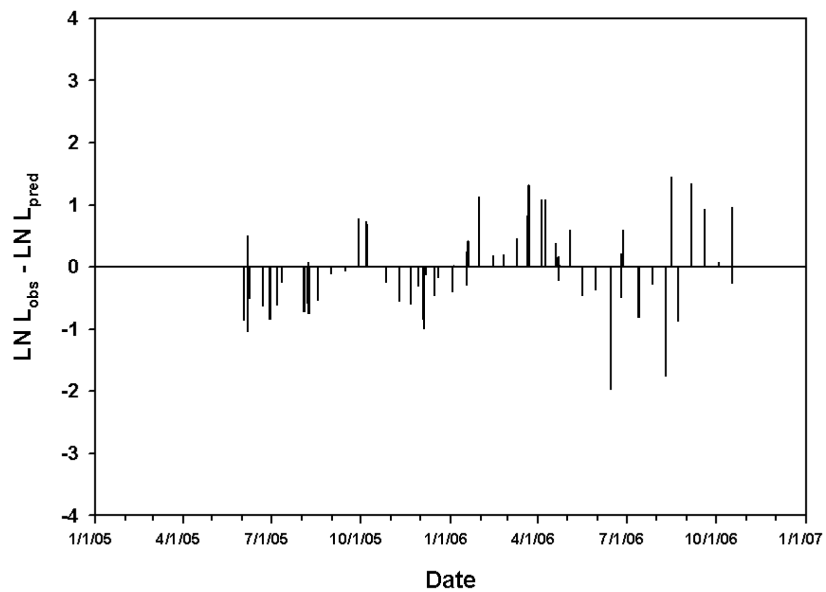

Figure 75. Time series of regression model residuals for AG-11.

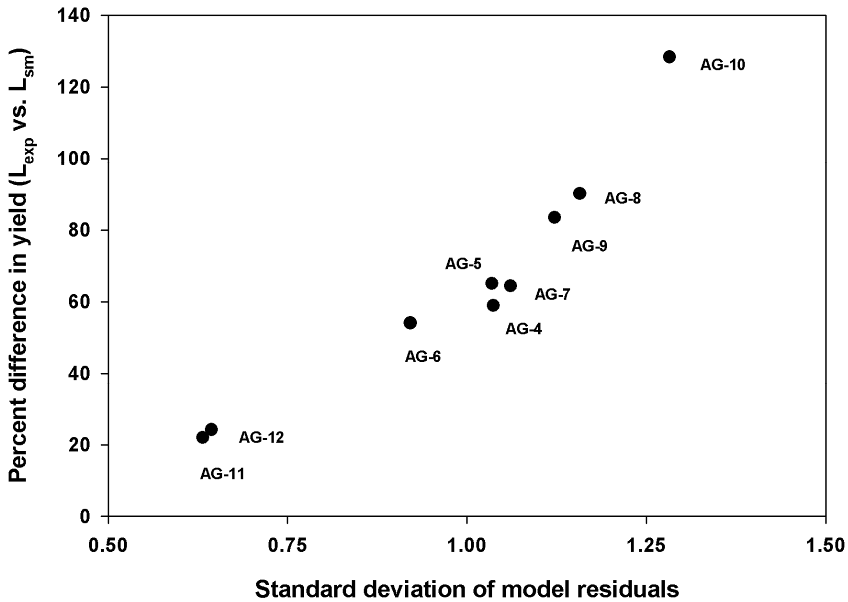

Figure 76. Percent difference in yield estimates via L_{exp} and L_{sm} estimators as a function of the standard deviation in the residuals of original calibrated regression model

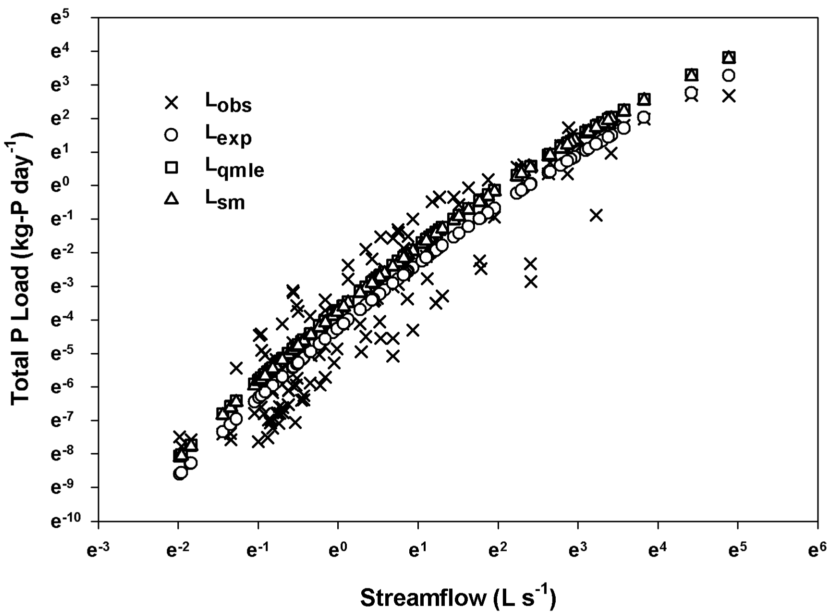

Figure 77. Observed and regression model-predicted instantaneous loads for site AG-5 as a function of observed streamflow.

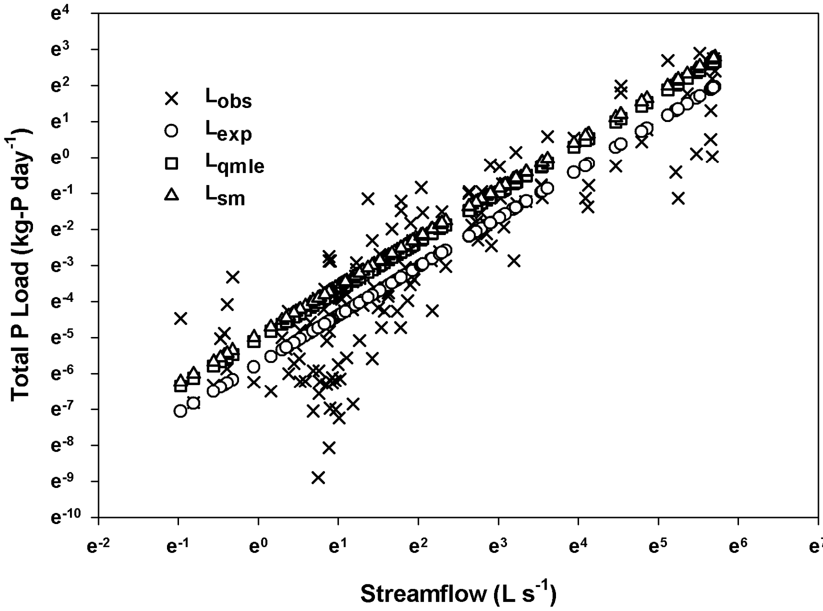

Figure 78. Observed and regression model-predicted instantaneous TP loads for site AG-10 as a function of observed streamflow.

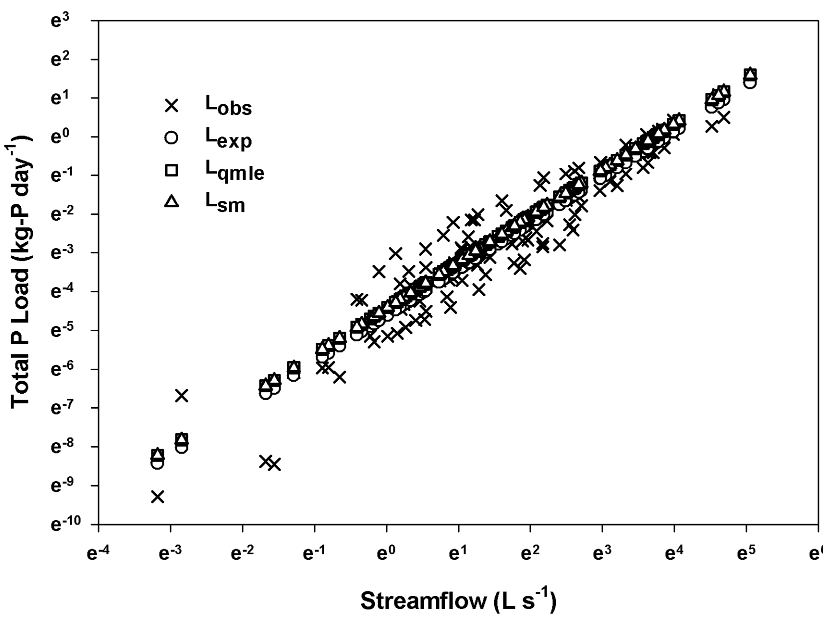

Figure 79. Observed and regression model-predicted instantaneous TP loads for site AG-11 as a function of observed streamflow.

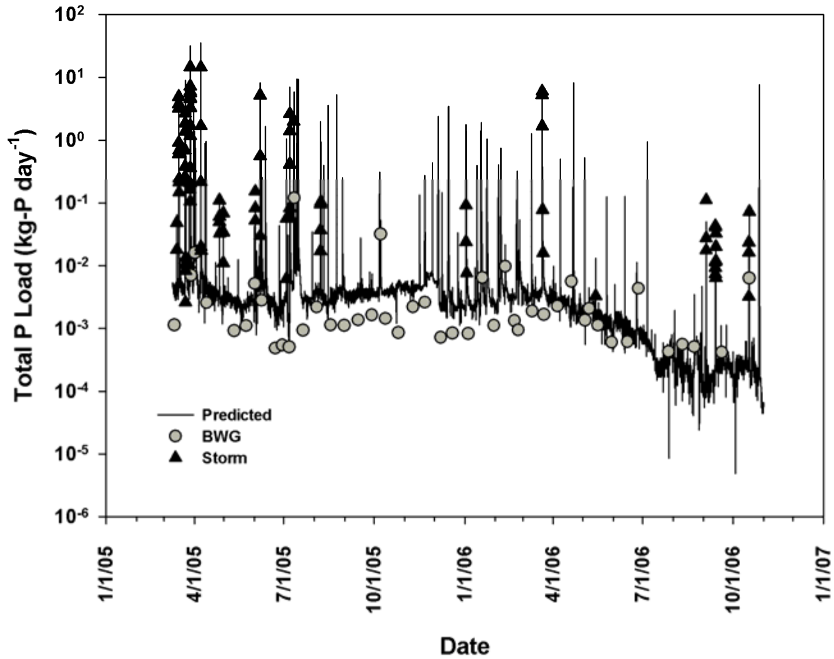

Figure 80. Time series of observed and regression model-predicted (L_{exp}) TP loads at site AG-5. Observed loads are shown by sample type (BWG and storm).

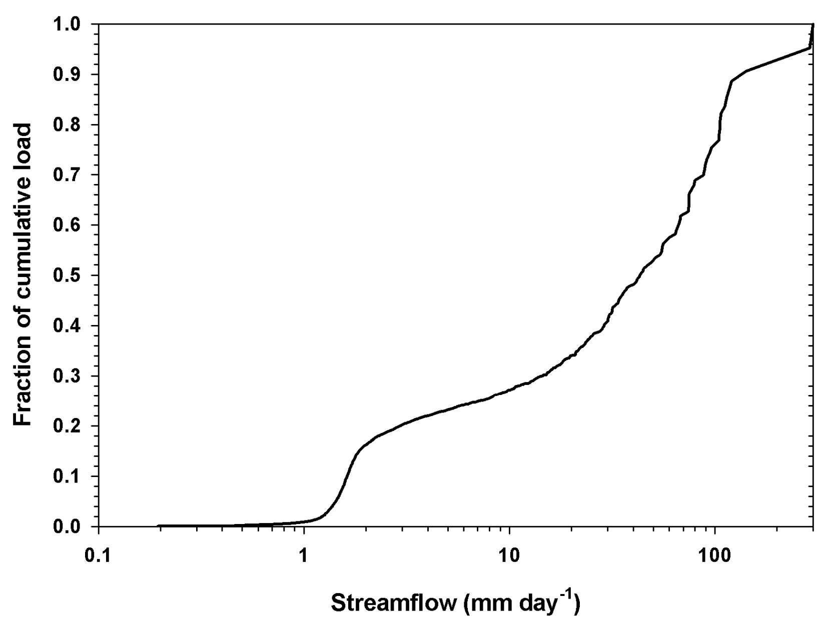

Figure 81. Cumulative TP load predicted (L_{exp}) for site AG-5 as a function of streamflow.

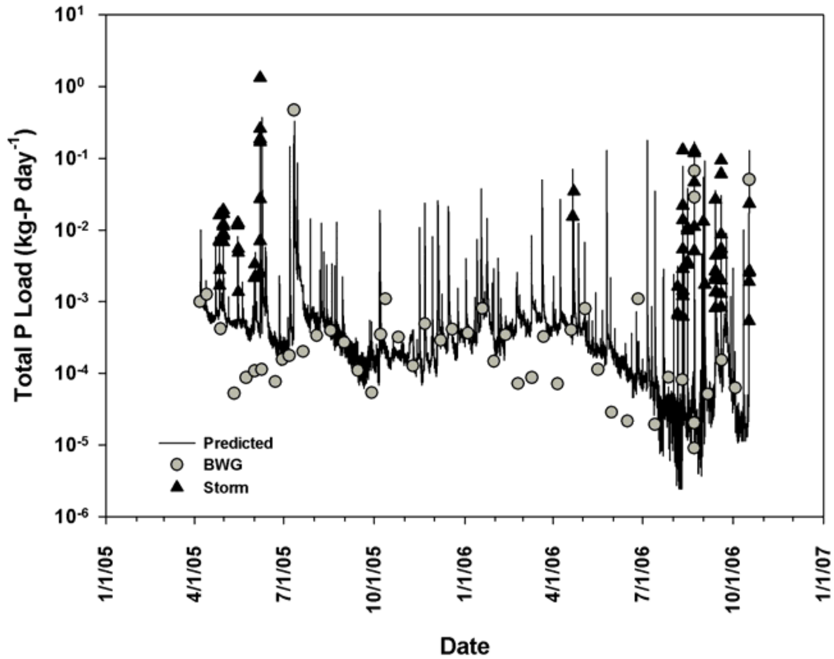

Figure 82. Time series of observed and predicted (L_{exp}) TP loads at site AG-7.

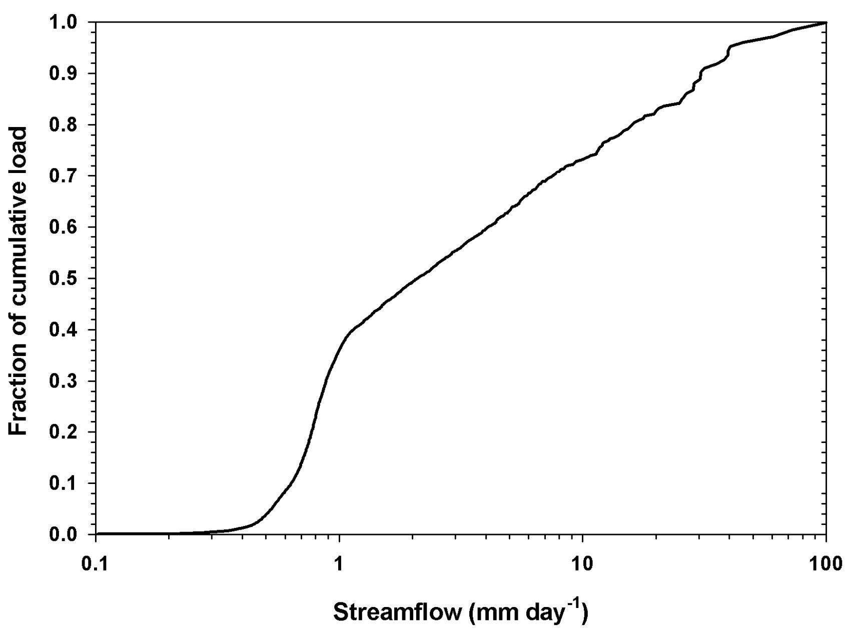

Figure 83. Cumulative TP load predicted (L_{exp}) for site AG-7 as a function of streamflow.

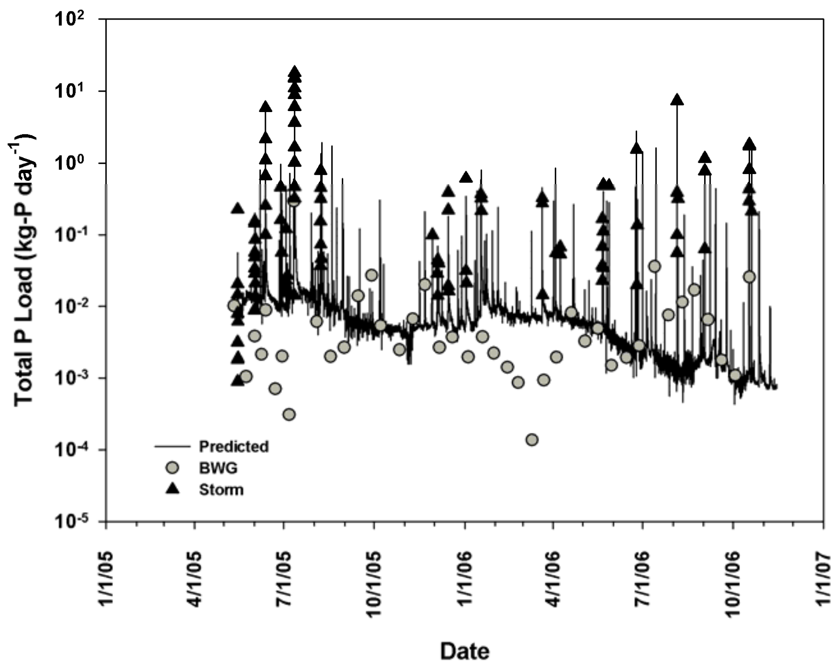

Figure 84. Time series of observed and predicted (L_{exp}) TP loads at site AG-10.

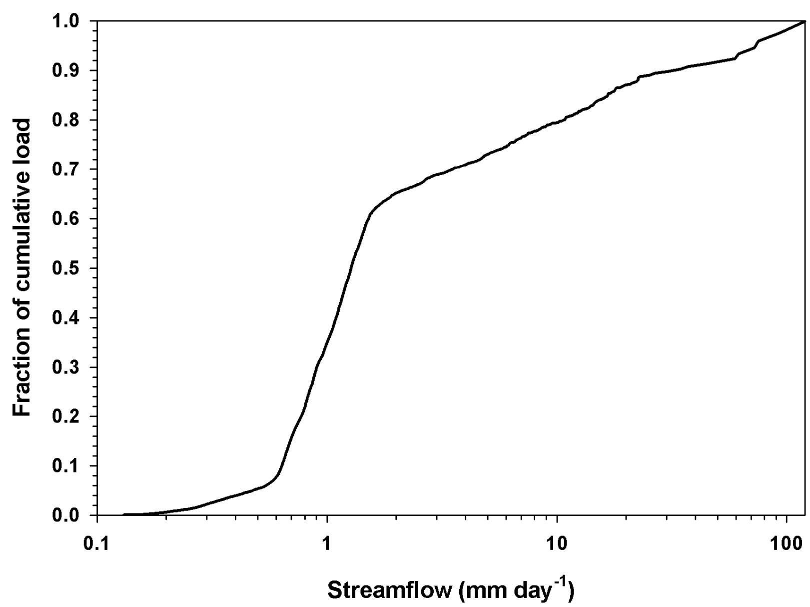

Figure 85. Cumulative TP load predicted (L_{exp}) for site AG-10 as a function of streamflow.

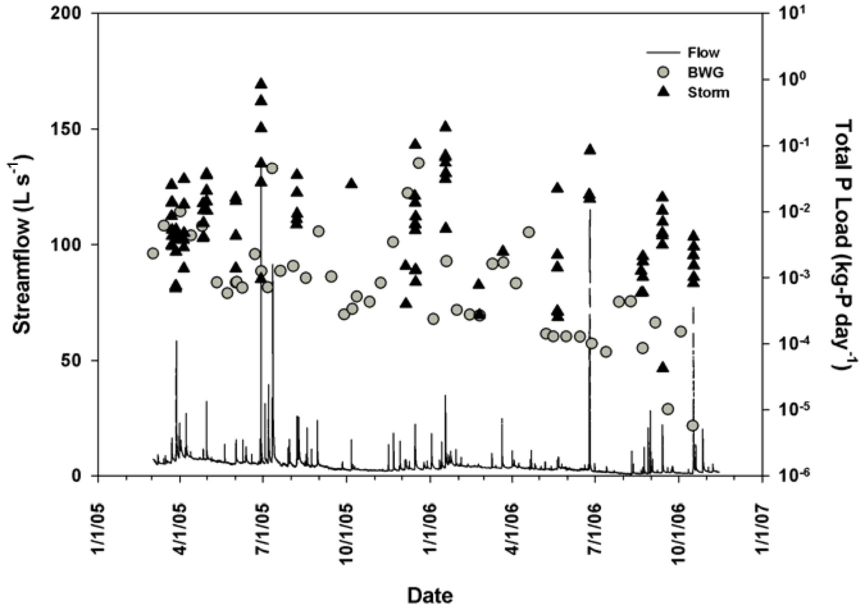

Figure 86. Time series of streamflow and observed TP loads at site FORS-3.

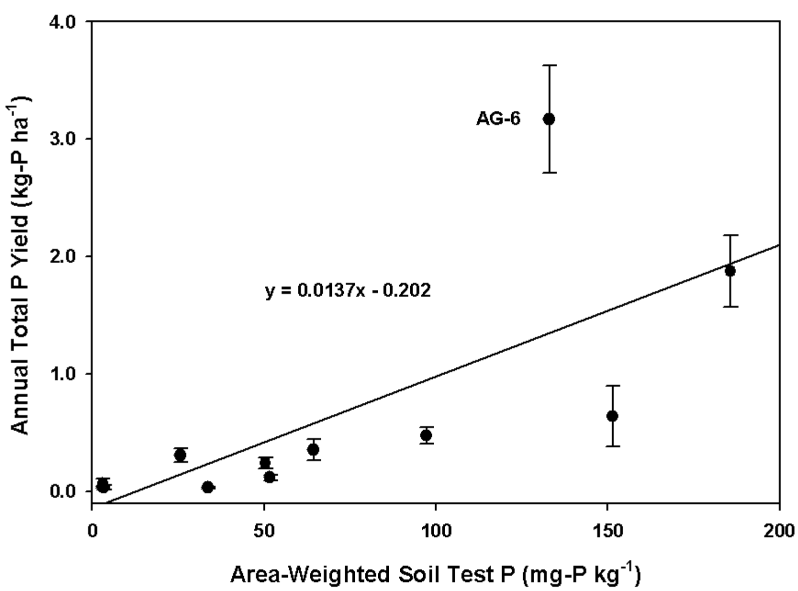

Figure 87. Relationship between estimated annual TP yield and observed area-weighted Mehlich-1 soil test P at study sites ($P = 0.003$; $R^2 = 0.6426$). Yields are based on use of flow-duration rating curve (L_{fdrc}) estimator. Error bars correspond to 95% confidence intervals for yield estimates.

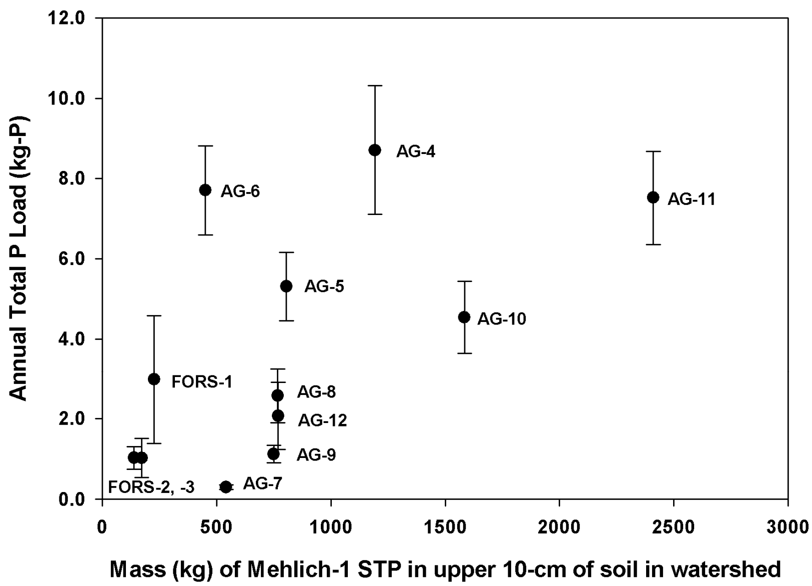

Figure 88. Scatter plot of estimated annual total P load and mass of Mehlich-1 soil test P at study sites. Loads are based on use of flow-duration rating curve (L_{fdrc}) estimator. Error bars correspond to 95% confidence intervals for yield estimates.

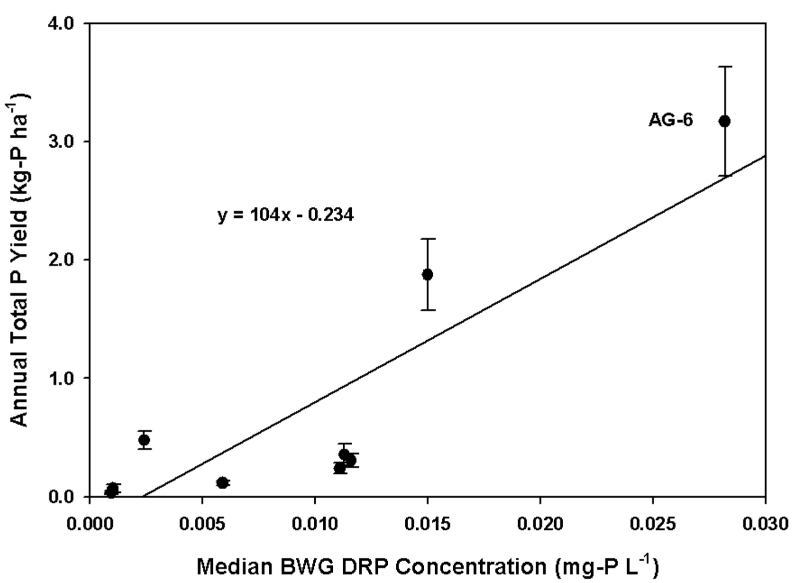

Figure 89. Relationship between estimated annual TP yield and observed median DRP concentrations in BWG samples at study sites ($P = 0.0003$; $R^2 = 0.7818$). Yields are based on use of flow-duration rating curve (L_{fdrc}) estimator. Error bars correspond to 95% confidence intervals for yield estimates.

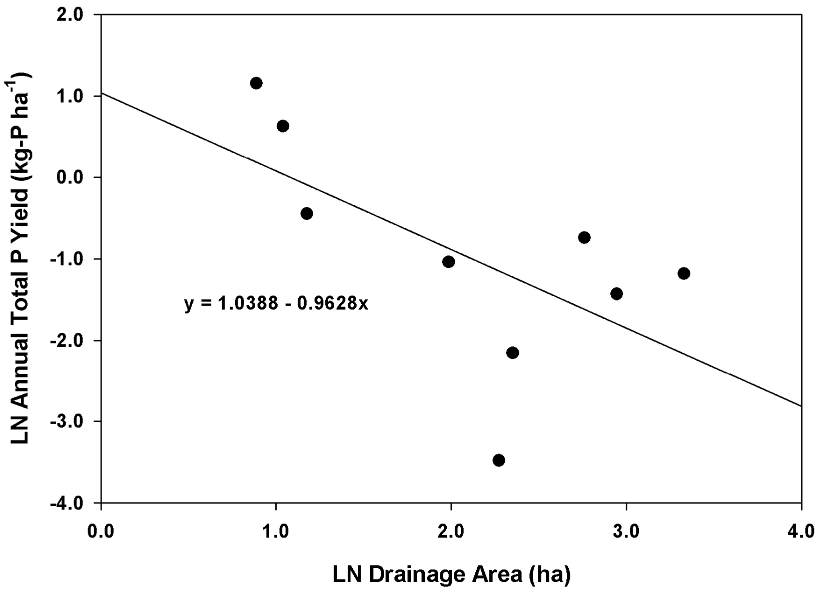

Figure 90. Relationship between LN-transformed annual TP yield and LN-transformed drainage area of the nine AG sites ($P = 0.0797$; $R^2 = 0.3747$). Annual TP yields are based on use of flow-duration rating curve (L_{fdrc}) load estimator.

APPENDIX A

SOILS IN STUDY WATERSHEDS

Soils in Study Watersheds

The names and symbols of the soil mapping units of the twelve project watersheds are provided in the tables on the following two pages. The data were obtained from digital, georeferenced soil maps available from the Natural Resource Conservation Service's Soil Data Mart (http:\\soildatamart.nrcs.usda.gov). The maps are based on the original soil surveys by McIntyre (1972) and Jordan et al. (1973). Spatial analysis tools available in ArcMap were used to delineate and estimate the areal coverage of the soils within each site's watershed boundary.

Site	Map symbol	Percent of watershed area
FORS-1	HIE	14.92
	HIE	11.01
	HJE3	0.56
	HJE3	6.50
	TdG	44.70
	TdG	0.56
	TlC	1.81
	TlC	3.44
	W	4.35
	WgD	12.16
FORS-2	FaC	5.17
	FaE	14.70
	TdG	50.76
	WgD	26.13
	WgD	3.25
FORS-3	EPF	6.52
	HIE	16.40
	HIE	8.50
	TdG	48.27
	WgD	20.30
AG-4	AwB	0.69
	AwB	1.93
	HLC	12.48
	HSC	3.18
	HSD	5.88
	MCE	33.62
	MoC2	3.06
	MuE2	15.77
	MuE2	3.40
	RbD3	2.48
	Sta	1.14
	TdG	13.76
	Wed	2.61
AG-5	HJC3	35.13
	HJE3	50.23
	HlE	14.64

Site	Map symbol	Percent of watershed area
AG-6	HJC3	16.13
	HJE3	51.13
	HlB	27.10
	HlE	5.65
AG-7	HJC3	2.38
	MiC2	8.59
	Sta	0.67
	ThE2	88.37
AG-8	HIC	24.30
	HIE	75.70
AG-9	HJE3	1.65
	HlB	4.48
	HlC	39.47
	MiC2	2.03
	MjC	1.65
	TcE	38.51
	ThE2	6.47
	W	5.74
AG-10	Con	0.91
	HIE	94.14
	HJE3	0.04
	HJE3	0.87
	TdG	0.00
	TlC	4.03
AG-11	FaC	0.61
	HIC	1.27
	HIE	50.44
	HJC3	14.17
	HJE3	15.41
	Toc	14.22
	W	3.88
AG-12	HIE	100.00

Key

Map symbol	Name
AwB	Augusta fine sandy loam, 2 to 6 percent slopes
Con	Congaree and Starr soils
EPF	Edneyville and Porters loams, 25 to 60 percent slopes
FaC	Fannin fine sandy loam, 6 to 10 percent slopes
FaE	Fannin fine sandy loam, 10 to 25 percent slopes
HIE	Hayesville sandy loam, 10 to 25 percent slopes
HJC3	Hayesville sandy clay loam, 6 to 10 percent slopes, severely eroded
HJE3	Hayesville sandy clay loam, 10 to 25 percent slopes, severely eroded
HLC	Hayesville and Rabun loams, 6 to 10 percent slopes
HSC	Hiwassee loam, 2 to 10 percent slopes
HSD	Hiwassee loam, 10 to 15 percent slopes
MCE	Musella cobbly loam, 6 to 25 percent slopes
MoC2	Masada fine sandy loam, 6 to 10 percent slopes, eroded
MuE2	Musella gravelly clay loam, 10 to 25 percent slopes, eroded
RbD3	Rabun clay loam, 10 to 15 percent slopes, severely eroded
Sta	Starr fine sandy loam
TcE	Tallapoosa fine sandy loam, 10 to 25 percent slopes
TdG	Tallapoosa soils, 25 to 70 percent slopes
TlC	Tusquitee loam, 6 to 10 percent slopes
Toc	Toccoa soils
Wed	Wehadkee soils
WgD	Wickham fine sandy loam, 10 to 25 percent slopes
HlB	Hayesville fine sandy loam, 2 to 6 percent slopes
HlE	Hayesville fine sandy loam, 10 to 25 percent slopes
MiC2	Madison gravelly sandy clay loam, 2 to 10 percent slopes, eroded
MjC	Madison fine sandy loam, 6 to 10 percent slopes
ThE2	Tallapoosa gravelly sandy clay loam, 10 to 25 percent slopes, eroded
W	Water

APPENDIX B

STREAMFLOW AND RAINFALL TIME SERIES AT STUDY SITES

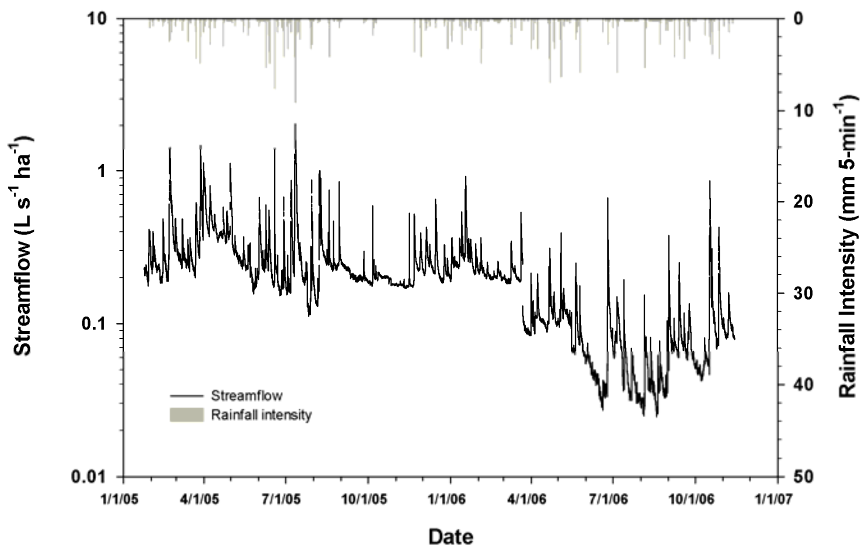

Figure B1. Site FORS-1 streamflow and rainfall time series.

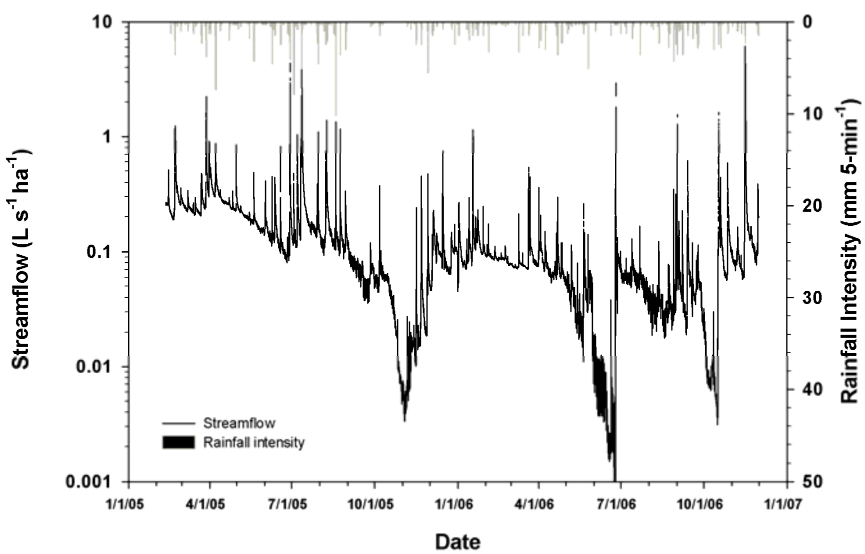

Figure B2. Site FORS-2 streamflow and rainfall time series.

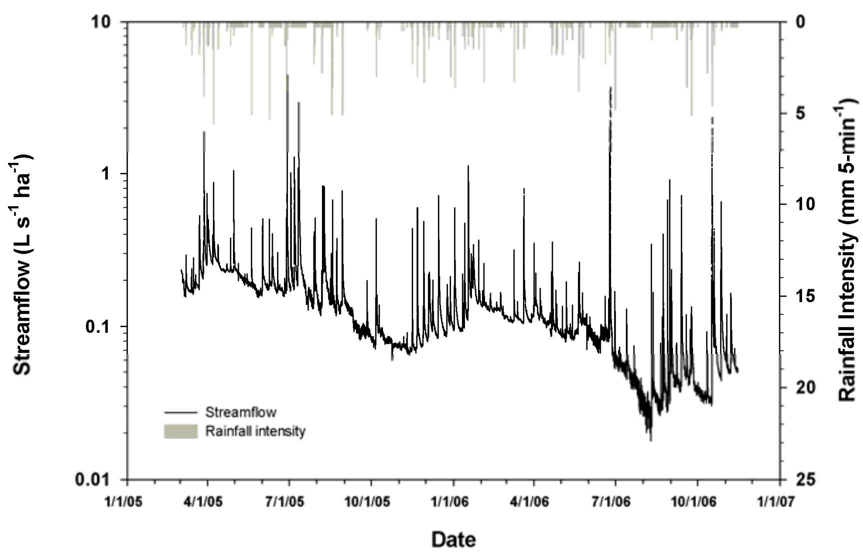

Figure B3. Site FORS-3 streamflow and rainfall time series.

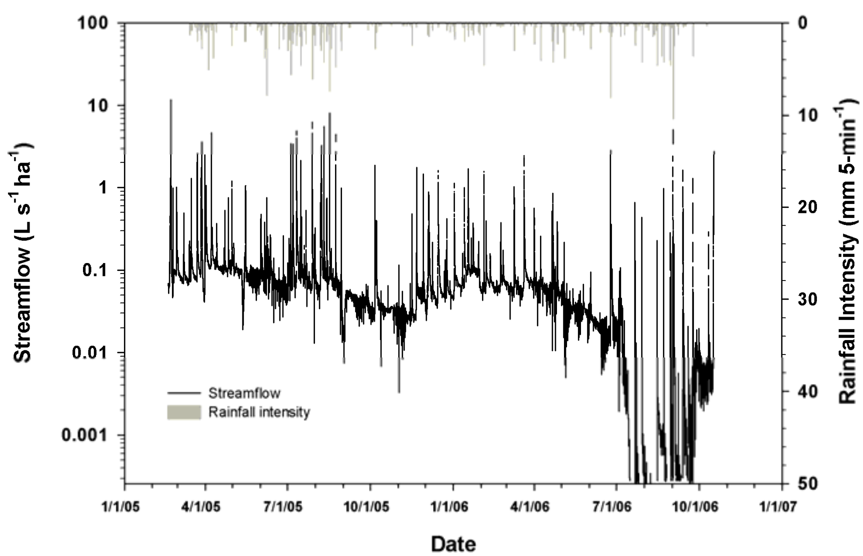

Figure B4. Site AG-4 streamflow and rainfall time series.

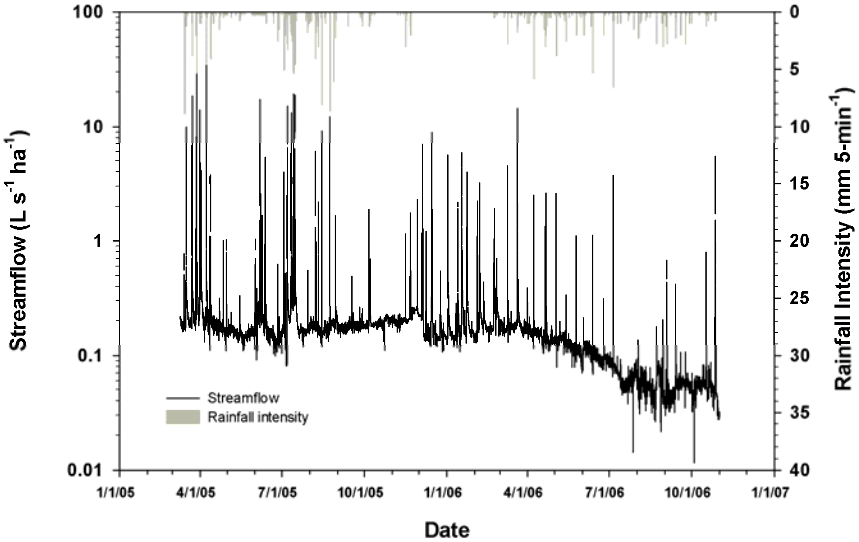

Figure B5. Site AG-5 streamflow and rainfall time series.

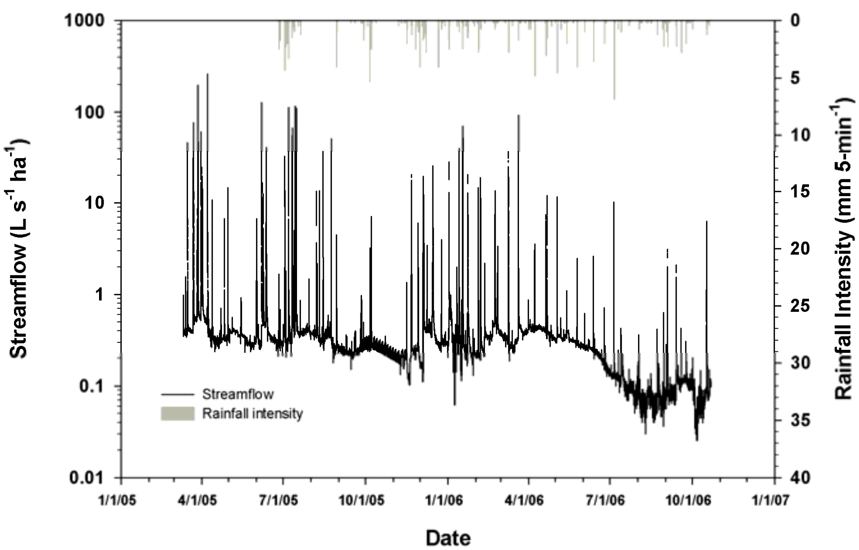

Figure B6. Site AG-6 streamflow and rainfall time series.

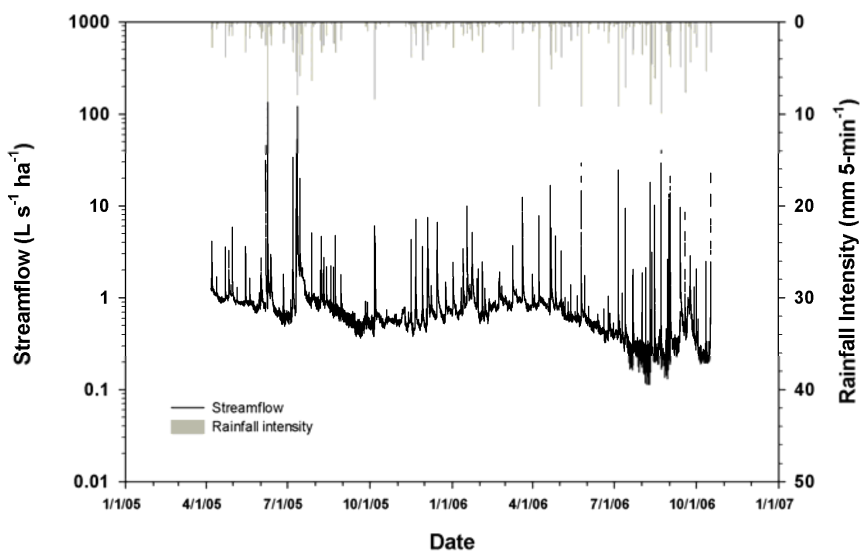

Figure B7. Site AG-7 streamflow and rainfall time series.

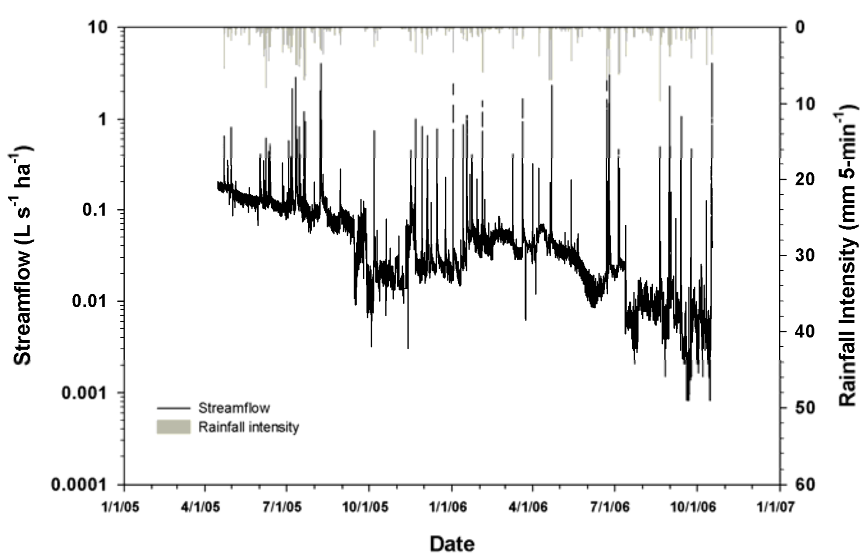

Figure B8. Site AG-8 streamflow and rainfall time series.

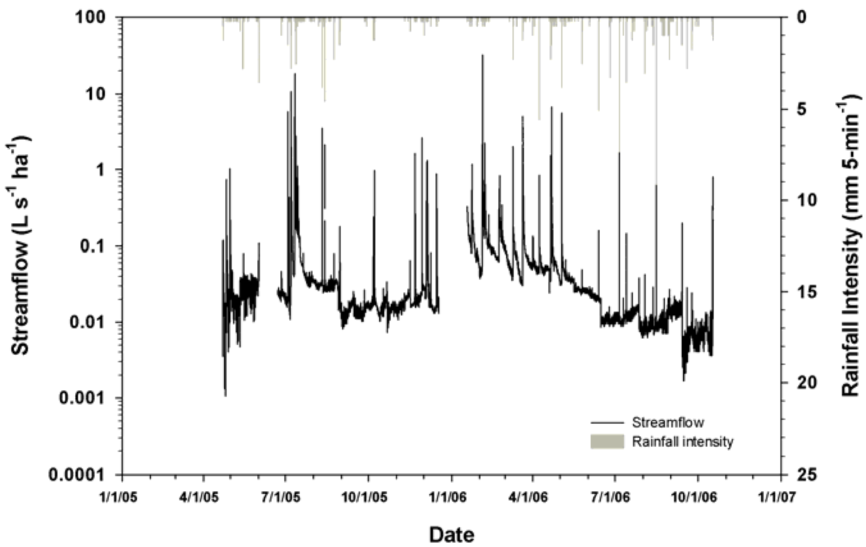

Figure B9. Site AG-9 streamflow and rainfall time series.

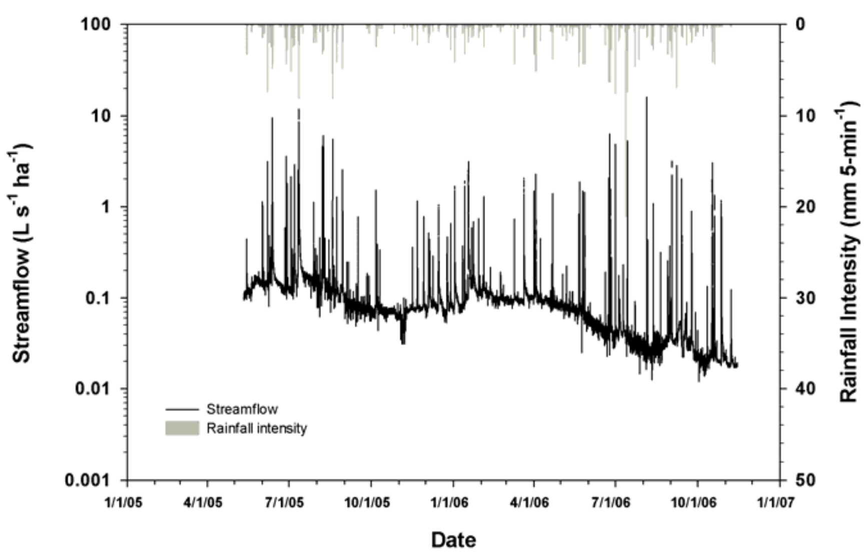

Figure B10. Site AG-10 streamflow and rainfall time series.

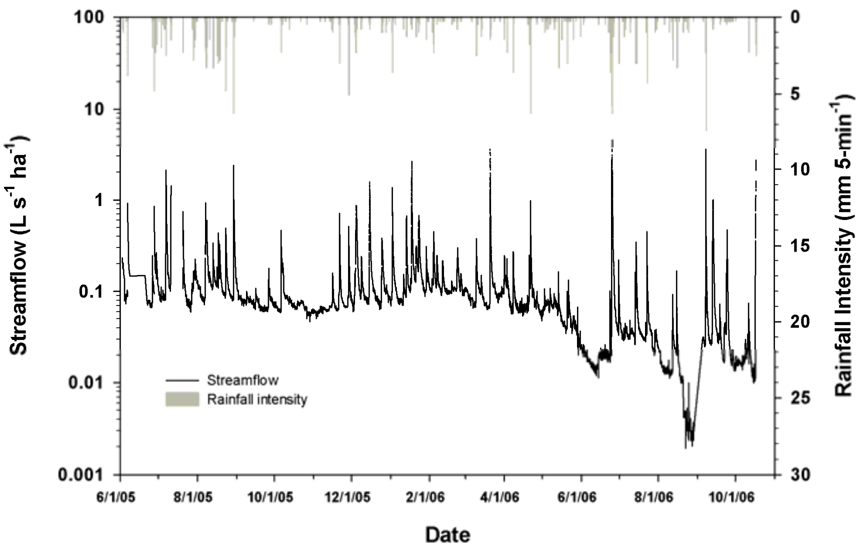

Figure B11. Site AG-11 streamflow and rainfall time series.

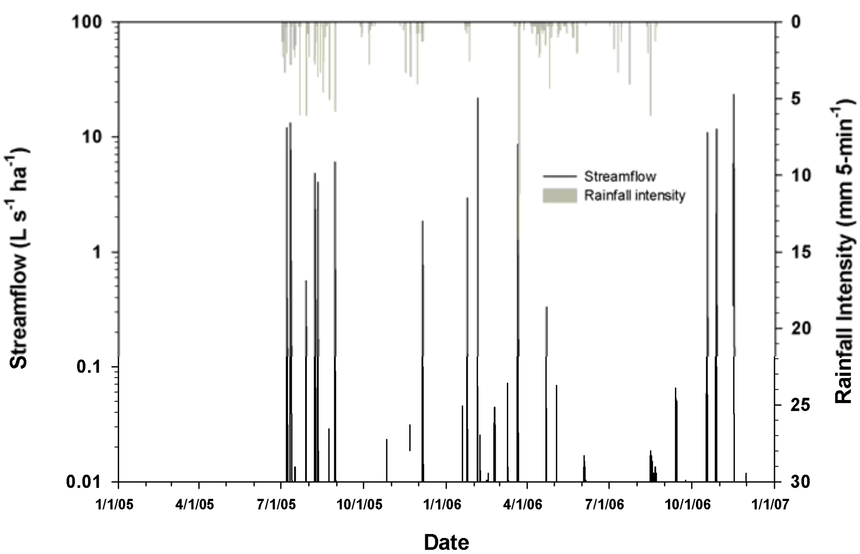

Figure B12. Site AG-12 streamflow and rainfall time series.

APPENDIX C

TOTAL PHOSPHORUS CONCENTRATION TIME SERIES AT STUDY SITES

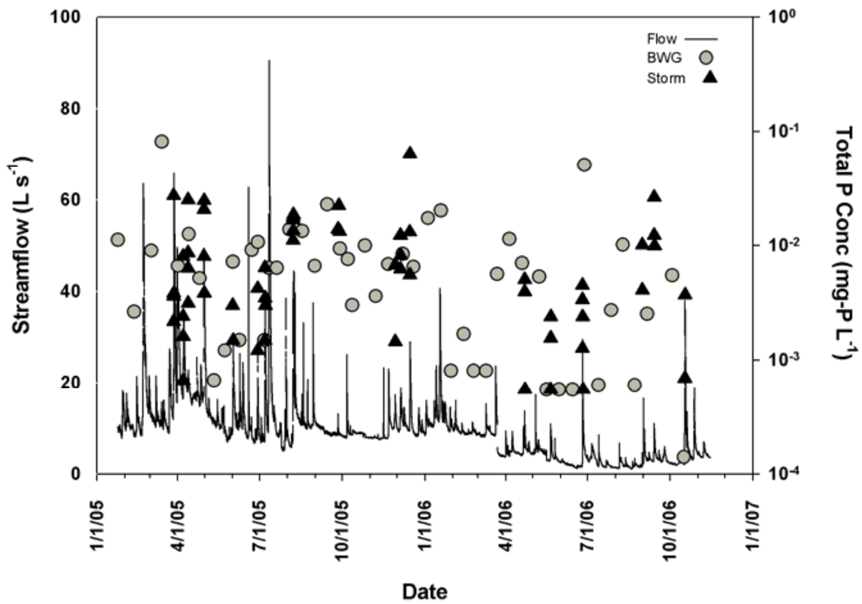

Figure C1. Site FORS-1 TP concentration and streamflow time series

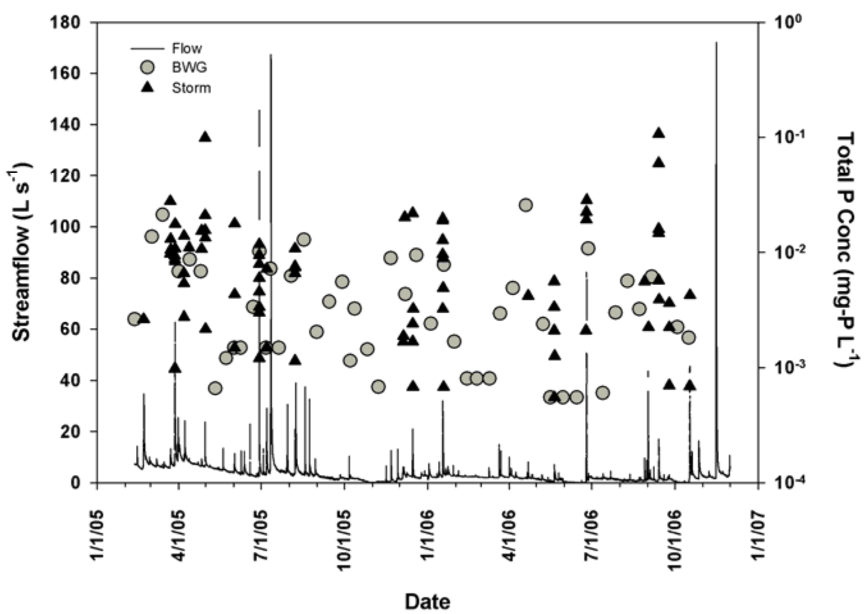

Figure C2. Site FORS-2 TP concentration and streamflow time series

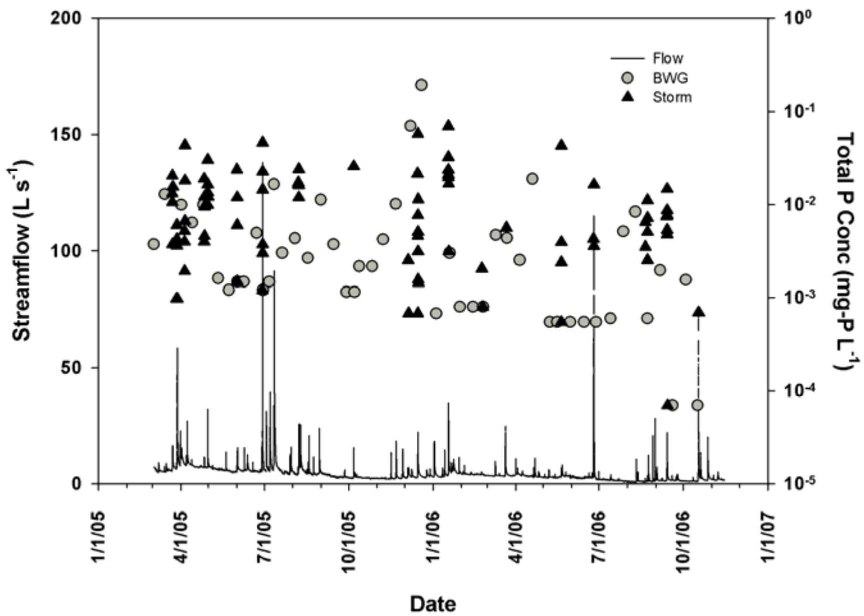

Figure C3. Site FORS-3 TP concentration and streamflow time series

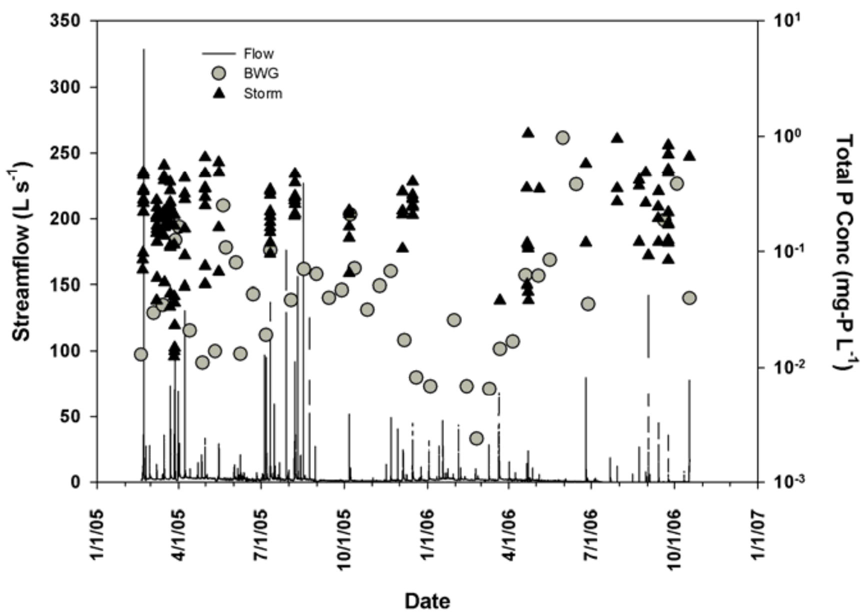

Figure C4. Site AG-4 TP concentration and streamflow time series

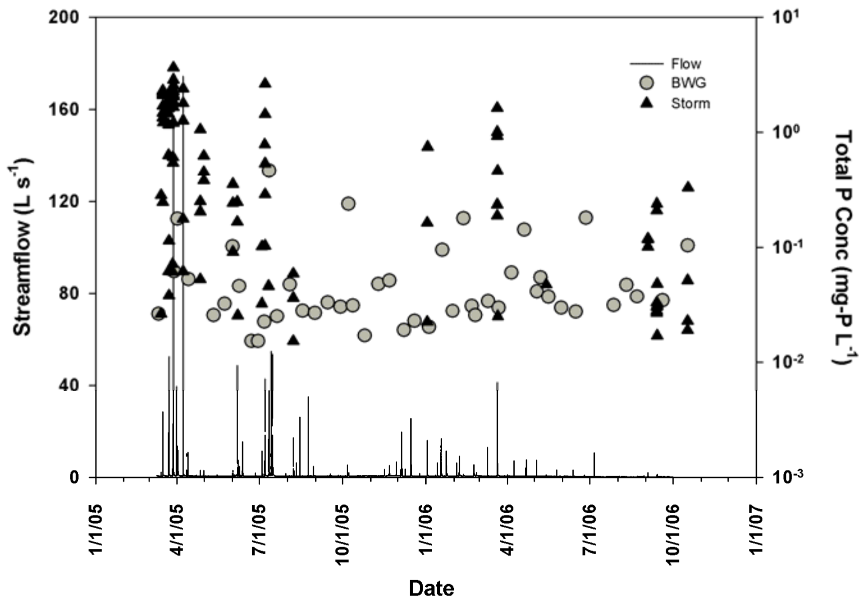

Figure C5. Site AG-5 TP concentration and streamflow time series

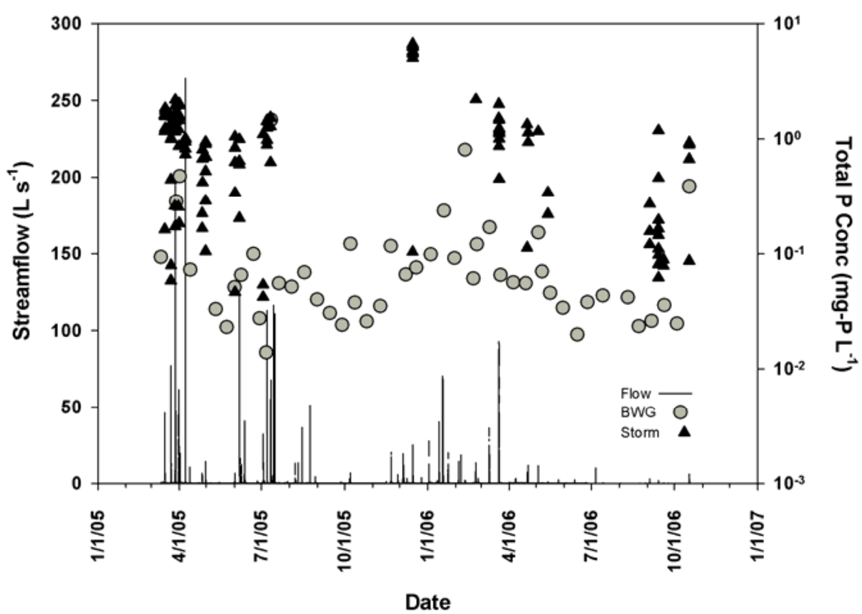

Figure C6. Site AG-6 TP concentration and streamflow time series.

.

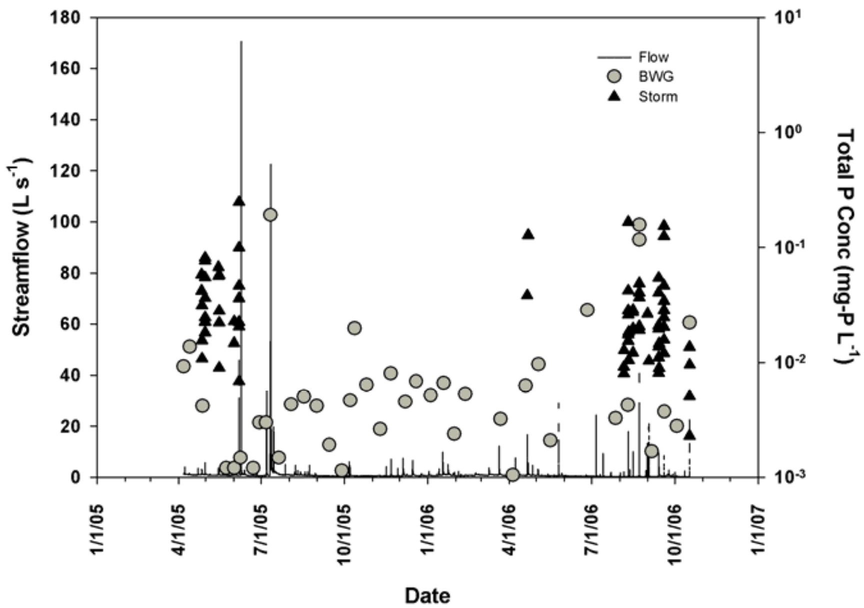

Figure C7. Site AG-7 TP concentration and streamflow time series.

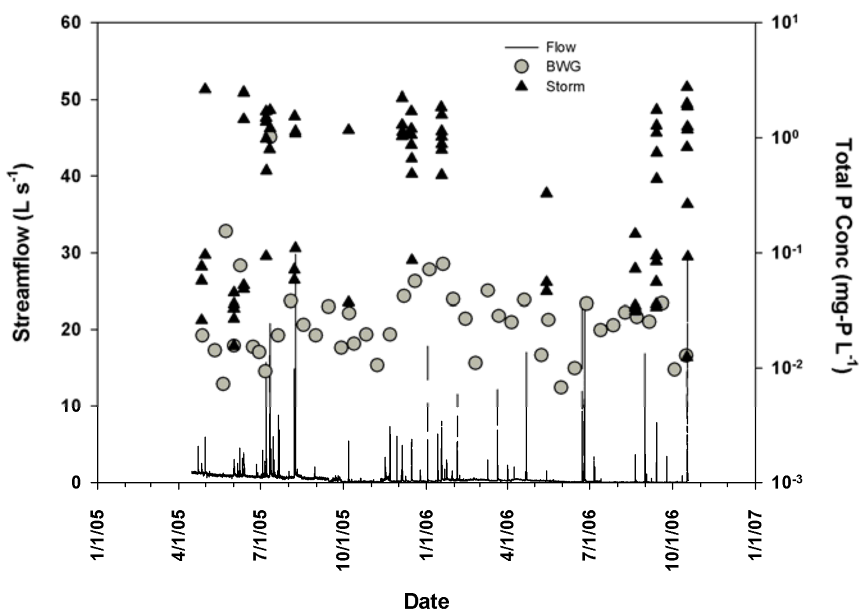

Figure C8. Site AG-8 TP concentration and streamflow time series.

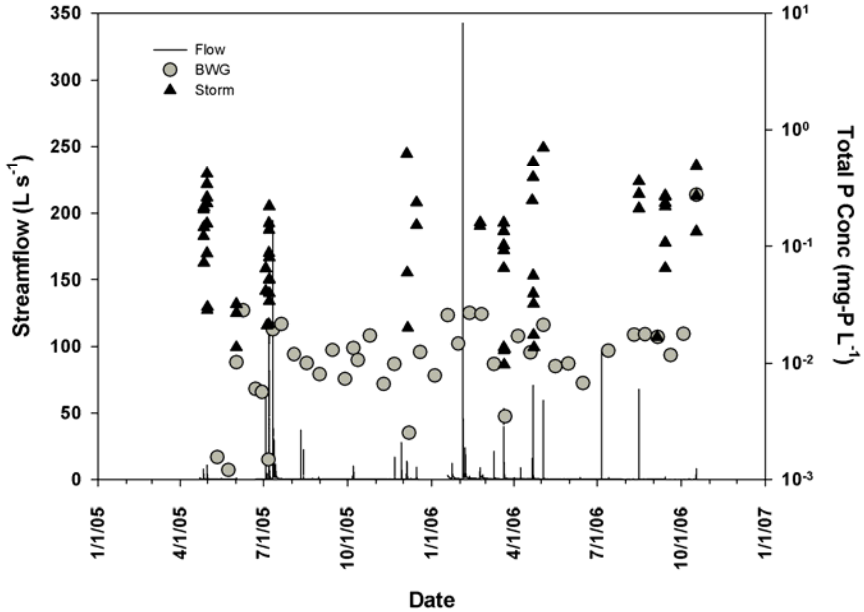

Figure C9. Site AG-9 TP concentration and streamflow time series.

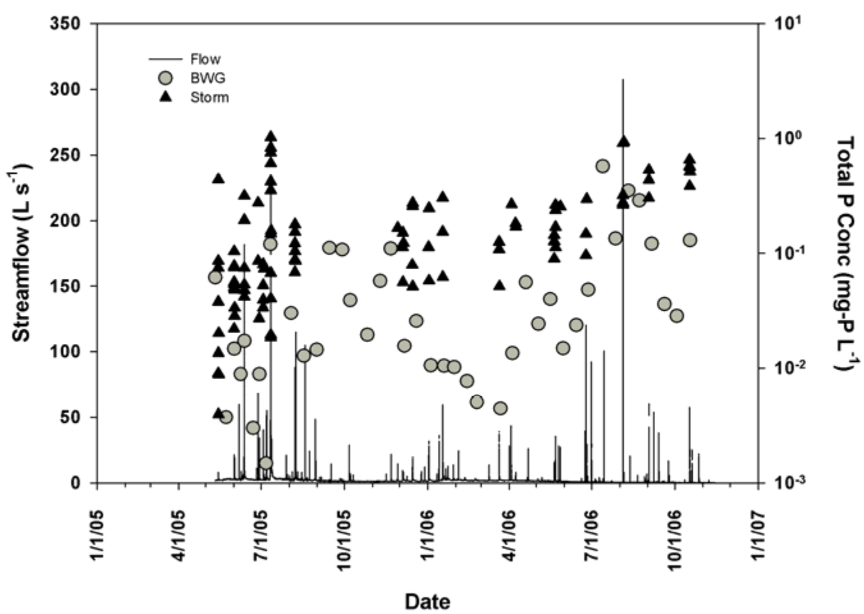

Figure C10. Site AG-10 TP concentration and streamflow time series.

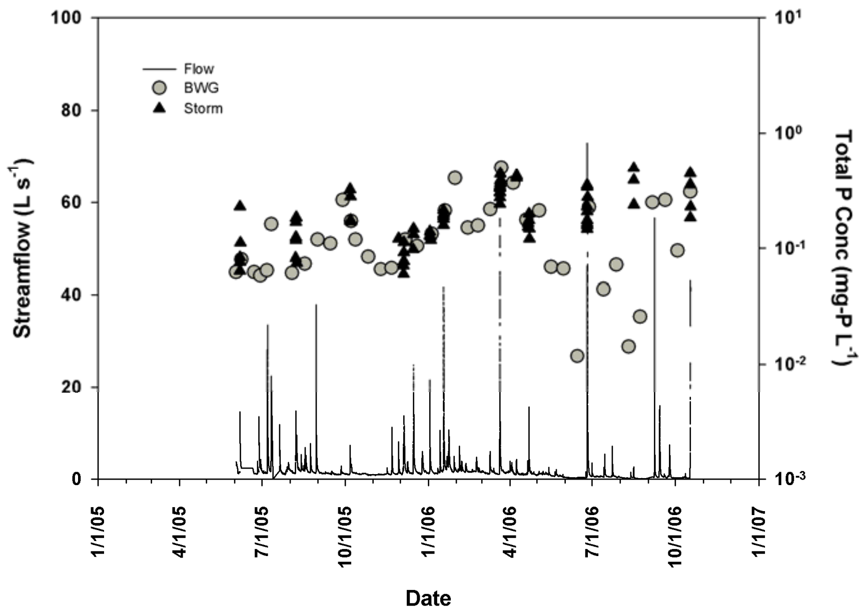

Figure C11. Site AG-11 TP concentration and streamflow time series.

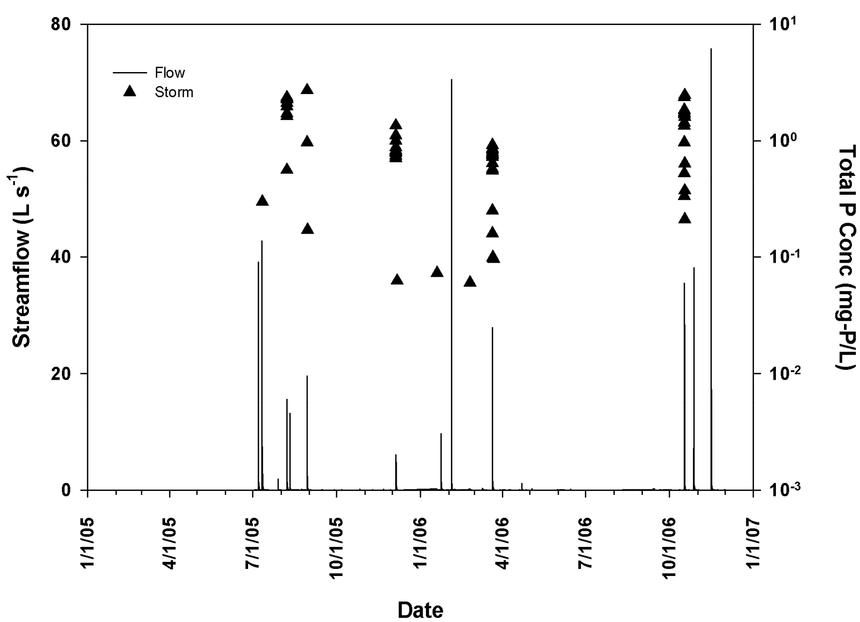

Figure C12. Site AG-12 TP concentration and streamflow time series.

APPENDIX D

SCATTER PLOTS OF STREAMFLOW AND TOTAL

PHOSPHORUS CONCENTRATION

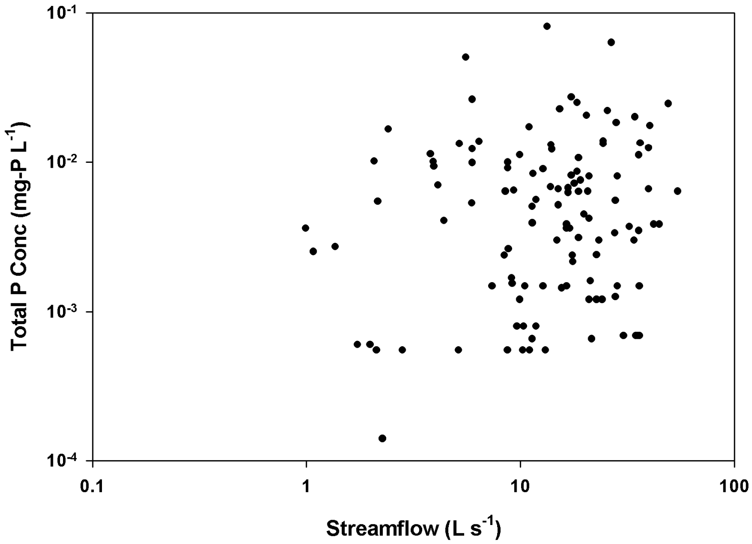

Figure D1. Scatter plot of TP concentration vs. streamflow in water quality samples collected at site FORS-1. Plot shows all samples (BWG and storm) collected at site.

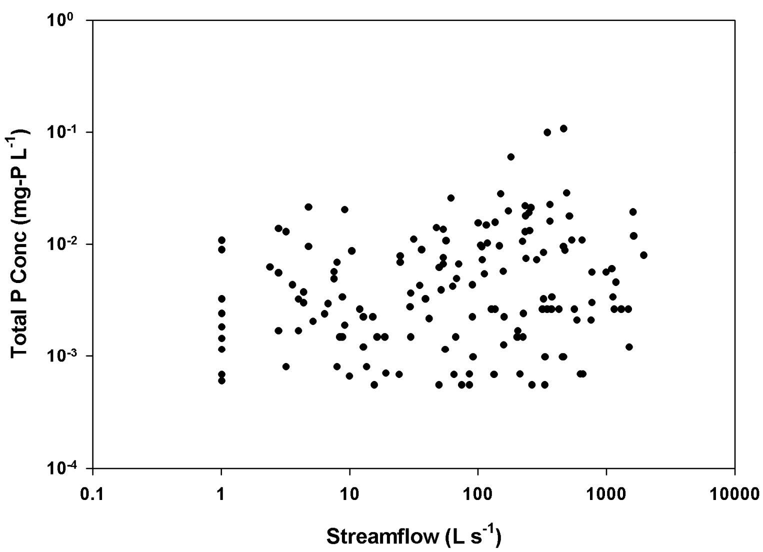

Figure D2. Scatter plot of TP concentration vs. streamflow in water quality samples collected at site FORS-2. Plot shows all samples (BWG and storm) collected at site.

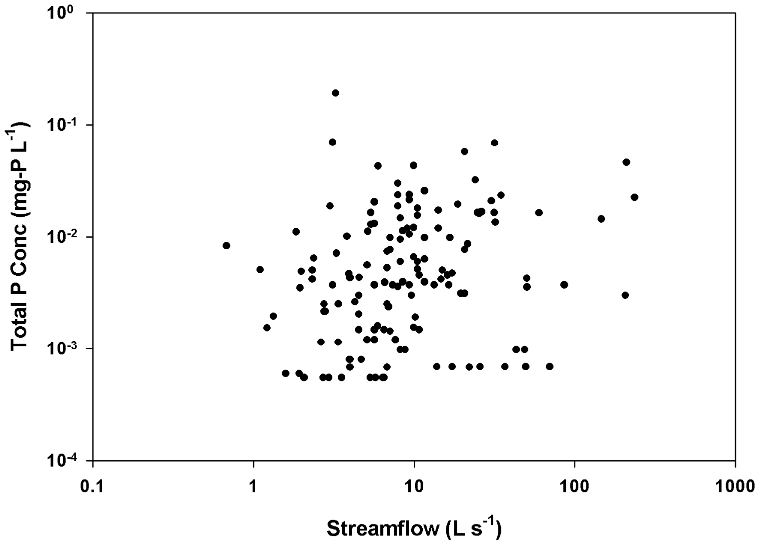

Figure D3. Scatter plot of TP concentration vs. streamflow in water quality samples collected at site FORS-3. Plot shows all samples (BWG and storm) collected at site.

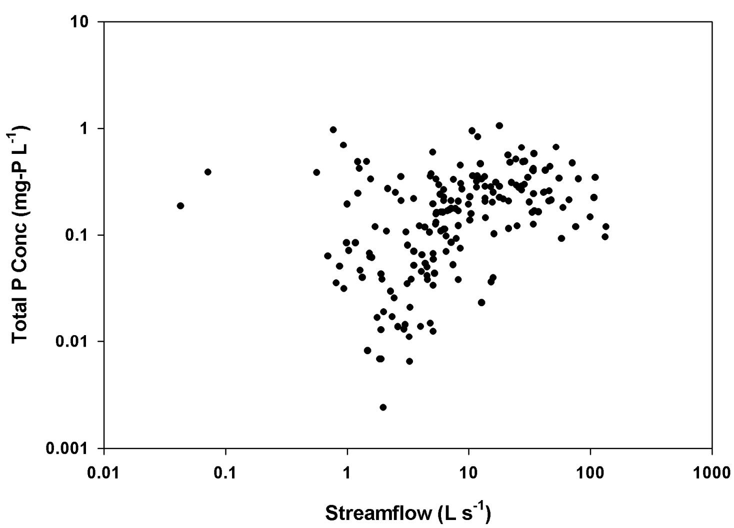

Figure D4. Scatter plot of TP concentration vs. streamflow in water quality samples collected at site AG-4. Plot shows all samples (BWG and storm) collected at site.

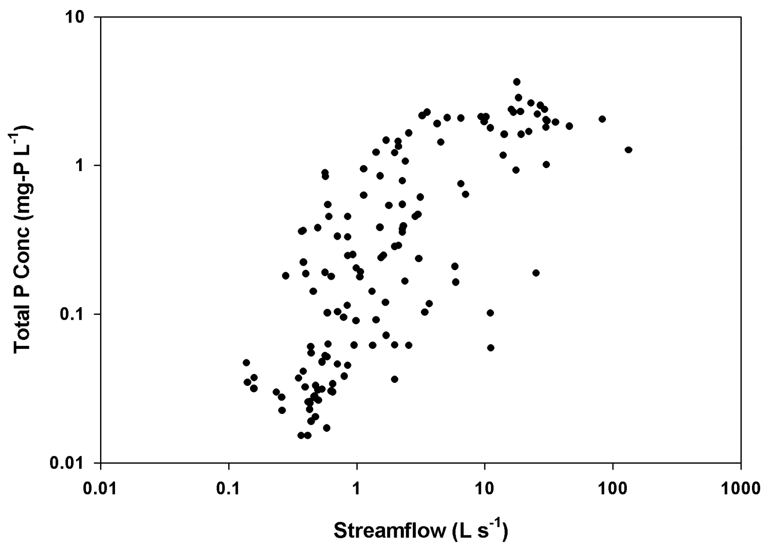

Figure D5. Scatter plot of TP concentration vs. streamflow in water quality samples collected at site AG-5. Plot shows all samples (BWG and storm) collected at site.

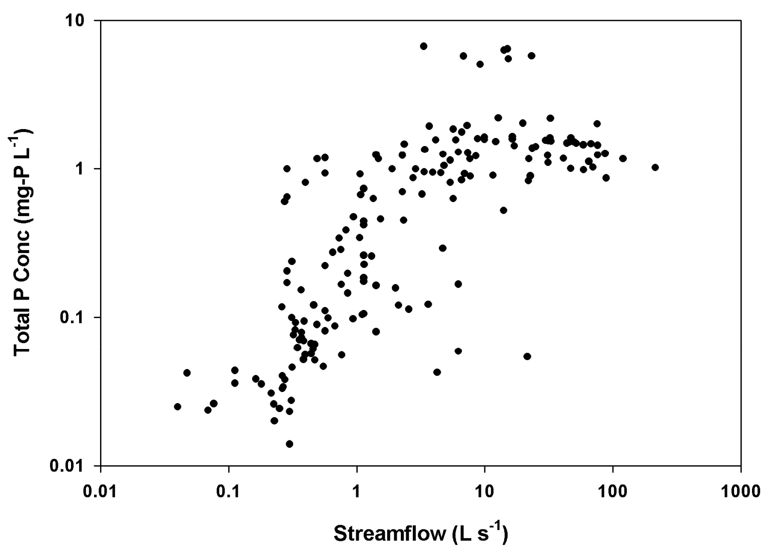

Figure D6. Scatter plot of TP concentration vs. streamflow in water quality samples collected at site AG-6. Plot shows all samples (BWG and storm) collected at site.

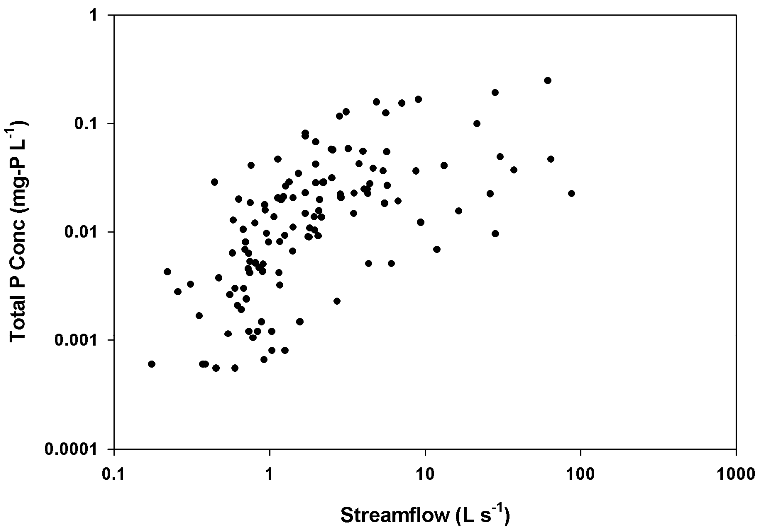

Figure D7. Scatter plot of TP concentration vs. streamflow in water quality samples collected at site AG-7. Plot shows all samples (BWG and storm) collected at site.

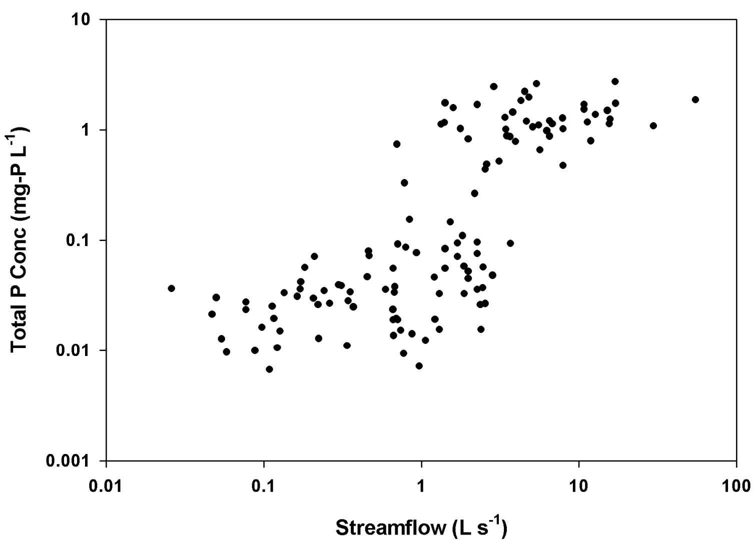

Figure D8. Scatter plot of TP concentration vs. streamflow in water quality samples collected at site AG-8. Plot shows all samples (BWG and storm) collected at site.

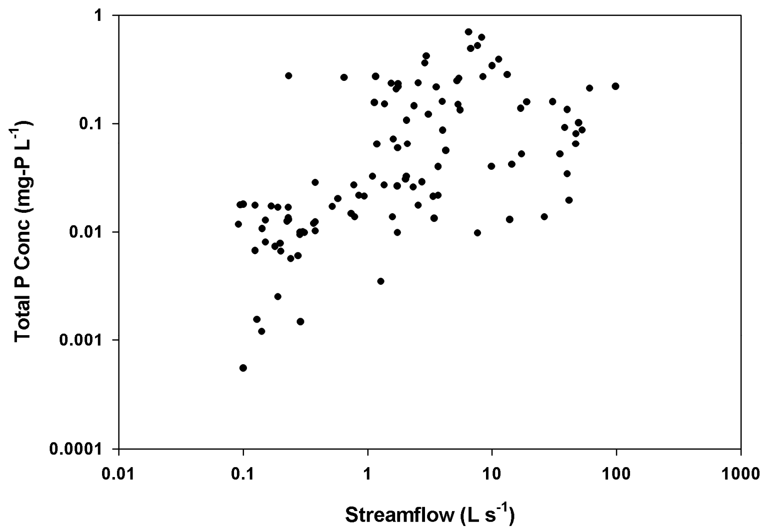

Figure D9. Scatter plot of TP concentration vs. streamflow in water quality samples collected at site AG-9. Plot shows all samples (BWG and storm) collected at site.

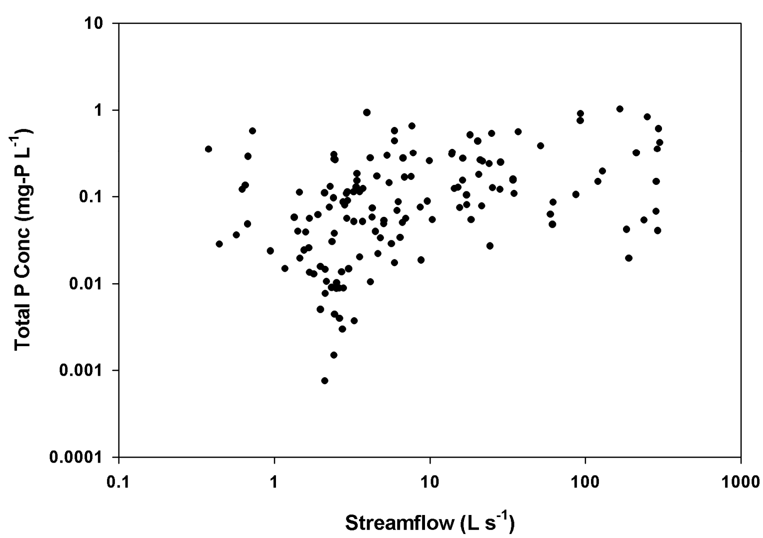

Figure D10. Scatter plot of TP concentration vs. streamflow in water quality samples collected at site AG-10. Plot shows all samples (BWG and storm) collected at site.

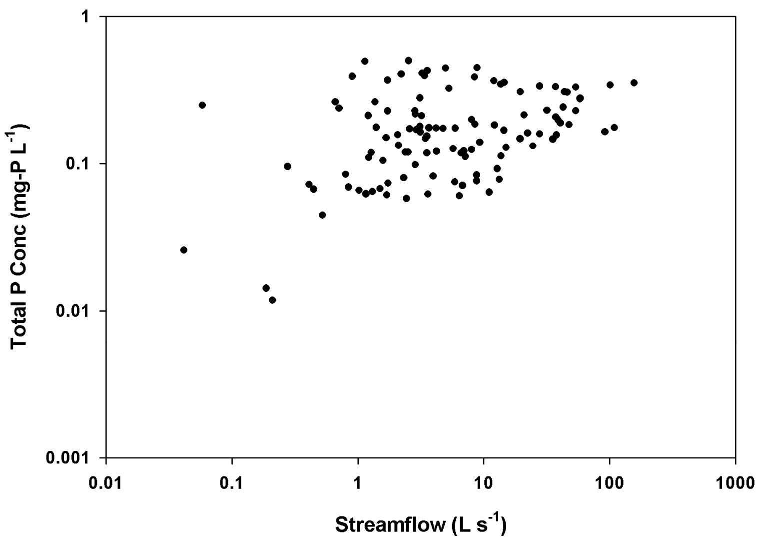

Figure D11. Scatter plot of TP concentration vs. streamflow in water quality samples collected at site AG-11. Plot shows all samples (BWG and storm) collected at site.

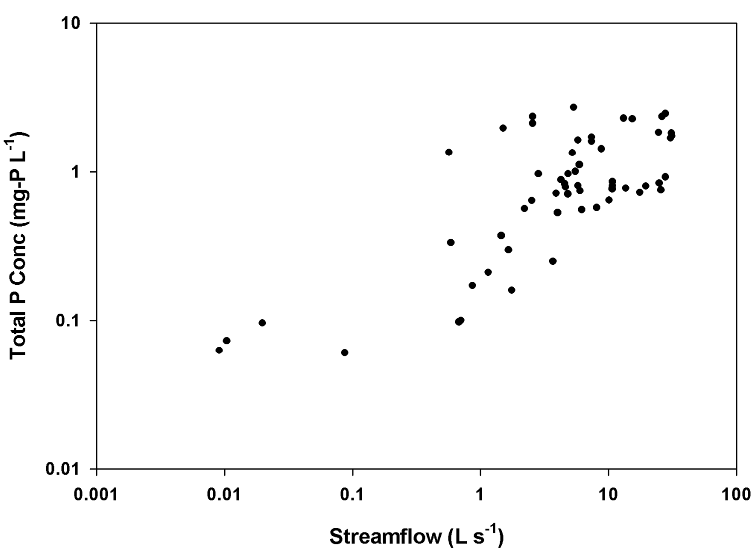

Figure D12. Scatter plot of TP concentration vs. streamflow in water quality samples collected at site AG-12. Plot shows all samples (BWG and storm) collected at site.

APPENDIX E

TOTAL PHOSPHORUS FLOW DURATION RATING CURVES

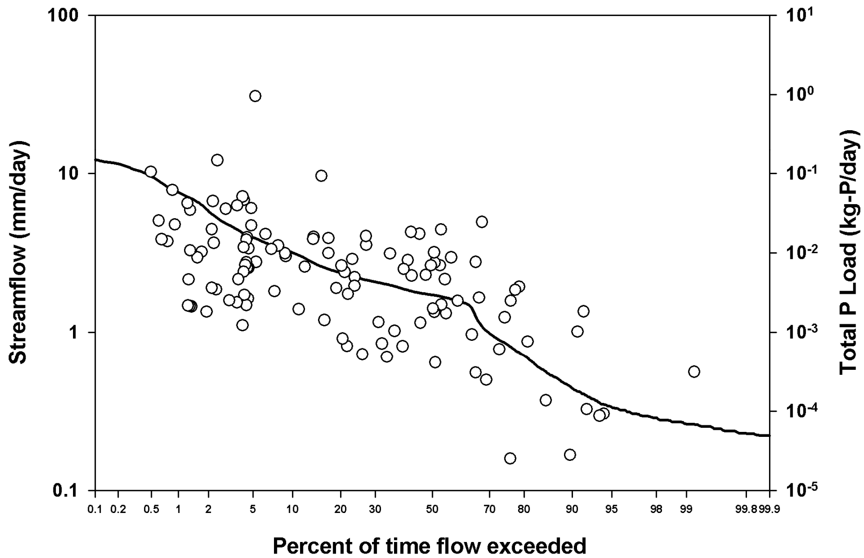

Figure E1. Instantaneous observed TP load and streamflow as a function of percent of time flow exceeded at FORS-1. Solid line represents streamflow. Circles represent observed TP load.

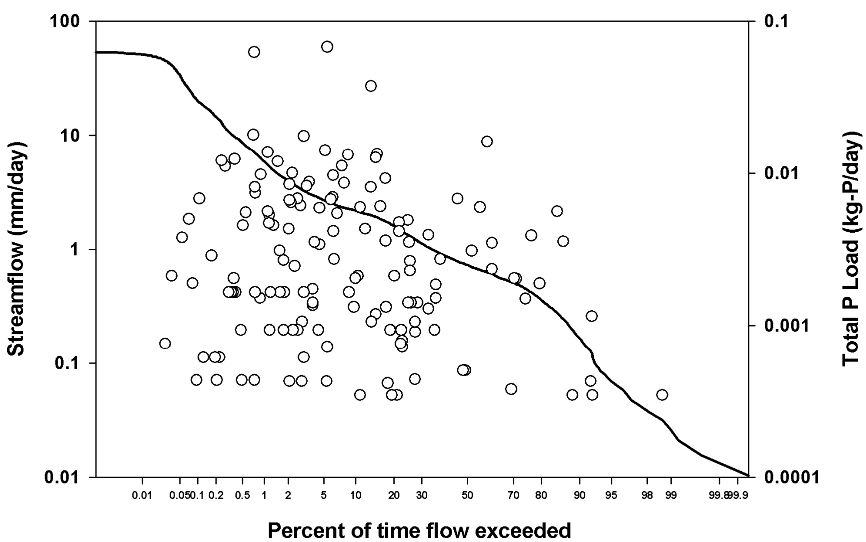

Figure E2. Instantaneous observed TP load and streamflow as a function of percent of time flow exceeded at FORS-2. Solid line represents streamflow. Circles represent observed TP load.

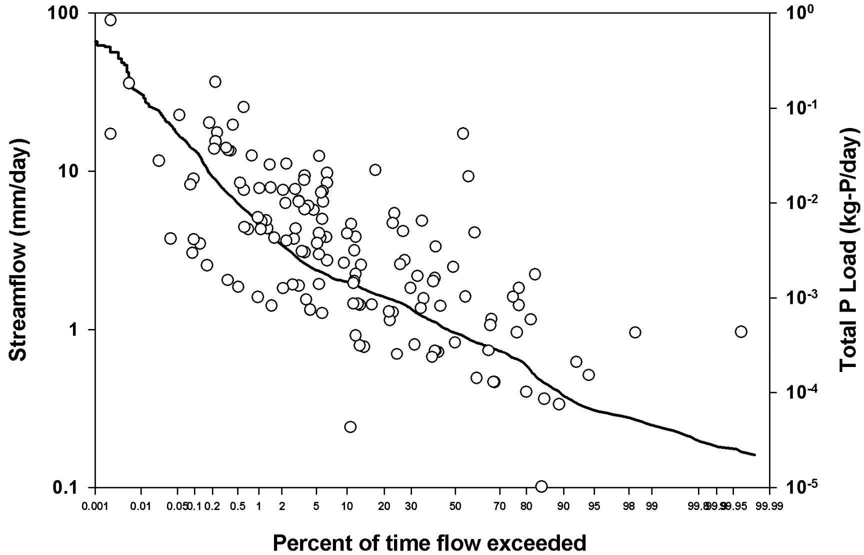

Figure E3. Instantaneous observed TP load and streamflow as a function of percent of time flow exceeded at FORS-3. Solid line represents streamflow. Circles represent observed TP load.

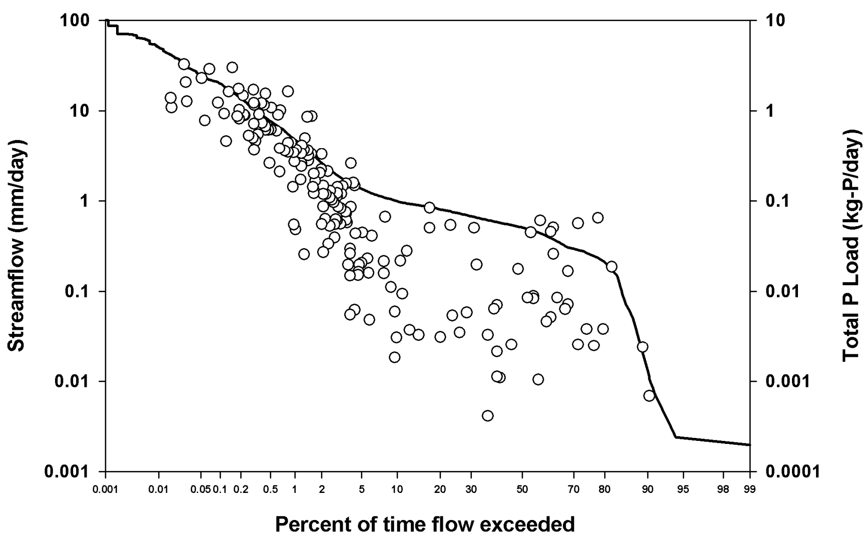

Figure E4. Instantaneous observed TP load and streamflow as a function of percent of time flow exceeded at AG-4. Solid line represents streamflow. Circles represent observed TP load.

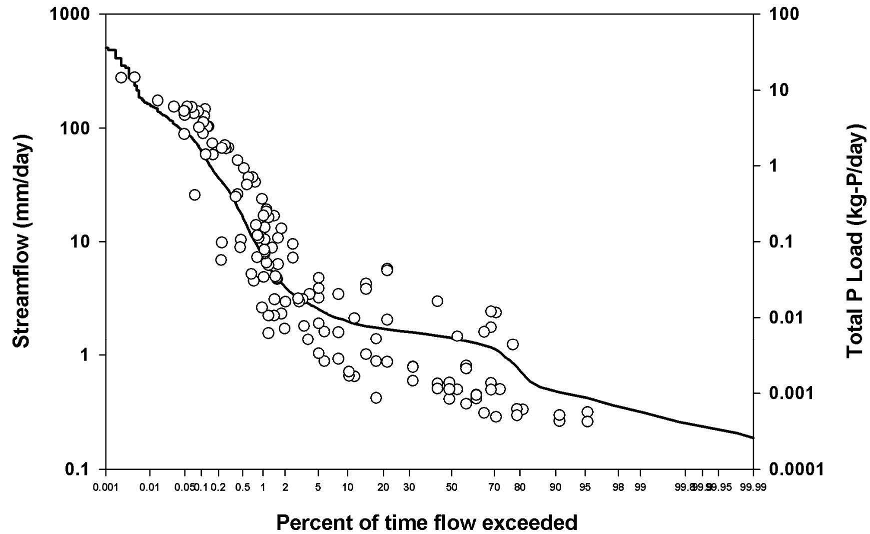

Figure E5. Instantaneous observed TP load and streamflow as a function of percent of time flow exceeded at AG-5. Solid line represents streamflow. Circles represent observed TP load.

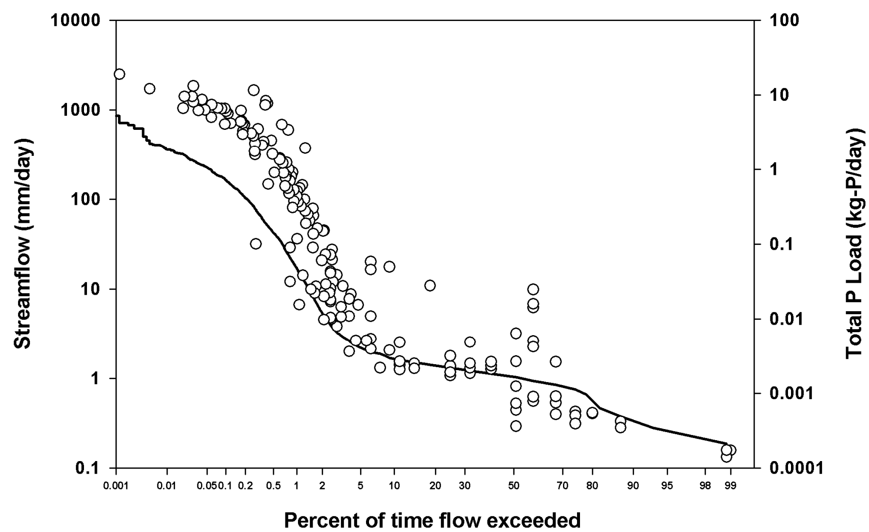

Figure E6. Instantaneous TP load and streamflow as a function of percent of time flow exceeded at AG-6. Solid line represents streamflow. Circles represent observed TP load.

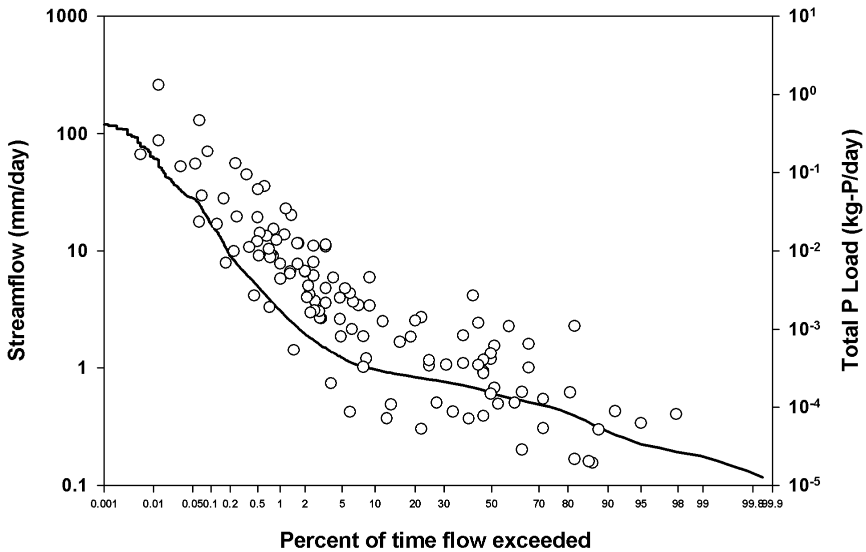

Figure E7. Instantaneous TP load and streamflow as a function of percent of time flow exceeded at AG-7. Solid line represents streamflow. Circles represent observed TP load.

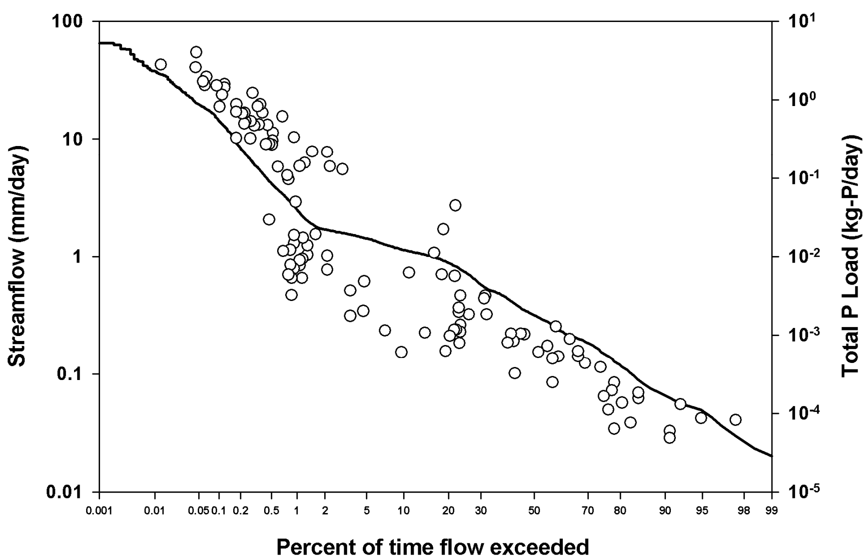

Figure E8. Instantaneous TP load and streamflow as a function of percent of time flow exceeded at AG-8. Solid line represents streamflow. Circles represent observed TP load.

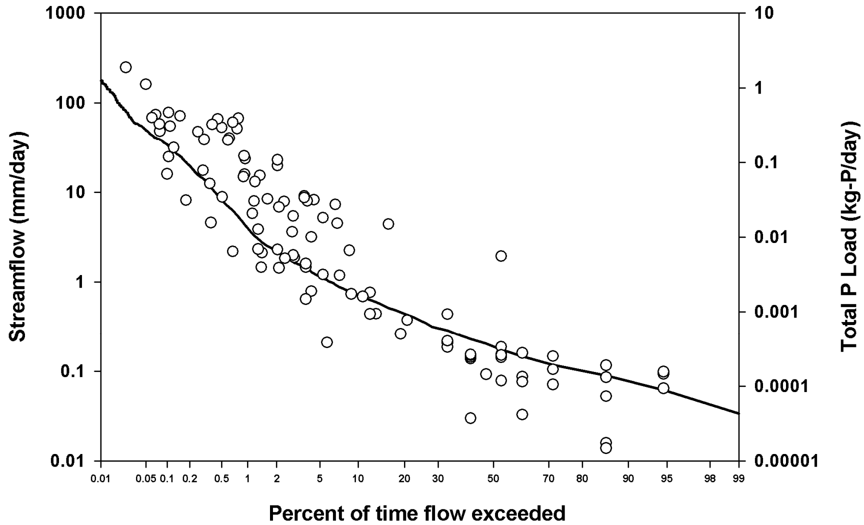

FigureE9. Instantaneous TP load and streamflow as a function of percent of time flow exceeded at AG-9. Solid line represents streamflow. Circles represent observed TP load.

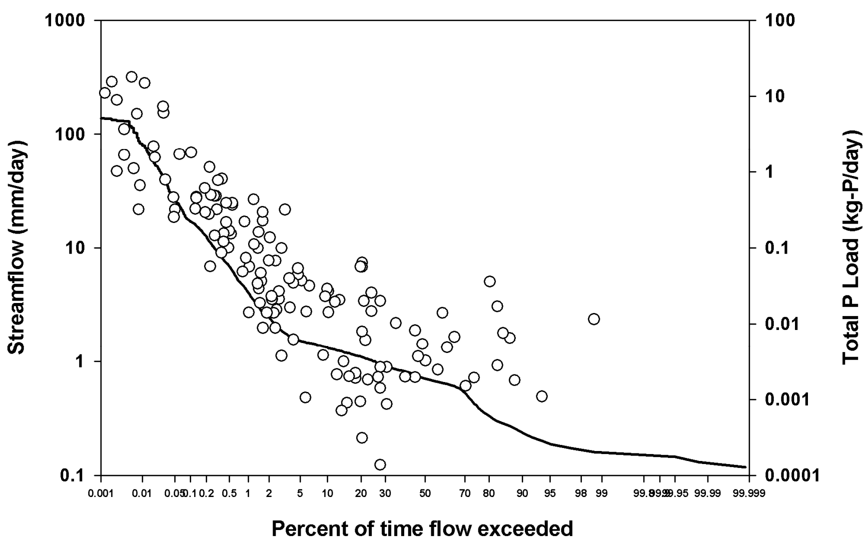

Figure E10. Instantaneous TP load and streamflow as a function of percent of time flow exceeded at AG-10. Solid line represents streamflow. Circles represent observed TP load.

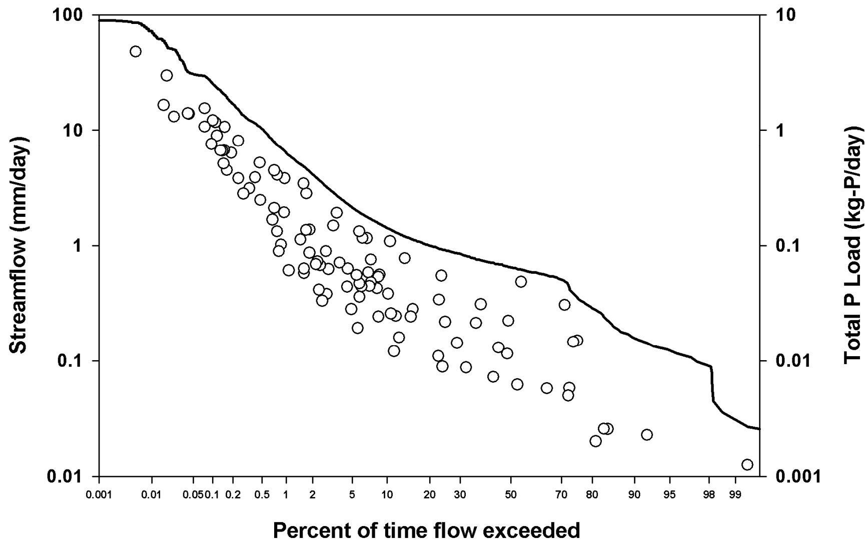

Figure E11. Instantaneous TP load and streamflow as a function of percent of time flow exceeded at AG-11. Solid line represents streamflow. Circles represent observed TP load.

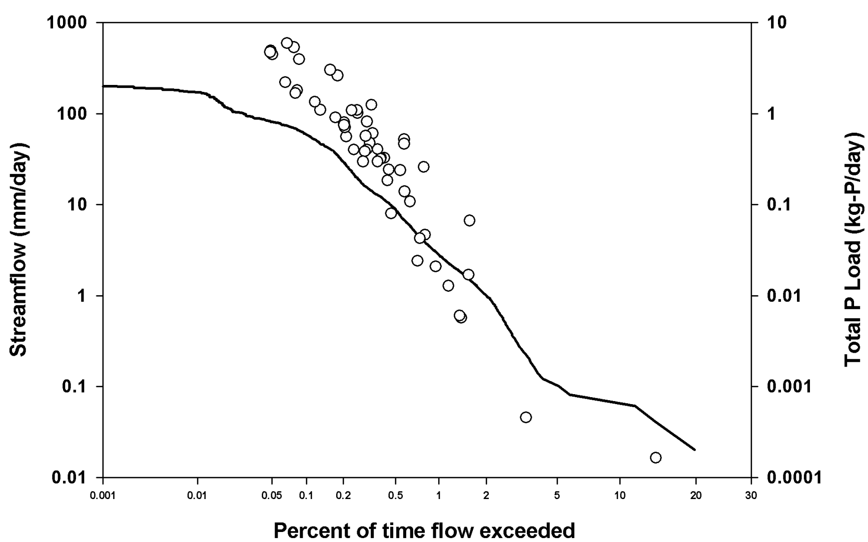

Figure E12. Instantaneous TP load and streamflow as a function of percent of time flow exceeded at-AG-12. Solid line represents streamflow. Circles represent observed TP load.

APPENDIX F

ESTIMATED TOTAL PHOSPHORUS LOADS BY ESTIMATOR

Table F1. Estimated annual yields (kg-P ha^{-1} yr^{-1}) of total P at study sites via three load estimation methods (planning-level, direct estimation, and linear regression).

	Planning-level					**FDRC**		**Linear Regression**					
Site	L_{bwg}	L_{stm}	L_{geo}	L_{geo} upper 95% CI	L_{geo} lower 95% CI	L_{fdrc}	L_{fdrc} 95% CI	L_{exp}	L_{exp} WMAE	L_{qmle}	L_{qmle} WMAE	L_{sme}	L_{sme} WMAE
FORS-1	0.041	0.025	0.025	0.066	0.018	0.068	0.036	NE	NE	NE	NE	NE	NE
FORS-2	0.003	0.014	0.014	0.027	0.009	0.037	0.010	NE	NE	NE	NE	NE	NE
FORS-3	0.009	0.022	0.017	0.045	0.012	0.033	0.016	NE	NE	NE	NE	NE	NE
AG-4	0.095	0.504	0.312	0.530	0.196	0.306	0.057	0.299	0.039	0.512	0.043	0.475	0.042
AG-5	0.200	3.455	1.412	6.157	1.149	1.874	0.302	1.770	0.154	3.035	0.175	2.921	0.171
AG-6	0.442	7.872	2.881	10.17	2.245	3.170	0.461	4.140	0.315	6.330	0.368	6.378	0.371
AG-7	0.009	0.060	0.031	0.099	0.024	0.031	0.006	0.029	0.004	0.050	0.004	0.047	0.004
AG-8	0.046	1.366	0.242	1.280	0.204	0.354	0.092	0.555	0.034	1.135	0.044	1.056	0.042
AG-9	0.022	0.202	0.073	0.337	0.016	0.116	0.020	0.089	0.013	0.168	0.015	0.164	0.015
AG-10	0.076	0.377	0.238	0.681	0.176	0.239	0.047	0.188	0.037	0.382	0.042	0.429	0.044
AG-11	0.379	0.593	0.514	0.520	0.258	0.476	0.074	0.470	0.040	0.574	0.041	0.573	0.041
AG-12	NA	0.710	0.617	1.055	0.389	0.639	0.258	1.078	0.075	1.327	0.081	1.339	0.082

CI=confidence interval. NA=not applicable. NE=not estimated WMAE=weighted mean absolute error. Flow-duration rating curve (FDRC) refers to direct estimation method.